3 8006 10039 0619

CoA Memo Aero No. 41

September, 1964

BOUNDARY LAYERS WITH SUCTION OR INJECTION

LEGE OF AERONAUTICS LIBRARY

T. N. STEVENSON

QUEEN MARY COLLEGE

UNIVERSITY OF LONDON

1964

Thesis submitted
in partial fulfilment of the regulations for
the degree of Doctor of Philosophy in
the Faculty of Engineering
of the University of London

ABSTRACT

Approximate integral equations are derived for the compressible laminar boundary layer with arbitrary pressure gradient and arbitrary suction or injection velocity through a porous wall. Reasonable agreement is obtained when particular solutions to the integral equations are compared with solutions by previous authors.

Experiments in an incompressible turbulent boundary layer over a porous surface reveal two laws for the inner and outer regions; laws which correlate previous experimental results. The laws are used to calculate shear distributions and variations of skin friction with Reynolds number and enable Preston tubes to be used to estimate skin friction over a porous surface.

The outer region theory is extended to boundary layers in small pressure gradients and at separation. The only universal functions required are obtained from zero pressure gradient flow. No other constants are used to calculate the mean velocity profiles for boundary layers in small pressure gradients, with suction or injection and at separation or reattachment. The theory agrees with the available experimental results for turbulent boundary layers in energy equilibrium.

Experiments in fully developed pipe flow show how the mean flow is altered when there is suction through a porous section of the pipe. An approximate theory for the inner region compares reasonably well with the experiments for small suction velocities.

CONTENTS

SYMBOLS

General

H	form parameter, δ_1/δ_2
u	velocity in x-direction
v	velocity in y-direction
x	co-ordinate along the surface
y	co-ordinate normal to the surface
δ	boundary layer thickness
δ_1	displacement thickness
δ_2	momentum thickness
μ	viscosity
ν	kinematic viscosity
ρ	density
τ_w	skin friction

Subscripts: w wall conditions

1 free stream conditions

PART I

a	speed of sound
a_2, b_2	function of p in equ. (7.15)
a_3, b_3	coefficients in equ. (8.21)
a_4	coefficient in equ. (8.29)
A, B	functions of p equ. (7.26)
B_1	constant $\left(B_1 x^{\epsilon} = T_w(x)\right)$
C	constant $\left(C x^{m} = u_1(x)\right)$
c_p	ratio of specific heats

SYMBOLS
(Continued)

PART I - Cont.

C, C'	$C = \frac{\mu T_0}{\mu_0 T}$ and $C' = \frac{\mu_w T_1}{\mu_1 T_w} = \frac{C_w}{C_1}$
D	defined by equ. (8.15)
E	$\Gamma(\frac{1}{3}) \cdot 6^{\frac{2}{3}} \cdot 2^{-\frac{1}{3}} 3^{-\frac{2}{3}}$
f	a stream function co-ordinate
f_w, F_w	blowing velocity parameters defined by equ. (8.9) and (10.3) respectively
f_w'', F_w''	skin friction parameters defined by equ. (8.10) and (10.5) respectively
F_1	defined by equ. (7.12)
G	constant $\left(G x^{\frac{m-1}{2}} = v_w(x) \right)$
$G(x, \Phi)$	defined by equ. (6.10)
h	total enthalpy $(i + \frac{u^2}{2})$
i	enthalpy
$I_n( )$	modified Bessel function
k	thermal conductivity
k_h	Stanton number or Stanton heat transfer coefficient, equ. (10.19)
K	constant $\left(K^2 x^{\frac{3m-1}{2}} = \tau_w(x) \right)$
K_1	defined by (equ. (8.28)
$K_n( )$	modified Bessel function of second kind
m	pressure gradient parameter $\left(u_1(x) = c x^m \right)$
m_1	function of Mach number, equ. (10.2)
M	Mach number $\left(= \frac{u}{a} \right)$
N	constant $\left(N x^{\frac{m+1+2\epsilon}{2}} = Nu \right)$
Nu	Nusselt number, equ. (8.7)

SYMBOLS
(Continued)

PART I - Cont.

p	static pressure and also Laplace transform notation
P	function of Φ , equ. (7.16)
P_1, P_2, P_3	coefficients in a series for $\frac{\partial z}{\partial \Phi}$, equ. (9.1)
q	$\frac{4}{3} p^{\frac{1}{2}} \Phi^{3/4}$
Q	function of Φ , equ. (7.16)
$Q_w(x)$	heat transfer per unit area to the wall, $\left(k \frac{\partial T}{\partial y}\right)_w$
$Q_w(X)$	heat transfer parameter, $k_o \left(\frac{\partial T}{\partial Y}\right)_w$
R, R_1	defined by equ. (8.20) and (8.30) respectively
R_e	Reynolds number, $\frac{x u_1}{\nu}$
$R(X, \Phi)$	defined by equ. (6.4)
S	$1 - \frac{h}{h_1}$
S_o	solution of equ. (7.2) when there is zero heat transfer
S_1	$S - S_o$
S_2, S_3	defined by equ. (7.17) and (7.18) respectively
t	defined by equ. (6.25) in section 6 and by equ. (7.11) in section 7.
T	temperature
$\mathcal{T}$	a temperature ratio parameter, equ. (3.6)
U	$\frac{\partial \psi}{\partial Y}$, equ. (5.14)
V	$-\frac{\partial \psi}{\partial X}$, equ. (5.15)
X, Y	defined by equ. (5.6)
$Z(x), Z(X)$	$(u_1^2 - u^2)$ and $(U_1^2 - U^2)$ respectively
γ	ratio of specific heats

SYMBOLS
(Continued)

PART I - Cont.

$\delta(t)$	a Delta function, an impulse function
ε	temperature gradient parameter $\left(B_1 x^{\varepsilon} = T_w(x)\right)$
η	transformed co-ordinate, equ. (3.6)
ξ	$V_w^2 x / u_1 \nu$
σ	Prandtl number
$\tau_w(x)$	a skin friction parameter, $\mu_0 \left(\frac{\partial U}{\partial Y}\right)_w$
Φ	modified stream function
ψ	stream function
ω	viscosity - temperature index $\left(\frac{\mu}{\mu_1} = \left(\frac{T}{T_1}\right)^{\omega}\right)$
$\overline{(\ )}$	Laplace transform notation, equ. (6.23)

Subscripts:

$_0$	stagnation conditions in isentropic flow outside the boundary layer
$_a$	constant reference conditions outside the boundary layer

PARTS II and III

$2a$	in Part II : inside diameter of Preston tube in Part III: inside diameter of the pipe
a_2	$\frac{u_\tau}{V_w}\left(\lambda^2 - 1\right)$
$2b$	outside diameter of Preston tube
b_2	λ / K
B, B_1, B_2, B_3, B_4	constants of integration with respect to y in equations (19.2),(28.6),(28.7), (28.8), and (28.10) respectively
c_f	skin friction coefficient,
C	constant in equ. (23.2)
C_n	profile parameters, $\int_0^{\eta} F^n(\eta_1)\, d\eta_1$

SYMBOLS (Continued)

PARTS II and III - Cont.

$(C_n)_1$	value of C_n when $\eta = 1$
d	outside diameter of Preston tube
D	pressure gradient parameter, $-\frac{\delta}{u_1}\cdot\frac{du_1}{dx}$
D_{APP}	apparent value of D, defined in section 31.4
D_{EXT}	value of D at the outer edge of the boundary layer
E, E_1	$(p\delta\, exp.S(y/\delta)+1)^{\frac{1}{2}}$, $(p\delta\, exp.S(1)+1)^{\frac{1}{2}}$
$F(y/\delta), F$	universal function of y/δ, equ. (25.6)
G	defined by equ. (31.22)
$I_m(t)$	integrals defined by equ. (23.10)
J_1, J_2	integrals defined by equ. (31.13)
J_3, J_4	integrals defined by equ. (34.10)
K	von Kármán's constant
M	defined by equ. (26.10)
n	constant in equ. (23.2)
N	$\frac{\delta}{D}\cdot\frac{dD}{dx}$
N_1	$G\sqrt{\frac{c_f}{2}}$
N_2	$\Delta/\delta G$
p	$\frac{1}{u_\tau^2}\cdot\frac{dP_1}{dx}$ (in Part II this is equal to $-\frac{u}{u_\tau^2}\cdot\frac{du_1}{dx}$)
P_1	ratio of static pressure to density
$(P-p_0)$	pressure recorded by the Preston tube relative to the static pressure
r	cylindrical co-ordinate measured from the centre line of the pipe

SYMBOLS (continued)

PARTS II and III - Cont.

R_x	Reynolds number, $\frac{x u_1}{\nu}$
R_{δ_2}	Reynolds number, $\frac{\delta_2 u_1}{\nu}$
$S(x)$	$\left(1 + \frac{v_w u_1}{u_\tau^2}\right)^{\frac{1}{2}}$
$S(y/\delta)$, S	universal function of y/δ
$S(1)$, S_1	value of S when $y/\delta = \eta = 1$
t	$\frac{a}{b}$ in section 23
u_τ	friction velocity, $\sqrt{\frac{\tau_w}{\rho}}$
u', v'	components of the velocity fluctuations
u_θ	value of u when $y = \delta_2$
v_r	velocity in the r- direction
$V_1(\xi), V_2(\xi)$	defined by equ. (33.3) and (33.10) respectively
Y	defined by equ. (13.17)
α, β	defined after equ. (23.16)
δ_0	value of y at which $F(y/\delta) = K$
Δ	defined by equ. (31.23)
ξ	$\frac{u_1}{u_\tau}$
η	y/δ
λ	defined by equ. (20.2)
ξ_3	function of x only, equ. (32.7), (33.1) and (34.3)
σ	area of Preston tube opening
τ	total shear stress = the sum of the viscous stress, $\mu \frac{\partial u}{\partial y}$, and the Reynolds stress, $-\rho \overline{u'v'}$.
$\phi(y/\delta)$	function of y/δ only, equ. (25.1)

SYMBOLS
(continued)

PARTS II and III - Cont.

$\overline{(\,)}$	time averaged mean value
$(\,)^*$	values which were obtained from the 'law of the wall equation' as described in section 21

Subscripts:

a	conditions at a 'transition point' between the logarithmic region and the sublayer region.
o	conditions when the blowing velocity is zero at the same R_x
ε	value determined from the experiments (from momentum traverses)

1. Introduction

In order to predict the skin friction or the heat transfer at the surface of a body moving through the atmosphere, it is essential to know the behaviour of the boundary layer over the body. The growth of a laminar boundary layer may be controlled by applying suction through a permeable surface or through discrete slots in the surface in order to prevent separation or delay transition to turbulent flow with its associated high skin friction. It may be necessary to heat a surface to prevent icing or alternatively to cool the surface to prevent it from reaching high temperatures. The high temperatures at high Mach numbers are due to the conversion of kinetic energy into heat energy by the shear stresses in the boundary layer. An effective method of cooling heated bodies is to inject a gas through a porous wall into the boundary layer, thus modifying the velocity and temperature profiles at the surface. A very small velocity through a porous surface has a significant effect on the boundary layer skin friction and heat transfer rates. Velocities of the order of 0·001 of the free stream velocity, injected into a laminar boundary layer can reduce the heat transfer rates by as much as 50%.

The present work falls easily into three parts. In Part I the laminar boundary layer is discussed and an approximate solution to the compressible laminar boundary layer equations with suction or injection is obtained. Part II deals with the incompressible turbulent boundary layer over porous surfaces through which there is a small suction or injection velocity. An experiment on a porous cylinder in axisymmetric flow reveals two laws for the inner and outer regions of turbulent boundary layers; laws which are shown to correlate the mean flow and the shear stress distributions in turbulent boundary layers in small pressure gradients, at separation or reattachment, and with suction or injection. The laws reduce to the well known 'law of the wall' and 'velocity defect law' when the suction or injection velocity and the pressure gradient are zero. In Part III an experiment in fully

developed turbulent pipe flow, when there is suction through a porous section of the pipe, is described and the results are compared with theory.

No attempt is made to evaluate the overall effect on aircraft performance and nowhere in the analysis has any account been taken of the pump power required and the duct losses associated with suction or injection installations. The stability of the laminar boundary layer is not considered although it is to be expected that injection will cause an earlier transition to turbulent flow.

PART I

LAMINAR BOUNDARY LAYERS OVER POROUS SURFACES WITH SUCTION OR INJECTION

2. Introduction

There are few exact solutions to the partial differential equations describing the laminar boundary layer over a porous surface, and these are for special cases such as the flow far from the leading edge of a flat plate with uniform suction. A few approximate analytical solutions have been published and several numerical solutions. However, in the solutions the normal velocity distributions at the wall have been severely limited by the transformations used. In the present theory, an extension of Lilley's method (1959) is used to obtain approximate solutions when there are arbitrary distributions of the normal velocity at the wall, the free stream velocity, and the wall temperature. Lilley considers boundary layers over solid surfaces and uses the Stewartson (1949) and Illingworth (1949) transformation together with the method of Lighthill (1950). Lighthill replaces a velocity in the boundary layer equations by its form near to the wall and quite accurate solutions for the skin friction and wall heat transfer rates are obtained, thus showing that the skin friction and heat transfer depend to a large extent on the local conditions near to the wall.

Illingworth (1954) has extended Lighthill's method to deal with variable freestream and wall temperature distributions in a compressible flow when both the Prandtl number, σ, and the viscosity-temperature index, ω, are equal to unity. Lilley assumes the viscosity to be proportional to the temperature across the boundary layer, but introduces a more accurate wall viscosity-temperature relationship and is able to include an arbitrary Prandtl number, which is, however, not too small compared with unity.

The present theory gives two integral equations, one for the skin friction and one for the heat transfer rate. In order to estimate

the accuracy of these equations, solutions are obtained and compared with those of Donoughe and Livingood (1954), Iglisch (1949), Lew and Fanucci (1955) and Low (1955). The accuracy of the integral equations is of the same order as that of Lighthill's equations which were for an impermeable wall.

In the following sections the methods for calculating incompressible and compressible laminar boundary layers with suction or injection through a permeable wall will be summarised before the new theory is outlined.

Chapter 1
A Review of Previous Work

3. The incompressible laminar boundary layer

The normal velocity at the wall, v_w, is considered to be very small so that the Navier-Stokes equations reduce to the usual boundary layer equations. For a perfect gas the equations of continuity, momentum, and energy for a steady laminar incompressible boundary layer flow in two dimensions, using the coordinate system shown in figure 1, are

$$\frac{\partial u}{\partial x} + \frac{\partial v}{\partial y} = 0 , \tag{3.1}$$

$$u \frac{\partial u}{\partial x} + v \frac{\partial u}{\partial y} = \frac{\mu}{\rho} \frac{\partial^2 u}{\partial y^2} - \frac{1}{\rho} \frac{\partial p}{\partial x} \tag{3.2}$$

and

$$u \frac{\partial T}{\partial x} + v \frac{\partial T}{\partial y} = \frac{\mu}{\rho c_p} \left(\frac{\partial u}{\partial y} \right)^2 + \frac{\mu}{\rho \sigma} \frac{\partial^2 T}{\partial y^2} . \tag{3.3}$$

u is the velocity in the x-direction which is in the direction of the free stream, v is the velocity in the y-direction normal to the surface, c_p is the specific heat at constant pressure, ρ is the density, μ is the viscosity, p is the static pressure and T is the temperature. The subscripts $_\infty$ and $_w$ will be used to denote free stream and wall conditions respectively. The boundary conditions are

$u = 0$ and $v = v_w(x)$ when $y = 0$,

and $u \longrightarrow u_1$ as $y \longrightarrow \infty$.

The simplest example of viscous flow over a porous surface with suction is that of a uniform stream over a semi-infinite flat plate far downstream of the leading edge. The velocity component, v, is everywhere constant and the 'asymptotic suction velocity profile' is given by

$$\frac{u}{u_1} = 1 - \exp\left(\frac{v_w y}{\nu}\right). \tag{3.4}$$

(A suction velocity corresponds to a negative value of v_w.) The solution (Griffith and Meredith 1936) is an exact solution of the Navier-Stokes equations. The corresponding axisymmetric solution for flow along an infinite circular cylinder has been found by Wuest (1955).

The boundary layer partial differential equations may be transformed to ordinary differential equations for flow over infinite wedges, that is flow in which the free-stream velocity and the difference between the wall and the stream temperatures are proportional to powers of the distance from the leading edge, i.e.

$$u_1 = c x^m \quad \text{and} \quad T_w - T_1 = B_1 x^\varepsilon \tag{3.5}$$

where c, m, B_1 and ε are constants. Flow satisfying these conditions is generally termed 'wedge type flow' or 'similarity flow'. The following transformations (Donoughe and Livingood 1954) are introduced

$$\eta = y\sqrt{\frac{u_1}{\nu x}}, \quad \mathcal{T} = \frac{T - T_1}{T_w - T_1} \quad \text{and} \quad f = \frac{\psi}{\sqrt{\nu x u_1}} \tag{3.6}$$

where η is the independent variable of Blasius and $\mathcal{T}$ and f are dependent variables representing the temperature and the stream function, ψ, for which $u = \frac{\partial \psi}{\partial y}$ and $v = -\frac{\partial \psi}{\partial x}$. The momentum and energy equations now reduce to the ordinary differential equations

$$f''' = m(f')^2 - \frac{m+1}{2} f f'' - m, \tag{3.7}$$

and

$$\mathcal{T}'' = -\frac{(m+1)}{2} \sigma f \mathcal{T}' + \varepsilon \sigma f' \mathcal{T}, \tag{3.8}$$

which were solved numerically for the skin friction and the heat transfer rates by Donoughe and Livingood when there is a blowing velocity through the wall and by Koh and Hartnett (1961) when there is suction. A summary of the earlier solutions for wedge type flow is given by Livingood and Donoughe (1955).

Solutions for wedge-type flow have been used as a first approximation in calculations of local heat transfer coefficients to bodies of arbitrary cross section (Eckert and Livingood 1953 and Staniforth 1951). In wedge-type flow the distribution of the blowing velocity, V_w, is limited to one of the form, $V_w \propto x^{\frac{m-1}{2}}$, which implies an infinite value of V_w at the leading edge of a flat plate (where $m=0$), which is contrary to the boundary layer approximations.

Iglisch (1949) obtained an exact solution for a uniform free-stream over a flat plate through which there is a constant suction velocity. The boundary layer equations were transformed to a non-linear second order parabolic equation which reduces to the Blasius form at the leading edge of the plate. Iglisch used an iterative process to calculate the velocity profiles along the plate and showed that the profiles approach the asymptotic form (equation 3.4) as $x \to \infty$. Approximate solutions to the same problem have been given by Schlichting (1942), Thwaites (1952) and Curle (1960). The experimental results of Kay (1952) and Head (1955) for a boundary layer over a flat plate with distributed suction are in agreement with Iglisch's theory.

Integral methods have been used in which a velocity profile, satisfying certain boundary conditions, is substituted into the momentum or energy integral equations, which may be derived as follows: the continuity equation (3.1) is multiplied by $\frac{u^{r+1}}{r+1}$ and added to the momentum equation (3.2) multiplied by u^r, and the resulting equation is integrated from the wall to the outer edge of the boundary layer. Thus (Wuest 1961)

$$\frac{1}{u_1^{r+1}} \frac{d}{dx}\left(u_1^{r+2} f_r\right) + \frac{g_r}{u_1} \frac{du_1}{dx} - \frac{v_w}{u_1} = \varrho_r \,, \qquad (3.9)$$

where $$f_r = \int_0^{\delta} \frac{u}{u_1}\left(1 - \left(\frac{u}{u_1}\right)^{r+1}\right) dy \,, \tag{3.10}$$

$$g_r = -(r+1)\int_0^{\delta} \frac{u}{u_1}\left(1 - \left(\frac{u}{u_1}\right)^{r-1}\right) dy \tag{3.11}$$

and $$e_r = -(r+1)\int_0^{\delta} \left(\frac{u}{u_1}\right)^r \frac{\partial}{\partial y}\left(\frac{\tau}{\rho u_1^2}\right) dy \,. \tag{3.12}$$

When $r=0$, equation (3.9) reduces to von Kármán's momentum integral equation,

$$\frac{1}{u_1^2}\frac{d}{dx}\left(u_1^2 \delta_2\right) + \frac{\delta_1}{u_1}\frac{du_1}{dx} - \frac{v_w}{u_1} = \frac{\tau_w}{\rho u_1^2} \,, \tag{3.13}$$

where $\delta_2 = f_0$ is the momentum thickness and $\delta_1 = g_0$ is the displacement thickness. When $r=1$ equation (3.9) reduces to the energy integral equation

$$\frac{1}{u_1^3}\frac{d}{dx}\left(u_1^3 \varepsilon\right) - \frac{v_w}{u_1} = \frac{2d}{\rho u_1^3} \tag{3.14}$$

where $\varepsilon = f_1$ is the energy thickness and $\mathcal{D}_1 = \frac{2d}{\rho u_1^3}$ is a dissipation term.

The integral methods which have been developed usually depend upon satisfying one or more of the integral equations (3.9) and a limited number of boundary conditions. The boundary conditions at the outer edge of the boundary layer are

$$u = u_1 \,, \quad y = \delta \qquad \text{and} \qquad \frac{\partial^n u}{\partial y^n} = 0$$

and the so-called compatibility conditions at the wall, where

$$u = 0 \,, \quad v = v_w \qquad \text{and} \qquad \tau_w = \mu\left(\frac{\partial u}{\partial y}\right)_w \,, \quad \text{are}$$

$$-v_w\left(\frac{\partial u}{\partial y}\right)_w = -\frac{1}{\rho}\frac{dp}{dx} + \nu\left(\frac{\partial^2 u}{\partial y^2}\right)_w \tag{3.15}$$

and $$-v_w\left(\frac{\partial^2 u}{\partial y^2}\right)_w = \nu\left(\frac{\partial^3 u}{\partial y^3}\right)_w \,. \tag{3.16}$$

Further compatibility equations may be derived by differentiating the momentum equation and finding the limit as $y \to 0$.

For flow over a solid surface it is possible to choose a polynomial in y/δ and evaluate the coefficients by satisfying certain boundary conditions. In this way a singly infinite set of velocity

profiles is obtained (Pohlhausen 1921), so that for a particular value of, for example, the form parameter, $H(=\frac{\delta_1}{\delta_2})$, only one profile will exist. Unfortunately this is not possible for flow over a porous surface because the same value of the form parameter can correspond to any number of combinations of the pressure gradient and the blowing or suction velocity. In other words a doubly infinite set of velocity profiles is really required.

Head (1961) discusses the various ways in which sets of velocity profiles may be built up by using either polynomials or sets of profiles from known exact solutions. The accuracy of the solution to a particular problem will depend largely on the set of velocity profiles which forms the basis of the method. A doubly infinite set of profiles will usually have a wider application than a singly infinite set.

Head concludes that the prediction of separation, with suction, using methods which depend on a singly infinite family of profiles satisfying the momentum equation and the first compatibility condition (Schlichting 1949, Braslow et al 1951) are not very satisfactory. The doubly infinite family of profiles which satisfy the momentum equation and the first and second compatibility conditions (Jorda 1952, van Ingen 1958) are better than the singly infinite methods but are not as accurate as the methods which satisfy the momentum and energy equations and the first or second compatibility conditions (Head 1957, 1961).

It would be interesting to know the solution to the boundary layer equations when suction is applied through slots in the surface rather than through a porous surface. Rheinboldt (1955) has considered two cases of discontinuous suction on a flat plate, (i) a solid surface followed by a porous section and (ii) one slot some distance after the leading edge. Rheinboldt uses a series expansion for the stream function near the wall which is matched to an asymptotic expansion further from the wall. Rheinboldt has also extended his method to flow around a cylinder with suction after a certain angle.

Finite difference methods have been used by Görtler (1948) and Schröder (1951) and more recently by Smith and Clutter (1963). The fundamental idea of finite difference methods is that of replacing the x-derivatives by finite differences, in order to approximate the partial differential equation by an ordinary differential equation. Care is required to ensure the stability of the numerical methods. The method of Smith and Clutter which is based on the method of Hartree and Womersley (1937), appears to be very powerful and has been used successfully for the case of discontinuous suction considered by Rheinboldt.

4. The compressible laminar boundary layer

If certain simplifying assumptions are introduced regarding μ, ρ and the Prandtl number σ, the compressible equations may be reduced to the incompressible form. If $\sigma = 1$ and $\mu \propto T$ so that $\mu\rho = \mu_1\rho_1$, the compressible form of the momentum equation becomes independent of the energy equation and the skin friction is then independent of the compressibility effects and of the thermal conditions at the wall, just as in the case of the incompressible boundary layer. Thus the ways in which heat transfer and dissipation modify the skin friction, i.e. by thickening the boundary layer and changing the viscosity, exactly cancel. Lew and Fanucci (1955) consider the boundary layer over a flat plate with constant suction under these conditions and reduce the problem to that solved by Iglisch.

Low (1955) has obtained numerical solutions to the momentum and energy equations when the pressure gradient is zero, the Prandtl number is 0·72 and the linear viscosity law holds. The momentum equation reduces to the Blasius form and the energy equation is solved by a method similar to that used by Polhausen (1921) for the compressible energy equation with zero transpiration. Low's solution is for similarity flow in which the normal velocity at the wall is proportional to $x^{-\frac{1}{2}}$.

Young (1948) obtained an exact solution to the compressible boundary layer equations far downstream from the leading edge of a flat plate with uniform suction and with zero heat transfer. Velocity and temperature profiles were evaluated with $\sigma = 0.76$, $\omega = 0.76$ and 1.0, and for various Mach numbers. (ω is defined by $\frac{\mu_1}{\mu} = \left(\frac{T_1}{T}\right)^{\omega}$).

The extension of compressible boundary layer methods of solution, to flow over permeable surfaces, is complicated if the wall temperature is not known, because the transformations which have been used do not transform v in a simple way: the product of the density and the suction or injection velocity is often an essential part of the transformation. However, solutions could probably be obtained if the suction or injection velocity were allowed to change so that $\rho_w v_w$ were of a certain form, implied by the transformation.

Chapter 2

An Approximate Theory for the Compressible Laminar Boundary Layer with Suction or Injection

5. The compressible equations

For a perfect gas the equations of continuity, momentum and energy for a steady laminar compressible boundary layer flow in two-dimensions are (Lilley 1959)

$$\frac{\partial \rho u}{\partial x} + \frac{\partial \rho v}{\partial y} = 0 \quad , \tag{5.1}$$

$$\rho u \frac{\partial u}{\partial x} + \rho v \frac{\partial u}{\partial y} - \rho_1 u_1 \frac{du_1}{dx} = \frac{\partial}{\partial y}\left(\mu \frac{\partial u}{\partial y}\right) \tag{5.2}$$

and $$\rho u \frac{\partial h}{\partial x} + \rho v \frac{\partial h}{\partial y} = \frac{\partial}{\partial y}\left(\frac{\mu}{\sigma} \frac{\partial}{\partial y}\left(h - (1-\sigma)\frac{u^2}{2}\right)\right) , \tag{5.3}$$

where h is the total enthalpy defined by the equation

$$h = i + \frac{u^2}{2} \quad . \tag{5.4}$$

i is the enthalpy.

The boundary conditions to be applied are:

(a) at $y = 0$, $u = 0$, $v = v_w(x)$, $T = T_w(x)$,

$\left(k \frac{\partial T}{\partial y}\right)_w = Q_w(x)$ and $\left(\mu \frac{\partial u}{\partial y}\right)_w = \tau_w(x)$.

(b) at $y \longrightarrow \infty$, $u = u_1(x)$, $T = T_1(x)$ and $\frac{\partial u}{\partial y} = \frac{\partial T}{\partial y} = 0$,

where k is the thermal conductivity, $Q_w(x)$ is the rate of heat transfer per unit area to the wall and $\tau_w(x)$ is the shear stress at the wall.

A stream function, ψ , which satisfies the continuity equation is defined

$$\frac{\rho u}{\rho_0} = \frac{\partial \psi}{\partial y} \quad \text{and} \quad \frac{\rho v}{\rho_0} = -\frac{\partial \psi}{\partial x} \tag{5.5}$$

where the subscript 0 refers to the stagnation conditions in the isentropic flow external to the boundary layer.

If the Stewartson (1949) and Illingworth (1949) transformation is used to change the (x, y) coordinates to (X, Y) coordinates where

$$X = \int_0^x \left(\frac{a_1}{a_0}\right)^{\frac{3\gamma-1}{\gamma-1}} dx, \quad \text{and} \quad Y = \frac{a_1}{a_0} \int_0^y \frac{\rho}{\rho_0} dy, \ , \tag{5.6}$$

the equations of momentum and energy become

$$U \frac{\partial U}{\partial X} + V \frac{\partial U}{\partial Y} = \frac{h}{h_1} U_1 \frac{dU_1}{dX} + \frac{\rho_0}{\rho_1} \nu_0 \frac{\partial}{\partial Y}\left(\frac{\rho \mu}{\rho_0 \mu_0} \frac{\partial U}{\partial Y}\right) \tag{5.7}$$

and $$U \frac{\partial h}{\partial X} + V \frac{\partial h}{\partial Y} = \frac{\rho_0 \nu_0}{\rho_1 \sigma} \frac{\partial}{\partial Y}\left\{\frac{\rho \mu}{\rho_0 \mu_0} \frac{\partial}{\partial Y}\left(h - (1-\sigma)\frac{U^2 a_1^2}{2 a_0^2}\right)\right\}, \tag{5.8}$$

where a is the speed of sound, γ is the ratio of the specific heats,

$$U = \frac{\partial \psi}{\partial Y} \quad \text{and} \quad V = -\frac{\partial \psi}{\partial X} \ . \tag{5.9}$$

During the transformation the following relations were used:

$$a_1^2 + \frac{\gamma-1}{2} u_1^2 = a_0^2 \ , \tag{5.10}$$

$$\left(\frac{a_1}{a_0}\right)^{\frac{3\gamma-1}{\gamma-1}} = \frac{a_1 \rho_1}{a_0 \rho_0} \ , \tag{5.11}$$

$$h = \frac{u^2}{2} + C_p T = \frac{u^2}{2} + \frac{a^2}{\gamma - 1} \quad , \tag{5.12}$$

and $$h_1 = \frac{a_0^2}{\gamma - 1} \quad . \tag{5.13}$$

The relations between $u(x)$ and $U(X)$, $\tau_w(x)$ and $\tau_w(X)$, $v_w(x)$ and $V_w(X)$ and between $Q_w(x)$ and $Q_w(X)$ which are implied by the transformation are:

$$u(x) = U(X) \frac{a_1}{a_0} \quad , \tag{5.14}$$

$$v_w(x) = \frac{\rho_0}{\rho_w} V_w(X) \left(\frac{a_1}{a_0}\right)^{\frac{3\gamma - 1}{\gamma - 1}} \quad , \tag{5.15}$$

$$\tau_w(x) = \tau_w(X) \frac{\mu_w \rho_w}{\mu_0 \rho_0} \left(\frac{a_1}{a_0}\right)^2 \quad \text{where} \quad \tau_w(X) = \mu_0 \left(\frac{\partial U}{\partial Y}\right)_w \quad , \tag{5.16}$$

and $$Q_w(x) = Q_w(X) \frac{k_w \rho_w}{k_0 \rho_0} \left(\frac{a_1}{a_0}\right) \quad \text{where} \quad Q_w(X) = k_0 \left(\frac{\partial T}{\partial Y}\right)_w \quad . \tag{5.17}$$

In the present theory, which follows that of Lilley (1959) but now includes the transpiration velocity, V_w , it is possible to consider a value for σ other than unity but it is not possible to include an arbitrary viscosity-temperature index. However a more accurate wall viscosity-temperature relationship will be included in the analysis. The method is basically the same as that used by Lighthill (1950); the argument being that the skin friction and the heat transfer rate at the wall are determined primarily by the local conditions near the wall, and consequently some of the terms in the equations will be replaced by their values at, or near to the wall. The theory is virtually the first stage of an iterative method in which a first approximation for certain terms is substituted into the equations which are then solved to obtain a more accurate second approximation.

Equations (5.7) and (5.8) can be written

$$U \frac{\partial U}{\partial x} + V \frac{\partial U}{\partial Y} = (1 - S) U_1 \frac{dU_1}{dx} + \nu_0 \frac{\partial}{\partial Y} \left(C \frac{\partial U}{\partial Y} \right) \tag{5.18}$$

and $$U \frac{\partial S}{\partial x} + V \frac{\partial S}{\partial Y} = \frac{\nu_0}{\sigma} \frac{\partial}{\partial Y} \left\{ C \frac{\partial}{\partial Y} \left(S + \frac{1 - \sigma}{2} \frac{U^2 a_1^2}{a_0^2 h_1} \right) \right\} \quad , \tag{5.19}$$

where $$\frac{\mu\rho\rho_0}{\mu_0\rho_0\rho_1} = \frac{\mu T_0}{\mu_0 T} = C(X,Y) = \left(\frac{T}{T_0}\right)^{\omega-1} \tag{5.20}$$

and $$S = 1 - h/h_1 . \tag{5.21}$$

Following the above discussion it will be assumed that C takes its wall value and is therefore a function of X but not of Y.

The momentum and energy equations, which are in terms of the independent variables (X,Y), are transformed to the (X,ψ) coordinates:

$$\left(\frac{\partial z}{\partial x}\right)_\psi = S\frac{dU_1^2}{dX} + \nu_0 U \frac{\partial}{\partial\psi}\left(C(X)\cdot\frac{\partial z}{\partial\psi}\right) , \tag{5.22}$$

and $$\frac{\partial S}{\partial X} = \frac{\nu_0}{\sigma}\frac{\partial}{\partial\psi}\left(C(X)\,U\frac{\partial}{\partial\psi}\left(S + \frac{1-\sigma}{2}\cdot\frac{U^2 a_1^2}{a_0^2 h_1}\right)\right) , \tag{5.23}$$

where $$z = U_1^2 - U^2 . \tag{5.24}$$

These equations which are in Von Mises' form, are for a pseudo-incompressible flow with a density and kinematic viscosity of ρ_0 and ν_0 respectively.

6. The transformed momentum equation

In this section certain approximations will be made to the transformed momentum equation (5.22). The Laplace transform of the resulting equation reduces to a modified Bessel equation which is then solved, and an integral equation for the skin friction is obtained.

A stream function, Φ, is introduced such that

$$\Phi = \psi - \psi_w , \tag{6.1}$$

where $$\psi_w = (\psi)_{Y=0} \quad \text{and} \quad \left(\frac{\partial\psi}{\partial X}\right)_{Y=0} = -V_w = \frac{d\psi_w}{dx} = -\left(\frac{\partial\Phi}{\partial x}\right)_\psi . \tag{6.2}$$

ψ_w is a function of X but is independent of Y.

Hence, using the independent variables (X,Φ), equation (5.22) may be written

$$\left(\frac{\partial z}{\partial X}\right)_\Phi + \left(\frac{\partial z}{\partial\Phi}\right)_x\left(\frac{\partial\Phi}{\partial x}\right)_\psi = S\left(\frac{dU_1^2}{dx}\right) + \nu_0 U C\frac{\partial^2 z}{\partial\Phi^2} . \tag{6.3}$$

If $$\left(\frac{\partial z}{\partial \bar{\Phi}}\right)_x \left(\frac{\partial \bar{\Phi}}{\partial x}\right)_\psi - S\frac{dU_1^2}{dx} = R(x,\bar{\Phi}) = \frac{\partial}{\partial x}\int_0^x R(x',\bar{\Phi})\,dx' \tag{6.4}$$

then, at $\bar{\Phi}=0$, $$\int_0^x R(x',\bar{\Phi})\,dx' = \int_0^x R(x',0)\,dx' \tag{6.5}$$

and, at $\bar{\Phi}=\infty$, $$\frac{\partial^2}{\partial \bar{\Phi}^2}\int_0^x R(x',\bar{\Phi})\,dx' = 0 \tag{6.6}$$

and $$\int_0^x R(x',\bar{\Phi})\,dx' = 0\,, \tag{6.7}$$

since $R(x,\infty)=0$.

Therefore, near $\bar{\Phi}=0$, equation (6.3) may be written approximately

as $$\frac{\partial}{\partial x}G(x,\bar{\Phi}) = \nu_0 UC\,\frac{\partial^2}{\partial \bar{\Phi}^2}G(x,\bar{\Phi})\,, \tag{6.8}$$

where $$G(x,\bar{\Phi}) = z(x,\bar{\Phi}) + \int_0^x R(x',0)\,dx'\,, \tag{6.9}$$

whilst for large values of $\bar{\Phi}$, $G(x,\bar{\Phi})$ has a similar form with

$$G(x,\bar{\Phi}) = z(x,\bar{\Phi}) + \int_0^x R(x',\bar{\Phi})\,dx' \tag{6.10}$$

such that $$G(x,\infty) = 0\,. \tag{6.11}$$

The boundary conditions for $G(x,\bar{\Phi})$ are

as $\bar{\Phi}\longrightarrow\infty$, $G(x,\bar{\Phi})\longrightarrow 0$, , (6.12)

as $x\longrightarrow 0$, $G(x,\bar{\Phi})\longrightarrow 0$, (6.13)

and as $\bar{\Phi}\to 0$, $$G(x,\bar{\Phi}) = U_1^2 - U^2 + \int_0^x\left(\frac{\partial z}{\partial \bar{\Phi}}\right)v_w\,dx' - \int_0^x S(x',0)\frac{dU_1^2}{dx'}\,dx'\,. \tag{6.14}$$

From the definition of S, (equation (5.21)), $$S(x',0) = 1 - \frac{h_w}{h_1}\,, \tag{6.15}$$

therefore

$$G(x,\bar{\Phi}) \underset{\bar{\Phi}\to 0}{=} U_1^2(0) - U^2 + \int_0^x \frac{h_w}{h}\frac{dU_1^2}{dx'}\,dx' + \int_0^x\left(\frac{\partial z}{\partial \bar{\Phi}}\right)v_w\,dx' \tag{6.16}$$

Expressions for U and $\frac{\partial z}{\partial \bar{\Phi}}$ which are accurate near the wall are now substituted into this equation. Following Fage and Falkner (1931), the

expression for the velocity, U, near the wall is

$$U = \frac{\tau_w(x)\, Y}{\mu_o} , \tag{6.17}$$

or since $$\psi = \int_0^Y U dY' = \frac{\tau_w(x)\, Y^2}{2\mu_o} + \psi_w(x) , \tag{6.18}$$

then $$U_{\Phi \to 0} = \left(\frac{2\tau_w(x)}{\mu_o}\, \Phi\right)^{\frac{1}{2}} . \tag{6.19}$$

and $$\left(\frac{\partial \psi}{\partial \Phi}\right)_{\Phi \to 0} = -\frac{2\tau_w(x)}{\mu_o} . \tag{6.20}$$

Thus, equation (6.8) is

$$\frac{\partial}{\partial x} G(x,\Phi) = \sqrt{\frac{2\mu_o \tau_w(x)\, C^2}{\rho_o^2}}\; \Phi^{\frac{1}{2}} \frac{\partial^2}{\partial \Phi^2} G(x,\Phi) \tag{6.21}$$

and the boundary condition at $\Phi \to 0$ is

$$G(x,\Phi)_{\Phi \to 0} = U_1^2(0) + \int_0^x \frac{h_w}{h_1} \frac{dU_1^2}{dx'} dx' - \frac{2\tau_w(x)}{\mu_o}\Phi - \int_0^x \frac{2\tau_w(x) V_w(x)}{\mu_o} dx' \tag{6.22}$$

Using the Laplace transform notation $$\bar{F}(p,\Phi) = \int_0^\infty e^{-pt} F(t,\Phi)\, dt \tag{6.23}$$

and the condition $\bar{G} = 0$ when $t = 0$, equation (6.21) may be written

$$p\bar{G} = \Phi^{\frac{1}{2}} \frac{\partial^2 \bar{G}}{\partial \Phi^2} , \tag{6.24}$$

where $$t = \int_0^x \left(\frac{2\mu_o}{\rho_o^2}\, \tau_w(x')\, C^2\right)^{\frac{1}{2}} dx' . \tag{6.25}$$

Equation (66) of Lighthill's paper (1950) is similar to the Bessel equation (6.24) and both satisfy similar boundary conditions. The solution of equation (6.24) is thus

$$\bar{G} = \left(\tfrac{2}{3} p^{\frac{1}{2}}\right)^{2/3} \Gamma\left(\tfrac{1}{3}\right) \bar{G}_{\Phi=0}\; \Phi^{\frac{1}{2}}\, I_{-\frac{2}{3}}\left(\tfrac{4}{3} p^{\frac{1}{2}} \Phi^{\frac{3}{4}}\right) +$$

$$\left(\tfrac{2}{3} p^{\frac{1}{2}}\right)^{-\frac{2}{3}} \Gamma\left(\tfrac{5}{3}\right) \left(-2\frac{\overline{\tau_w(t)}}{\mu_o}\right) \Phi^{\frac{1}{2}}\, I_{\frac{2}{3}}\left(\tfrac{4}{3} p^{\frac{1}{2}} \Phi^{\frac{3}{4}}\right) . \tag{6.26}$$

where $$G_{\Phi=0} = U_1^2(0) + \int_0^x \frac{h_w}{h_1} dU_1^2 + \int_0^x -\frac{2\tau_w(x') V_w(x')}{\mu_o} dx' , \tag{6.27}$$

and $I_{-\frac{2}{3}}(\_)$ and $I_{\frac{2}{3}}(\_)$ are modified Bessel functions of the first kind. Now $\bar{G} \to 0$ as $\Phi \to \infty$, therefore, from the properties of Bessel functions, the coefficients of $I_{-\frac{2}{3}}$ and $I_{\frac{2}{3}}$ must be equal and opposite. Hence

$$\overline{G}_{\Phi=0} = \frac{3^{\frac{4}{3}}\,\Gamma(\frac{5}{3})}{2^{\frac{1}{3}}\,\Gamma(\frac{1}{3})\mu_0}\, p^{-\frac{2}{3}}\,\overline{\tau_w(t)} \,. \tag{6.28}$$

This equation is inverted by the Convolution Theorem to give

$$U_1^2(0) + \int_0^x \frac{h_w(x')}{h_1}\,\frac{dU_1^2(x')}{dx'}\,dx' - \frac{2}{\mu_0}\int_0^x \tau_w(x')\,v_w(x')\,dx' =$$

$$\frac{3^{\frac{1}{3}}\,2}{\Gamma(\frac{1}{3})(\rho_0\mu_0)^{\frac{2}{3}}}\int_0^x C(x')\,\tau_w(x')^{3/2}\left(\int_{x'}^x \left(\tau_w(\bar{z})^{\frac{1}{2}}\,C(\bar{z})\,d\bar{z}\right)^{-\frac{1}{3}} dx' \,. \tag{6.29}$$

This is the integral equation for the skin friction in the pseudo-incompressible flow.

7. The transformed energy equation

If the expression for U in equation (5.14) is substituted into the equation for the total enthalpy (equ. 5.12) then

$$h_1 = \left(1 + \frac{\gamma-1}{2a_0^2}\,U_1^2\right)\frac{a_1^2}{\gamma-1} \tag{7.1}$$

Therefore the transformed energy equation (5.23) can be written

$$\frac{\partial S}{\partial x} - \frac{\nu_0}{\sigma}\,C\,\frac{\partial}{\partial\psi}\left(U\,\frac{\partial S}{\partial\psi}\right) = -\frac{(1-\sigma)}{\sigma\,U_1^2}\,\nu_0 C\left(\frac{\frac{\gamma-1}{2a_0^2}\,U_1^2}{1+\frac{\gamma-1}{2a_0^2}\,U_1^2}\right)\frac{\partial}{\partial\psi}\left(U\,\frac{\partial z}{\partial\psi}\right) \tag{7.2}$$

When $\sigma = 1$ the right hand side of this equation is zero. For other values of σ the expressions for U and $\frac{\partial z}{\partial\psi}$ from the solution of the momentum equation could be substituted into the right hand side and the method of variation of parameters could be used to find the complete solution of the equation. Bernard Le Fur (1959) solved the equation in this way for incompressible flow and thus found the heat transfer correction term to allow for the recovery enthalpy. However for incompressible flow the right hand side, which represents the frictional heating term, is usually neglected.

For simplicity, the full solution will not be found in this way. As a first approximation it will be assumed that the changes in U and C between the cases of heat transfer and zero heat transfer are negligible. This is the method used by Lilley (1959), and quite satisfactory solutions were obtained.

The boundary conditions for S are $S(x,\infty)=0$ and $S\to 0$ as $x\to 0$. Near to the wall, S has the form

$$S_{\psi\to 0} = 1 - \frac{h_w}{h_1} + \sigma \frac{Q_w(x)}{h_1}\sqrt{\frac{2\Phi}{\mu_0 \tau_w(x)}}, \tag{7.3}$$

where $Q_w(x)$ is the rate of heat transfer to the wall, $\left(Q_w(x) = k_0\left(\frac{\partial T}{\partial Y}\right)_w\right)$. Equation (7.3) is derived by writing the total enthalpy in the form

$$h_{\psi\to 0} = h_w + Y C_p \left(\frac{\partial T}{\partial Y}\right)_w, \tag{7.4}$$

and substituting the expression for Y from equation (6.18).

If $S_0(x,\psi)$ is the complete solution of equation (7.2) when there is zero heat transfer, and $S(x,\psi)$ is the solution with heat transfer, then $S_1(x,\psi)$ (which is defined $S_1 = S - S_0$) is the solution of the equation

$$\frac{\partial S_1}{\partial x} = \frac{\nu_0}{\sigma} C \frac{\partial}{\partial \psi}\left(U \frac{\partial S_1}{\partial \psi}\right). \tag{7.5}$$

S_1 satisfies the boundary conditions

$$S_1 \to 0 \quad \text{as} \quad \psi \to \infty \quad \text{and as} \quad x \to 0,$$

and $$S_1 = \frac{h_{w_0}(x) - h_w(x)}{h_1} + \frac{\sigma Q_w(x)}{h_1}\sqrt{\frac{2\Phi}{\mu_0 \tau_w(x)}} \tag{7.6}$$

as $\Phi\ (=\psi-\psi_w) \to 0$. h_{w_0} is the wall enthalpy with zero heat transfer.

Equation (7.5) in terms of the coordinates (x, Φ) is

$$\left(\frac{\partial S_1}{\partial \Phi}\right)_x v_w + \frac{\partial S_1}{\partial x} = \frac{\nu_0}{\sigma} C(x) \frac{\partial}{\partial \Phi}\left(U \frac{\partial S_1}{\partial \Phi}\right), \tag{7.7}$$

which will be solved by a similar method to that used for the momentum equation: the forms for U and $\frac{\partial S_1}{\partial \Phi}$, which are accurate near the wall, will be substituted into equation (7.7). Now equation (6.19) is

$$U_{\Phi \to 0} = \sqrt{\frac{2\tau_w(x)}{\mu_0}}\, \Phi^{\frac{1}{2}} + O[\Phi] \tag{7.8}$$

and from equation (7.6),

$$\left(\frac{\partial S_1}{\partial \Phi}\right)_{\Phi \to 0} = \frac{\sigma Q_w(x)}{h_1}\sqrt{\frac{2}{\mu_0 \tau_w(x)}}\, \frac{1}{2}\Phi^{-\frac{1}{2}}, \tag{7.9}$$

therefore equation (7.7) may be written

$$\frac{\sigma V_w Q_w}{h_1}\sqrt{\frac{1}{2\mu_0 \tau_w(x)}}\cdot \Phi^{-\frac{1}{2}} + \frac{\partial S_1}{\partial x} = \frac{\nu_0}{\sigma} C \sqrt{\frac{2\tau_w(x)}{\mu_0}}\, \frac{\partial}{\partial \Phi}\left(\Phi^{\frac{1}{2}} \frac{\partial S_1}{\partial \Phi}\right). \tag{7.10}$$

If $$t = \int_0^x \frac{C}{\rho_0 \sigma}\sqrt{2\mu_0 \tau_w(z)}\, dz \tag{7.11}$$

and $$F_1(x) = -\frac{\sigma^2 V_w Q_w \rho_0}{h_1 C 2\mu_0 \tau_w} \tag{7.12}$$

then equation (7.10) simplifies to

$$\Phi^{-\frac{1}{2}} F_1(t) = \frac{\partial S_1}{\partial t} - \frac{\partial}{\partial \Phi}\left(\Phi^{\frac{1}{2}} \frac{\partial S_1}{\partial \Phi}\right), \tag{7.13}$$

or in the Laplace transform notation (equ. 6.23)

$$\overline{F_1(p)}\cdot \Phi^{-\frac{1}{2}} = p\bar{S}_1 - \frac{\partial}{\partial \Phi}\left(\Phi^{\frac{1}{2}} \frac{\partial \bar{S}_1}{\partial \Phi}\right). \tag{7.14}$$

The homogeneous form of this Bessel equation is equivalent to equation (21) in Lighthill's paper and has the solution

$$\bar{S}_1 = a_2 \Phi^{\frac{1}{4}} I_{-\frac{1}{3}}\left(\frac{4}{3} p^{\frac{1}{2}} \Phi^{\frac{3}{4}}\right) + b_2 \Phi^{\frac{1}{4}} I_{\frac{1}{3}}\left(\frac{4}{3} p^{\frac{1}{2}} \Phi^{\frac{3}{4}}\right) \tag{7.15}$$

where a_2 and b_2 must be determined from the boundary conditions.

The complete solution of equation (7.14) will now be found by the method of variation of parameters (see for example Piaggo 1952).

A solution is assumed to be

$$\bar{S}_1 = P(\bar{\Phi})\bar{S}_2 + Q(\Phi).\bar{S}_3 \tag{7.16}$$

where $$\bar{S}_2 = \bar{\Phi}^{\frac{1}{4}} I_{-\frac{1}{3}}(q), \tag{7.17}$$

$$\bar{S}_3 = \bar{\Phi}^{\frac{1}{4}} I_{\frac{1}{3}}(q) \tag{7.18}$$

and $$q = \frac{4}{3} p^{\frac{1}{2}} \bar{\Phi}^{\frac{3}{4}}. \tag{7.19}$$

The equations to determine P and Q are

$$\frac{dP}{d\bar{\Phi}} = - \frac{\bar{S}_3 \bar{\Phi}^{-1} \bar{F}_1}{\bar{S}_2' \bar{S}_3 - \bar{S}_3' \bar{S}_2} \tag{7.20}$$

and $$\frac{dQ}{d\bar{\Phi}} = \frac{\bar{S}_2 \bar{\Phi}^{-1} \bar{F}_1}{\bar{S}_2' \bar{S}_3 - \bar{S}_3' \bar{S}_2}, \tag{7.21}$$

where the prime indicates a differential with respect to $\bar{\Phi}$. From equations (7.17) and (7.18)

$$\bar{S}_2' \bar{S}_3 - \bar{S}_3' \bar{S}_2 = \bar{\Phi}^{\frac{1}{2}} \left\{ I_{\frac{1}{3}}(q)\, I'_{-\frac{1}{3}}(q) - I_{-\frac{1}{3}}(q).\, I'_{\frac{1}{3}}(q) \right\}. \tag{7.22}$$

Now the Wronskian, $W\left(I_{\frac{1}{3}}(\xi), I_{-\frac{1}{3}}(\xi)\right)$ $\left(= I_{\frac{1}{3}}(\xi) I'_{-\frac{1}{3}}(\xi) - I'_{\frac{1}{3}}(\xi).\, I_{-\frac{1}{3}}(\xi)\right)$

is equal to $-\frac{2}{\xi\pi} \sin\frac{\pi}{3}$ (Erdélyi 1953), and therefore

$$\bar{S}_2' \bar{S}_3 - \bar{S}_3' \bar{S}_2 = -\bar{\Phi}^{1/2} \left\{ \frac{3}{2\pi\bar{\Phi}} \sin\frac{\pi}{3} \right\}. \tag{7.23}$$

Equations (7.20) and (7.21) may now be written

$$P = \int^{\bar{\Phi}} \left(\frac{\bar{F}_1 2\pi}{3 \sin \pi/3} \right). I_{\frac{1}{3}}(q).\, \bar{\Phi}^{-\frac{1}{4}}\, d\bar{\Phi} \tag{7.24}$$

and $$Q = -\int^{\bar{\Phi}} \left(\frac{\bar{F}_3 2\pi}{3 \sin \pi/3} \right) I_{-\frac{1}{3}}(q)\, \bar{\Phi}^{-\frac{1}{4}}\, d\bar{\Phi}. \tag{7.25}$$

The complete solution of equation (7.14) is obtained by substituting (7.17), (7.18), (7.24) and (7.25) into equation (7.16). Thus

$$\bar{S}_1(p,\Phi) = \Phi^{\frac{1}{4}} I_{-\frac{1}{3}}(q)\left(\frac{2\pi \bar{F}_1}{3\sin\pi/3}\right)\int_0^{\Phi} I_{\frac{1}{3}}(q)\,\Phi^{-\frac{1}{4}}\,d\Phi + \Phi^{\frac{1}{4}} I_{\frac{1}{3}}(q)\,B(p) -$$

$$\Phi^{\frac{1}{4}} I_{\frac{1}{3}}(q)\left(\frac{2\pi \bar{F}_1}{3\sin\pi/3}\right)\int_0^{\Phi} I_{-\frac{1}{3}}(q)\,\Phi^{-\frac{1}{4}}\,d\Phi + \Phi^{\frac{1}{4}} I_{-\frac{1}{3}}(q)\,A(p), \qquad (7.26)$$

where $A(p)$ and $B(p)$ are to be found from the boundary conditions. As $\Phi \to \infty$ then $\bar{S}_1 \to 0$, therefore from the properties of modified Bessel functions, the coefficients of $I_{\frac{1}{3}}$ and $I_{-\frac{1}{3}}$ must be equal and opposite. Hence

$$\frac{2\pi \bar{F}_1 p^{-\frac{1}{2}}}{3\sin\pi/3}\int_0^{\infty}\left(I_{\frac{1}{3}}(q) - I_{-\frac{1}{3}}(q)\right)dq + A + B = 0$$

$$\text{or} \quad -\frac{4}{3}\bar{F}_1 p^{-\frac{1}{2}}\int_0^{\infty} K_{\frac{1}{3}}(q)\,dq + A + B = 0 \qquad (7.27)$$

where $K_{\frac{1}{3}}(q)$ is a modified Bessel function of the second kind. From Erdélyi (1954 c) the integral,

$$\int_0^{\infty} K_{\nu}(\beta c)\,c^{\alpha-1}\,dc = 2^{\alpha-2}\beta^{-\alpha}\Gamma\left(\tfrac{1}{2}\alpha + \tfrac{1}{2}\nu\right)\Gamma\left(\tfrac{1}{2}\alpha - \tfrac{1}{2}\nu\right),$$

providing $(\alpha \mp \nu) > 0$ and $\beta > 0$, and therefore equation (7.27) reduces to

$$-\frac{2}{3}\Gamma\left(\tfrac{2}{3}\right)\Gamma\left(\tfrac{1}{3}\right)p^{-\frac{1}{2}}\bar{F}_1 + A + B = 0 \quad . \qquad (7.28$$

The boundary conditions at the wall are:

$$\Phi = 0 \quad , \quad S_1 = \frac{h_{wo}(x) - h_w(x)}{h_1} = F_2 \qquad (7.29)$$

and $$\Phi^{\frac{1}{2}}\frac{\partial S_1}{\partial \Phi} = \frac{\sigma Q_w}{h_1}\sqrt{\frac{1}{2\mu_o \tau_{w(x)}}} = F_3 \; . \qquad (7.30)$$

(F_2 and F_3 are defined by these equations). As $\Phi \to 0$ equation (7.26) reduces to

$$\bar{S}_1(p,\Phi) = A\left(\frac{3}{2}\right)^{\frac{1}{3}} \frac{p^{-\frac{1}{6}}}{\Gamma(\frac{2}{3})} ,$$

and its differential with respect to Φ reduces to

$$\Phi^{\frac{1}{2}} \frac{\partial \bar{S}_1}{\partial \Phi} = B\left(\frac{3}{2}\right)^{\frac{2}{3}} \frac{p^{\frac{1}{6}}}{\Gamma(\frac{1}{3})}$$

and therefore from the boundary conditions (7.29) and (7.30)

$$A = \left(\frac{2}{3}\right)^{\frac{1}{3}} \Gamma(\tfrac{2}{3})\, p^{\frac{1}{6}}\, \overline{F_2(p)} ,$$

and $$B = p^{-\frac{1}{6}} \Gamma(\tfrac{1}{3}) \left(\tfrac{2}{3}\right)^{\frac{2}{3}} \overline{F_3}(p) .$$

The expressions for A and B are substituted into equation (7.28) which is rearranged to give

$$\bar{F}_3 = \left(\frac{2}{3}\right)^{\frac{1}{3}} \Gamma(\tfrac{2}{3}) p^{-\frac{1}{3}} \bar{F}_1 - \left(\frac{3}{2}\right)^{\frac{1}{3}} \frac{\Gamma(\frac{2}{3})\, p^{\frac{1}{3}} \bar{F}_2}{\Gamma(\frac{1}{3})} . \tag{7.31}$$

By the Convolution Theorem the inverse transform of $p^{\frac{1}{3}}\bar{F}_2$ is

$$p^{\frac{1}{3}}\bar{F}_2 = \frac{1}{\Gamma(\frac{2}{3})} \int_0^t (t-t_1)^{-\frac{1}{3}} \left(\frac{\partial F_2(t_1)}{\partial t_1} + \delta(t_1) F_2(t_1) \right) dt_1 ,$$

where δ is the Delta function (an impulse function). Equation (7.11) is used to transform from the t to the x-coordinate. Thus

$$p^{\frac{1}{3}}\bar{F}_2 = \frac{1}{\Gamma(\frac{2}{3})} (\rho_0 \sigma)^{\frac{1}{3}} (2\mu_0)^{\frac{1}{6}} \int_0^x \left(\int_{x_1}^x C(z)\, \tau_w^{\frac{1}{2}}(z)\, dz \right)^{-\frac{1}{3}} \frac{d}{dx_1} \left(\frac{h_{w_0} - h_w}{h_1} \right) dx_1$$

where the expression is written in Stieltjès form for shortness.

Similarly,

$$p^{-\frac{1}{3}}\bar{F}_1 = \frac{\sigma^{5/3} \rho_0^{2/3}}{\Gamma(\frac{1}{3})(2\mu_0)^{2/3}} \int_0^x \left(\int_{x_1}^x C\, \tau_w^{\frac{1}{2}} dz \right)^{-\frac{2}{3}} \frac{v_w Q_w}{h_1 \tau_w^{1/2}}\, dx_1$$

and therefore the inverse transform of equation (3.21) is

$$Q_w(x) = -\frac{\Gamma(\frac{2}{3})\, \sigma^{2/3} \tau_w^{\frac{1}{3}}(x)}{\Gamma(\frac{1}{3})\, (3\rho_0\mu_0)^{1/3}} \int_0^x \left(\int_{x_1}^x C(z)\, \tau_w^{\frac{1}{2}}(z)\, dz \right)^{-\frac{2}{3}} \frac{v_w Q_w \rho_0}{\tau_w^{\frac{1}{2}}}\, dx_1$$

$$- \frac{3^{\frac{1}{3}} \tau_w^{\frac{1}{2}} (\rho_0\mu_0)^{\frac{1}{3}} h_1}{\Gamma(\frac{1}{3})\, \sigma^{\frac{2}{3}}} \int_0^x \left(\int_{x_1}^x C(z) \tau_w^{\frac{1}{2}}(z)\, dz \right)^{-\frac{1}{3}} \frac{d}{dx_1} \left(\frac{h_{w_0} - h_w}{h_1} \right) dx_1 . \tag{7.32}$$

This is the integral equation for the heat transfer rate to the wall in the pseudo-incompressible flow, and it will be discussed in section 10.

8. The incompressible boundary layer

When the flow is incompressible the integral equations for the skin friction (6.29) and the heat transfer rate (7.32) reduce to

$$u_1^2(x) = \frac{2.3^{1/3}}{\Gamma(\frac{1}{3})}(\mu\rho)^{2/3}\int_0^x\left(\int_{x_1}^x \tau_w^{1/2}\,dz\right)^{-\frac{1}{3}}\tau_w^{3/2}\,dx_1 + \frac{2}{\mu}\int_0^x v_w\tau_w\,dx_1 \qquad (8.1)$$

and

$$Q_w(x) = -k\left(\frac{3\sigma\rho}{\mu^2}\right)^{1/3}\frac{\tau_w^{\frac{1}{2}}}{\Gamma(\frac{1}{3})}\int_0^x\left(\int_{x_1}^x \tau_w^{1/2}\,dz\right)^{-1/3}dT_w(x_1) -$$

$$\left(\frac{\sigma^2\rho^2}{3\mu}\right)^{\frac{1}{3}}\frac{\Gamma(\frac{2}{3})}{\Gamma(\frac{1}{3})}\tau_w^{1/2}\int_0^x\left(\int_{x_1}^x \tau_w^{1/2}\,dz\right)^{-2/3}\frac{v_w Q_w}{\tau_w^{1/2}}\,dx_1 \qquad (8.2)$$

where T is the temperature (on a temperature scale with the free stream zero). In obtaining the incompressible equations, it is assumed that μ and ρ are constant, and that the frictional heating term $\frac{\mu}{\rho c_p}\left(\frac{\partial u}{\partial y}\right)^2$, in the energy equation (3.3) is negligible.

8.1 Wedge-type flow

Equations (8.1) and (8.2) will now be compared with the known exact solutions for wedge type flow (Donoughe and Livingood 1954). For similarity or wedge type flow, the free stream velocity, $u_1(x)$, the skin friction, $\tau_w(x)$, the blowing velocity, $v_w(x)$, and the local Nusselt number, $Nu(x)$, may be expressed as powers of x as follows:

$$u_1(x) = c\,x^m, \qquad (8.3)$$

$$\tau_w(x) = K^2 x^{\frac{3m-1}{2}}, \qquad (8.4)$$

$$v_w(x) = G\,x^{\frac{m-1}{2}}, \qquad (8.5)$$

and $$\eta_u(x) = N x^{\frac{m+1+2\varepsilon}{2}}, \tag{8.6}$$

where the local Nusselt number is defined

$$\eta_u(x) = -\frac{Q_w(x).\,x}{k\,T_w} \tag{8.7}$$

and m is the pressure gradient parameter and ε is the wall temperature gradient parameter:

$$\varepsilon = \frac{x}{T_w}\frac{dT_w(x)}{dx} \quad ; \quad T_w(x) = B_1 x^{\varepsilon}. \tag{8.8}$$

(c, K, G, N and B_1 are constants.)

These conditions are the same as those used by Brown and Donoughe (1952), Emmons and Leigh (1953) and Donoughe and Livingood (1954). They are the conditions for similarity between the velocity and temperature profiles when the Prandtl number, $\sigma = 1$.

It is convenient to write the equations in terms of the blowing velocity parameter, f_w , the skin friction parameter, f_w'' , and the Reynolds number, R_e , where

$$f_w = -\frac{2}{m+1}\,v_w(x)\left(\frac{x}{u_1(x).\nu}\right)^{\frac{1}{2}} = -\frac{2}{m+1}\,\frac{v_w}{u_1}\,R_e^{1/2}, \tag{8.9}$$

$$f_w'' = \tau_w(x)\left(\frac{x}{\rho u_1^3/\mu}\right)^{\frac{1}{2}} = \frac{c_f}{2}R_e^{1/2} \tag{8.10}$$

and $$R_e = \frac{x u_1}{\nu}. \tag{8.11}$$

Equations (8.3) to (8.7) are substituted into the integral equations (8.1) and 8.2), and after evaluating the 'Beta type' integrals (Dwight 1960), the equations reduce to

$$1 + \frac{(m+1)}{2m} f_w f_w'' = \frac{2^{7/3}\,(f_w'')^{4/3}\,\Gamma\left(\frac{2}{3}\right)\Gamma\left(\frac{9m+1}{3m+3}\right)}{3^{1/3}(m+1)^{2/3}\,\Gamma\left(\frac{1}{3}\right)\Gamma\left(\frac{11m+3}{3m+3}\right)} \tag{8.12}$$

and $$\eta_u R_e^{-\frac{1}{2}} = \left(\frac{\eta_u R_e^{-\frac{1}{2}}}{f_w''^{\frac{1}{3}}}\right)_{v_w=0}\left(\frac{f_w''^{1/3}}{1 - \frac{D f_w}{f_w''^{1/3}}}\right), \tag{8.13}$$

where $$\left(Nu\, R_e^{-\frac{1}{2}}\right)_{V_w=0} = \frac{2^{4/3}\,\sigma^{1/3} f_w''^{1/3}(m+1)^{-2/3}\,\varepsilon\,\Gamma(\frac{2}{3})\,\Gamma\left(\frac{4\varepsilon}{3(m+1)}\right)}{3^{1/3}\,\Gamma(\frac{1}{3})\,\Gamma\left(\frac{4\varepsilon}{3(m+1)}+\frac{2}{3}\right)} \qquad (8.14)$$

and $$D = \frac{\sigma^{2/3}(m+1)^{2/3}\,\Gamma(\frac{2}{3})\,\Gamma\left(\frac{4\varepsilon}{3(m+1)}+\frac{1}{3}\right)}{3^{2/3}\,2^{1/3}\,\Gamma\left(\frac{4\varepsilon}{3m+3}+\frac{2}{3}\right)} \; . \qquad (8.15)$$

When $V_w = 0$ these equations are identical to those obtained by Lighthill (1950).

If the skin friction parameter, f_w'', is evaluated from equation (8.12) for particular values of f_w and m, and compared with the exact results of Donoughe and Livingood, then quite large errors are apparent ranging from 8% to 24%. One reason for the large error is that it contains the combined errors of the blowing term and the zero blowing term. However an improved solution for f_w'' is obtained if we assume that equation (8.12) is only used to determine $\Delta f_w''$, the difference between the skin friction with blowing and that without blowing, i.e.

$$\Delta f_w'' = \left(f_w''\right)_{\text{FROM EQU. 8.12}} - \left(f_w''\right)_{\text{EQU. 8.12 WHEN } V_w=0} .$$

The variation of the skin friction parameter with pressure gradient and injection parameter, f_w, evaluated in this way, is shown in fig.2. The above correction has been used for these calculations only. It is not used for any of the other solutions. The solution tends to diverge as $m \to 0$. This is due to the similarity condition imposed on V_w, i.e. $V_w = G x^{\frac{m-1}{2}}$, which implies an infinite blowing or suction velocity at the leading edge when the free stream pressure gradient parameter is less than one. The present theory is perfectly well behaved when there are realistic blowing or suction velocity distributions. (This is shown later in this section.)

A more accurate and more satisfactory similarity solution which uses a better approximation for the blowing velocity term in the momentum equation is presented in section 9.

The Nusselt number has been evaluated using equation (8.13) and its variations with different pressure gradients, wall temperature gradients and blowing velocities are shown in figures 3, 4 and 5. During the calculations the exact values obtained by Donoughe and Livingood were used for $\left(\eta_u R_e^{-1/2}\right)_{v_w(x)=0}$ and for f_w''.

Injection through a porous wall modifies the velocity profile by reducing the velocity gradients and the shear stresses. The temperature is coupled to the velocity profile through the convective terms (and the frictional heating term) in the energy equation. Injection reduces the temperature gradients so that the flow near the wall is closer to the wall temperature and the heat transfer rates are reduced. The smaller shear stresses near the wall result in a reduction of the viscous dissipation or the frictional heating and therefore the heat transfer rate to a cool wall would be reduced.

8.2 Uniform free stream and constant blowing velocity

If the momentum equation (8.1) is partially inverted (see Appendix A) then

$$\tau_w(x) = \frac{(\rho\mu)^{2/3}}{\Gamma(\frac{2}{3})\,3^{1/3}} \left\{ -\frac{1}{\mu}\int_0^x \left(\int_{x_1}^x \tau_w^{1/2}\, dz \right)^{-\frac{2}{3}} v_w \tau_w\, dx_1 + \frac{1}{2}\int_0^x \left(\int_{x_1}^x \tau_w^{1/2}\, dz \right)^{-\frac{2}{3}} d\left(u_1^2(x_1)\right) \right\} \tag{8.16}$$

where the last term is a Stieltjès integral and therefore has a value when the free stream velocity, u_1, is constant.

When the blowing velocity, v_w, is zero and there is a uniform free stream, then from equation (8.1) the skin friction is

$$\tau_w(x) = K^2 x^{-\frac{1}{2}} \tag{8.17}$$

and

$$K = \frac{u_1^{3/4}\, 3^{1/3}\, (\mu\rho)^{\frac{1}{4}}}{2^{7/3}\left(\Gamma(\frac{2}{3})\right)^{3/8}} . \tag{8.18}$$

Equation (8.17) will be used as a first approximation to $\tau_w(x)$. On substituting (8.17) into the right hand side of equation (8.16) and integrating, the second approximation for $\tau_w(x)$ becomes

$$(\tau_w)_{\substack{2nd.\\ APPROX.}} = \frac{(\rho\mu)^{2/3}}{\Gamma(\frac{2}{3})3^{\frac{1}{3}}}\left\{-\frac{v_w}{\mu}K^{4/3}\left(\frac{4}{3}\right)^{1/3}\Gamma(\tfrac{1}{3})\Gamma(\tfrac{2}{3}) + \frac{1}{2}c^2K^{-2/3}\left(\frac{3}{4}\right)^{2/3}x^{-1/2}\right\}. \tag{8.19}$$

Now the dimensionless form of the flow through the wall is defined by equation (8.9) as

$$f_w = -\frac{2v_w R_e^{1/2}}{u_1} \qquad \text{where} \quad R_e = \frac{u_1 x}{\nu}$$

and therefore equation (8.19) may be written

$$(\tau_w)_{2nd.\ APPROX} = (1 - Rx^{1/2})K^2x^{-1/2} \tag{8.20}$$

where $Rx^{1/2} = -\dfrac{2^{1/4}\Gamma(\frac{1}{3})\Gamma(\frac{2}{3})^{1/4}}{3^{4/3}} f_w$. (R is not a function of x)

If equation (8.20) were substituted into the right hand side of equation (8.16) and integrated, a third approximation for $\tau_w(x)$ would be found; and if this procedure were continued, an equation for $\tau_w(x)$ of the form

$$\tau_w(x) = K^2x^{-\frac{1}{2}}\left(1 - a_3(Rx^{1/2}) - b_3(Rx^{1/2})^2 \ldots\right)_{|Rx^{1/2}|<1} \tag{8.21}$$

could be obtained.

The first two terms will now be considered and this implies that $Rx^{1/2}$ is small, i.e. the velocity through the wall is small. The equation for $\tau_w(x)$ thus obtained will be compared with the calculations of Iglisch (1949) and Curle (1960).

In order to find the value of a_3 in equation (8.21), the expression for $\tau_w(x)$ will be substituted into the terms on the right hand side of equation (8.16). Three different approximate methods will be used.

OF AERONA... LIBRARY

First Method

$\int_{x_1}^{x} \tau_w^{1/2}\, dz$ will be put equal to $\frac{4}{3}\tau_w(x_1)^{1/2} x_1^{1/4}\left(x^{3/4} - x_1^{3/4}\right)$

which is correct only when $V_w = 0$. On substituting $\tau_w(x) = K^2 x^{-\frac{1}{2}}\left(1 - a_3 R x^{1/2}\right)$ into the integrals of equation (8.16):

$$\int_0^x \left(\int_{x_1}^{x} \tau_w^{\frac{1}{2}} dz\right)^{-\frac{2}{3}} V_w \tau_w dx_1 \simeq V_w\left(\frac{4}{3}\right)^{\frac{1}{3}} K^{4/3}\left\{\Gamma\left(\tfrac{1}{3}\right)\Gamma\left(\tfrac{2}{3}\right) - \tfrac{1}{3} a_3 \frac{R x^{1/2}\Gamma^2\left(\tfrac{1}{3}\right)}{\Gamma\left(\tfrac{2}{3}\right)}\right\} \quad (8.22)$$

and $\frac{\varepsilon^2}{2}\left(\int_0^x \tau_w^{1/2} dz\right)^{-\frac{2}{3}} \simeq \frac{c^2}{2}\left(\frac{3}{4}\right)^{\frac{2}{3}} K^{-\frac{2}{3}} x^{-\frac{1}{2}}\left(1 + \tfrac{1}{3} a_3 R x^{1/2} \ldots\right)$. (8.23)

Hence on substituting (8.22) and (8.23) into (8.16) then

$$\tau_w(x) = K^2 x^{-\frac{1}{2}}\left(1 + \left(\tfrac{1}{3} a_3 - 1\right) R x^{1/2} \ldots\right). \quad (8.24)$$

Therefore from (8.21) and (8.24) $a_3 = 3/4$ and so

$$\tau_w(x) = K^2 x^{-\frac{1}{2}}\left(1 - \tfrac{3}{4} R x^{1/2} \ldots\right). \quad (8.25)$$

Second Method

If the approximation which Lighthill (1950) suggested is used, i.e.

$$\int_{x_1}^{x} \tau_w^{\frac{1}{2}} dz \simeq (x - x_1)\,\tau_w^{\frac{1}{2}} \quad (8.26)$$

then from equation (8.16), the value of $\tau_w(x)$ when $V_w = 0$ is modified to

$$\tau_w(x) = K_1^2 x^{-\frac{1}{2}}, \quad (8.27)$$

where $$K_1 = \frac{\mu_1^{3/4}(\mu\rho)^{\frac{1}{4}}}{2^{3/8}\left(\Gamma\left(\frac{2}{3}\right)\right)^{3/8}}, \quad (8.28)$$

and equation (8.21) is modified to

$$\tau_w(x) = K_1^2 x^{-\frac{1}{2}}\left(1 - a_4\left(R_1 x^{1/2}\right) \ldots\right), \quad (8.29)$$

where $R_1 x^{\frac{1}{2}} = -\dfrac{\Gamma(\frac{1}{3})\Gamma^{\frac{1}{4}}(\frac{2}{3})\, f_w}{2^{3/4}\, 3^{1/4}} = -1.31\, f_w$. (8.30)

Equation (8.29) is substituted into equation (8.16). Thus

$$\tau_w = K_1^2 x^{-\frac{1}{2}}\left(1 + \tfrac{1}{3}(a_4 - 1) R_1 x^{1/2} \ldots\right)$$

and so from equation (8.29)

$$\tau_w = K_1^2 x^{-\frac{1}{2}}\left(1 - \tfrac{3}{4} R_1 x^{1/2} \ldots\right) . \qquad (8.31)$$

Third Method

In the first and second methods the approximations were used to evaluate both terms on the right hand side of equation (8.16). The second term can however be evaluated without using an approximation. The expression which is obtained in place of (8.23) is

$$\frac{c^2}{2}\left(\frac{3}{4}\right)^{2/3} K^{-\frac{2}{3}} x^{-\frac{1}{2}}\left(1 + \tfrac{1}{5} a_3 R x^{\frac{1}{2}} \ldots\right) \qquad (8.32)$$

and the final equation for $\tau_w(x)$ is given by

$$\tau_w(x) = K^2 x^{-\frac{1}{2}}\left(1 - \tfrac{5}{6} R x^{\frac{1}{2}} \ldots\right) . \qquad (8.33)$$

In order to compare equations (8.25), (8.31) and (8.33) with previous work, the function ξ is introduced such that

$$\xi = \frac{V_w^2 x}{(u_1 \nu)} . \qquad (8.34)$$

From equation (8.20) $R x^{1/2} = 3\xi^{\frac{1}{2}}$, and from equation (8.30) $R_1 x^{1/2} = 2.62\, \xi^{1/2}$. Therefore equation (8.25) is

$$\frac{\tau_w(x)}{K^2 x^{-\frac{1}{2}}} = 1 + 2.25\, \xi^{1/2} \qquad |\xi| < \tfrac{1}{3} , \qquad (8.35)$$

equation (8.31) is $\dfrac{\tau_w(x)}{K_1^2 x^{-\frac{1}{2}}} = 1 + 1.96\, \xi^{1/2} = 1 + 0.982\, f_w$, $|\xi| < 0.38$ (8.36)

and equation (8.21) is $$\frac{\tau_w(x)}{K^2 x^{-\frac{1}{2}}} = 1 + 2{\cdot}5\left(\frac{6}{5}\right)^{\frac{1}{2}} = 1 + 1{\cdot}25 f_w \cdot \qquad \left|\frac{6}{5}\right| < \frac{1}{3} \tag{8.37}$$

These skin friction solutions are presented in figure 6 and compare quite well with the theories of Curle and Iglisch.

9. A more accurate similarity solution

The approximation for $\frac{\partial z}{\partial \Phi}$ which was used in section 6 gives reasonable solutions when there is a realistic blowing distribution. However, in similarity flow, the blowing or suction distribution of the form $V_w \propto x^{\frac{m-1}{2}}$, which implies infinite velocities at the leading edge, mathematically requires a better approximation for $\frac{\partial z}{\partial \Phi}$ in order that the skin friction solution does not diverge as $m \to 0$.

In this section a more accurate similarity solution of the momentum equation for incompressible flow is outlined. More terms are considered in the series for $\frac{\partial z}{\partial \Phi}$, and the boundary condition $\frac{\partial z}{\partial \Phi} \to 0$ as $\Phi_1 \to 0$ is satisfied.

The solution for $\frac{\partial z}{\partial \Phi}$ when $V_w = 0$ is derived in Appendix B and it is shown that an exponential term, $\exp\left(-\left(\frac{2}{3}\right)^2 \Phi_1^{3/2} t^{-1}\right)$, ensures that $\frac{\partial z}{\partial \Phi} \to 0$ as $\Phi_1 \to \infty$. This exponential term is then used in the approximate series for $\frac{\partial z}{\partial \Phi}$ when there is suction or injection.

The details of the method, which is very similar to that used in solving the energy equation (section 7), are given in Appendix B3. A series for $\frac{\partial z}{\partial \Phi_1}$ of the form

$$\frac{\partial z}{\partial \Phi} = \left(P_1 + P_2 \Phi_1^{\frac{1}{2}} + P_3 \Phi_1 \ldots\right) \exp\left(\frac{-\left(\frac{2}{3}\right)^2 \Phi_1^{3/2}}{t}\right) \tag{9.1}$$

is used in place of $\frac{2\tau_w}{\mu\rho}$ which was used in the original analysis in section 6. The Laplace Transform of the momentum equation is again reduced to a modified Bessel equation and the method of Variation of Parameters is used to find the particular integral. Finally, after

taking the inverse transform, the following equation for the skin friction is obtained:

$$1 = \frac{2^{7/3}\,\Gamma\left(\frac{2}{3}\right)\Gamma\left(\frac{9m+1}{3m+3}\right)}{3^{1/3}(m+1)^{2/3}\,\Gamma\left(\frac{1}{3}\right)\Gamma\left(\frac{11m+3}{3m+3}\right)} \cdot \left(f_w''\right)^{4/3} -$$

$$\Gamma\left(\frac{9m+1}{3m+3}\right)\left\{\frac{\frac{4}{3}f_w f_w''}{\Gamma\left(\frac{12m+4}{3m+3}\right)} - \frac{2^{8/3}f_w}{3^{5/3}f_w''^{1/3}}\,\frac{\left(m+\frac{f_w'' f_w (m+1)}{2}\right)\cdot\Gamma\left(\frac{2}{3}\right)}{\Gamma\left(\frac{13m+5}{3m+3}\right)\cdot(m+1)^{1/3}} + \right.$$

$$\left.\frac{\Gamma\left(\frac{2}{3}\right)2^{7/3}\,f_w^2\,(m+1)^{1/3}}{\Gamma\left(\frac{1}{3}\right)\Gamma\left(\frac{14m+6}{3m+3}\right)f_w''^{2/3}\,3^{4/3}}\left(m+\frac{f_w'' f_w (m+1)}{2}\right)\right\}. \qquad (9.2)$$

The skin friction parameter, f_w'', has been evaluated from this equation (by a 'trial and error' method) and is presented in figure 8 showing the variations with the pressure gradient parameter, m, and the blowing velocity parameter, f_w. The solution for f_w'' when f_w is zero is the solution obtained by Lighthill (1950). The curves compare reasonably well with the exact solutions obtained by Donoughe and Livingood (1954) and Koh and Hartnett (1960).

10. Solutions to the compressible equations

Equations (5.14) to (5.7), which express the pseudo-incompressible forms of velocity, wall shear stress and heat transfer rate in terms of the original compressible forms, are used to change the integral momentum and energy equations (6.29 and 7.32) into their compressible forms. Thus

$$a_o^2\left[M_1^2(0)+\int_0^{x}\frac{h_w}{h_1}\,dM_1^2\right]=\frac{2}{\mu_o\rho_o}\int_0^{x}\frac{\tau_w}{C_w}\,m_1^{\frac{2(2\gamma-1)}{\gamma}}\rho_w v_w\,dx_1+$$

$$\frac{3^{1/3}2}{\Gamma(\frac{1}{3})(\mu_o\rho_o)^{2/3}}\int_0^{x}\frac{\tau_w^{3/2}}{C_w^{1/2}}\,m_1^{\frac{3\gamma-2}{\gamma}}\left(\int_{x_1}^{x}\frac{C_w^{\frac{1}{2}}\tau_w^{\frac{1}{2}}}{m_1}\,dz\right)^{-\frac{1}{3}}dx_1 \qquad (10.1)$$

and

$$Q_w=-\frac{\Gamma(\frac{2}{3})\sigma^{\frac{2}{3}}\rho_w\tau_w^{\frac{1}{2}}\mu_w m_1}{\Gamma(\frac{1}{3})3^{1/3}(\rho_o\mu_o)^{\frac{1}{3}}C_w^{\frac{1}{2}}}\int_0^{x}\left(\int_{x_1}^{x}\frac{C_w^{\frac{1}{2}}\tau_w^{\frac{1}{2}}}{m_1}\,dz\right)^{-\frac{2}{3}}\frac{v_w Q_w C_w^{\frac{1}{2}}}{\mu_w\tau_w^{\frac{1}{2}}m_1}\,dx_1-$$

$$\frac{3^{\frac{1}{3}}(\mu_o\rho_o)^{\frac{1}{3}}\tau_w^{\frac{1}{2}}\rho_w m_1\mu_w}{\Gamma(\frac{1}{3})\sigma^{2/3}C_w^{1/2}\rho_o\mu_o}\int_0^{x}\left(\int_{x_1}^{x}\frac{C_w^{\frac{1}{2}}\tau_w^{\frac{1}{2}}}{m_1}\,dz\right)^{-\frac{1}{3}}d\left(h_{w_o}-h_w\right), \qquad (10.2)$$

where $m_1=\left(1+\frac{\gamma-1}{2}M_1^2(x)\right)^{\frac{\gamma}{2(\gamma-1)}}$.

Convenient dimensionless forms of these equations are obtained by introducing a blowing parameter, F_w, a skin friction parameter, F_w'', and a heat transfer parameter, $S(x)$, which are defined:

$$F_w(x)=-2\rho_w v_w\left(\frac{x}{u_a\rho_a\mu_a}\right)^{1/2}\left(\frac{i_a}{i_w}\right)^{\frac{\omega-1}{2}}=-2\frac{\rho_w v_w}{\rho_a u_a}Re^{\frac{1}{2}}\left(\frac{i_a}{i_w}\right)^{\frac{\omega-1}{2}}, \qquad (10.3)$$

$$F_w''(x)=\tau_w\left(\frac{x}{\rho_a u_a^3\mu_a}\right)^{1/2}\left(\frac{i_a}{i_w}\right)^{\frac{\omega-1}{2}}=\frac{\tau_w}{\rho_a u_a^2}Re^{\frac{1}{2}}\left(\frac{i_a}{i_w}\right)^{\frac{\omega-1}{2}} \qquad (10.4)$$

and

$$S(x)=(\text{STANTON No})\,Re^{\frac{1}{2}}\left(\frac{i_a}{i_w}\right)^{\frac{\omega-1}{2}}$$

$$=\left(\frac{Q_w(x)}{\rho_a u_a\left(h_w(+0)-h_{w_o}(+0)\right)}\right)\sqrt{\frac{\rho_a u_a x}{\mu_a}}\left(\frac{i_a}{i_w}\right)^{\frac{\omega-1}{2}} \qquad (10.5)$$

where i is the enthalpy $\left(h=i+u^2/2\right)$ and the subscript 'a' denotes a constant reference condition in the isentropic flow outside

the boundary layer. It is assumed that the viscosity ~ temperature relationship is $\mu_w \propto T_w^{\omega}$, where ω is a constant, and that γ, the ratio of the specific heats, is 1.4. Equations (9.3), (9.4) and (9.5) together with the relations,

$$C_w = \frac{\mu_w T_o}{\mu_o T_w} = \left(\frac{T_o}{T_w}\right)^{1-\omega} = \left(\frac{h_1}{i_w}\right)^{\omega-1} \tag{10.6}$$

from equation (5.20), and for isentropic flow

$$\frac{T_o}{T_a} = \left(1 + \frac{M_a^2}{5}\right) = \frac{h_1}{i_a} = \left(\frac{a_o}{a_a}\right)^2 \tag{10.7}$$

and $$\frac{\rho_a}{\rho_o} = \left(1 + \frac{M_a^2}{5}\right)^{-5/2} = \left(\frac{i_a}{h_1}\right)^{5/2}, \tag{10.8}$$

are used to change equations (9.1) and (9.2) into the dimensionless forms:

$$\frac{M_1^2(0)}{M_a^2} + \int_0^x \frac{i_w}{h_1} \cdot \frac{dM_1^2(z)}{M_a} = -\int_0^x \frac{F_w'' F_w}{x_1}\left(\frac{m_1}{m_a}\right)^{\frac{18}{7}} dx_1 \; +$$

$$\frac{3^{\frac{1}{3}}2}{\Gamma(\frac{1}{3})}\int_0^x \frac{F_w''^{3/2}}{x_1^{3/4}}\left(\frac{i_a}{i_w}\right)^{\frac{1-\omega}{4}}\left(\frac{m_1}{m_a}\right)^{\frac{11}{7}}\left(\int_{x_1}^x \frac{F_w''^{\frac{1}{2}}}{z^{1/4}}\left(\frac{i_a}{i_w}\right)^{\frac{3}{4}(1-\omega)}\left(\frac{m_a}{m_1}\right)dz\right)^{-\frac{1}{3}} dx_1, \tag{10.9}$$

and

$$S(x) = \frac{-3^{\frac{1}{3}}F_w''^{\frac{1}{2}}}{\Gamma(\frac{1}{3})\sigma^{\frac{2}{3}}}\left(\frac{m_a}{m_1}\right)\left(\frac{i_a}{i_1}\right)^{\frac{1-\omega}{4}}\int_0^x\left(\int_{x_1}^x \frac{F_w''^{\frac{1}{2}}}{z^{1/4}}\left(\frac{i_a}{i_w}\right)^{\frac{3}{4}(1-\omega)}\left(\frac{m_a}{m_1}\right)dz\right)^{-\frac{1}{3}}\frac{d(h_w - h_{w_o})}{h_w(+0) - h_{w_o}(+0)}$$

$$+\frac{\Gamma(\frac{2}{3})}{3^{\frac{1}{3}}2\Gamma(\frac{1}{3})}\left(\frac{i_a}{i_w}\right)^{\frac{1-\omega}{4}} x^{\frac{1}{4}}\sigma^{\frac{2}{3}}F_w''^{\frac{1}{2}}\left(\frac{m_a}{m_1}\right)\int_0^x\left(\int_{x_1}^x\left(\frac{i_a}{i_w}\right)^{\frac{3}{4}(1-\omega)}\frac{F_w''^{\frac{1}{2}}m_a\,dz}{z^{\frac{1}{4}}m_1}\right)^{-\frac{2}{3}}$$

$$\frac{F_w m_1 S(x_1)}{F_w'' m_a x^{3/4}}\left(\frac{i_a}{i_w}\right)^{\frac{1-\omega}{4}} dx_1. \tag{10.10}$$

These equations may be solved by methods similar to those used by Lilley (1959). However at present only the simple solutions for flow over a flat plate will be considered.

When there is a uniform free stream and constant wall enthalpy, equations(10.9) and (10.10) reduce to

$$1 = -\int_0^{x} \frac{F_w'' F_w}{x_1}\,dx_1 + \frac{3^{\frac{1}{3}}2}{\Gamma(\frac{1}{3})}\int_0^{x} \frac{F_w''^{\frac{3}{2}}}{x_1^{3/4}}\left(\int_{x_1}^{x} \frac{F_w''^{\frac{1}{2}}}{z^{\frac{1}{4}}}\,dz\right)^{-\frac{1}{3}} dx_1 \qquad (10.11)$$

and $$S(x) = -\frac{3^{\frac{1}{3}} F_w''^{\frac{1}{2}} x^{\frac{1}{4}}}{\Gamma(\frac{1}{3})\sigma^{\frac{2}{3}}}\left(\int_0^{x} \frac{(F_w'')^{\frac{1}{2}}}{z^{\frac{1}{4}}}\,dz\right)^{-\frac{1}{3}} +$$

$$\frac{\Gamma(\frac{2}{3})\, x^{\frac{1}{4}}}{2\Gamma(\frac{1}{3})\, 3^{1/3}}\sigma^{\frac{2}{3}} F_w''^{\frac{1}{2}}\int_0^{x}\left(\int_{x_1}^{x} \frac{F_w''^{\frac{1}{2}}}{z^{\frac{1}{4}}}\,dz\right)^{-\frac{2}{3}}\left\{\frac{S(x) F_w}{F_w''^{\frac{1}{2}} x_1^{3/4}}\right\} dx_1 . \qquad (10.12)$$

These are equivalent to the incompressible equations and they will have similar solutions providing that f_w, f_w'' and $\eta_{\infty} R_e^{-\frac{1}{2}}$ in the incompressible solutions are replaced by F_w, F_w'' and $S(x)$ for the compressible solutions.

When the suction or injection velocity through the porous surface is constant, the solution to equation (10.11), by comparison with equations (8.36) and (8.37), is approximately

$$\frac{\tau_w(x)}{\tau_w(x)_{v_w=0}} = \frac{F_w''}{(F_w'')_{v_w=0}} = 1 + 0{\cdot}92\, F_w \qquad (10.13)$$

or $$1 + 1{\cdot}25\, F_w \,. \qquad (10.14)$$

Lew and Fanucci (1955) present a curve for the skin friction with uniform suction for the compressible boundary layer. $\frac{\tau_w}{\rho_w v_w u_1}$ is plotted against $\sqrt{\frac{2\xi}{C'}}\cdot\frac{T_1}{T_w}$,

where $C' = \frac{\mu_w T_1}{\mu_1 T_w}$ and $\xi = \left(\frac{v_w}{u_1}\right)^2 \left(\frac{u_1 x}{\nu_1}\right)$. These terms are related to F_w and F_w'' by the equations:

$$\frac{-\tau_w}{\rho_w v_w u_1} = \frac{2F_w''}{F_w} \tag{10.15}$$

and $$\sqrt{\frac{2\xi}{C'}} \cdot \frac{T_1}{T_w} = \sqrt{2\xi} \cdot \left(\frac{T_1}{T_w}\right)^{\frac{\omega+1}{2}} = \frac{\sqrt{2}}{2} \cdot F_w \,. \tag{10.16}$$

In figure 7 it is shown that equations (10.13) and (10.14) agree reasonably well with Lew and Fanucci's curve.

The similarity solutions of the compressible boundary layer equations for a uniform free stream and constant wall enthalpy, by comparison with equations (9.2) and (8.14), are

$$1 = \frac{2^{\frac{1}{3}}\Gamma\left(\frac{2}{3}\right) F_w''^{\frac{4}{3}}}{3^{\frac{1}{3}}} - 4F_w F_w'' + \left(\frac{2}{3}\right)^{\frac{2}{3}} F_w^2 F_w''^{\frac{2}{3}} \Gamma\left(\frac{1}{3}\right) - \left(\frac{2}{3}\right)^{\frac{4}{3}} F_w^3 F_w''^{\frac{1}{3}} \Gamma\left(\frac{2}{3}\right) \tag{10.17}$$

and $$k_h R_e^{\frac{1}{2}} = \left(k_h R_e^{\frac{1}{2}}\right)_{v_w=0} \left\{1 - \frac{E f_w}{(f_w'')^{\frac{1}{3}}} \left(\frac{i_w}{i_1}\right)^{\frac{1-\omega}{3}}\right\}^{-1}, \tag{10.18}$$

where $E = \frac{\Gamma\left(\frac{1}{3}\right) \sigma^{\frac{2}{3}}}{2^{1/3} 3^{2/3}}$ and k_h is the Stanton heat transfer coefficient given by

$$k_h = -\frac{Q_w(x)}{\rho_1 u_1 (h_w - h_{w_0})} \,. \tag{10.19}$$

The variation of the skin friction parameter, calculated from equation (10.17), is compared with those presented by Low (1955) and Brown and Livingood (1952) in figures 9 and 10. (In Low's paper $(f_w'')_{LOW} \equiv 4 F_w''$ and $(f_w)_{LOW} \equiv F_w$.) The reduction in the Stanton heat transfer coefficient with injection is shown in figure 11.

11. Résumé

Approximate integral equations have been derived for the compressible laminar boundary layer with injection through a porous wall. The equations for the skin friction and the heat transfer to

the wall reduce to those presented by Lilley (1959) when the transpiration velocity is zero, and to those of Lighthill (1950) when the transpiration velocity is zero and the flow is incompressible. In order to estimate the accuracy of these integral equations, solutions are obtained for the special cases which have been solved by previous authors.

The incompressible forms of the integral equations have been solved for similarity flow and for flat plate flow with continuous suction or injection, and the solutions have been compared with the known exact solutions. The uniform suction or injection solution is close to the exact solution and it is to be expected that other 'realistic' distributions of pressure gradient and blowing velocity will give reasonable solutions. However when similarity flow is considered the blowing velocity is 'unrealistic' because infinite velocities are implied at the leading edge in most cases, and this causes a singularity in the skin friction solution, although the energy equation is still well behaved. It is shown how a better approximation for $\frac{\partial z}{\partial \Phi}$ removes the singularity and gives a solution close to the exact solution.

Solutions to the compressible integral equations have been found for certain cases and these compare favourably with the few solutions which have been published.

If improved velocity and temperature distributions near the wall were used, then the accuracy of the method would be improved. A suitable improved velocity distribution is given by Spalding (1958).

The present theory (Stevenson 1961) has been extended by Craven (1962) to include the effects of foreign gas injection. Injection through a porous wall adds mass to the wall region but not momentum in the x-direction. The injected gas, which is accelerated in the x-direction by the viscous forces, results in lower velocity gradients adjacent to the wall and consequently lower skin frictions. If a certain volume of a light gas is injected then the reduction in skin friction is less than with the same volume of air because the mass to accelerate is less. However if an equal mass of a light gas is

injected then the velocity gradients near to the wall and the resulting skin friction are less than with air injection. Some of the curves (Craven 1962) showing the reductions in skin friction and heat transfer at a Mach number of 4, using helium and hydrogen as the injected gases, are compared with those for air in figures 12 and 13.

A light gas injected through a wall diffuses into the boundary layer but its concentration near the wall is high and therefore the density is low, and the effect of pressure gradients will be similar to those which occur with a hot wall, i.e. near the wall, the effects of pressure gradient will be enhanced because the lighter gas will be accelerated or decelerated more easily by the external pressure gradient.

PART II

TURBULENT BOUNDARY LAYERS OVER POROUS SURFACES WITH SUCTION OR INJECTION

12. Introduction

There is no adequate theory for shear flow turbulence and the semi-empirical theories which have been published require experimental results to determine whether certain terms are constants, and if so, what values these take. There have been many experiments in turbulent boundary layers over solid surfaces but there are relatively few which include suction or injection and these show considerable scatter in the results.

In chapter 1 there is a review of the experimental results and theories which have been published, but the review does not include a discussion of the approximations which are used in order to solve the boundary layer equations, because it is more convenient to discuss these when considering a new theory for turbulent boundary layers in chapter 6.

Hartnett et al (1960) discuss the experimental results of Mickley and Davis (1957) for incompressible flow and those of Tenderland and Okuno (1956) and Pappas and Okuno (1960) for compressible flow, and compare these with the theoretical predictions of Dorrance and Dore (1954) and Rubesin (1954). Hartnett suggests that the skin friction results of Mickley and Davis are possibly low. The present experiments in an axisymmetric incompressible boundary layer over a porous cylinder were intended to check those of Mickley and Davis. The experiments, which are compared with the existing theories, reveal two laws, one for the inner region of the turbulent boundary layer and one for the outer region. The laws are

valid for both suction and injection providing there is no pressure gradient, and they reduce to the 'law of the wall' and the 'velocity defect law' when the transpiration velocity is zero. The laws are shown to agree with the experimental results of Mickley and Davis (1957), Black and Sarnecki (1958) and Dutton (1960).

The law for the inner region is used to derive an equation relating the pressure recorded by a Preston tube on a porous surface to the local skin friction. The law for the outer region is used to calculate the variations in skin friction with Reynolds number for a range of injection velocities.

The law for the outer region with suction or injection is a special case of a more general theory for the outer region of turbulent boundary layers which is derived in chapter 6. The new approximate theory correlates the mean velocity in the outer region of incompressible turbulent boundary layers in small pressure gradients, at separation, and with injection or suction through a porous wall. It is probably the first theory to correlate equilibrium turbulent boundary layers under all these conditions.

The theory initially uses a dimensional analysis to show that the outer region depends on a function of the form $f\left(\frac{u_1}{u_\tau}, Q\right) - f\left(\frac{u}{u_\tau}, Q\right)$, and not necessarily on a velocity defect term, $(u_1 - u)$, which has been used by Clauser (1954), Mickley and Smith (1963) and Black and Sarnecki (1958). (Q is a dimensionless parameter independent of y : it could be a pressure gradient parameter or injection velocity parameter. u is the mean velocity in the x-direction and u_1 is the velocity at the outer edge of the boundary layer where $y = \delta$). An outer region which depends on a velocity defect term is a special case of the present theory.

The theory shows that the outer region equation follows immediately from the inner region equation if an overlap region is to exist between the inner and outer solutions. Even if there is an unknown constant with respect to y in the inner region equation, the constant can be eliminated in the outer region solution simply by applying the

boundary condition at the edge of the boundary layer.

The theory is shown to be consistent with the turbulent shear stress distributions at separation, and with suction or injection.

Chapter 1

13. A Review of Previous Work

The momentum and continuity equations for the mean flow in a two-dimensional turbulent boundary layer with zero pressure gradient are approximately (Townsend 1956a)

$$2u\frac{\partial u}{\partial x} + \frac{\partial uv}{\partial y} + \frac{\partial}{\partial x}\left(\overline{u'^2} - \overline{v'^2}\right) + \frac{\partial \overline{u'v'}}{\partial y} = \nu\frac{\partial^2 u}{\partial y^2}$$

and $$\frac{\partial u}{\partial x} + \frac{\partial v}{\partial y} = 0 \ ,$$

where u and v are the mean velocities in the x and y directions, and u' and v' are the components of the velocity fluctuations. In most cases the term $\frac{\partial}{\partial x}\left(\overline{u'^2} - \overline{v'^2}\right)$ is small, and it is neglected in the following analyses. It will be assumed that $\frac{\partial u}{\partial x}$ and $\frac{\partial v}{\partial y}$ are very small in the inner region (the region close to the wall) and the momentum and continuity equations therefore simplify to

$$v_w\frac{\partial u}{\partial y} + \frac{\partial \overline{u'v'}}{\partial y} = \nu\frac{\partial^2 u}{\partial y^2} \ ,$$

or $$v_w\frac{du}{dy} = \frac{1}{\rho}\frac{d\tau}{dy} \ , \qquad (13.1)$$

where τ is the total shear stress which is the sum of the viscous shear stress, $\mu\frac{\partial u}{\partial y}$, and the Reynolds stress, $-\rho\overline{u'v'}$. (The approximations are discussed in more detail in chapter 6). Most of the theories for suction or injection are based on the momentum transfer theory of Prandtl, together with the assumption that the mixing length is proportional to the distance from the wall. This yields

$$\frac{\tau}{\rho} = K^2 y^2 \left(\frac{\partial u}{\partial y}\right)^2 , \qquad (13.2)$$

where K is von Kármán's constant. This equation is further substantiated by Townsend (1956b) who considers regions of turbulent shear flow in which there is equilibrium between the local rates of energy production and dissipation.

In the sublayer, the region very close to the wall where the Reynolds stresses are assumed to be negligibly small compared with the viscous stresses, equation 13.1 may be integrated twice with respect to y. After substituting the wall conditions, the solution reduced to

$$\frac{y u_\tau}{\nu} = \frac{u_\tau}{v_w} \text{LOG}_e \left(1 + \frac{v_w u}{u_\tau^2}\right) , \qquad (13.3)$$

where u_τ is the friction velocity $\left(= \sqrt{\frac{\tau_w}{\rho}}\right)$.

The equation for the inner turbulent region will now be derived, and it will be shown how this equation reduces to those obtained by various authors by substituting the appropriate boundary conditions.

If equation 13.2 is substituted into equation 13.1, then

$$v_w \frac{du}{dy} = \frac{d}{dy}\left(K^2 y^2 \left(\frac{du}{dy}\right)^2\right) . \qquad (13.4)$$

This equation is integrated twice with respect to y, to give

$$\frac{1}{K} \text{LOG}_e \frac{y u_\tau}{\nu} = \frac{2 u_\tau}{v_w} \left(\frac{v_w u}{u_\tau^2} - c\right)^{\frac{1}{2}} + d \qquad (13.5)$$

where c and d are in general functions of v_w and u_τ but are independent of y.

13.1 Kay (1948)

Kay considers the asymptotic suction case and uses the boundary conditions

$\frac{du}{dy} = 0$ and $u = u_1$ at $y = \delta$.

If these conditions are used together with equation 13.5 then,

$$C = \frac{V_w u_1}{u_\tau^2} \quad , \quad d = -\frac{1}{K} \log_e \frac{\delta u_\tau}{\nu}$$

and therefore equation 13.5 reduces to $\frac{u}{u_1} = 1 + \frac{V_w}{4K^2 u_1} \log_e^2 \left(\frac{y}{\delta}\right)$. (13.6)

This is the equation obtained by Kay, but his experimental results for suction did not agree with the equation. This is because the mixing length hypothesis is not valid in the outer region where the boundary conditions were applied.

13.2 Clarke, Menkes and Libby (1955).

Clarke et al write equation 13.5 in the following form

$$\frac{u}{u_\tau} = A + B \log_e \left(\frac{u_\tau y}{\nu}\right) + \frac{1}{4K^2} \frac{V_w}{u_\tau} \log_e^2 \left(\frac{y u_\tau}{\nu}\right) \ldots \quad (13.7)$$

When $V_w = 0$ this equation reduced to the accepted 'law of the wall' equation,

$$\frac{u}{u_\tau} = A + B \log_e \left(\frac{y u_\tau}{\nu}\right) . \quad (13.8)$$

However Clarke et al overlook the implicit relation between A , B and. V_w . (see section 20 for more details).

13.3 Rubesin (1954), Dorrance and Dore (1954) and Mickley and Davis (1957)

Rubesin and Dorrance and Dore consider the compressible boundary layer, and obtain integral equations for the sublayer region and for the inner turbulent region. Mickley and Davis write the equations in incompressible form, assuming that they hold on either side of a transition point at $y = y_a$. At this point the velocities and shear stresses are matched —

$$\text{At } y = y_a \text{ , } u = u_a \text{ and } \left(\mu \frac{\partial u}{\partial y}\right)_a = \left(\rho K^2 y^2 \left(\frac{\partial u}{\partial y}\right)^2\right)_a . \quad (13.9)$$

The velocity-shear relationship which is valid in the sublayer, and which is assumed to hold in the inner turbulent region, is obtained

by integrating equation 13.1 and substituting the wall conditions. Hence

$$\rho u v_w = \tau - \tau_w \quad . \tag{13.10}$$

Equations 13.9 and 13.10 are combined at $y=y_a$ to give

$$u_a v_w + u_\tau^2 = \left(K^2 y^2 \left(\frac{\partial u}{\partial y}\right)^2\right)_a \quad . \tag{13.11}$$

If this condition together with $u=u_a$ at $y=y_a$ is used to determine c and d in equation 13.5, then

$$c=-1 \quad \& \quad d = \frac{1}{K} \log_e \frac{y_a u_\tau}{\nu} - \frac{2u_\tau}{v_w}\left(\frac{v_w u}{u_\tau^2}+1\right)^{\frac{1}{2}} . \tag{13.12}$$

Therefore equation 13.5 may be written

$$\log_e \frac{u_\tau y}{\nu} - \log_e \frac{u_\tau y_a}{\nu} = \frac{2K u_\tau}{v_w}\left\{\left(\frac{v_w u}{u_\tau^2}+1\right)^{\frac{1}{2}} - \left(\frac{v_w u_a}{u_\tau^2}+1\right)^{\frac{1}{2}}\right\} . \tag{13.13}$$

This is the equation presented by Mickley and Davis.

Mickley and Davis have published a very comprehensive set of experimental results of the mean flow in a turbulent boundary layer in a wind tunnel which had a porous wall 12 feet long and 1 foot wide. Blowing velocity ratios, v_w/u_1, which were constant in a particular experiment, ranged between 0 and 0.01 and free stream velocities between 17 and 60 feet per second. A small pressure gradient was present in the experiments but does not seem to be included in the skin friction calculations. This is discussed further in section 21 where it is shown that the effect of the small pressure gradient increases the skin friction by as much as 80% when $\frac{v_w}{u_1} = 0.003$, although it has negligible effect when there is no blowing velocity.

Mickley and Davis compare their experimental results with equation 13.13 by plotting $\log\left(\frac{yu_\tau}{\nu}\right)$ against $\left(1+\frac{v_w u}{u_\tau^2}\right)^{\frac{1}{2}}$ and they show that a straight line of the predicted slope, $\frac{2Ku_\tau}{v_w}$, is obtained and also that von Kármán's constant, K, is independent of v_w. However it was not possible to correlate the variations in the conditions at the edge of the sublayer where $y=y_a$. It was shown that the velocity defect term,

$\frac{u_1-u}{u_\tau}$, only correlated the velocity profiles in the outer region when v_w was zero.

13.4 Black and Sarnecki (1958)

If it is assumed that the shear relation of equation 13.10 is valid at the same time as the linear mixing length equation 13.2, then $c=-1$ and equation 13.5 may be written

$$\frac{1}{K}\log_e\left(\frac{yu_\tau}{\nu}\right)=\frac{2}{v_w}\left(v_w u+u_\tau^2\right)^{\frac{1}{2}}+d\,. \tag{13.14}$$

(As $v_w\to 0$ then $d\to\frac{2u_\tau}{v_w}-B$ where B is the constant in the no-blowing law of the wall equation 13.8).

If d is made equal to $\frac{1}{K}\log_e\frac{ku_\tau}{\nu}$ then

$$u_\tau^2+v_w u=\left(\frac{v_w}{2K}\log_e\frac{y}{k}\right)^2, \tag{13.15}$$

where k is the constant of integration. This is the equation which Black and Sarnecki call the bilogarithmic law. The equation is rewritten

$$\frac{u}{u_1}-\frac{1}{4K^2}\frac{v_w}{u_1}\left(\log_e\frac{u_1y}{\nu}\right)^2=\left[\frac{1}{4K^2}\frac{v_w}{u_1}\left(\log_e\frac{u_1k}{\nu}\right)^2-\frac{u_\tau^2}{v_w u_1}\right]-\left(\frac{1}{2K^2}\frac{v_w}{u_1}\log_e\frac{u_1k}{\nu}\right)\log_e\frac{u_1y}{\nu}, \tag{13.16}$$

so that the left hand side of the equation contains only the quantities which are easily measured, and the right hand side is linear in $\log\frac{yu_1}{\nu}$. When there is injection it is convenient to introduce the substitution

$$\frac{1}{2K}\sqrt{\frac{v_w}{u_1}}\cdot\log_e\frac{u_1y}{\nu}=Y \tag{13.17}$$

and hence equation 13.16 becomes

$$\frac{u}{u_1}-Y^2=\left(n_2^2-b_2^2\right)+2n_2Y \tag{13.18}$$

where $$n_2=-\frac{1}{2K^2}\sqrt{\frac{v_w}{u_1}}\cdot\log_e\frac{u_1k}{\nu}\,, \tag{13.19}$$

and $$b^2 = \frac{u_e^2}{V_w U_\infty} \quad . \qquad (13.20)$$

If experimental results are plotted as $\left(\frac{u}{U_\infty} - Y^2\right)$ against Y, straight lines are obtained in the inner region where the mixing length hypothesis applies and the skin friction may be obtained from the gradient and the intercept.

Von Kármán's constant, K, in the mixing length theory should be independent of the transpiration velocity providing $|V_w|$ is small compared with the velocity U. The experiments of Black and Sarnecki, Mickley and Davis and the present results confirm that K is independent of V_w.

Black and Sarnecki's theory enables the skin friction to be determined from a velocity profile without assuming a form for k, the unknown constant of integration with respect to y. This was not possible with Mickley and Davis' theory.

13.5 Turcotte (1960) and Leadon (1961)

Turcotte assumes that the shear stress in the fully turbulent portion of the boundary layer is unaffected by injection and suggests a similarity parameter V_w/U_{e_0}. (The subscript $_0$ refers to zero blowing conditions.) However in a reply to Turcotte's paper, Leadon shows that the shear stress assumption is incorrect. Leadon suggests that a proper similarity parameter should include the free stream velocity.

In the next chapter the present experimental results will be described and compared with the various theories.

Chapter 2

Experiments on Injection into an Incompressible Turbulent Boundary Layer

14. Apparatus

The first model which was used is shown in figure 14. This

consisted of an 8" long, 4" diameter porous tube which was mounted as part of a long cylinder extending from the contraction to the working section of the College of Aeronautics 3 feet x 3 feet open circuit wind tunnel, which has the fan at the end of the diffuser. Air from the compressor flowed along the inside of the cylinder, through an inch thick felt filter and then through the porous tube. The rig, without the porous tube, had originally been used for base pressure measurements. A large aerofoil in the wind tunnel contraction supported the cylinder and there was a small vertical support after the working section.

A material was required, which was smooth as far as the boundary layer was concerned, and which was porous so that a uniform flow of air, rather than a series of jets, could be forced through it. The material, which best suits this specification, is Porosint Grade A made by Sintered Products Limited. Porosint is a sintered bronze material with quite a smooth surface because the holes are only about 10 microns in diameter. The material consists of spherical granules which are welded together at their points of contact, and through a microscope, the holes in the surface have a sort of bell-mouthed appearance. The pressure drop across the porous tube was far higher than the kinetic energy $(\frac{1}{2}\rho V_w^2)$ of the air passing through the tube, so that turning vanes were not required inside the tube.

A micrometer screw traversing gear (fig. 14), which was calibrated to 0.001 inch, enabled boundary layer profiles to be taken on the top and bottom surfaces of the cylinder at any longitudinal position. Mean velocity profiles through the boundary layer were measured with a pitot tube which had a rectangular cross section 0.014 inch x 0.1 inch and the readings were corrected for the transverse total pressure gradient by the method of Young and Maas (1936). Hot wire traverses using a 0.001 inch diameter platinum wire gave the same velocity profiles as those with the pitot tube but hot wires were not used all the time because they needed recalibrating too frequently. This was probably because of the dust in the laboratory. Traverses using a

static tube 0.064 inch diameter did not detect any change in the static pressure through the boundary layer.

The air flow to the porous tube was measured with an orifice plate in the supply pipe. The orifice plate calibration was checked by taking momentum traverses across the end of the supply pipe. A thick felt filter was positioned in the pipe to simulate the correct pressure range across the orifice. The velocity distribution, $V_w(z)$, through the porous tube was estimated with a hot wire anemometer when there was no flow through the wind tunnel.

A Betz manometer was used to record the pressure difference across the orifice plate and two Chattock gauges were used to measure the free stream velocity and the pitot tube pressure.

The Preston tubes which were used consist of a tube 3 inches in length and 0.064" outside diameter soldered onto a 0.004 inch thick curved metal strip at the downstream end (see figure 15b). The tubes had a very slight curvature so that an elastic band, at the downstream end, held the mouth of the tube against the model.

Pitot and static traverses in the working section showed that the velocity outside the boundary layer was constant to within 0.35%.

Pitot tube traverses in the boundary layer on the cylinder showed that the mean velocity profiles changed slightly from day to day. A series of Preston tubes around the cylinder showed variations in $(P-p_0)$ of ±10% (fig. 15c). $(P-p_0)$ is the pressure recorded by the Preston tube relative to the static pressure. It was thought that the variations were due to changes in the position of transition, however, using surface flow indicators, moving the position of a roughness strip (a strip of course sandpaper around the cylinder), and trying various transition wires, still resulted in day to day variations. The trouble was eventually traced to the large aerofoil in the wind tunnel contraction. Ailerons were fixed onto the aerofoil and it was found that a fraction of a degree change in the angle of the ailerons completely altered the flow on the model. The trouble was due to a very slight rotation of

the flow in the working section and the day to day variations were due to slight changes in the local incidence along the span of the aerofoil due to temperature changes.

The aerofoil section was removed and the cylinder air supply was fed from downstream of the working section and at the same time the length of porous tube was increased from 8 inches to 24 inches. Porosint is only made in 8 inch lengths and three tubes had to be used. The v_w distribution along the porous tube is shown in fig. 19. An elliptic nose was used on the model, which is shown in figures 16, 17 and 18. The supporting wires allowed the model to be aligned with the air flow.

The distribution of $(P-p_0)$ around the cylinder was within ±1% (fig. 15d) and pitot traverses on the top and bottom of the cylinder at a particular x-position were the same. There were no day to day variations.

15. Momentum equation for axisymmetric flow

The integral momentum equation for a steady incompressible turbulent boundary layer along a cylinder with zero pressure gradient is (Young 1939)

$$\frac{d\delta_2}{dx} - \frac{v_w}{u_1} = \frac{\tau_w}{\rho u_1^2} = \frac{c_f}{2} \qquad (15.1)$$

where c_f is the local skin friction coefficient and the momentum thickness, δ_2, is defined

$$\delta_2 = \int_0^{\delta} \left(1+\frac{y}{r}\right)\frac{u}{u_1}\left(1-\frac{u}{u_1}\right)dy \ , \qquad (15.2)$$

where $2r$ is the outside diameter of the cylinder and y is measured from the surface of the cylinder. The displacement thickness, δ_1, is defined

$$\delta_1 = \int_0^{\delta} \left(1+\frac{y}{r}\right)\left(1-\frac{u}{u_1}\right)dy \qquad (15.3)$$

The differences between flat plate and axisymmetric flow are discussed in section 18.

16. Experimental results

The mean velocity profiles were measured at several positions along the cylinder and for several values of the blowing velocity, with a constant free stream velocity of 50 feet per second. Curves of $\frac{u}{U_1}\left(1-\frac{u}{U_1}\right)\left(1+\frac{y}{r}\right)$ against y were plotted (see figs. 21 and 22) and integrated graphically to find the momentum thickness, δ_2. The variations in δ_2 along the cylinder are shown in figure 20, and it was necessary to estimate $\frac{d\delta_2}{dx}$ from these curves in order to evaluate the skin friction using the integral momentum equation (15.1). The estimated accuracy of the skin friction measurements is ±10% in c_f when $v_w = 0$ and ±0.0003 when there is a blowing velocity.

Some velocity profiles at a particular position on the cylinder for different blowing velocities are shown in figure 23. (The x-coordinate is measured from the beginning of the porous tube.)

17. A comparison with the previous theories

A few of the experimental results in the region near the wall are plotted as $\log \frac{yu_\tau}{\nu}$ against $\left(1+\frac{v_w u}{u_\tau^2}\right)^{\frac{1}{2}}$ in figure 24 and are shown to agree with Mickley and Davis' equation (13.13). The straight lines in figure 24 have gradients of $\frac{2Ku_\tau}{v_w}$, where $K = 0.418$, and therefore the experimental points confirm that K is independent of v_w.

Some of the velocity profiles are plotted in the way suggested by Black and Sarnecki (see section 13.4) in figure 25. The skin friction predicted from the slope and intercept of the straight logarithmic part of the curves agree with the measured skin friction (see table 1). It is only possible to estimate the skin friction from the gradient and intercept with an accuracy of about ±15%.

The variation in skin friction with Reynold's number will be discussed in section 26.

18. Axisymmetric flow

It is necessary to discuss the likely differences between axisymmetric and flat plate flow. A few reports on the subject have been

published and they indicate that the boundary layer in the present experiments is almost the same as that on a flat plate. Landweber (1949) and Eckert (1952) assumed that the velocity profiles on a cylinder could be represented by a 1/7 power law, and that the relationship between the wall shear stress and the boundary layer thickness for the cylinder is identical to that on a flat plate, from which they calculated the boundary layer growth using the integral momentum equation. If δ/r, the ratio of the boundary layer thickness to the radius of the cylinder, is 0.5 then Eckert's theory suggests that the skin friction on the cylinder is 5% greater than on a flat plate.

Ginevskii and Solodkin (1958) and Sparrow et al (1963) consider the boundary layer to be composed of a laminar region near the wall and a turbulent outer region. Ginevskii and Solodkin follow the analysis of Prandtl and assume that the mixing length is proportional to the distance from the wall and Sparrow follows the analysis of Deissler and Loeffler (1959) and assumes that the logarithmic region extends to the outer edge of the boundary layer. The theories suggest that the skin friction in the present experiments would be 5 to 10% greater than on a flat plate.

When y , the distance from the wall, is small compared with the radius of the cylinder very little difference is to be expected between flat plate and axisymmetric flow and the velocity profiles are close to those predicted by the 'law of the wall' equation. Richmond (1957) and Yasuhara (1959) measured velocity profiles on cylinders and estimated the skin friction by comparing the profiles with the law of the wall equation. Their results are roughly in agreement with the theories.

The theories and experiments for axisymmetric flow indicate that the skin friction in the present experiments may be slightly higher, perhaps 5% higher, than that on a flat plate.

Chapter 3

A Law of the Wall for Turbulent Boundary Layers with Suction or Injection

19. The law of the wall equation

The equation for the inner turbulent region, equation 13.14, may be written

$$\frac{2u_\tau}{V_w}\left\{\left(\frac{V_w u}{u_\tau^2}+1\right)^{\frac{1}{2}}-1\right\} = \frac{1}{K}\log_e\frac{yu_\tau}{\nu} - \left(d+\frac{2u_\tau}{V_w}\right). \qquad (19.1)$$

This is similar in form to that given by Townsend (1956b) and reduces to the familiar law of the wall equation when $V_w = 0$, i.e.

$$\frac{u}{u_\tau} = \frac{1}{K}\log_e\frac{yu_\tau}{\nu} + B \qquad (19.2)$$

The experimental curves for flow over a permeable or impermeable wall may now be compared on one figure if $\log\frac{yu_\tau}{\nu}$ is plotted against $\frac{2u_\tau}{V_w}\left\{\left(\frac{V_w u}{u_\tau^2}+1\right)^{\frac{1}{2}}-1\right\}$ and the inner turbulent region should plot as a series of parallel lines if the mixing length coefficient K is independent of V_w. The present experimental results were plotted in this way and it was found that they plotted very close to the accepted impermeable wall curve (fig. 25). The experimental results show that the term $\left(d+\frac{2u_\tau}{V_w}\right)$ in equation 19.1 varies very little with suction or injection.

There still remains some doubt as to the values for the constants K and B in the 'law of the wall' equation when there is no suction or injection. However the values which were found by Dutton (1959) will be used, and therefore the 'law of the wall' equation with suction or injection is

$$\frac{2u_\tau}{V_w}\left\{\left(1+\frac{V_w u}{u_\tau^2}\right)^{\frac{1}{2}}-1\right\} = 5.5\log_{10}\frac{yu_\tau}{\nu} + 5.8 \qquad (19.3)$$

In the following sections this equation will be compared with previous experimental results.

20. A comparison between equation (19.3) and that suggested by Black and Sarnecki (1958)

Black and Sarnecki wrote their bilogarithmic law in the form

$$\frac{u}{u_\tau} = a_2 + b_2 \log_e \frac{u_\tau y}{\nu} + \frac{1}{4K^2}\frac{V_w}{u_\tau}\left(\log_e \frac{u_\tau y}{\nu}\right)^2 \qquad (20.1)$$

with $a_2 = \frac{u_\tau}{V_w}(\lambda^2 - 1)$, $b_2 = \frac{\lambda}{K}$ and

$$\lambda = -\frac{1}{2K}\frac{V_w}{u_\tau}\log_e \frac{u_\tau k}{\nu}. \qquad (20.2)$$

Several dimensionless parameters which might provide a possible criterion for specifying conditions at the edge of the sublayer ($y = y_a$) were considered. Eight possible equations for λ were obtained by considering the sublayer equation (13.3), and λ was then plotted against V_w/u_τ and compared with the experimental results. There is a considerable scatter in the experimental results, but Black and Sarnecki chose the equation for λ which seemed to predict most accurately the actual variation for layers on smooth and nearly homogeneous walls. The equation is

$$\lambda = \sqrt{1+2m} - \frac{m}{NK}\log_e\left\{\frac{N_3}{2m}\log_e(1+2m)\right\} \qquad (20.3)$$

where $m = \frac{u_a V_w}{2u_\tau^2}$ and $N_3 = \frac{u_a}{u_\tau}$; $m > -\frac{1}{2}$.

This equation is presented in figure 27 together with some experimental results, and is reproduced from Black and Sarnecki's paper.

The equivalent variation which is implied by the 'law of the wall with suction or injection', equation (19.3) is

$$\lambda = \frac{5.8}{2}\frac{V_w}{u_\tau} + 1 \qquad (20.4)$$

and is also shown in figure 27.

21. To estimate the skin friction from a velocity traverse

The 'law of the wall' equation with suction or injection (equation 19.3) may be written in the form

$$\frac{2}{5.5}\frac{u_\tau}{V_w}\left\{\left(1+\frac{V_w u_1}{u_\tau^2}\cdot\frac{u}{u_1}\right)^{\frac{1}{2}}-1\right\}-\frac{5.8}{5.5}+\text{LOG}_{10}\frac{u_1}{u_\tau}=\text{LOG}_{10}\frac{yu_1}{\nu} \qquad (21.1)$$

From this equation a set of curves of $\frac{V_w}{u_1}$ against $\text{LOG}_{10}\frac{yu_1}{\nu}$ has been evaluated for particular values of $c_f\left(=2\left(\frac{u_\tau}{u_1}\right)^2\right)$ at fixed values of $\frac{u}{u_1}$ (fig. 28). If the value of $\frac{V_w}{u_1}$ is known for a particular profile, then figure 28 may be used to plot curves of $\frac{u}{u_1}$ against $\text{LOG}_{10}\frac{yu_1}{\nu}$ for particular values of c_f. If the experimental profile is plotted on these curves, then the skin friction may be estimated as in figure 29. The values of u_τ which are estimated in this way will be denoted by u_τ^* and the experimental values obtained from momentum traverses by $u_{\tau E}$.

Some velocity profiles are shown plotted as $\frac{2u_\tau^*}{V_w}\left(\left(\frac{V_w u}{u_\tau^{*2}}+1\right)^{\frac{1}{2}}-1\right)$ against $\text{LOG}_{10}\frac{yu_\tau^*}{\nu}$ in figure 30. Values for the friction velocity u_τ^* (or the skin friction c_f^*) were estimated in this way from the velocity profiles and the results are given in table 1.

The skin friction results which were calculated from the momentum traverses as described in Section 16 are also given in table 1. The value of c_f^* may be estimated from a velocity profile very accurately whereas the experimentally measured skin frictions are only accurate to ± 0.0003. The differences between the experimentally determined skin friction measurements and those estimated from the law of the wall equation 19.3 or 21.1 are within the experimental accuracy. Therefore the hypothesis that 'the unknown function of $\frac{V_w}{u_\tau}$ in equation 19.1 is approximately constant' is in agreement with the present experimental results.

The experimental results presented in Black and Sarnecki's report are plotted in figure 31. Only the straight logarithmic portions are plotted for clarity. The positions of the experimental straight

lines with regard to the straight line of equation 19.3 do not show any trend with changes in V_w. The position of the straight line is very dependent on the accuracy of u_{τ_E} and for $V_w \simeq 0$, a $\pm 10\%$ error in u_{τ_E} results in equation 19.3 plotting as the chain dotted lines in fig.31.

Mickley and Davis do not seem to include the pressure gradient term in their skin friction calculations. Some of their values for C_{f_E} are given in table 2, together with modified values which include the pressure gradient term. These are compared with values of C_f^* which are estimated from the law of the wall equation. Some of Mickley and Davis' velocity profiles are compared with equation 19.3 in fig. 32.

The law of the wall equation with suction or injection shows reasonable agreement with the available experimental results.

Chapter 4

The Use of Preston Tubes to Measure the Skin Friction on a Permeable Wall

22. Measurement of Skin Friction

It is very difficult to obtain an accurate measurement of the local skin friction in turbulent boundary layers. Pitot tube traverses may be used together with von Kármán's momentum integral equation to relate the local shear stress to the changes in the momentum thickness (see section 16), but the method requires the differentiation of experimental results in the streamwise direction which is rather inaccurate, and the method is also very sensitive to three dimensional effects.

Accurate measurements of the velocity profile very close to the wall have been made (Wills 1963) in order to find the velocity gradient and hence the skin friction, but large corrections to the instrumentation calibrations are required due to the presence of the wall and the method is extremely difficult. Dhawan (1952) and Smith and Walker (1958) have made successful measurements with skin friction balances which consist of an isolated portion of the surface connected to strain gauge balances. Ludwieg (1950) measured the heat transfer rates to the wall

and related these to the skin friction, and it was shown that the 'law of the wall' (with zero transpiration) held in pressure gradients just as it did in zero pressure gradient.

Stanton tubes and Preston tubes may be used to estimate the skin friction. Stanton tubes (Stanton et al 1920) are very small pitot tubes which are used in the linear velocity profile in the sublayer region and Preston tubes (Preston 1954) are pitot tubes which are used in the universal logarithmic region. Preston tubes were originally calibrated in pipe flow on the assumption that the law of the wall was the same in pipe and boundary layer flows, but there is now some doubt as to the exact calibration curve (see the discussion - Head and Rechenberg 1962). Further work is continuing to determine the best calibration curve since the use of Preston tubes is the easiest method of estimating skin friction.

The theory presented in this chapter shows how Preston tubes may be used to estimate the skin friction in turbulent boundary layers over porous walls through which there is a small normal velocity. The theory gives an equation which may be used with the Preston tube calibration curve (whichever calibration curve is eventually chosen). The theory follows that of Hsu (1955) but the equations now include the suction or injection velocity at the wall. The final equation is relatively simple to apply and the skin friction results which are obtained in an experiment compare favourably with those obtained using the integral momentum equation.

23. Theory

The law of the wall equation for turbulent boundary layers with zero pressure gradient and zero transpiration velocity, which is valid in the inner turbulent region, is

$$\frac{u}{u_\tau} = \frac{1}{K} \log_e \frac{y u_\tau}{\nu} + B = f\left(\frac{y u_\tau}{\nu}\right) \qquad (23.1)$$

where K and B are constants. Hsu (1955) fits a power law profile to this region of the form

$$\frac{u}{u_\tau} = C\left(\frac{y u_\tau}{\nu}\right)^n \qquad (23.2)$$

where C and n are constants which best fit the experimental results. (Hsu uses the values, $C = 8.61$ and $n = \frac{1}{7}$.)

If there is suction or injection through a porous wall then the law of the wall equation is modified to (equ. 19.3)

$$2\frac{u_\tau}{V_w}\left\{\left(1 + \frac{V_w u}{u_\tau^2}\right)^{\frac{1}{2}} - 1\right\} = \frac{1}{K}\,\mathrm{LOG}_e\frac{y u_\tau}{\nu} + B \qquad (23.3)$$

In the last chapter it was shown that K and B are approximately independent of V_w and u_τ and therefore take the values for the case of zero transpiration. Some of the experimental results are plotted as $2\frac{u_\tau}{V_w}\left(\left(1 + \frac{V_w u}{u_\tau^2}\right)^{\frac{1}{2}} - 1\right)$ against $\mathrm{LOG}_{10}\frac{y u_\tau}{\nu}$ in fig. 34 and are compared with an equation of the form

$$2\frac{u_\tau}{V_w}\left(\left(1 + \frac{V_w u}{u_\tau^2}\right)^{\frac{1}{2}} - 1\right) = C\left(\frac{y u_\tau}{\nu}\right)^n . \qquad (23.4)$$

The equation shows reasonable agreement in the overlap or logarithmic region and it is now rearranged to give the equation for the velocity, u:

$$u = C^2\frac{V_w}{4}\left(\frac{u_\tau y}{\nu}\right)^{2n} + C u_\tau\left(\frac{u_\tau y}{\nu}\right)^n . \qquad (23.5)$$

It will be assumed that the presence of the pitot tube does not affect the flow in the boundary layer and that the pressure recorded by the pitot tube is an average of the integrated pressure over the open portion of the tube:

$$(P - p_o) = \frac{\rho}{\pi 2a^2}\int_\sigma u^2\, d\sigma \qquad (23.6)$$

where $(P - p_o)$ is the pressure recorded by the tube relative to the static pressure, p_o, and σ refers to the area of the tube opening. A pitot tube which touches the wall and has a circular cross section of inside diameter $2a$ and outside diameter $2b$ is considered. Equation 23.6 is written

$$(P - p_o)\pi a^2 = \frac{1}{2}\rho\int_{b-a}^{b+a} 2u^2\sqrt{a^2 - (y-b)^2}\; dy \;, \qquad (23.7)$$

$$\text{or } (P-p_o)\pi a^2 = \frac{1}{2}\rho \int_{-\frac{\pi}{2}}^{\pi/2} 2u^2 a^2 \cos^2\phi \, d\phi \qquad (23.8)$$

where $y - b = a \sin\phi$, or $\frac{y}{b} = (1 + t\sin\phi)$; $t = \frac{a}{b}$.

The equation for u , equation 23.5, is substituted into equation 23.8 and the subsequent equation integrated to give

$$(P-p_o) = \rho\left\{\frac{C^4 v_w^2}{16}\left(\frac{u_z}{\nu}\right)^{4n} b^{4n} I_3(t) + C^3 \frac{u_z v_w}{2}\left(\frac{u_z b}{\nu}\right)^{3n} I_2(t) + C^2 u_z^2 \left(\frac{u_z b}{\nu}\right)^{2n} I_1(t), \right. \qquad (23.9)$$

where

$$I_m(t) = \int_{-\frac{\pi}{2}}^{\frac{\pi}{2}} (1 + t\sin\phi)^{(m+1)n} \cos^2\phi \, d\phi \,. \qquad (23.10)$$
$$m = 1, 2, 3$$

Equation 23.9 can be written,

$$\frac{(P-p_o)\pi d^2}{4\rho\nu^2} = \left\{\frac{C^4}{16}\left(\frac{v_w}{u_z}\right)^2\left(\frac{u_z d}{2\nu}\right)^{2+4n} I_3(t) + \frac{C^3}{2}\left(\frac{v_w}{u_z}\right)\left(\frac{u_z d}{2\nu}\right)^{2+3n} I_2(t) + C^2\left(\frac{u_z d}{2\nu}\right)^{2+2n} I_1(t) \right. \qquad (23.11)$$

where $d = 2b$

When $v_w = 0$ this equation reduces to

$$\frac{\tau_w d^2}{4\rho\nu^2} = k\left(\frac{(P-p_o)d^2}{4\rho\nu^2}\right)^{\frac{1}{n+1}} , \qquad (23.12)$$

$$\text{or } \log\frac{\tau_w d^2}{4\rho\nu^2} = \log k + \frac{1}{n+1}\log\left(\frac{(P-p_o)d^2}{4\rho\nu^2}\right) \qquad (23.13)$$

$$\text{where } k = \left(\frac{\pi}{C^2 I_1(t)}\right)^{\frac{1}{n+1}} . \qquad (23.14)$$

Hsu evaluated $I_1(t)$ for different values of t (see table 3) and showed that the value of k changes very little with t providing that t is less than about 0.6, i.e. if a thick walled tube is used then $I_1(t) \simeq I_1(0)$. There is doubt as to the appropriate values for the constants K and B in the law of the wall equation and therefore corresponding doubt with regard to the values for C and n . Hsu used the values, C = 8.61 and

$n = 1/7$, and therefore equation 23.13 reduces to

$$\alpha = \bar{2}\cdot 6274 + 0\cdot 875\beta \qquad (23.15)$$

when $t = 0$, and

$$\alpha = \bar{2}\cdot 6298 + 0\cdot 875\beta \qquad (23.16)$$

when $t = 0.5$, where

$$\alpha = \log_{10}\frac{\tau_w d^2}{4\rho\nu^2} \qquad \text{and} \qquad \beta = \log_{10}\frac{(p-p_0)d^2}{4\rho\nu^2}.$$

The calibration formula which Preston (1954) obtained for pipe flow is

$$\alpha = \bar{2}\cdot 604 + 0\cdot 875\beta, \qquad (23.17)$$

the formula suggested by the Staff of the N.P.L. (1961) is

$$\alpha = \bar{2}\cdot 647 + 0\cdot 875\beta, \qquad (23.18)$$

and that suggested by Smith and Walker (1958) is

$$\alpha = \bar{2}\cdot 634 + 0\,877\beta. \qquad (23.19)$$

If it is assumed that $I_1(t) = I_1(0)$ then equation 23.13 reduces to equation 23.18 when $n = 1/7$ and $C = 8\cdot 4$, and to equation 23.19 when $n = 0\cdot 14$ and $C = 8\cdot 48$. The resulting equations for u/u_τ (from equ. 23.2) are

$$\frac{u}{u_\tau} = 8.4\left(\frac{yu_\tau}{\nu}\right)^{1/7} \qquad (23.20)$$

and

$$\frac{u}{u_\tau} = 8\cdot 48\left(\frac{yu_\tau}{\nu}\right)^{1/7} \qquad (23.21)$$

These are compared with some 'law of the wall' equations in figure 35. It is difficult to decide which are the correct values for C and n but Hsu's theory gives an equation of the right form and the values of C and n may be adjusted to suit the calibration curve which is eventually

chosen.

When there is a normal velocity at the wall, equation 23.11 must be used. C and n are independent of V_w and therefore have the values obtained for the case of zero transpiration, and the integrals, $I_1(t), I_2(t), I_3(t)$, may be evaluated for the particular pitot tube which is being used in the experiment. Some values for I_1, I_2 and I_3 are given in table 4. Equation 23.11 is therefore of the form

$$(P-p_0)\,g_1 = V_w^2\,u_\tau^{4/7}\,g_2 + V_w\,u_\tau^{3/7}\,g_3 + u_\tau^{2/7}\,g_4, \qquad (23.22)$$

where g_1, g_2, g_3 and g_4 are known. Curves of $(P-p_0)$ against c_f may be plotted for particular values of V_w and u_τ.

If it is assumed that $I_3(t) \simeq I_2(t) \simeq I_1(t) \simeq I_1(0) = \pi/2$ equation 23.11 reduces to

$$\left\{\frac{(P-p_0)d^2}{4\rho\nu^2}\right\}^{\frac{1}{2}} = \frac{c^2 V_w}{2^{5/3}u_\tau}\left(\frac{u_\tau d}{2\nu}\right)^{1+2n} + \frac{c}{2^{1/2}}\left(\frac{u_\tau d}{2\nu}\right)^{1+n}, \qquad (23.23)$$

and this is the equation which will be used to calculate the skin friction in the experiment described below. Hsu's values for C and n are used in the calculations.

24. Experiment using Preston tubes

The Preston tube is described in section 14 and was used on the second model (fig. 16). The Preston tube was placed at different positions on the surface of the cylinder and the pressures, which were recorded for different blowing velocities with a constant free stream velocity of 50 feet per second, are shown in fig. 36. There is a certain length at the beginning of the porous surface during which the boundary layer is adjusting itself to the new conditions. In this region the x-derivatives, which were assumed to be negligible in the theory, are probably large and the inner region equation 19.3 will not be valid. (The Preston tubes would probably indicate too high a skin friction in the region.) Therefore the

Preston tube results will only be compared with the momentum traverses over the latter portion of the porous tube.

The Preston tube, which has an outside diameter of 0.064 inches with t equal to 0.68, was always within the overlap region during the experiments. Curves of $(P-p_0)$ against c_f were evaluated for several blowing velocities from equation 23.23 (fig. 37) and the curves are used to estimate the skin friction from the Preston tube readings. The skin friction results are shown in fig. 38.

In section 21 it was shown how the skin friction may be obtained for a particular suction or injection velocity from a velocity profile using equation 19.3. The skin friction results estimated in this way, and those obtained using the momentum integral method (section 16), are compared with the skin friction results using Preston tubes in fig. 38 and they agree quite well.

Chapter 5

A Modified Velocity Defect Law for Turbulent Boundary Layers with Suction or Injection

25. The modified velocity defect equation.

For a turbulent boundary layer with zero pressure gradient over an impermeable wall, von Kármán showed that the equation for the mean velocity distribution in the inner and outer regions is given by

$$\frac{u}{u_\tau} = \frac{1}{K} \log_e\left(\frac{y u_\tau}{\nu}\right) + \phi\left(y/\delta\right) \tag{25.1}$$

where $\phi(y/\delta)$ is a function of y/δ only, having the constant value $\phi(0)$ throughout the inner region. It follows that

$$\frac{u_1-u}{u_\tau} = -\frac{1}{K} \log_e\left(y/\delta\right) + \phi(1) - \phi\left(y/\delta\right) = \frac{f(y/\delta)}{K} \tag{25.2}$$

is the equation for the outer region, the velocity defect equation, whereas

$$\frac{u}{u_\tau} = \frac{1}{K} \log_e\left(\frac{y u_\tau}{\nu}\right) + \phi(0) \tag{25.3}$$

is the law of the wall equation for the inner region. f is a function of y/δ only.

In the case of a permeable wall, these laws are modified as a result of the finite transpiration velocity at the wall. When the external pressure gradient is zero, it is found that 'the law of the wall with suction or injection', (equation 19.3) is

$$\frac{2u_\tau}{v_w}\left\{\left(1+\frac{v_w u}{u_\tau^2}\right)^{\frac{1}{2}}-1\right\} = \frac{1}{K}\log_e\left(\frac{yu_\tau}{\nu}\right) + B \qquad (25.4)$$

where K and B take the same values as for the case $v_w=0$ over the range of transpiration velocities which result in a measurable skin friction. Following von Kármán it is now postulated that the equation for the inner and outer regions is

$$\frac{2u_\tau}{v_w}\left\{\left(1+\frac{v_w u}{u_\tau^2}\right)^{\frac{1}{2}}-1\right\} = \frac{1}{K}\log_e\left(\frac{yu_\tau}{\nu}\right) + \Phi(y/\delta) \qquad (25.5)$$

where B in equation 25.4 is equal to $\Phi(0)$. It follows that

$$\frac{2u_\tau}{v_w}\left\{\left(1+\frac{v_w u_1}{u_\tau^2}\right)^{\frac{1}{2}}-\left(1+\frac{v_w u}{u_\tau^2}\right)^{\frac{1}{2}}\right\} = -\frac{1}{K}\log_e y/\delta + \Phi(1) - \Phi(y/\delta)$$
$$= \frac{1}{K}F(y/\delta) \qquad (25.6)$$

This is the modified velocity defect law for turbulent boundary layers with suction or injection but with zero pressure gradient. In the next chapter it will be shown that this equation is a special case of a more general 'law for the outer region'.

Townsend (1956a) plots $\frac{u_1-u}{u_\tau}$ against y/δ_0 for various values of x for the case of zero blowing, and verifies that $f(y/\delta)$ is a universal function when there is no pressure gradient. δ_0 is defined as the value of y at which $\frac{u_1-u}{u_\tau}=1$.

When there is injection, the term δ_0 will be defined as the value of y at which $\frac{2u_\tau}{v_w}\left\{\left(1+\frac{v_w u_1}{u_\tau^2}\right)^{\frac{1}{2}}-\left(1+\frac{v_w u}{u_\tau^2}\right)^{\frac{1}{2}}\right\}=1$.
The present experimental results and those of Mickley and Davis (1957) are plotted as $\frac{2u_\tau}{v_w}\left\{\left(1+\frac{v_w u_1}{u_\tau^2}\right)^{\frac{1}{2}}-\left(1+\frac{v_w u}{u_\tau^2}\right)^{\frac{1}{2}}\right\}$ against y/δ_0 in figs. 39 and 40, and the results fall close to the zero blowing curve

presented by Townsend (1956a). $F(y/\delta)$ is therefore the same function as $f(y/\delta)$ in the velocity defect equation (25.2).

For high blowing velocities u_τ has negligible effect on the outer region and equation 25.6 reduces to

$$F(y/\delta) = 2K\left(\frac{u_1}{v_w}\right)^{\frac{1}{2}}\left(1-\left(\frac{u}{u_1}\right)^{\frac{1}{2}}\right). \qquad (25.7)$$

The experimental results (fig. 41) again verify that $F(y/\delta)$ is a universal function.

The logarithmic plot of the velocity defect curve is shown in fig. 42. There is some scatter in the value of $\Phi(1)$ but it is no greater than that for the case of zero blowing (Coles 1961). (The scatter will be discussed in section 30.1.)

Equation 25.6 is now written in the form

$$\frac{u}{u_1} = \frac{u_\tau^2}{u_1 v_w}\left\{\left(\left(1+\frac{v_w u_1}{u_\tau^2}\right)^{\frac{1}{2}} - \frac{F(y/\delta)}{2K}\frac{v_w}{u_\tau}\right)^2 - 1\right\}. \qquad (25.8)$$

This equation has been used to evaluate the velocity profiles, $\frac{u}{u_1}$ against y/δ, for particular values of $\frac{v_w}{u_1}$ and some of the profiles are presented in figs. 43 to 46.

In fig. 47 equation 25.8 is compared with one of the experimental injection profiles, and in fig. 48 it is compared with a near asymptotic suction profile which was measured by Dutton (1960). There is very good agreement.

Tewfik (1963) did an experiment using a very similar rig to that used in the present experiments except that the cylinder was 2 inches diameter. The velocity profiles which were measured by Tewfik for a particular blowing velocity, collapsed onto one curve which is shown in fig. 49. The curve is similar in shape to that given by equation 25.8 and the skin friction appears to be in the range 0.001 to 0.0015. This range is again obtained if the profiles are compared with the 'law of the wall equation with suction or injection' (fig. 59). Tewfik measured the skin friction by momentum traverses and obtained values considerably higher in the range 0.0015 to 0.002.

26. Variation of skin friction with Reynolds number

If the continuity and momentum equations for a turbulent boundary layer (section 13) are integrated from 0 to δ then

$$V = -\int_0^{\delta} \frac{\partial u}{\partial x}\, dy_1 + v_w \tag{26.1}$$

and

$$\frac{\partial}{\partial x}\int_0^{\delta} u^2\, dy_1 + u_1 V = -\frac{\tau_w}{\rho}\,, \tag{26.2}$$

where the variations with x of the mean square turbulent velocity components $\overline{u'^2}$ and $\overline{v'^2}$ have been neglected. Thus when equation 26.1 is substituted into 26.2, the shear stress at the wall is given by

$$-\frac{\tau_w}{\rho} = v_w u_1 + \frac{\partial}{\partial x}\int_0^{\delta} u^2\, dy_1 - u_1 \frac{\partial}{\partial x}\int_0^{\delta} u\, dy_1\,, \tag{26.3}$$

or, in a form which includes the momentum defect term,

$$-\frac{\tau_w}{\rho} = v_w u_1 + \frac{\partial}{\partial x}\int_0^{\delta} (u^2 - uu_1)\, dy_1\,. \tag{26.4}$$

A more convenient form can be derived if we define the functions ξ, S, η, C_n and δ_2 as

$$\xi(x) = \frac{u_1}{u_\tau(x)}\,; \quad S(x) = \left(1 + \frac{v_w u_1}{u_\tau^2}\right)^{\frac{1}{2}}\,; \quad \eta(x) = y/\delta(x)\,,$$

$$C_n = \int_0^{\eta} F^n(\eta_1)\, d\eta_1 \quad \left(\text{with } (C_n)_1 = \int_0^{1} F^n(\eta_1)\, d\eta_1\right), \text{ and} \tag{26.5}$$

$$\delta_2 = \int_0^{1} \delta(x)\, \frac{u(x_1,\eta)}{u_1}\left(1 - \frac{u(x_1,\eta)}{u_1}\right) d\eta_1 \tag{26.6}$$

where F is the universal function of y/δ.

Thus equation 26.4 reduces to

$$0 = \frac{1}{\xi^2} + \frac{v_w}{u_1} - \frac{d\xi}{dx}\,\delta_2'\,, \tag{26.7}$$

where the prime denotes differentiation with respect to ξ. The modified velocity defect equation (25.8) may be written

$$u = u_1 - sF u_\tau + \frac{F^2 v_w}{4}\,, \tag{26.8}$$

and equation 25.5, when $\eta = 1$, reduces to

$$\frac{2u_\tau}{V_w}(s-1) = \frac{1}{K}\log_e\left(\frac{\delta u_\tau}{\nu}\right) + \Phi(1), \tag{26.9}$$

or $$\delta = \frac{\nu}{u_\tau}\exp M, \tag{26.10}$$

where $$M = K\left\{\frac{2}{\varphi}\frac{u_1}{V_w}(s-1) - \Phi(1)\right\}. \tag{26.11}$$

The velocity distribution of equation 26.8 is substituted into the integral for the momentum thickness, δ_2, and the integral is evaluated. The errors involved in assuming that $F(y/\delta)$ is universal in the sublayer region are negligibly small. Hence

$$\delta_2 = \frac{\nu}{u_1}e^M\varphi\left(\frac{s(C_1)_1}{\varphi} - \frac{V_w(C_2)_1}{4u_1} - \frac{s^2(C_2)_1}{\varphi^2} + \frac{V_w(C_3)_1 s}{2u_1\varphi} - \frac{(C_4)_1 V_w^2}{16u_1^2}\right) \tag{26.12}$$

The profile parameters C_1, C_2, C_3 and C_4 have been evaluated using the universal function, $F(y/\delta)$, together with equation 26.5 and are shown in fig. 50.

The equation relating the skin friction to the Reynolds number, $R_{\delta_2}\left(=\frac{\delta_2 u_1}{\nu}\right)$, for a particular value of $\frac{V_w}{u_1}$ is therefore

$$R_{\delta_2} = \left(\delta(C_1)_1 - \frac{V_w(C_2)_1\varphi}{4u_1} - \frac{s^2(C_2)_1}{\varphi} + \frac{V_w(C_3)_1 s}{2u_1} - \frac{(C_4)_1 V_w^2\varphi}{16u_1^2}\right)e^M. \tag{26.13}$$

In order to calculate the Reynolds number from this equation, only the skin friction and the blowing velocity parameter need be specified - no experimental results are required. The variation of skin friction with Reynolds number, evaluated from equation 26.13 is presented in figs. 51 and 52.

The Reynolds number, $R_x\left(=\frac{xu_1}{\nu}\right)$ is obtained by integrating equation 26.7 Thus

$$R_x = \frac{u_1}{\nu}\int_0^\varphi \frac{\delta_2'}{\left(\frac{1}{\xi^2} + \frac{V_w}{u_1}\right)}\,d\xi. \tag{26.14}$$

This equation was integrated numerically and the resulting curves of C_f against R_x are presented in fig. 53. During the calculations the values which were used for $\Phi(1)$, C_1 and C_2 differ slightly from those used by Coles (see table 5) but the final skin friction ~ Reynolds number curves when $V_w = 0$ are quite close.

Mickley and Davis' experimental results when corrected for pressure gradient as described in section 21 agree with the theory (see figs. 52 and 53), and the present experimental results (figs. 54 and 55) are shown to agree reasonably well considering that the measurements are in axisymmetric flow, where skin frictions 5% higher than those on a flat plate are to be expected (see section 18).

Rubesin (1954) presented a theory for injection and evaluated the variations of C_f with R_x by assuming that the law of the wall region extended to the edge of the boundary layer. The constants in the law of the wall are changed from their no-blowing experimental values, to values which give the correct $C_f \sim R_x$ variation when $V_w = 0$. These constants were then used for the case with blowing, together with the assumption that $\frac{u}{u_\tau}$ at the edge of the sublayer is independent of V_w. The curves of $C_f \sim R_x$ which were obtained by Rubesin are compared with the present theory in fig. 53. Rubesin's theory (which is also for compressible flow) gives higher values of skin friction than the present theory, the present experiments, and the experiments of Mickley and Davis. Rubesin's theory compares very well with the experimental results in compressible flow (Tenderland and Okuno 1956) and it was for this reason that Hartnett et al (1960) suggested that Mickley and Davis' results were possibly low (see fig. 57). However, care should be taken when comparing experimental results with an equilibrium theory. Coles (1961) has shown that an incompressible turbulent boundary layer is not in an equilibrium (fully developed, normal, ideal, asymptotic) state until the Reynolds number, R_{δ_2}, is greater than about 3000. The relaxation length, the distance the boundary layer requires to adjust itself to an equilibrium state, is probably related to the boundary layer

thickness, such that flows at a particular Reynolds number have similar relaxation lengths. If this is the case, then the Reynolds number at which the boundary layer actually attains an equilibrium state will be larger for a higher Mach number. (For the higher Mach number at the same Reynolds number, x is smaller.) The incompressible turbulent boundary layer in Mickley and Davis' experiments would probably be in equilibrium because their porous section was 12 feet in length. On the model used in the present experiments the boundary layer is certainly not in an equilibrium state for the first 12 inches of the porous cylinder but is probably close to equilibrium when x is greater than 12 inches. (This is indicated by the rapid change in Preston tube readings over the first part of the porous cylinder (see fig. 36)). The experiments in compressible flow (Tenderland and Okuno 1956, Pappas and Okuno 1960) were on models less than 12 inches in length and the boundary layers were possibly a long way from a fully developed (or equilibrium) state.

Squire (1963) discusses available experimental and theoretical results and compares them in three figures which are reproduced as figs. 56, 57 and 58. The figures have axes $\frac{\tau_w}{\tau_{w_0}} \sim \frac{\rho_w v_w}{\rho_1 u_{\tau_0}}$, $\frac{c_f}{c_{f_0}} \sim \frac{2\rho_w v_w}{\rho_1 u_1 c_{f_0}}$ and $\frac{c_f}{c_{f_0}} \sim \frac{\rho_w v_w}{\rho_1 u_1}$ where the subscript $_0$ refers to conditions when the blowing velocity is zero. The present theoretical curves are also shown in the figures and it is seen that the plot of c_f/c_{f_0} against $\frac{2\rho_w v_w}{\rho_1 u_1 c_{f_0}}$ is the only one which collapses the theoretical curves onto one curve.

Chapter 6

The Outer Region of Turbulent Boundary Layers

27. Introduction

It will be shown that the modified velocity defect law with suction or injection is a special case of a more general law for the outer region of turbulent boundary layers. The theory initially uses a dimensional analysis to show that the outer region depends on a

function of the form $f\left(\frac{u_1}{u_\tau}, Q\right) - f\left(\frac{u}{u_\tau}, Q\right)$ and not necessarily on a velocity defect term, $(u_1 - u)$, which has been used by Clauser (1954), Mickley and Smith (1963) and Black and Sarnecki (1958). (Q is a dimensionless parameter independent of y; it could be a blowing velocity parameter, or a pressure gradient parameter.)

Clauser (1954), realising that the past history of the boundary layer is very important, managed to adjust the pressure gradient in his experiments so that the mean velocity profiles at different positions along the flow collapsed onto one curve when $\frac{u_1 - u}{u_\tau}$ was plotted against y/δ. Clauser's experiments are a special case of the present theory.

Mickley and Smith (1963) found by experiment that the outer region of turbulent boundary layers with small injection velocities through a porous wall, collapsed onto one curve when $\frac{u_1 - u}{(u_\tau)_m}$ was plotted against y/δ. $(u_\tau)_m$ corresponds to the maximum value of the shear stress which occurs in the particular profile. (For boundary layers with injection the maximum shear stress does not occur at the wall.) However with suction the maximum shear stress occurs at the wall but the velocity profiles do not appear to collapse onto one curve when a velocity defect term, $\frac{u_1 - u}{u_\tau}$, is used (see Black and Sarnecki 1958). The equation given by the present theory is more general than that of Mickley and Smith.

Coles (1956) introduced a wake function, $\omega(y/\delta)$, which represents the departure of the mean velocity profile from the 'Law of the wall' velocity profile. The wake function, which is tabulated by Coles, is considered to be independent of the skin friction and pressure gradient. The velocity profile is written

$$\frac{u_1 - u}{u_\tau} = -\frac{1}{K} \log_e \frac{y}{\delta} + \frac{B}{K}\left\{2 - \omega(y/\delta)\right\}$$

The function, $\omega(y/\delta)$, is normalised so that $\omega(0) = 0$, $\omega(1) = 2$ and $\int_0^1 \omega \cdot d(y/\delta) = 1$. Coles analysed available experimental data and showed that the wake function represented the velocity profiles reasonably well except near separation where the 'law of the wake' reduces to

$$\frac{u}{u_1} = \frac{1}{2}\omega(y/\delta),$$

which is presented in fig; 60. The equation does not compare favourably with the experimental results at separation. The 'law of the wake' is not based on any similarity concept and goes beyond the limits of dimensional analysis. Black and Sarnecki (1958) were unsuccessful when they tried to use Coles' wake function when there was suction or injection.

It is well known that the inner region of a turbulent boundary layer adjusts itself to the local wall conditions reasonably quickly whereas the outer region with its slow rates of energy transfer, takes some time to relax to its new form. The present approximate theory will not hold during this relaxation period, however it is shown to be quite useful when considering non-equilibrium layers.

In the following sections the inner region solutions will be reviewed before the new theory is introduced.

28. The inner region

The momentum and continuity equations for the mean flow in a two-dimensional turbulent boundary layer are approximately (Townsend 1956a) :

$$2u\frac{\partial u}{\partial x}+\frac{\partial uv}{\partial y}+\frac{\partial}{\partial x}\left(\overline{u'^2}-\overline{v'^2}\right)+\frac{\partial \overline{u'v'}}{\partial y}=-\frac{dP_1}{dx}+\nu\frac{\partial^2 u}{\partial y^2} \qquad (28.1)$$

and $$\frac{\partial u}{\partial x}+\frac{\partial v}{\partial y}=0 \qquad (28.2)$$

where $\frac{dP_1}{dx}\left(=-u_1\frac{du_1}{dx}\right)$ is the pressure gradient. In most cases the term $\frac{\partial}{\partial x}\left(\overline{u'^2}-\overline{v'^2}\right)$ is small and it will be neglected in the following analysis. We shall assume that $\frac{\partial u}{\partial x}$ and $\frac{\partial v}{\partial y}$ are very small in the inner region, the region very close to the wall. This assumption will be checked once we have the solution for u in the inner region. The momentum and continuity equations therefore simplify to

$$v_w\frac{\partial u}{\partial y}+\frac{\partial \overline{u'v'}}{\partial y}=u_1\frac{du_1}{dx}+\nu\frac{\partial^2 u}{\partial y^2} \qquad (28.3)$$

in the inner region. The equation is integrated with respect to y in order to obtain the equation for the shear stress distribution in the inner region:

$$\frac{\tau}{\rho} = \frac{\tau_w}{\rho} + v_w u - u_1 \frac{du_1}{dx} y . \qquad (28.4)$$

(τ is the total shear stress, the sum of the viscous shear stress $\mu \frac{\partial u}{\partial y}$ and the Reynolds stress $-\rho \overline{u'v'}$)

The momentum transfer or the mixing length hypothesis of Prandtl, together with the usual assumption that the mixing length is proportional to the distance from the wall, yields the relation between the shear stress and the velocity gradient; $\tau = \rho K^2 y^2 \left(\frac{\partial u}{\partial y}\right)^2$, (28.5) where K is von Kármán's constant. This equation will not be valid in the region very close to the wall where the viscous shear stress predominates.

The mixing length hypothesis was used by Rubesin, Dorrance and Dore, and Black and Sarnecki to derive the equations for a turbulent boundary layer with transpiration through a porous wall (section 13). Stratford (1959a) uses the same hypothesis when considering a turbulent boundary layer with negligible wall shear stress: however Stratford is able to derive the same equation by dimensional arguments.

Equation 28.5 is further substantiated by Townsend (1956b) who considers regions of turbulent shear flow in which there is equilibrium between the local rates of energy production and dissipation.

Rotta (1962) reviews the inner region approximations in detail and shows that the available experimental results verify equation 28.5.

The total shear stress in equation 28.4 is eliminated by using equation 28.5, and the resulting equation is integrated with respect to y when (a), the blowing velocity is zero, (b) the pressure gradient is zero, (c) the pressure gradient and the skin friction are zero, (d) the blowing velocity and the pressure gradient are zero, and (e) the blowing velocity and wall shear stress are zero.—

(a) When $\frac{v_w}{u_1} = 0$

$$K\frac{u}{u_\tau} = 2(py+1)^{\frac{1}{2}} + \log_e\left|\frac{(py+1)^{1/2}-1}{(py+1)^{1/2}+1}\right| + B_1(u_\tau, p) \qquad (28.6)$$

where $p = -\frac{u_1}{u_\tau^2}\frac{du_1}{dx}$, and $B_1(u_\tau, p)$ is independent of y.

(b) When $\frac{du_1}{dx} = 0$

$$2\frac{u_\tau}{v_w}\left\{\left(\frac{v_w u}{u_\tau^2}+1\right)^{\frac{1}{2}}-1\right\} = \frac{1}{K}\log_e\frac{yu_\tau}{\nu} + B_2\left(\frac{v_w}{u_\tau}\right) \qquad (28.7)$$

where B_2 is independent of y. This is the law of the wall equation with suction or injection which was described in section 19.

(c) When $\frac{du_1}{dx} = \tau_w = 0$

$$2\left(\frac{u}{v_w}\right)^{\frac{1}{2}} = \frac{1}{K}\log_e\frac{yv_w}{\nu} + B_3 \qquad (28.8)$$

where B_3 is a constant.

(d) When $\frac{v_w}{u_1} = \frac{du_1}{dx} = 0$

$$\frac{u}{u_\tau} = \frac{1}{K}\log_e\frac{yu_\tau}{\nu} + B \qquad (28.9)$$

where B is a constant. Equation 28.9 is the 'law of the wall' equation. Millikan (1938) derived the same equation by dimensional analysis.

(e) When $\tau_w = v_w = 0$

$$u = 2y^{1/2}\left(\frac{dP_1}{dx}\cdot\frac{1}{K^2}\right)^{\frac{1}{2}} + B_4, \qquad (28.10)$$

where B_4 is independent of y.

In deriving equations 28.6 to 28.10 it has been assumed that the region, in which equation 28.5 is valid, is independent of the conditions at the outer edge of the boundary layer, and therefore δ and

u_1 do not appear in the equations.

When $\beta \to 0$ in equation 28.6 or $\frac{V_w}{u_1} \to 0$ in equation 28.7, the equations must reduce to the zero pressure gradient equation 28.9. Therefore

$$B_1(u_\tau, \beta) \underset{\text{as } \beta \to 0}{\longrightarrow} KB - 2 + \log_e\left(\frac{4u_\tau}{\beta\nu}\right), \tag{28.11}$$

and $$B_2\left(\frac{V_w}{u_\tau}\right) \underset{\text{as } V_w \to 0}{\longrightarrow} B. \tag{28.12}$$

Similarly, as the wall shear stress approaches zero, equation 28.6 must reduce to 28.10 and equation 28.7 must reduce to 28.8. Hence

$$B_1(u_\tau, \beta) \underset{\text{as } u_\tau \to 0}{\longrightarrow} \frac{B_4 K}{u_\tau} \tag{28.13}$$

and $$B_2\left(\frac{V_w}{u_\tau}\right) \longrightarrow B_3 + \frac{1}{K}\log_e \frac{V_w}{u_\tau}. \tag{28.14}$$

Stratford (1959a) and Townsend (1960) show that B_4 in the separation equation 28.10 is negligibly small when the Reynolds number, $R_x > 10^6$.

Before the momentum equation 28.1 was solved it was assumed that $\frac{\partial u}{\partial x}$ and $\frac{\partial v}{\partial y}$ were very small in the inner region. At separation for example, this may be checked by using the equation for the velocity distribution in the inner region (equ. 28.10) with $B_4 = 0$. Thus if the terms $\frac{\partial u}{\partial x}$ and $\frac{\partial v}{\partial y}$ are neglected, we are assuming that

$$\frac{4}{3K^2}\, y \frac{d}{dx}\left(-u_1 \frac{du_1}{dx}\right) \ll -u_1 \frac{du_1}{dx}$$

$$\text{or } \frac{4}{3K^2}\frac{y}{\delta}\left\{\frac{\delta}{D}\frac{dD}{dx} - 2D - \frac{d\delta}{dx}\right\} \ll 1 \tag{28.15}$$

where $D\left(= -\frac{\delta}{u_1}\frac{du_1}{dx}\right)$ is a pressure gradient parameter. The various terms in the expression 28.15 have been evaluated using the separation experimental results of Schubauer and Klebanoff (1951) and it is found that the convective terms, $u\frac{\partial u}{\partial x} + v\frac{\partial u}{\partial y}$, are only 2% of the

pressure gradient term. At separation the equation for the total shear stress in the inner region (equ. 28.4) reduces to

$$\frac{\tau}{\frac{1}{2}\rho u_1^2} = -\frac{2}{u_1}\frac{du_1}{dx}\cdot y = 2D\,y/\delta \,. \qquad (28.16)$$

This equation is compared with Schubauer and Klebanoff's measured values of shear stress in fig. 88. The theoretical line is quite close to the experimental shear stress distribution throughout the inner region and it is therefore further justification for neglecting the convective terms. The same arguments may be applied to boundary layers in a pressure gradient or with suction or injection.

29. Equations for the outer region

The method follows that of von Kármán but now includes an unknown function of $\frac{u}{u_\tau}$ and Q in place of the usual $\frac{u}{u_\tau}$ in the zero pressure gradient equation. Q may be a dimensionless pressure gradient parameter or a transpiration velocity parameter or a combination of these, or any other relevant parameters. The equation for an overlap region, a region in which the inner and outer solutions are valid, is written in the form

$$f_1\left(\frac{u}{u_\tau}, Q\right) = \frac{1}{K}\log_e\frac{yu_\tau}{\nu} + C_1 \,, \qquad (29.1)$$

where C_1 is a constant and f_1 is the unknown function of $\frac{u}{u_\tau}$ and Q. Following von Kármán it is now postulated that the boundary layer profile in the outer region is given by

$$f_1\left(\frac{u}{u_\tau}, Q\right) = \frac{1}{K}\log_e\frac{yu_\tau}{\nu} + \phi\left(y/\delta\right) \,, \qquad (29.2)$$

where $\phi(y/\delta)$ is a universal function taking the constant value C_1 in the overlap region. When $y/\delta = 1$ it follows that

$$f_1\left(\frac{u_1}{u_\tau}, Q\right) = \frac{1}{K}\log_e\frac{u_\tau\delta}{\nu} + \phi(1) \,, \qquad (29.3)$$

and thus

$$f_1\left(\frac{u_1}{u_\tau}, Q\right) - f_1\left(\frac{u}{u_\tau}, Q\right) = -\frac{1}{K}\log_e y/\delta + \phi(1) - \phi(y/\delta). \tag{29.4}$$

Equations 29.1, 29.2 and 29.4 are rearranged to give the three equations which will be referred to as 'the equations for the outer region':

(a) from equ. 29.1

$$K\left\{f_1\left(\frac{u}{u_\tau}, Q\right) - C_1\right\} - \log_e \frac{\delta u_\tau}{\nu} = f\left(\frac{u}{u_\tau}, \frac{u_1}{u_\tau}, Q\right) = \log_e y/\delta \tag{29.5}$$

in the overlap region.

(b) from equ. 29.2

$$K\left\{f_1\left(\frac{u}{u_\tau}, Q\right) - C_1\right\} - \log_e \frac{\delta u_\tau}{\nu} = \log_e y/\delta + \phi(y/\delta) - C_1 = S(y/\delta) \tag{29.6}$$

in the outer region.

(c)

$$K\left\{f_1\left(\frac{u}{u_\tau}, Q\right) - f_1\left(\frac{u}{u_\tau}, Q\right)\right\} = f\left(\frac{u_1}{u_\tau}, Q\right) - f\left(\frac{u}{u_\tau}, \frac{u_1}{u_\tau}, Q\right) = S(1) - S(y/\delta) = F(y/\delta) \tag{29.7}$$

in the outer region.

f is a function of $\frac{u}{u_\tau}$, $\frac{u_1}{u_\tau}$ and Q only, because $\frac{\delta u_\tau}{\nu}$ may be written in terms of $\frac{u_1}{u_\tau}$ and Q (equ. 29.3). The outer region includes the overlap region and the outer region equations 29.6 and 29.7 are valid in the overlap region where $S(y/\delta) = \log_e y/\delta$.

In appendix C the same outer region equations are derived by a method similar to that of Millikan (1938). It is assumed that the inner region does not depend on the conditions at the outer edge of the boundary layer and that the outer region is independent of the viscosity, ν . The dimensional equations for the inner and outer regions are written in the form:

Inner region $$f_1\left(\frac{u}{u_\tau}, Q\right) = g\left(\frac{y u_\tau}{\nu}\right) \tag{29.8}$$

Outer region $$F_2\left(\frac{u}{u_\tau}, \frac{u_1}{u_\tau}, Q\right) = G(y/\delta). \tag{29.9}$$

COLLEGE OF AERONAUTICS LIBRARY

When the skin friction is zero, a constant reference velocity must replace u_τ in the equations. Equations (29.8) and (29.9) do not imply similar velocity profiles or self preserving flow (Townsend 1956a). In the appendix it is shown that an overlap region will exist in which equations (3.8) and (3.9) are valid, providing the equations are of the form

$$f_1\left(\frac{u}{u_\tau}, Q\right) = \frac{1}{K} \log_e \frac{y u_\tau}{\nu} + C_1 , \tag{29.10}$$

and $$F_2\left(\frac{u}{u_\tau}, \frac{u_1}{u_\tau}, Q\right) = \frac{1}{K} \log_e y/\delta + C_2 , \tag{29.11}$$

in the overlap region. The equations for the outer region, equations (29.5), (29.6) and (29.7), follow by a method similar to that at the beginning of this section.

Thus, if we know the equation for the overlap region in the form

$$f\left(\frac{u}{u_\tau}, \frac{u_1}{u_\tau}, Q\right) = \log_e y/\delta , \tag{29.12}$$

then the equations for the whole of the outer region are automatically

$$f\left(\frac{u}{u_\tau}, \frac{u_1}{u_\tau}, Q\right) = S(y/\delta), \tag{29.13}$$

and $$f\left(\frac{u_1}{u_\tau}, Q\right) - f\left(\frac{u}{u_\tau}, \frac{u_1}{u_\tau}, Q\right) = S(1) - S(y/\delta) = F(y/\delta), \tag{29.14}$$

where S and F are functions of y/δ only and must be determined from experiment. However they should take the same numerical values in a boundary layer with a pressure gradient or with transpiration, as they do in a boundary layer with zero pressure gradient. It is reasonable to expect similarity of the turbulent structure based on y/δ in the outer region in this way, but in the inner region it is more difficult because similarity could be based on $\frac{y u_\tau}{\nu}$ or $\frac{y u}{\nu}$.

Ultimately the theoretical equations must be compared with experimental results. If there is satisfactory agreement then the original assumptions are justified. We cannot expect agreement when the turbulence

is not fully developed, as for example at very low Reynolds numbers, just after transition.

When the inner region equations were derived in section 28, the equation which was integrated was independent of both ν and δ i.e. from equations (28.4) and (28.5)

$$K y \frac{du}{dy} = \left(u_\tau^2 + v_w u - u_1 \frac{du_1}{dx} \cdot y \right)^{\frac{1}{2}} , \qquad (29.15)$$

which is independent of ν and δ. It is therefore not surprising that the equations (28.6) to (28.10) are solutions for the overlap region.

In the following sections the equations for the overlap region will be used to derive the equations for the outer region, which will then be compared with some experimental results in zero pressure gradient and at separation.

30. The functions $S(y/\delta)$ and $F(y/\delta)$

30.1 Zero pressure gradient

The law of the wall equation for turbulent boundary layers with zero pressure gradient (equ. 28.9) is

$$\frac{u}{u_\tau} = \frac{1}{K} \log_e \frac{y u_\tau}{\nu} + B , \qquad (30.1)$$

where K and B are constants. The equations for the outer region are derived by rearranging this equation to give

$$\log_e y/\delta = K\left(\frac{u}{u_\tau} - B\right) - \log_e \frac{u_\tau \delta}{\nu} \qquad (30.2)$$

in the overlap region, and replacing $\log_e y/\delta$ by $S(y/\delta)$ to give

$$S(y/\delta) = K\left(\frac{u}{u_\tau} - B\right) - \log_e \frac{u_\tau \delta}{\nu} \qquad (30.3)$$

in the outer region.

When $y/\delta = 1$ then $S(1) = K\left(\frac{u_1}{u_\tau} - B\right) - \log_e \frac{u_\tau \delta}{\nu}$ (30.4)

and therefore $S(1) - S(y/\delta) = K\left(\frac{u_1 - u}{u_\tau}\right) = F(y/\delta)$. (30.5)

This is the accepted 'velocity defect equation' for the outer region with zero pressure gradient and zero transpiration. If experimental results are plotted as y/δ_0 against $\frac{u_1-u}{u_\tau}$, they fall close to a single curve (see Clauser 1954 or Townsend 1956a). δ_0 is defined as the value of y at which $F(y/\delta)=K$.

It is difficult to find the exact value of the constant, $S(1)$, because the equation for $S(1)$ includes the skin friction, the boundary layer thickness and the constants in the law of the wall equation; all of which are difficult to determine. Some experimental results are plotted as $S(y/\delta)$ against y/δ in fig. 61.

$S(1)$ is related to Coles' constant, $\phi(1)$ $\left(=\frac{u_1}{u_\tau}-\frac{1}{K}\text{LOG}_e\frac{\delta u_\tau}{\nu}\right)$ by the equation

$$S(1)=K\left(\phi(1)-B\right). \tag{30.6}$$

Coles (1961) has recalculated the majority of the published zero pressure gradient turbulent boundary layer mean flow results, and has evaluated the size of the wake component which is related to $\phi(1)$. Coles shows that the wake component, and therefore $\phi(1)$, is constant above Reynolds numbers of $R_{\delta_2}>3000$ in equilibrium flows.

Coles uses a value of 7.9 for $\phi(1)$ and values of 0.4 and 5.1 for K and B. If these are substituted into equation 30.6 then $S(1)=1.1$.

30.2 With transpiration

The equation for the inner region of a turbulent boundary layer over a porous surface with suction or injection (equ. 28.7) is

$$\frac{2u_\tau}{v_w}\left(\left(1+\frac{v_w u}{u_\tau^2}\right)^{\frac{1}{2}}-1\right)=\frac{1}{K}\text{LOG}_e\frac{yu_\tau}{\nu}+B_2\,, \tag{30.7}$$

where B_2 is, in general, a function of v_w and u_τ. The equations for the outer region are obtained by rearranging equation 30.7 to give

$$\text{LOG}_e\frac{y}{\delta}=2K\frac{u_\tau}{v_w}\left\{\left(1+\frac{v_w u}{u_\tau^2}\right)^{\frac{1}{2}}-1\right\}-BK-\text{LOG}_e\frac{u_\tau\delta}{\nu} \tag{30.8}$$

in the overlap region, and thus

$$S(y/\delta) = 2K\frac{u_\tau}{V_w}\left\{\left(1+\frac{V_w u}{u_\tau^2}\right)^{\frac{1}{2}}-1\right\} - BK - \log_e\frac{u_\tau\delta}{\nu}, \qquad (30.9)$$

and $$F(y/\delta) = 2K\frac{u_\tau}{V_w}\left\{\left(1+\frac{V_w u_1}{u_\tau^2}\right)^{\frac{1}{2}}-\left(1+\frac{V_w u}{u_\tau^2}\right)^{\frac{1}{2}}\right\} \qquad (30.10)$$

in the outer region. Equation (30.10) is the 'modified velocity defect law with suction or injection' which was discussed in section 25. The experimental results again verify that the function, $F(y/\delta)$, is the same as that in the velocity defect equation (see figs. 39 to 41). Some experimental results are plotted as $S(y/\delta)$ against y/δ in fig. 62 and are reasonably close to the zero pressure gradient curve.

30.3 <u>At separation</u>

Stratford (1959a) and Townsend (1960) show that the equation for the inner region at separation (equ. (28.10) with $B_4=0$) is

$$u = \frac{2}{K}\left(\frac{dP_1}{dx}\cdot y\right)^{\frac{1}{2}}, \qquad (30.11)$$

where $\frac{dP_1}{dx}$ is the pressure gradient. The equation, which is valid in the overlap region, is rearranged to give

$$\log_e y/\delta = 2\log_e\left(\frac{Ku}{2\delta^{\frac{1}{2}}\left(\frac{dP_1}{dx}\right)^{\frac{1}{2}}}\right) \qquad (30.12)$$

and therefore the equations for the outer region are

$$S(y/\delta) = 2\log_e\left(\frac{Ku}{2\delta^{\frac{1}{2}}\left(\frac{dP_1}{dx}\right)^{\frac{1}{2}}}\right) \qquad (30.13)$$

and $$F(y/\delta) = 2\log_e\left(\frac{u_1}{u}\right). \qquad (30.14)$$

Some of the experimental results of Schubauer and Klebanoff (1951) and Stratford (1959b) are plotted as y/δ_0 against $\frac{2}{K}\log_e \frac{u_1}{u}$ in fig. 60. The results again fall close to the zero pressure gradient curve. (The scatter is due to B_4 not being exactly zero.). The separation of turbulent boundary layers is discussed in more detail in section 31.2

To sum up, the equations for the outer region, together with the solutions for the overlap region, have been compared with experimental results in order to confirm that S and F are functions y/δ only. In the remainder of Part 2 it will be assumed that $F(y/\delta)$ and $S(y/\delta)$ are universal functions. The values for $S(y/\delta)$ which are used in the calculations are given in table 6, and were evaluated using $F(y/\delta)$ from the velocity defect curve with zero pressure gradient, together with a value for $\phi(1)$ of 1.05, which best fits the experimental results. (If it had been realised at the time that Coles' constants gave a value for $\phi(1)$ of 1.1, then this value might have been used instead of 1.05).

31. Turbulent boundary layers in a pressure gradient

31.1 The equations

The equation for the overlap region of a turbulent boundary layer in a pressure gradient (equ. 28.6) is

$$K\frac{u}{u_\tau} = 2(py+1)^{\frac{1}{2}} + \log_e\left|\frac{(py+1)^{\frac{1}{2}}-1}{(py+1)^{\frac{1}{2}}+1}\right| + B_1(u_\tau, p), \qquad (31.1)$$

where $p = -\frac{u_1}{u_\tau^3}\cdot\frac{du_1}{dx}$ and B_1 is independent of y. In section 29 it was shown that an equation for $\log_e y/\delta$, which is valid in the overlap region, is also valid in the outer region provided $\log_e y/\delta$ is replaced by $S(y/\delta)$. The equation for the outer region is therefore

$$K\frac{u}{u_\tau} = 2E + \log_e\left|\frac{E-1}{E+1}\right| + B_1(u_\tau, p), \qquad (31.2)$$

where $$E = (p\delta \exp S + 1)^{\frac{1}{2}}. \qquad (31.3)$$

At the outer edge of the boundary layer

$$K\frac{u_1}{u_\tau} = 2E_1 + \log_e\left|\frac{E_1-1}{E_1+1}\right| + B_1(u_\tau,\rho), \tag{31.4}$$

where $$E_1 = \left(\rho\delta\exp.S_1+1\right)^{\frac{1}{2}} \quad ; \quad S_1 = S(1). \tag{31.5}$$

Equation (31.2) is subtracted from equation (31.4) in order to eliminate the unknown function, B_1, and the equation is then rearranged:

$$\frac{u}{u_1} = 1 - \left\{E_1 - E + \frac{1}{2}\log_e\left|\frac{E_1-1}{E_1+1}\cdot\frac{E+1}{E-1}\right|\right\}\frac{2}{K}\frac{u_\tau}{u_1}. \tag{31.6}$$

E may be written in terms of the pressure gradient parameter, D

$$\left(D = -\frac{\delta}{u_1}\cdot\frac{du_1}{dx} = \rho\delta\left(\frac{u_\tau}{u_1}\right)^2\right),$$

$$E = \left\{D\left(\frac{u_1}{u_\tau}\right)^2\exp.S + 1\right\}^{\frac{1}{2}}. \tag{31.7}$$

Several velocity profiles, $\frac{u}{u_1}$ against y/δ, which have been calculated from equation 31.6 for particular values of D are shown in figs. 63 and 64.

31.2 Velocity profiles at separation or reattachment

When the skin friction is zero, the equation for the outer region, equation 31.6, reduces to

$$\frac{u}{u_1} = 1 - \frac{2D^{\frac{1}{2}}}{K}\left\{\exp.\frac{S_1}{2} - \exp.\frac{S}{2}\right\}, \tag{31.8}$$

where $$D = \frac{K^2}{4\exp.S_1}\left(1-\frac{B_4}{u_1}\right)^2 \quad ; \quad B_4 = \frac{B_1 u_\tau}{K}. \tag{31.9}$$

These equations are more general than those in the previous section on separation (section 30.3), where B_4 was assumed to be zero.

It is not possible to deduce the value of D at which separation or reattachment occurs because the form of B_1 is not known. However when

separation does occur in an experiment, the value of D and the velocity profile should correspond to one of the family of profiles represented by equation 31.8.

The reattachment profiles after a separation bubble which were measured by McGregor (1954) are shown in fig. 65 and the separation profile which was measured by Schubauer and Klebanoff (1951) is shown in figs. 66 and 67. Some of the zero skin friction profiles of Stratford (1959b) are shown in fig. 68. The shape of the experimental profiles are in good agreement with the theoretical curves of equation (31.8), and the theoretical values of D agree with those in the experiments

If $\frac{u}{u_1}$ from equation (31.8) is substituted into the equations for the displacement thickness, δ_1^* , and the momentum thickness, δ_2 then

$$\delta_1^* = \delta \int_0^1 \left(1 - \frac{u}{u_1}\right) d\left(y/\delta\right) = \frac{2\delta D^{\frac{1}{2}}}{K}\left(\exp.\frac{S_1}{2} - J_1\right), \qquad (31.10)$$

and

$$\delta_2 = \delta \int_0^1 \left(1 - \frac{u}{u_1}\right)\frac{u}{u_1}\, d\left(y/\delta\right)$$

$$= 2\frac{\delta D^{\frac{1}{2}}}{K}\left\{\exp.\frac{S_1}{2} - J_1 - \frac{2D^{\frac{1}{2}}}{K}\left(\exp.S_1 + J_2 - 2J_1 \exp.\frac{S_1}{2}\right)\right\}, \qquad (31.12)$$

where $J_1 = \int_0^1 \exp.\frac{S}{2}\, d\left(y/\delta\right)$ and $J_2 = \int_0^1 \exp.S.\, d\left(y/\delta\right)$. (31.13)

J_1 and J_2 are constants. The form parameter, H , at separation or reattachment is therefore

$$H = \frac{\delta_1^*}{\delta_2} = \frac{1}{1 - 5.09\, D^{\frac{1}{2}}} = \frac{1}{1 - 1.51\,\frac{\delta_1^*}{\delta}} \qquad (31.14)$$

where $$\frac{2}{K}\left(\frac{\exp.S_1 + J_2 - J_1 . 2\exp.\frac{S_1}{2}}{\exp.\frac{S_1}{2} - J_1}\right) = 5.09.$$

The errors introduced into J_1 and J_2 by neglecting differences in the sublayer region are negligible.

Separation and reattachment occur when B_4 is very nearly zero. This corresponds to a value for D of 0.0153 and a value for H of 2.69. When $B_4=0$ the equation for the velocity profile reduces to

$$\frac{u}{u_1} = \exp\left(\frac{S-S_1}{2}\right). \tag{31.15}$$

This is consistent with equation (30.14).

31.3 A hypothetical equation for the inner region

It will be assumed that B_4 at separation is zero. The equation for the overlap region (equ. 28.6) is

$$K\frac{u}{u_\tau} = 2(py+1)^{\frac{1}{2}} + \log_e \frac{(py+1)^{\frac{1}{2}}-1}{(py+1)^{\frac{1}{2}}+1} + B_1(u_\tau, p) \tag{31.16}$$

where $p = -\frac{u_1}{u_\tau^2}\cdot\frac{du_1}{dx}$. When $p \to \infty$ equation (31.16) must reduce to the zero pressure gradient 'law of the wall' equation. A simple form for B_1 which satisfies the two limiting conditions is

$$B_1(u_\tau, p) = KB - 2 + \log_e\left(1+\frac{4u_\tau}{p\nu}\right) \tag{31.17}$$

where K and B are the constants which occur in the law of the wall equation. Their product is approximately 2 (see table 7). Thus

$$B_1 \simeq \log_e\left(1+\frac{4u_\tau}{p\nu}\right). \tag{31.18}$$

If this is substituted into equation (31.16) then

$$K\frac{u}{u_\tau} = 2(py+1)^{\frac{1}{2}} + \log_e\left|\frac{(py+1)^{\frac{1}{2}}-1}{(py+1)^{\frac{1}{2}}+1}\right| + \log_e\left(1+\frac{4u_\tau}{p\nu}\right), \tag{31.19}$$

where ϕy may be written

$$\phi y = P\left(\frac{u_1}{u_2}\right)^2\left(\frac{u_1 y}{\nu}\right) \quad ; \quad P = -\frac{\nu}{u_1^2}\cdot\frac{du_1}{dx} \quad . \tag{31.20}$$

The hypothetical velocity profiles in the inner region may now be evaluated for particular values of $\frac{u_1}{u_2}$ and P. Some of the profiles, when $c_f = 0.002$ and 0.0002, are shown in figs. 69 and 70. The figures are interesting because they show that the inner region profiles with pressure gradient are almost the same as those with zero pressure gradient at the same value of skin friction. This has been shown experimentally by Ludwieg and Tillmann (1949).

31.4 The experimental results of Schubauer and Klebanoff (1951)

Schubauer and Klebanoff present some results for a boundary layer in a pressure gradient. The variation of the pressure gradient in their experiment is shown in fig. 74 in terms of the pressure gradient parameter, $D\left(=-\frac{\delta}{u_1}\frac{du_1}{dx}\right)$. For several feet, the pressure gradient parameter is larger than that at the separation point. It is now suggested that the boundary layer is adjusting itself as quickly as possible, trying to attain an energy equilibrium state, but not succeeding until the separation point is reached. It is only be separating that the boundary layer is able to modify the external flow sufficiently to reduce the external pressure gradient and thus achieve an equilibrium state.

The law of the wall (eq. 28.9) has been used to estimate the skin friction from the velocity profiles of Schubauer and Klebanoff (see figs. 71 and 72). The family of equilibrium velocity profiles for each of these values of skin friction were then plotted using equation (31.6) (Fig. 73 is given as an example). The apparent pressure gradient parameters for the velocity profiles of Schubauer and Klebanoff were then estimated from these curves. The "apparent pressure gradient parameters" are shown in fig. 74. Some of the profiles in the inner region are shown in fig. 75.

31.5 The experimental results of Clauser (1954)

Clauser measured the mean velocity profiles in turbulent boundary layers subject to two small pressure gradients. The pressure gradients were adjusted so that the mean velocity profiles at different positions along the flow collapsed onto one curve when $\frac{u_1-u}{u_\tau}$ was plotted against y/δ . The experimental curves are shown in figs. 75 and 76.

Equation (31.6) is now rearranged to give

$$\frac{u_1-u}{u_\tau} = \left(E_1 - E + \tfrac{1}{2}\log_e\left|\frac{E_1-1}{E_1+1}\cdot\frac{E+1}{E-1}\right|\right)\frac{2}{K}, \qquad (31.21)$$

where $E = \left(p\delta \exp s + 1\right)^{\frac{1}{2}}$.

This equation is used to evaluate curves of $\frac{u_1-u}{u_\tau}$ against y/δ for particular values of $p\delta$. In figs. 75 and 76 it is shown that these curves are of the same shape as those measured by Clauser.

The theoretical variations of Δ and G will now be compared with Clauser's experimental values. Δ and G are defined

$$G = \frac{\int_0^\infty \left(\frac{u_1-u}{u_\tau}\right)^2 d\left(y/\delta\right)}{\int_0^\infty \left(\frac{u_1-u}{u_\tau}\right) d\left(y/\delta\right)}, \qquad (31.22)$$

and

$$\frac{\Delta}{\delta} = \int_0^\infty \frac{u_1-u}{u_\tau}\, d\left(y/\delta\right). \qquad (31.23)$$

The displacement thickness, δ_1 , and the momentum thickness, δ_2 , are related to G and Δ by the equations

$$\delta_1 = \sqrt{\frac{c_f}{2}}\,\Delta \qquad (31.24)$$

and

$$\delta_2 = \sqrt{\frac{c_f}{2}}\left(1 - G\sqrt{\frac{c_f}{2}}\right)\Delta. \qquad (31.25)$$

The theoretical curves of $\left(\frac{u_1-u}{u_\tau}\right)$ and $\left(\frac{u_1-u}{u_\tau}\right)^2$ against y/δ, which are evaluated from equation (31.21), are integrated to obtain the variations in the parameters G and $\frac{\Delta}{\delta}$ with $\rho\delta$. (The errors which are introduced by neglecting differences in the sublayer region are small). The theoretical curves of G and $\frac{\Delta}{\delta}$ against $\rho\delta$ are shown in fig. 78, and the curve of G against $\frac{\Delta}{\delta}$ is compared with Clauser's experimental points in fig. 79.

The parameters $\rho\delta$, G and $\frac{\Delta}{\delta}$ are infinite at separation and it is often more convenient to use the parameters, N_1 and N_2, which are defined,

$$N_1 = G\sqrt{\frac{c_f}{2}} \tag{31.26}$$

and

$$N_2 = \frac{\Delta}{\delta G} \,. \tag{31.27}$$

Thus,

$$H = \frac{1}{1-N_1} \tag{31.28}$$

and

$$-\frac{\delta_2}{u_1}\cdot\frac{du_1}{dx} = N_1 N_2 (1-N_1) D \,, \tag{31.29}$$

where D is the pressure gradient parameter.

The theoretical variation of H with $-\frac{\delta_2}{u_1}\frac{du_1}{dx}$ is shown in fig. 80. It must be noted that these curves are for layers in energy equilibrium. If the boundary layer is not in equilibrium then D would be the 'apparent pressure gradient parameter', and in adverse pressure gradients the true external pressure gradient parameter would be larger than this. This is illustrated in fig. 81 where the measured pressure gradient parameters in Schubauer and Klebanoff's experiments are compared with the equilibrium theory.

Turbulent boundary layers in pressure gradients are usually not in equilibrium, and this accounts for the considerable scatter in the curves of H against D which occurs in the literature (see the review by Rotta 1962). The pressure gradient parameters are invariably based on

that of the free stream velocity gradient. However it has been shown that the boundary layer cannot adjust itself quickly enough to the external pressure gradient and it is for this reason that the 'apparent pressure gradient' has been introduced.

From equations (31.24), (31.26) and (31.27), the ratio of the displacement thickness to the boundary layer thickness is

$$\frac{\delta_1}{\delta} = N_1 N_2 \quad . \tag{31.30}$$

The theoretical curves of H against $\frac{\delta_1}{\delta}$ are presented in fig. 77 and are compared with some measurements near separation reproduced from the report by Sandborn (1959).

31.6 The experimental results of von Doenhoff and Tetervin (1943)

Von Doenhoff and Tetervin showed experimentally that curves of $\frac{u}{u_1}$ against H for particular values of y/δ_2 were almost independent of the skin friction and pressure gradient. y/δ_2 is expressed in terms of y/δ by the equation

$$y/\delta_2 = y/\delta \cdot \frac{1}{N_1 N_2 (1 - N_1)} \quad . \tag{31.31}$$

The theoretical velocity profiles of figs. 63 and 64 are used to plot curves of $\frac{u}{u_1}$ against H for particular values of the skin friction. The curves are compared with the experimental results of von Doenhoff and Tetervin in fig. 82 and with the results of Schubauer and Klebanoff in fig. 83.

The present theory is used to evaluate the curve of $\frac{u_\theta}{u_1}$ against H, and in figure 84 this is compared with the semi-empirical curves of Ludwieg and Tillmann, and Spence (see Duncan, Thom and Young 1960). u_θ is the value of u at $y = \delta_2$.

The velocity profiles, and the parameters based on the profile shapes, which are predicted by the present theory, compare extremely

well with previous theories and experimental results.

Chapter 7

Shear Stress Distributions

32. The integrated momentum equation

In the previous sections the momentum equation,

$$\frac{\partial}{\partial x}\left(\overline{u'^2}-\overline{v'^2}\right)+2u\frac{\partial u}{\partial x}+\frac{\partial \overline{u'v'}}{\partial y}=u_1\frac{du_1}{dx}+\nu\frac{\partial^2 u}{\partial y^2} \qquad (32.1)$$

was considered, and it was assumed that $\frac{\partial}{\partial x}\left(\overline{u'^2}-\overline{v'^2}\right)$, $\frac{\partial u}{\partial x}$ and $\frac{\partial v}{\partial y}$ were small in the inner region. The momentum equation therefore reduces to

$$\frac{\partial \overline{u'v'}}{\partial y}=u_1\frac{du_1}{dx}+\nu\frac{d^2u}{dy^2}-uv_w \qquad (32.2)$$

in the inner region. This equation was subsequently solved by making certain approximations and an equation for the mean flow in the overlap region was obtained. The dimensional equations for the outer region were then used to derive the equation for the velocity distribution in the outer region. The outer region includes the logarithmic overlap region, and by comparison with experimental velocity profiles, is valid for almost all of the boundary layer; all except the region very close to the wall where y/δ is less than about 0.02. (Excluding boundary layers with suction which have a relatively large sublayer and in this case the outer solution is only valid to about $0.06\,y/\delta$.)

Variations in the x-direction will now be considered by substituting the outer region velocity distribution into an integrated momentum equation. The errors which are introduced by neglecting the differences in the sublayer region are insignificant. The term $\frac{\partial}{\partial x}\left(\overline{u'^2}-\overline{v'^2}\right)$ in equation (32.1) is usually small and will be neglected in the following analysis.

In order to obtain the integrated momentum equation, first of all the continuity equation, $\frac{\partial u}{\partial x} + \frac{\partial v}{\partial y} = 0$, is substituted into the momentum equation (32.1) and the resulting equation is integrated with respect to y giving

$$\int_0^y \frac{\partial u^2}{\partial x} dy + uv = u_1 \frac{du_1}{dx} y + \frac{\tau}{\rho} - \frac{\tau_w}{\rho} . \qquad (32.3)$$

(τ is the total shear stress $\left(= \mu \frac{\partial u}{\partial y} - \rho \overline{u'v'} \right)$). The continuity equation is integrated with respect to y to give

$$v = - \int_0^y \frac{\partial u}{\partial x} . dy + v_w , \quad \text{and} \qquad (32.4)$$

the resulting equation is substituted into equation 32.3. Thus

$$\frac{\tau}{\rho} = \frac{\tau_w}{\rho} + v_w u - u_1 \frac{du_1}{dx} y + \int_0^y \frac{\partial u^2}{\partial x} dy - u \int_0^y \frac{\partial u}{\partial x} . dy , \qquad (32.5)$$

or $$\frac{\tau}{\rho} = \frac{\tau_w}{\rho} + v_w u - u_1 \frac{du_1}{dx} y + 2 \int_0^\eta u \frac{\partial u}{\partial x} \delta \, d\eta - u \int_0^\eta \frac{\partial u}{\partial x} \delta \, d\eta \qquad (32.6)$$

where $\eta = y/\delta$. It is convenient to write $\frac{\partial u}{\partial x}$ in the form:

$$\frac{\partial u}{\partial x} = \frac{du_1}{dx} + \frac{\partial (u - u_1)}{\partial \xi} . \frac{d\xi}{dx} + \frac{\partial (u - u_1)}{\partial \eta} \frac{\partial \eta}{\partial x} , \qquad (32.7)$$

where ξ is a function of x only. The free stream velocity, u_1 , and the boundary layer thickness, δ , are also functions of x only and therefore $\frac{\partial u_1}{\partial \eta} = 0$ and $\frac{\partial \eta}{\partial x} = - \frac{y}{\delta^2} \frac{d\delta}{dx} = - \frac{\eta}{\delta} \frac{d\delta}{dx}$.
Thus, equation (32.7) may be written,

$$\frac{\partial u}{\partial x} = \frac{du_1}{dx} + \frac{\partial (u - u_1)}{\partial \xi} \frac{\partial \xi}{\partial x} - \frac{\eta}{\delta} \frac{\partial u}{\partial \eta} \frac{d\delta}{dx} . \qquad (32.8)$$

This expression for $\frac{\partial u}{\partial x}$ is substituted into the integrated momentum equation (32.6) and the equation is rearranged:

$$\frac{\tau}{\rho} = \frac{\tau_w}{\rho} + V_w u + \frac{du_1}{dx}\left\{2\delta\int_0^\eta u\,d\eta - uy - u_1 y\right\} + \frac{d\xi}{dx}\left\{2\delta\int_0^\eta u\,\frac{\partial(u-u_1)}{\partial\xi}d\eta - \delta u\int_0^\eta \frac{\partial(u-u_1)}{\partial\xi}\,d\eta\right\} + \frac{d\delta}{dx}\left\{\int_0^\eta u^2 d\eta - u\int_0^\eta u\,d\eta\right\}. \tag{32.9}$$

In the following sections this equation will be used to evaluate the shear stress distributions in boundary layers at separation and with suction or injection.

33. Boundary layers with suction or injection

The equation for the outer region of turbulent boundary layers with suction or injection in zero pressure gradient (equ. 25.8) may be written,

$$\frac{u}{u_1} = 1 - \frac{F(y/\delta)}{K\xi}\left(1 + \frac{V_w}{u_1}\xi^2\right)^{\frac{1}{2}} + \frac{F^2(y/\delta)}{4K^2}\cdot\frac{V_w}{u_1}, \tag{33.1}$$

where $\frac{V_w}{u_1}$ is constant and $\xi = \frac{u_1}{u_2}$. Thus

$$\frac{1}{u_1}\frac{\partial(u-u_1)}{\partial\xi} = F(\eta)\,V_1(\xi) \tag{33.2}$$

where $$V_1(\xi) = \frac{1}{K}\left(\frac{1}{\xi^2}\left(1 + \frac{V_w}{u_1}\xi^2\right)^{\frac{1}{2}} - \frac{V_w}{u_1}\left(1 + \frac{V_w}{u_1}\xi^2\right)^{-\frac{1}{2}}\right). \tag{33.3}$$

Equation (32.9) can therefore be written in the form,

$$\frac{\tau}{\rho u_1^2} = \frac{\tau_w}{\rho u_1^2} + \frac{V_w u}{u_1^2} + \frac{d\xi}{dx}\cdot\delta\cdot\left\{2V_1(\xi)\int_0^\eta \frac{u}{u_1}F(\eta)\,d\eta - \frac{u}{u_1}V_1(\xi)\int_0^\eta F(\eta)\,d\eta\right\} + \frac{d\delta}{dx}\left\{\int_0^\eta\left(\frac{u}{u_1}\right)^2 d\eta - \frac{u}{u_1}\int_0^\eta \frac{u}{u_1}\,d\eta\right\}, \tag{33.4}$$

and by using equation (33.1) to eliminate $\frac{u}{u_1}$ in equation (33.4), an equation is obtained for the shear stress distribution in terms of the four integrals,

$$\left(C_n = \int_0^{\eta} F^n(\eta)\, d\eta\right)_{n=1,2,3,4.} \tag{33.5}$$

The integrals have been evaluated numerically and are shown in fig. 50.

When $y = \delta$ equation (33.4) reduces to

$$0 = \frac{c_f}{2} + \frac{v_w}{u_1} + \frac{d\xi}{dx}\,\delta\left\{2V_1(\xi)\int_0^{\eta}\frac{u}{u_1}F(\eta)\,d\eta - V_1(\xi)\int_0^{1}F(\eta)\,d\eta\right\}$$

$$+ \frac{d\delta}{dx}\left\{\int_0^1\left(\frac{u}{u_1}\right)^2 d\eta - \frac{u}{u_1}\int_0^1\frac{u}{u_1}\,d\eta\right\}. \tag{33.6}$$

This equation relates the terms $\delta\frac{d\xi}{dx}$ and $\frac{d\delta}{dx}$. Thus, if the skin friction coefficient, c_f, and the transpiration velocity ratio, $\frac{v_w}{u_1}$, are specified then the shear stress distribution, $\frac{\tau}{\rho u_\tau^2}$, through the boundary layer for different values of $\frac{d\delta}{dx}$ may be evaluated.

The equation which relates the growth of the boundary layer to the change in skin friction (equ. 30.9) is

$$S(1) = 2K\frac{u_\tau}{v_w}\left\{\left(1 + \frac{v_w u_1}{u_\tau^2}\right)^{\frac{1}{2}} - 1\right\} - KB_2 - \log_e\frac{u_\tau\delta}{\nu}. \tag{33.7}$$

In section 19 it was shown that K and B are approximately constant and therefore take their values for the case $v_w = 0$ over the range of transpiration velocities which result in a measurable skin friction. The equation for δ is obtained by rearranging equation (33.7):

$$\delta = \frac{\xi}{\zeta}\frac{\nu}{u_1}\exp\left(2K\frac{u_1}{v_w}\frac{1}{\zeta}\left\{\left(1 + \frac{v_w}{u_1}\zeta^2\right)^{\frac{1}{2}} - 1\right\} - KB - S(1)\right). \tag{33.8}$$

Therefore $$\frac{d\delta}{dx} = \frac{\delta}{\xi}\frac{d\xi}{dx}\left\{1 + 2KV_2\left(\frac{\xi}{\delta}\right)\right\}, \qquad (33.9)$$

where $$V_2\left(\frac{\xi}{\delta}\right) = \frac{\xi}{\delta}\left(1 + \frac{V_w}{u_1}\frac{\xi^2}{\delta}\right)^{-\frac{1}{2}} - \frac{u_1}{V_w}\frac{1}{\frac{\xi}{\delta}}\left\{\left(1 + \frac{V_w}{u_1}\frac{\xi^2}{\delta}\right)^{\frac{1}{2}} - 1\right\}. \qquad (33.10)$$

If this equation for $\frac{d\delta}{dx}$ is used, together with the previous equation for the shear stress distribution, then $\frac{\tau}{\rho u_1^2}$ becomes a function of c_f and $\frac{V_w}{u_1}$ only. A shear stress distribution which corresponds to B = constant is shown in fig. 85 and compares favourably with the curve calculated by Leadon (1961) from the experimental results of Mickley and Davis (1957).

Shear stress distributions with suction are shown in fig. 87 and they are of the same shape as that calculated from experimental results by Dutton (1960).

If the blowing velocity ratio is large ($\frac{V_w}{u_1} > 0.005$) then the skin friction is small and $\frac{V_w}{u_1}\frac{\xi^2}{\delta} \gg 1$. In this case equations (33.1), (33.2) and (33.3) simplify to

$$\frac{u}{u_1} = \left(1 - \frac{F}{2K}\left(\frac{V_w}{u_1}\right)^{\frac{1}{2}}\right)^2, \qquad (33.11)$$

and $$V_1\left(\frac{\xi}{\delta}\right) = 0 = \frac{1}{u_1}\cdot\frac{\partial(u-u_1)}{\partial\frac{\xi}{\delta}}. \qquad (33.12)$$

The shear distribution is now fully defined by the equations

$$\frac{\tau}{\rho u_1^2} = \frac{c_f}{2} + \frac{V_w}{u_1}\cdot\frac{u}{u_1} + \frac{d\delta}{dx}\left\{\int_0^{\eta}\left(\frac{u}{u_1}\right)^2 d\eta - \frac{u}{u_1}\int_0^{\eta}\frac{u}{u_1}\,d\eta\right\}, \qquad (33.13)$$

and (when $y/\delta = 1$)

$$0 = \frac{c_f}{2} + \frac{V_w}{u_1} + \frac{d\delta}{dx}\left\{\int_0^{1}\left(\frac{u}{u_1}\right)^2 d\eta - \int_0^{1}\frac{u}{u_1}\,d\eta\right\}. \qquad (33.14)$$

The boundary layer growth, $\frac{d\delta}{dx}$, is governed primarily by the blowing velocity ratio, $\frac{v_w}{u_1}$: the skin friction has a negligible effect.

Equations (33.13) and (33.14) were used to calculate the shear stress distributions shown in fig. 86.

34. Boundary layers in a pressure gradient

The equation for the mean velocity in turbulent boundary layers in a pressure gradient but without suction or injection (equ. 31.6) is

$$\frac{u}{u_1} = 1 - \left\{ E_1 - E + \frac{1}{2} \log_e \left| \frac{E_1 - 1}{E_1 + 1} \cdot \frac{E+1}{E-1} \right| \right\} \frac{2}{K} \frac{u_\tau}{u_1} , \qquad (34.1)$$

where $$E = \left(p\delta \exp .S + 1 \right)^{\frac{1}{2}} . \qquad (34.2)$$

If $\xi = p\delta = -\frac{u_1}{u_\tau^2} \cdot \delta \cdot \frac{du_1}{dx}$, (this satisfies the condition $\xi = \xi(x)$)

then $$\frac{\partial (u-u_1)}{\partial \xi} = \left(-\frac{E_1}{p\delta} + \frac{E}{p\delta} \right) \frac{u_\tau}{K} - \left(\frac{u-u_1}{u_\tau} \right) \frac{\partial u_\tau}{\partial p\delta} \cdot \frac{1}{K} . \qquad (34.3)$$

$p\delta$ is not a particularly useful variable because $p\delta \to \infty$ as separation is approached. Equation (34.3) will now be written in terms of

$D \left(= -\frac{\delta}{u_1} \frac{du_1}{dx} = p \frac{\delta u_\tau^2}{u_1^2} \right)$. Thus

$$\frac{\partial (u-u_1)}{\partial \xi} \cdot \frac{d\xi}{dx} = (E_1 - E) \frac{u_\tau}{K} \left(\frac{1}{D} \cdot \frac{dD}{dx} - \frac{2D}{\delta} \right) - \frac{1}{K} \log_e \left| \frac{E_1 - 1}{E_1 + 1} \cdot \frac{E+1}{E-1} \right| du_\tau / dx \qquad (34.4)$$

where E in terms of D is

$$E = \frac{1}{u_\tau} \left(D u_1^2 \exp .S + u_\tau^2 \right)^{\frac{1}{2}} . \qquad (34.5)$$

Either equation (34.3) or (34.4) may be used together with equation (32.9) to evaluate the shear stress distribution through the boundary layer.

If the skin friction is very small ($u_\tau \to 0$) then the

equations simplify considerably:

$$\frac{u}{u_1}_{\text{as } u_2 \to 0} = 1 - \frac{2D^{\frac{1}{2}}}{K}\left(\exp\frac{S_1}{2} - \exp\frac{S}{2}\right), \tag{34.6}$$

and $$\left(\frac{\partial(u-u_1)}{\partial\xi}\cdot\frac{d\xi}{dx}\right)_{\text{as } u_2 \to 0} = -(u_1-u)\left(\frac{1}{2D}\cdot\frac{dD}{dx} - \frac{D}{\delta}\right). \tag{34.7}$$

Equation (34.7) is substituted into the equation for the shear stress distribution (equ. 32.9). Thus

$$\frac{\tau}{\rho u_1^2} = \frac{\delta}{u_1}\frac{du_1}{dx}\left\{-\eta - \frac{u}{u_1}\eta + 2\int_0^\eta \frac{u}{u_1}\,d\eta\right\} +$$

$$\left(\frac{\delta}{2D}\cdot\frac{dD}{dx} - D\right)\left\{-2\int_0^\eta\left(1-\frac{u}{u_1}\right)\frac{u}{u_1}\,d\eta + \frac{u}{u_1}\int_0^\eta\left(1-\frac{u}{u_1}\right)d\eta\right\} +$$

$$\frac{d\delta}{dx}\left\{\int_0^\eta\left(\frac{u}{u_1}\right)^2 d\eta - \frac{u}{u_1}\int_0^\eta\frac{u}{u_1}\,d\eta\right\}, \tag{34.8}$$

or $$\frac{\tau}{\rho u_1^2} = D\left\{\eta - 2J_4 + \frac{u}{u_1}J_3\right\} + N\left\{J_4 - J_3 - \frac{u}{u_1}\frac{J_3}{2} + \frac{1}{2}\frac{u}{u_1}\eta\right\}$$

$$+ \frac{d\delta}{dx}\left\{J_4 - J_3\frac{u}{u_1}\right\}, \tag{34.9}$$

where $$N = \frac{\delta}{D}\cdot\frac{dD}{dx}, \quad J_3 = \int_0^\eta\frac{u}{u_1}\,d\eta \quad \& \quad J_4 = \int_0^\eta\left(\frac{u}{u_1}\right)^2 d\eta. \tag{34.10}$$

Equation (34.9) gives the shear stress distribution through turbulent boundary layers at separation , at reattachment and with negligible wall shear stress.

The shear stress distributions in fig. 88 have been calculated for the conditions $N = 0$ and 0.1, and $D = 0.013$. This value of D corresponds to that of the separation profile measured by Schubauer and Klebanoff (1951). It is significant that the theoretical shear stress curve for $N = 0$ is close to Schubauer and Klebanoff's experimental points, because the present theory is expected to correspond to equilibrium conditions, and true equilibrium conditions correspond to very small changes in the x-direction and therefore $N\left(= \frac{\delta}{D}\frac{dD}{dx}\right) \simeq 0$.

It has been suggested by Coles (1956) and Rotta (1962) that the shear stress measurements of Schubauer and Klebanoff are about 30% too high. If this is the case then the present theoretical curves do not compare quite so well with the experimental measurements as they would appear to do in fig. 88. However Newman's (1951) shear stress measurements at separation are even higher than those of Schubauer and Klebanoff.

It must be noted that the terms containing the turbulent velocity components, apart from the $\overline{u'v'}$ term, have been neglected in the integrated momentum equation : in particular the integral, $\int_0^{\eta} \frac{\partial \overline{u'^2}}{\partial x} d\eta$ has not been included in the calculations. However the contribution from these terms is probably small.

35. Suggestions for Future Work

An 'apparent pressure gradient', D_{APP}, has been introduced when considering non-equilibrium boundary layers with an external pressure gradient parameter, D_{EXT}. It would be useful to measure velocity profiles in various pressure gradients in order to find the relation between $\frac{dD_{EXT}}{dx}$ and $\frac{dD_{APP}}{dx}$, and the experiments may help in formulating a theory.

A recent report by Libby et al (1964) considers equilibrium boundary layers in pressure gradients, and a theory is outlined which enables velocity profiles to be defined by two parameters S_L and η_1. ($S_L = \left(\frac{\tau_w}{\tau}\frac{\partial}{\partial\eta}\cdot\frac{\tau}{\tau_w}\right)_{\eta=\eta_1}$ and $\eta = y/\delta$). Libby considers the

self preserving flows obtained by Clauser (1954) and by Ludwieg and Tillmann (1949) and those which exist for zero pressure gradient. (A self preserving flow is one which satisfies the equation

$$\frac{u_1 - u}{u_\tau} = f\left(y/\delta\right) \tag{35.1}$$

where $f(y/\delta)$ is the same function for all the velocity profiles in the flow. $f(y/\delta)$ may differ from one self preserving flow to another.) The values of S_L and η_1 are chosen so that the theoretical profile is the same shape as that of a self preserving set of profiles. The theoretical profile is then used together with the momentum integral equation to calculate the variations of c_f, δ and u_1 along the flow. The theoretical variations are shown to agree with the experiments. The present outer region theory may be used to preduct the velocity profiles, and it is suggested that these are used with the momentum integral equation in place of the profiles used by Libby.

PART III

TURBULENT FLOW IN A POROUS PIPE

36. Introduction

The turbulent structure in a pipe is different from that in a boundary layer. For example boundary layers have a region at their outer edge which exhibits intermittency, i.e. the flow is partly rotational and partly irrotational, whereas in fully developed turbulent pipe flow there is no intermittency. Also the turbulence in pipe flow is constrained between the walls whereas that in a boundary layer may increase or decrease depending on the external pressure gradient. The mean velocity profiles in a fully developed turbulent pipe flow are the same at different positions along the pipe and the pressure gradient and the skin friction are constant.

Yuan et al (1957, 1958, 1961) studied the effect of injection through a porous walled pipe into fully developed turbulent pipe flow. A 5-inch diameter porous stainless steel pipe 24 inches in length was connected as part of a long 5-inch diameter pipe. Pitot tube and thermocouple traverses were made and the velocity and temperature distributions were shown to compare reasonably well with an approximate theory in the outer region. The theory was based on the mixing length hypothesis and the boundary conditions were applied at the centre of the pipe.

The present experiments in the Aeronautical Laboratory at Queen Mary College show how the mean flow is altered when there is suction through a porous section of a pipe. First of all an approximate theory will be presented, the experiments will then be described and the results will be compared with the theory.

Chapter 1

Theory

37. The continuity and the momentum equation

The boundary layer or viscous flow equations of continuity and momentum for axisymmetric incompressible flow, in cylindrical coordinates (x, r) have the following forms (see Laufer 1954) :

$$\frac{\partial u}{\partial x} + \frac{1}{r}\frac{\partial r V_r}{\partial r} = 0 \quad , \tag{37.1}$$

$$u\frac{\partial u}{\partial x} + V_r\frac{\partial u}{\partial r} = -\frac{dP_1}{dx} - \frac{\partial \overline{u'^2}}{\partial x} - \frac{1}{r}\frac{\partial r\overline{u'v'_r}}{\partial r} + \nu\frac{\partial^2 u}{\partial r^2} + \frac{\nu}{r}\frac{\partial u}{\partial r}, \tag{37.2}$$

where V_r is the mean velocity in the r-direction. The term $\frac{\partial \overline{u'^2}}{\partial x}$ in this equation will be small, as it is in turbulent boundary layers, and it is neglected in the following analysis.

The boundary conditions for fully developed turbulent pipe flow with suction or injection through the wall are:

(i) at $r = 0$

$$\overline{u'v'_r} = 0 \ , \ V_r = 0 \ , \ u = u_1 \ \ \& \ \ \frac{\partial u}{\partial r} = 0$$

(ii) at $r = a$, where a is the radius of the pipe,

$$\overline{u'v'_r} = 0 \ , \ V_r = (V_r)_w \ , \ u = 0$$

$$\text{and } \nu\frac{\partial u}{\partial r} = -u_\tau^2 \ . \tag{37.3}$$

$$\text{Now } \frac{\partial r V_r u}{\partial r} = u\frac{\partial r V_r}{\partial r} + r V_r\frac{\partial u}{\partial r} \tag{37.4}$$

$$\text{and } \frac{1}{r}\left(\frac{\partial}{\partial r}\cdot r\left(\overline{u'v'_r} - \nu\frac{\partial u}{\partial r}\right)\right) = \frac{1}{r}\frac{\partial}{\partial r}\left(r\overline{u'v'_r}\right) - \nu\frac{\partial^2 u}{\partial r^2} - \frac{\nu}{r}\frac{\partial u}{\partial r} \ . \tag{37.5}$$

Equation (37.4) is rearranged and the continuity equation is used to eliminate $\frac{\partial r v_r}{\partial r}$, thus

$$\frac{1}{r}\frac{\partial r v_r u}{\partial r} + u\frac{\partial u}{\partial x} = v_r \frac{\partial u}{\partial r} . \qquad (37.6)$$

Equations (37.5) and (37.6) are added to the momentum equation (37.2) to give

$$2u\frac{\partial u}{\partial x} + \frac{1}{r}\frac{\partial r v_r u}{\partial r} = -\frac{dP_i}{dx} - \frac{1}{r}\left(\frac{\partial}{\partial r} r\left(\overline{u'v_r'} - \nu\frac{\partial u}{\partial r}\right)\right) \qquad (37.7)$$

which is multiplied by r and integrated with respect to r from 0 to a to give the following integrated momentum equation :

$$\frac{\partial}{\partial x}\int_0^a r u^2 dr = \frac{dP_i}{dx}\cdot\frac{a^2}{2} - a u_z^2 . \qquad (37.8)$$

The equation can be rewritten in terms of y, where $y(=a-r)$ is the distance from the wall,

$$\frac{2a}{u_i^2}\frac{\partial}{\partial x}\left(u_i^2\int_a^a \left(1-\tfrac{y}{a}\right)\left(\frac{u}{u_i}\right)^2 d\left(\tfrac{y}{a}\right)\right) = -\left(\frac{1}{\frac{1}{2}u_i^2}\frac{dP_i}{dx}\right)\frac{a}{2} - c_f \qquad (37.9)$$

Similarly the continuity equation (37.1) is multiplied by r and integrated from $r=0$ to a, thus

$$\frac{\partial}{\partial x}\int_0^a r u\, dr = a(v_r)_{w,} \qquad (37.10)$$

$$\text{or}\quad a\frac{\partial}{\partial x} u_i \int_0^a \frac{u}{u_i}\left(1-\tfrac{y}{a}\right) d\left(\tfrac{y}{a}\right) = v_w . \qquad (37.11)$$

where v is the velocity in the y direction. When v_w is zero the velocity profiles are similar, $\frac{dR}{dx}$ is constant, and equation (37.9) reduces to the well known equation relating the pressure drop along a pipe to the skin friction, namely

$$c_f = -\frac{a}{2}\left(\frac{1}{\frac{1}{2}u_i^2}\cdot\frac{dP_i}{dx}\right) . \qquad (37.12)$$

38. An approximate solution for the inner region

The theory follows that used for the turbulent boundary layer. It is assumed that the terms $\frac{\partial u}{\partial x}$ and $\frac{\partial r v_r}{\partial r}$ are negligibly small in the inner region compared with the other terms in the momentum equation, which therefore simplifies to

$$\frac{\partial r v_r u}{\partial r} = -r\frac{dP_i}{dx} - \frac{\partial}{\partial r}\left(\frac{r\tau}{\rho}\right) \tag{38.1}$$

where the shear stress, τ is $\rho\overline{u'v_r'} - \mu\frac{\partial u}{\partial r}$. The continuity equation implies that

$$r v_r = a(v_r)_w . \tag{38.2}$$

Equation (38.1) is integrated,

$$r v_r u = -\frac{r^2}{2}\frac{dP_i}{dx} - \frac{r\tau}{\rho} + \text{constant} = a(v_r)_w , \tag{38.3}$$

and when $r = a$ this reduces to

$$0 = -\frac{a^2}{2}\frac{dP_i}{dx} - \frac{a\tau_w}{\rho} + \text{constant} . \tag{38.4}$$

Equation (38.4) is subtracted from (38.3) to give

$$r v_r u = a(v_r)_w u = (a^2 - r^2)\frac{dP_i}{dx}\cdot\frac{1}{2} - \frac{r\tau}{\rho} + \frac{a\tau_w}{\rho} , \tag{38.5}$$

or, in terms of y ,

$$-a v_w u = y(2a - y)\frac{dP_i}{dx}\cdot\frac{1}{2} - (a - y)\frac{\tau}{\rho} + \frac{a\tau_w}{\rho} . \tag{38.6}$$

This equation is more complicated than that obtained for the boundary layer flow. However if it is assumed that y is small compared with the radius of the pipe, it reduces to:

$$\frac{\tau}{\rho} = y\frac{dP_i}{dx} + v_w u + \frac{\tau_w}{\rho} , \tag{38.7}$$

which is the same as that for boundary layer flow. Again it will be assumed that

$$\frac{y}{\left(\frac{\tau}{\rho}\right)^{\frac{1}{2}}} \cdot \frac{du}{dy} = K \tag{38.8}$$

where K is von Kármán's constant, so that equation (38.7) becomes

$$y\frac{du}{dy} = K\left(y\frac{dP_1}{dx} + v_w u + \frac{\tau_w}{\rho}\right)^{\frac{1}{2}}. \tag{38.9}$$

Equation (38.9) is non-linear and only two special linear cases will be considered: (i) when $v_w = 0$ and (ii) when $\frac{dP_1}{dx} = 0$.

(i) <u>When $v_w = 0$</u> the solution of equation (38.9) is (see section 28):

$$K\frac{u}{u_\tau} = 2(py+1)^{\frac{1}{2}} + \log_e\left|\frac{(py+1)^{\frac{1}{2}}-1}{(py+1)^{\frac{1}{2}}+1}\right| + B_1(u_\tau, p) \tag{38.10}$$

where $p = \frac{1}{u_\tau^2}\frac{dP_1}{dx}$, and B_1 is independent of y. However for fully developed turbulent pipe flow, from equation (36.12),

$$\frac{y}{\rho}\frac{dp}{dx} = -\frac{2y}{a}\frac{\tau_w}{\rho} \tag{38.11}$$

and therefore, consistent with the previous assumption that y is small compared with a, equation (38.9) reduces to

$$y\frac{du}{dy} = K\left(\frac{\tau_w}{\rho}\right)^{\frac{1}{2}} = K u_\tau \tag{38.12}$$

which has the solution

$$\frac{u}{u_\tau} = \frac{1}{K}\log_e\frac{y u_\tau}{\nu} + B \tag{38.13}$$

where B is a constant. This is of course the 'law of the wall' equation. Values of 0.4 and 5.1 will be used for K and B in the calculations for pipe flow.

(ii) When $\frac{dp_1}{dx} = 0$ the solution of equation (38.9) is

$$\frac{2u_\tau}{v_w}\left(\left(1 + \frac{v_w u}{u_\tau^2}\right)^{\frac{1}{2}} - 1\right) = \frac{1}{k} \log_e \frac{y u_\tau}{\nu} + B_2 (v_w, u_\tau) \qquad (38.14)$$

where B_2 is independent of y.

When there is suction through a permeable section of the pipe the pressure gradient is reduced and the skin friction is increased. Consequently, consistent with the assumption that y is small compared with a, equation (38.14) should be a reasonable solution for all moderate suction velocities. (Obviously if the suction velocity is too large the original assumptions made in reducing the Navier Stokes equations to the boundary layer equations will be invalid.)

When air is forced through the permeable wall into the pipe, the pressure gradient increases and the skin friction is reduced. In this case the pressure gradient term in equation (37.9) will increase to become of comparable magnitude to the skin friction term and therefore equation (38.14) will not be valid with injection.

Chapter 2

Suction Experiments in Fully Developed Turbulent Pipe Flow

39. Apparatus

The apparatus is shown in figures 89 to 92. A 36 foot length of 3.625 inches internal diameter steel pipe was connected at its downstream end with a flexible tube to a D.C. centrifugal fan (220 V, 26 amp.) Air entered the pipe through a cylindrical air clearer made from Vyon, a porous plastic sheet material. Vyon, which is manufactured by Porous Plastics Limited, retains particles down to about 25 microns.

25 feet downstream of the inlet there was a 32 inch porous section, which consisted of 4 interlocking 8 inch lengths of porosint similar to those used in the boundary layer experiment described in Part 2.

The porous section of the pipe was enclosed by a chamber consisting of a 3 foot length of 1 foot diameter pipe with end plates. The chamber was connected by means of six $1\frac{3}{8}$ inch rubber tubes to a six inch diameter flexible tube attached to a D.C. centrifugal fan (220 V. 6 amp.) which provided a pressure difference across the porous tube up to a maximum of 19 inches of water.

Static pressure tappings, each consisting of a small piece of 1/16 inch outside diameter brass tube cemented into a hole in the pipe or porous tube so that it fitted flush with the inside surface, were placed at 1 foot intervals along the pipe upstream of the porous section and at intervals of $2\frac{3}{8}$ inches along the porous section. A pitot tube or a static tube was fixed to a micrometer screw traversing gear which could be positioned at any of four stations along the suction chamber. The details of the traversing gear and one of the stations are shown in figure 92. The pitot or static tube passed through a shaped piece of tufnol which was fixed with araldite to the body of the suction chamber and also to a slot $1\frac{3}{8}$" by $\frac{1}{8}$" in the porous tube. Air could only enter the suction chamber by passing through 3/16" of porosint. A suction velocity of 0.25 ft./sec. through the porous tube required a pressure drop of 15 inches of water across the tube and consequently the small changes in static pressure along the pipe did not cause significant variations in the suction velocity. Another traversing micrometer was positioned 3 feet upstream of the porous section. The pressure drop across the porous tube was measured from one tube of a vertical multi-tube manometer and the static and pitot pressures were measured on an inclined multitube manometer which was calibrated against a Betz manometer.

The pitot tube was electrically insulated from the traversing micrometer and the suction chamber, and it was arranged so that an electric circuit was completed as the pitot tube touched the porous wall. The pitot tube and the static tube are the same as those used in the boundary layer experiment.

A disc inserted between two of the pipes 2 feet from the

inlet protruded 1/16" into the pipe to act as a trip device to ensure a fixed transition from laminar to turbulent flow.

40. Experimental results

Static tube traverses across the porous tube did not detect any change in pressure, even with the maximum suction velocities. The static tube confirmed that the pressure tappings along the porous tube were not affected by the suction velocities. The static pressure at the first tapping downstream of the suction chamber was almost independent of changes in the suction velocity, and this tapping was used as a datum i.e. throughout a set of traverses at different stations along the pipe for a particular suction velocity, this static pressure was kept constant by adjusting the speed of the fan connected downstream of the pipe.

The pitot tube was traversed across the pipe at each of the five stations along the pipe for suction velocities ranging from 0 to 0.275 ft/sec. During one set of traverses at different suction velocities, the datum static pressure was kept constant and during the other set of traverses the suction velocity was adjusted so that there was zero pressure gradient along the porous tube. The static pressure variations along the pipe are shown in figure 93, and the velocity distributions along the centre line of the pipe are shown in figure 94.

The mean velocity profiles at the station upstream of the suction chamber are compared with the 'law of the wall', equation (38.13) in figure 95. The skin friction indicated by the law of the wall equation agrees with that calculated from the pressure drop along the pipe using equation (37.12). The measured velocity profiles fall on the universal outer region curve for fully developed turbulent pipe flow (fig. 96.).

The velocity profiles at the stations along the suction chamber are shown in figures 97 to 99. Curves of $\frac{u}{u_1}\left(1-y/a\right)$ against y/a (fig. 100), and $\left(\frac{u}{u_1}\right)^2\left(1-y/a\right)$ against y/a (fig. 101) were plotted and, using equations (37.11) and (37.9), the suction velocity and the skin

friction were evaluated. The pressure distribution along the porous section is not uniform because the bore of the tubes are tapered by as much as 0,015". The variations in the pressure gradient cause uncertainties of ± 15% in the value of the skin friction coefficients.

Figure 102 shows the velocity profiles at different positions along the pipe when the suction velocity was 0.274 ft/sec. The lower curve corresponds to fully developed turbulent pipe flow with zero suction, the next curve is the velocity profile 6 inches after the beginning of the porous section, the next after 14inches, then 22 inches and the higher curve is the profile 30 inches after the beginning of the porous section. It can be seen that the velocity profile changes very quickly near to the wall but changes more slowly towards the outer region. There is the added complication that the ratio $\left|\frac{V_w}{u_1}\right|$ increases along the porous tube because the velocity u_1 decreases from 88 to 78 ft./sec. An increase of $\left|\frac{V_w}{u_1}\right|$ would give a higher velocity ratio $\frac{u}{u_1}$ at a particular distance from the wall and the changes in $\frac{u}{u_1}$ between the last three stations could be due to this effect.

In figures 103 and 104 the measured velocity profiles are compared with the inner region equation (38.14) (assuming that B_2 is equal to its zero suction value i.e. $B_2 = B$). The agreement is very good for the lower suction velocities but gradually, as the suction velocity is increased, the theory becomes less favourable. The differences between theory and experiment could be due to curvature effects (in the theory it was assumed that y was negligibly small compared with a) or to pressure gradient effects, but is more probably due to $\left|\frac{V_w}{u_1}\right|$ increasing along the porous section. The latter effect is indicated by the following diagram:

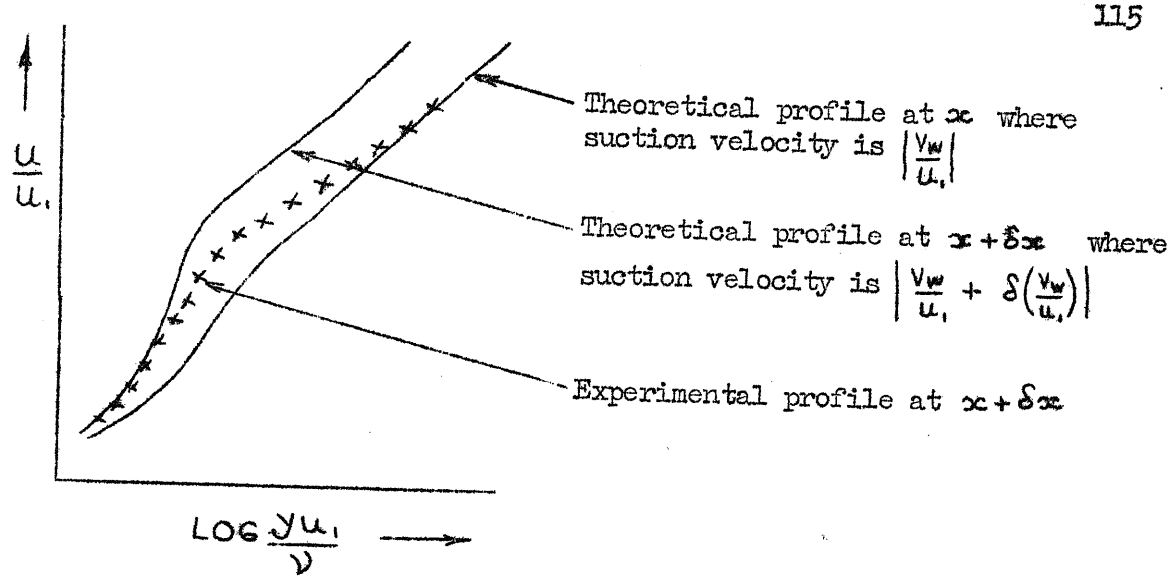

The diagram shows a velocity profile satisfying local conditions near to the wall but being influenced by upstream conditions towards the outer region.

In the region near the wall the effect of suction is just the same as that in turbulent boundary layers. Suction removes mass from the wall region but it does not remove momentum in the x-direction. The momentum is dissipated in the form of heat by the viscosity and therefore there are higher velocity gradients and therefore a fuller velocity profile i.e. the velocity u at a particular value of y is higher with suction than without suction.

The experimental rig used for the suction experiments has been used for provisional injection experiments by connecting the chamber to a compressed air supply. The effect of injection on the velocity profiles is shown in figs. 99, 100, 101, and 105.

The suction chamber has also been positioned near to the inlet of the pipe in order to study boundary layers with suction in the entry length. Some of the velocity profiles are shown in fig. 106. More detailed experiments in the entry length and with injection are planned.

41. Suggestions for Future Work

It is suggested that the outer region boundary layer analysis

be extended to the flow near the centre line of a pipe. The universal function, $S(y/\delta)$, will obviously not apply to pipe flow, where there is no intermittency, but a function of y/a will probably exist which enables the velocity profiles in pipe flow to collapse onto one curve. The analysis will be quite simple for pipe flow without suction or injection and for pipe flow with suction but with zero pressure gradient. However the analysis will be far more complicated in other cases, i.e. when the non-linear inner region equation has to be solved. The analysis will enable flows in slowly diverging or converging circular ducts to be predicted, and possibly will predict separation of a fully developed flow in a diverging duct. It will be interesting to calculate the shear stress distribution across the pipe with and without suction.

CONCLUSIONS

1. Laminar Theory

Approximate integral equations have been derived for the compressible laminar boundary layer with arbitrary pressure gradient. and arbitrary suction or injection velocities through a porous wall. In particular the incompressible forms of the integral equations have been solved for similarity flow and for flat plate flow with continuous suction or injection. The uniform suction or injection solutions are close to the exact solutions and it is to be expected that other realistic distributions of pressure gradient and blowing velocity will give reasonable solutions.

Solutions to the compressible integral equations for a uniform free stream over a flat plate, when there is constant wall enthalpy and the suction or injection velocity is uniform or satisfies similarity conditions, are shown to compare favourably with solutions obtained by previous authors.

2. Turbulent Boundary Layers

The skin friction in the axisymmetric incompressible turbulent

boundary layer experiments on the porous cylinder may be 5% greater than on a flat plate and the shape of the profiles may not be exactly the same as those on a flat plate but the experiments have been useful in formulating two laws for the inner and outer regions, laws which correlate the previous experimental results of Mickley and Davis, Dutton, and Black and Sarnecki. The laws reduce to the 'law of the wall' and the 'velocity defect law' when the injection or suction velocity is zero. The laws have been used to calculate shear distributions and variations of skin friction with Reynolds number and have made it possible to estimate the local skin friction over porous surfaces by using Preston tubes.

The total shear stress distribution with suction is a different shape from that with injection but the two constituent parts, $\mu \frac{\partial u}{\partial y}$ and $-\rho\overline{u'v'}$ are similar, as is shown in figure 107. The actual distribution of the Reynolds stress, $-\rho\overline{u'v'}$, is modified slightly by the appropriate conditions in the inner region, but the turbulent structure in boundary layers with suction or injection will be basically the same.

The outer region theory has been extended to turbulent boundary layers in pressure gradients and at separation. The outer region equation together with the equation for the overlap region has been used to evaluate mean velocity profiles. The only universal functions which were used were obtained from the zero pressure gradient flow. No other constants were required to calculate the velocity profiles for boundary layers in small pressure gradients, with suction or injection and at separation or reattachment. The total shear stress variation across a boundary layer at separation has been evaluated.

The theory agrees very well with the available experimental results for turbulent boundary layers in energy equilibrium.

3. Turbulent Pipe Flow

Experiments in fully developed turbulent pipe flow have shown how the mean flow is altered when there is suction through a porous section of the pipe. An approximate theory, similar to that for the

boundary layer, is presented and compared with the experimental profiles in the inner region. For small suction velocities the theory agrees reasonably well and, within experimental accuracy, the skin friction predicted by the theory is correct.

REFERENCES

Black, T.J. and Sarnecki, A.J. (1958) The turbulent boundary layer with suction and injection. ARC.20,501.

Braslow, A.L., Burrows, D.L., Tetervin, N. and Visconti, F. (1951) Experimental and theoretical studies of area suction for the control of the laminar boundary layer on an NACA.64 A010 airfoil. NACA Rpt.1025.

Brown, W.B. and Donoughe, P.L. (1952) Tables of exact laminar boundary layer equations which result in specific-weight flow profiles locally exceeding free stream values. NACA.TN.2800.

Clarke, J.H., Menkes, H.R. and Libby, P.A. (1955) A provisional analysis of turbulent boundary layers with injection. J. Aero. Sci. 22, pp.255-260.

Clauser, F.H. (1954) Turbulent boundary layers in adverse pressure gradients. J. Aero. Sci. 21, pp.91-108.

Coles, D. (1954) The problem of the turbulent boundary layer. ZAMP. 5, pp.181-202.

Coles, D. (1956) The law of the wake in the turbulent boundary layer. J. Fluid Mech. 1, pp.191-226.

Coles, D. (1961) The turbulent boundary layer in a compressible fluid. Rand Corporation, Santa Monica. P.2417.

Craven, A.H. (1960) Boundary layers with suction and injection. College of Aeronautics Rpt. Aero 136.

Craven, A.H. (1962) The compressible laminar boundary layer with foreign gas injection. College of Aeronautics Rpt. Aero 155.

Curle, N. (1960) The estimation of laminar skin friction, including the effects of distributed suction. Aero. Quart. 11, pp.1-21.

Deissler, R.G. and Loeffler, A.L. Jr. (1959) Analysis of turbulent flow and heat transfer on a flat plate at high Mach numbers with variable fluid properties. NASA. Rpt. R-17.

Dhawan, S. (1952) Direct measurements of skin friction. NACA.TN.2567.

von Doenhoff, A.E. and Tetervin, N. (1943) Determination of general relations for the behaviour of turbulent boundary layers. NACA.Rpt.772.

Doncughe, P.L. and Livingood, J.N.B. (1954) Exact solutions of laminar boundary layer equations with constant property values for porous wall with variable temperature. NACA.TN.3151.

Dorrance, W.H. and Dore, F.J. (1954) The effect of mass transfer on the compressible turbulent boundary layer skin friction and heat transfer. J. Aero. Sci. 21. pp.404-410.

Duncan, W.J., Thom, A.S. and Young, A.D. (1960) The Mechanics of Fluids. Edward Arnold Ltd. p.342.

Dutton, R.A. (1959) The velocity distribution in a turbulent boundary layer on a flat plate. ARC.CP. No.453. ARC.Rpt.19576.

Dutton, R.A. (1960) The effects of distributed suction on the development of turbulent boundary layers. R & M.3155.

Dwight, H.B. (1960) Tables of Integrals and other Mathematical Data. Macmillan Co. New York. 3rd Edition. p.196.

Eckert, E.R.G. & Livingood, J.N.B. (1953) Method for calculation of laminar heat transfer in air flow around cylinders of arbitrary cross section. NACA.Rpt.1118.

Eckert, H.U. (1952) Simplified treatment of the turbulent boundary layer along a cylinder in compressible flow. J. Aero. Sci. 19, pp.23-29.

Emmons, H.W. & Leigh, D.C. (1953) Tabulation of the Blasius function with blowing and suction. ARC.CP.No.157.

Erdélyi, A. (1953) Higher Trancendental Functions. McGraw-Hill Book Co. Inc., New York. Vol.2, p.80.

Erdélyi, A. (1954) Tables of Integral Transforms. McGraw-Hill Book Co. Inc., New York. (a) Vol.1, p.125. (b) Vol.2, p.181.

Fage, A. & Falkner, V.M. (1931) Relation between heat transfer and surface friction for laminar flow. R.& M.1408.

Ginevskii, A.S. & Solodkin, E.E. (1958) Effect of transverse curvature of the surface on the characteristics of an axi-symmetrical turbulent boundary layer. Prikladnaya Matematika i Mekhanika. 22, pp.819-825.

Gortler, H. (1948) Ein Differenzenverfahren zur Berechnung Laminarer Grenzschichten. Ing. Archiv. 16, p.173.

Griffith, A.A. and Meredith, F.W. (1936) Unpublished. See 'Modern Developments in Fluid Dynamics'. ed. Goldstein, 1938, p.534.

Hartnett, J.P., Masson, D.J., Gross, J.F. and Gazley, C. Jr. (1960) Mass-transfer cooling in a turbulent boundary layer. J. Aerospace Sci.27, p.623.

Hartree, D.R. and Womersley, J.R. (1937) A method for the numerical or mechanical solution of certain types of partial differential equations. Proc. Roy. Soc. London, A.101, pp.353-366.

Head, M.R. (1957) An approximate method of calculating the laminar boundary layer in two-dimensional incompressible flow. ARC., R.& M.3123.

Head, M.R. (1961) Approximate methods of calculating the two-dimensional laminar boundary layer with suction. Boundary Layer and Flow Control. Pergamon Press, p.801.

Head, M.R. and Rechenberg, I. (1962) The Preston tube as a means of measuring skin friction. ARC.23,459. FM.3153.

Hsu, E.Y. (1955) Measurement of local turbulent skin friction by means of surface pitot tubes. David W. Taylor Model Basin. Rpt.957. NS715-102.

Iglisch, R. (1949) Exact calculation of the laminar boundary layer in longitudinal flow over a flat plate with homogeneous suction. NASA. TM.1205.

Illingworth, C.R. (1949) Steady flow in the laminar boundary layer. Proc. Roy. Soc. (A) 199, pp.533-558.

Illingworth, C.R. (1954) Separation of a compressible laminar boundary layer. Quart. Mech. and Appl. Maths. Vol.7, pp.8-34.

van Ingen, J.L. (1958) Een Twee-parameter methode voor de Berekening van de Laminaire Grenslaag met Afzuiging. Memo. MT Tech. Hogeschool Delft, Vliegtuigbouwkunde.

Kay, J.M. (1948) Boundary layer flow along a flat plate with uniform suction. ARC. R.& M. 2628.

Klebanoff, P.S. and Diehl, Z.W. (1951) Some features of artificially thickened fully developed turbulent boundary layers with zero pressure gradient. NACA. TN.2475.

Koh, J.C.Y. and Hartnett, J.P. (1961) Skin friction and heat transfer for incompressible laminar flow over porous wedges with suction and variable wall temperature. Int. J. Heat Mass Transfer. Vol.2, pp.185-198.

Landweber, L. (1949) Effect of transverse curvature on frictional resistance. David W. Taylor Model Basin, USN. Rpt.689.

Laufer, J. (1954) The structure of turbulence in fully developed pipe flow. NACA. Rpt.1174.

Leadon, B.M. (1961) Comments on "A sublayer theory for fluid injection". Jnl. Aerospace Sci. Vol.28, pp.826-827.

Le Fur, B. (1959) Heat transfer and recovery factor in a laminar boundary layer with arbitrary pressure gradient and wall temperature distribution. J. Aerospace Sci. Vol.26, pp.682-683.

Lew, H.G. and Fanucci, J.B. (1955) On the laminar compressible boundary layer over a flat plate with suction or injection. J. Aero. Sci. Vol.22, pp.589-592.

Libby, P.A., Baronti, P.O. and Napolitano, L. (1964) Study of the incompressible turbulent boundary layer with pressure gradient. AIAA. J. Vol.2, pp.445-452.

Lighthill, M.J. (1950) Contribution to the theory of heat transfer through a laminar boundary layer. Proc. Roy. Soc. A. Vol.202, pp.359-377.

Lilley, G.M. (1959) A simplified theory of skin friction and heat transfer for a compressible laminar boundary layer. College of Aeronautics Note No.93.

Livingood, J.N.B. and Donoughe, P.L. (1955) Summary of laminar boundary layer solutions for wedge-type flow over convection and transpiration cooled surfaces. NACA. TN.3588.

Low, G.M. (1955) The laminar compressible boundary layer with fluid injection. NACA. TN.3404.

Ludwieg, H. (1950) Instrument for measuring wall shearing stress of turbulent boundary layers. NACA. TM.1284.

Ludwieg, H. and Tillmann, W. (1949) Investigation of the wall shearing stress in turbulent boundary layers. NACA. TM.1285.

McGregor, I. (1954) Regions of localised boundary layer separation and their role in the stalling of aerofoils. Ph.D. Thesis. Faculty of Eng. Univ. of London.

Mickley, H.S. and Davis, R.S. (1957) Momentum transfer for flow over a flat plate with blowing. NACA. TN.4017.

Mickley, H.S. and Smith, K.A. (1963) Velocity defect law for a transpired turbulent boundary layer. AIAA. J. 1, p.1685.

Millikan, C.B. (1938) A critical discussion of turbulent flows in channels and circular tubes. Proc. 5th Int. Cong. for App. Mech. Wiley, pp.386-392.

Nash, J.F. (1960) A correlation of skin friction measurement in compressible turbulent boundary layers with injection. ARC.22,386.

Newman, B.G. (1951) Skin friction in a retarded turbulent boundary layer near separation. Aero. Res. Consultative Comm. (Australia). Rpt. ACA.53.

Pappas, C.C. and Okuno, A.J. (1960) Measurements of the skin friction of the compressible turbulent boundary layer on a cone with foreign gas injection. J. Aerospace Sci. 27, p.321.

Piaggio, H.T.H. (1952) Differential Equations. G. Bell & Sons, Ltd. London, p.88.

Pohlhausen, K. (1921) On the approximate integration of the differential equation of the laminar boundary layer. Z. Angew. Math. Mech.1, p.252.

Preston, J.H. (1954) Determination of turbulent skin friction by means of pitot-tubes. J. Roy. Aero. Soc. 58, p.109.

Rheinboldt, W. (1955) On the calculation of steady boundary layers for continuous suction, with discontinuously variable suction velocity. NASA. TT.F29. 1961.

Richmond, R.L. (1957) Experimental investigation of thick axially symmetric boundary layers on cylinders at subsonic and supersonic speeds. Guggenheim Aero. Lab. California Inst. of Tech. Memo.39.

Rotta, J.C. (1962) Turbulent Boundary Layers in Incompressible Flow. Progress in Aero. Sci. Pergamon Press.

Rubesin, M.W. (1954) An analytical estimation of the effect of transpiration cooling. NACA. TN.3341.

Sandborn, V.A. (1959) An equation for the mean velocity distribution of boundary layers. NASA. Memo. 2.5.59E.

Schlichting, H. (1942) Die Grenzschicht an der ebenen Platte mit Absaugung und Ausblasen, Luftfahrtforsch.10, p.293.

Schlichting, H. (1949) An approximate method for the calculation of the laminar boundary layer with suction for bodies of arbitrary shape. NACA. TM.1216.

Schröder, K. (1951) Verwendung der Differenzenrechnung zur Berechnung der laminaren Grenzschicht. Math.Nachr. 4, p.439.

Schubauer, G.B. and Klebanoff, P.S. (1951) Investigation of separation of the turbulent boundary layer. NACA. TN.2133.

Schultz-Grunow, F. (1947) New frictional resistance law for smooth plates. NACA. TN.1257.

Smith, A.M.O. and Clutter, D.W. (1963) Solution of the incompressible laminar boundary layer equations. AIAA. J. 1, p.2062.

Smith, D.W. and Walker, J.W. (1958) Skin friction measurements in incompressible flow. NACA. TN.4231.

Spalding, D.B. (1958) Heat transfer from surfaces of non-uniform temperature. J. Fluid Mech. 4, pp.22-32

Sparrow, E.M., Eckert, E.R.G. and Minkowycz, W.J. (1963) Heat transfer and skin friction for turbulent boundary layer flow longitudinal to a circular cylinder. J. App. Mech.30, pp.37-43

Squire, L.C. (1963) Some notes on turbulent boundary layers with fluid injection at high supersonic speeds. RAE Tech. Note Aero.2904.

Staff of Aerodynamics Div. N.P.L.(1961) On the measurement of local surface friction on a flat plate by means of Preston tubes. R.& M. No.3185.

Staniforth, R. (1951) Contributions to the theory of effusion cooling of gas turbine blades. General Discussion on Heat Transfer. ASME. Sept.11-13.

Stanton, T.E., Marshall, D. and Bryant, C.N. (1920) On the conditions at the boundary of a fluid in turbulent motion. Proc. Roy. Soc. (A), Vol.97, p.413.

Stevenson, T.N. (1961) Laminar boundary layer with injection through a permeable wall. College of Aeronautics Rpt.145.

Stewartson, K. (1949) Correlated incompressible and compressible boundary layers. Proc. Roy. Soc. A. 200, p.84.

Stratford, B.S. (1959a) The prediction of separation of the turbulent boundary layer. J. Fluid Mech. 5, pp.1-16.

Stratford, B.S. (1959b) An experimental flow with zero skin friction throughout its region of pressure rise. J. Fluid Mech. 5, pp.17-35.

Tenderland, T. and Okuno, A.F. (1956) The effect of fluid injection on the compressible turbulent boundary layer. NACA. RM.A56D05. NACA/TIL 5126.

Tewfik, O.E. (1963) Some characteristics of the turbulent boundary layer with air injection. AIAA. J. 1, pp.1306-1312.

Torda, T.P. (1952) Boundary layer control by continuous surface suction or injection. J. Math. Phys. 31, p.206.

Townsend, A.A. (1956a) Structure of Turbulent Shear Flow. Cambridge Univ. Press.

Townsend, A.A. (1956b) The properties of equilibrium boundary layers. J. Fluid Mech. 1, pp.561-573.

Townsend, A.A. (1960) The development of turbulent boundary layers with negligible wall stress. J. Fluid Mech. 8, pp.143-155.

Turcotte, D.L. (1960) A sublayer theory for fluid injection into the incompressible turbulent boundary layer. J. Aerospace Sci. 27, pp.675-678.

Wills, J.A.B. (1963) A note on a method of measuring skin friction. N.P.L. Aero. Note 1011.

Wuest, W. (1955) Asymptotische Absaugegrenzschichten an längsangeströmten zylindrischen Körpern. Ing. Archiv. 23, p.198.

Wuest, W. (1961) Survey of calculation methods of laminar boundary layers with suction in incompressible flow. Boundary Layer and Flow Control. Pergamon Press, p.771.

Yasuhara, M. (1959) Experiments on axi-symmetric boundary layers along a cylinder in incompressible flow. Trans. Japan Soc. Aero. Space Sci. 2, pp.72-76.

Young, A.D. (1939) The calculation of the total and skin friction drags of bodies of revolution at zero incidence. R.& M. 1874.

Young, A.D. (1948) Note on the velocity and temperature distributions attained with suction on a flat plate of infinite extent in compressible flow. Quart. J. Mech. Appl. Math. 1, pp.70-75.

Young, A.D. and Maas, J.N. (1936) The behaviour of a pitot tube in a transverse total pressure gradient. R.& M.1770.

Yuan, S.W. and Barazotti (1958) Experimental investigation of turbulent pipe flow with coolant injection. Heat Transfer and Fluid Mech. I. California, pp. 25-39.

Yuan, S.W. and Brogren, E.W (1961) Turbulent flow in a circular pipe with porous wall. Phy. of Fluids 4, pp.368-372.

Yuan, S.W. and Galowin, L.S. (1957) Transpiration cooling in the turbulent flow through a porous-wall pipe. 9th Int. Congr. App. Mech. Brussels, pp.331-340.

ACKNOWLEDGMENTS

The author would like to acknowledge:

the help and encouragement given during the many discussions with Professor A.D. Young and Professor G.M. Lilley,

the consideration and co-operation of Dr. Whitehead and the technicians at Queen Mary College,

the co-operation of the drawing office and workshop staff at The College of Aeronautics,

the valuable daily talks with Dr. M. Gaster,

and the financial support of The College of Aeronautics.

APPENDIX A

A Partial Inversion of the Momentum Equation

Equation (6.28) is

$$\bar{G} = \frac{3^{4/3}\,\Gamma(\frac{5}{3})\,\rho^{-2/3}\,\overline{\tau_w}}{2^{1/3}\,\Gamma(\frac{1}{3})\,\mu_0}\,, \tag{A.1}$$

where, for incompressible flow,

$$\mu_0 = \mu \quad \& \quad G = u_1^2 + \int_0^x -\frac{2\tau_w v_w\,dx_1}{\mu}\,. \tag{A.2}$$

Equation (A.1) is rearranged to give

$$\overline{\tau_w} = \frac{2^{\frac{1}{3}}\,\Gamma(\frac{1}{3})\,\mu\rho^{\frac{1}{3}}\bar{G}}{3^{4/3}\,\Gamma(\frac{5}{3})}\,, \tag{A.3}$$

and the inversion of this equation is

$$\tau_w = \frac{2^{\frac{1}{3}}\,\mu}{3^{4/3}\,\Gamma(\frac{5}{3})}\int_0^t \frac{1}{(t-t_1)^{2/3}}\left\{\frac{\partial u_1^2}{\partial t_1} - \frac{2\tau_w v_w}{\mu}\right\}dt_1\,. \tag{A.4}$$

Using equation (6.25), the equation for the skin friction, in terms of x, is

$$\tau_w(x) = \frac{(\rho\mu)^{2/3}}{\Gamma(\frac{2}{3})\cdot 3^{\frac{1}{3}}}\left\{\frac{1}{2}\int_0^x\left(\int_{x_1}^x \tau_w^{\frac{1}{2}}dz\right)^{-\frac{2}{3}} d\left(u_1^2(x_1)\right) - \frac{1}{\mu}\int_0^x\left(\int_{x_1}^x \tau_w^{\frac{1}{2}}dz\right)^{-\frac{2}{3}} v_w\tau_w\,dx_1\right\} \tag{A.5}$$

The term involving $u_1^2(x)$ is a 'Stieltjès integral' and it has a value when the free stream velocity, u_1, is a constant. The equation is first used in section (8.2) as equation (8.16).

APPENDIX B

A More Accurate Skin Friction Solution

B.1 The series for $\frac{\partial z}{\partial \Phi}$

In section 6, the inaccuracy of the skin friction solution is largely due to the poor approximation used for $\frac{\partial z}{\partial \Phi}$. More terms are now considered in the series for $\frac{\partial z}{\partial \Phi}$ with the hope of obtaining better solutions. The following analysis for incompressible flow is similar to that used to solve the energy equation in section 7.

The equation of motion in Von Mises form is

$$\left(\frac{\partial z}{\partial \Phi}\right)_x \left(\frac{\partial \Phi}{\partial x}\right)_\psi + \left(\frac{\partial z}{\partial x}\right)_\Phi = \mu\rho u \left(\frac{\partial^2 z}{\partial \Phi^2}\right)_x , \tag{B.1}$$

where $z = u_1^2 - u^2$, $\frac{\partial \psi}{\partial x} = -\rho v$, $\frac{\partial \psi}{\partial y} = \rho u$ and

$$\left(\frac{\partial \psi}{\partial x}\right)_{y=0} = -\rho v_w = \left(\frac{\partial \psi_w}{\partial x}\right) . \tag{B.2}$$

Following Lighthill (1950) an expression for the velocity, u, namely $u = \left(\frac{2\tau_w}{\mu\rho}\right)^{\frac{1}{2}} \Phi^{\frac{1}{2}} + O[\Phi]$ which is most accurate near the wall is substituted into equation (B.1). A series for $\frac{\partial z}{\partial \Phi}$ of the form $\frac{\partial z}{\partial \Phi} = P_1 + P_2 \Phi^{\frac{1}{2}} + P_3 \Phi + O[\Phi^{3/2}]$ will be considered. Only the first term of this series was considered in the previous analysis in section 6.

Equation (B.1) may now be written

$$\frac{\partial^2 z}{\partial \Phi^2} - \Phi^{-\frac{1}{2}} \frac{\partial z}{\partial t} = P_4 \Phi^{-\frac{1}{2}} + P_5 + P_6 \Phi^{\frac{1}{2}} \cdots\cdots \tag{B.3}$$

where $t = \int_0^x (2\mu\rho\tau_w)^{\frac{1}{2}} \, dx$, (B.4)

$$P_4 = P_1 \left(\frac{\rho v_w}{(2\mu\rho\tau_w)^{\frac{1}{2}}}\right) , \quad P_5 = P_2 \frac{\rho v_w}{(2\mu\rho\tau_w)^{1/2}} \text{ and } P_6 = P_3 \frac{\rho v_w}{(2\mu\rho\tau_w)^{\frac{1}{2}}} \tag{B.5}$$

(P_1, P_2 and P_3 are functions of x only.)

Using the Laplace transform notation $\bar{z} = \int_0^\infty e^{-pt} z\, dt$ and the condition $z = 0$ when $t = 0$, equation (B.3) is

$$\frac{\partial^2 \bar{z}}{\partial \Phi^2} - \Phi_1^{-\frac{1}{2}} p \bar{z} = \bar{P}_4 \Phi_1^{-\frac{1}{2}} + \bar{P}_5 + \bar{P}_6 \Phi_1^{\frac{1}{2}}, \tag{B.6}$$

and the homogeneous part of this equation has the solution (see section 6)

$$\bar{z} = A \Phi_1^{\frac{1}{2}} I_{-\frac{2}{3}}(q) + B \Phi_1^{\frac{1}{2}} I_{\frac{2}{3}}(q) \tag{B.7}$$

where $q = \frac{4}{3} p^{\frac{1}{2}} \Phi_1^{3/4}$.

A and B must be determined from the boundary conditions. The complete solution to equation (B.6) will now be found by the method of variation of parameters. A solution is assumed to be

$$\bar{z} = P(\Phi_1) \bar{z}_1 + Q(\Phi_1) \bar{z}_2 , \tag{B.8}$$

where $\bar{z}_1 = \Phi_1^{1/2} I_{-\frac{2}{3}}(q)$ and $\bar{z}_2 = \Phi_1^{\frac{1}{2}} I_{\frac{2}{3}}(q)$. (B.9)

The equations to determine P and Q are thus

$$\frac{dP}{d\Phi} = \bar{z}_2 \left(\frac{\bar{P}_4 \Phi_1^{-\frac{1}{2}} + \bar{P}_5 + \bar{P}_6 \Phi_1^{\frac{1}{2}}}{\bar{z}_2 \bar{z}_1' - \bar{z}_1 \bar{z}_2'} \right), \tag{B.10}$$

and $$\frac{dQ}{d\Phi} = -\bar{z}_1 \left(\frac{\bar{P}_4 \Phi_1^{-\frac{1}{2}} + \bar{P}_5 + \bar{P}_6 \Phi_1^{\frac{1}{2}}}{\bar{z}_2 \bar{z}_1' - \bar{z}_1 \bar{z}_2'} \right), \tag{B.11}$$

where the prime denotes differentiation with respect to Φ_1.

Now the Wronskian (Erdélyi 1953), $W\left(I_{\frac{2}{3}}(q), I_{-\frac{2}{3}}(q)\right)$ is equal to $-\frac{2}{\pi q} \sin \frac{2}{3}\pi$, and therefore $\bar{z}_2 \bar{z}_1' - \bar{z}_1 \bar{z}_2' = \frac{3}{2\pi} \sin \frac{2}{3}\pi$ so that

$$P = -\frac{2\pi}{3 \sin \frac{2}{3}\pi} \int_0^{\Phi} \left(\bar{P}_4 \Phi_1^{-\frac{1}{2}} + \bar{P}_5 + \bar{P}_6 \Phi_1^{\frac{1}{2}} \right) \Phi_1^{\frac{1}{2}} I_{\frac{2}{3}}(q)\, d\Phi_1 , \tag{B.12}$$

and

$$Q = \frac{2\pi}{3 \sin \frac{2}{3}\pi} \int_0^{\Phi} \left(\bar{P}_4 \Phi_1^{-\frac{1}{2}} + \bar{P}_5 + \bar{P}_6 \Phi_1^{\frac{1}{2}} \right) \Phi_1^{\frac{1}{2}} I_{-\frac{2}{3}}(q)\, d\Phi_1 . \tag{B.13}$$

The solution to equation (B.6) is thus

$$\bar{z} = a\bar{\Phi}^{\frac{1}{2}} I_{-\frac{2}{3}}(q) + b\bar{\Phi}^{\frac{1}{2}} I_{\frac{2}{3}}(q) - \frac{2\pi}{3\sin\frac{2}{3}\pi}\bar{\Phi}^{\frac{1}{2}} I_{-\frac{2}{3}}(q)\int_0^{\bar{\Phi}} \left(\bar{P}_4\bar{\Phi}^{-\frac{1}{2}} + \bar{P}_5 + \bar{P}_6\bar{\Phi}^{\frac{1}{2}}\right) I_{\frac{2}{3}}(q)\bar{\Phi}^{\frac{1}{2}} d\bar{\Phi}$$

$$+ \frac{2\pi}{3\sin\frac{2}{3}\pi}\bar{\Phi}^{\frac{1}{2}} I_{\frac{2}{3}}(q)\int_0^{\bar{\Phi}} \left(\bar{P}_4\bar{\Phi}^{-\frac{1}{2}} + \bar{P}_5 + \bar{P}_6\bar{\Phi}^{\frac{1}{2}}\right)\bar{\Phi}^{\frac{1}{2}} I_{-\frac{2}{3}}(q)\, d\bar{\Phi}, \qquad \text{(B.14)}$$

where a and b are to be determined from the boundary conditions : $\bar{z} = \overline{u_1^2}$ and $\frac{\partial \bar{z}}{\partial \bar{\Phi}} = -\frac{2\overline{\tau_w}}{\mu\rho}$ at $\bar{\Phi} = 0$. Therefore from equation (B.14), $a = \Gamma(\frac{1}{3})(\frac{2}{3})^{\frac{2}{3}}\beta^{1/3}\overline{u_1^2}$ and $b = (\frac{2}{3})^{\frac{1}{3}}\Gamma(\frac{2}{3})\beta^{-\frac{1}{3}}\left(\frac{2\overline{\tau_w}}{\mu\rho}\right)$. Thus equation (B.14) may be written

$$\bar{z} = a q^{\frac{2}{3}} m^{\frac{1}{2}} I_{-\frac{2}{3}}(q) + b q^{\frac{2}{3}} m^{\frac{1}{2}} I_{\frac{2}{3}}(q) - \frac{M}{m^{\frac{1}{2}}} q^{\frac{2}{3}} I_{-\frac{1}{3}}(q)\int_0^{q} \left(\bar{P}_4 q^{\frac{1}{3}} + \bar{P}_5 m^{\frac{1}{2}} q + \right.$$

$$\left. \bar{P}_6 m q^{\frac{5}{3}}\right) I_{\frac{2}{3}}(q)\, dq + \frac{M}{m^{1/2}} q^{\frac{2}{3}} I_{\frac{2}{3}}(q)\int_0^{q} \left(\bar{P}_4 q^{\frac{1}{3}} + \bar{P}_5 m^{\frac{1}{2}} q + \bar{P}_6 m q^{5/3}\right) I_{-\frac{2}{3}}(q)\, dq, \qquad \text{(B.15)}$$

where $M = \frac{2\pi m^2}{3\sin\frac{2}{3}\pi}\cdot\frac{4}{3}$ and $m = \left(\frac{3}{4}\right)^{4/3}\beta^{-\frac{2}{3}}$.

This equation is now differentiated with respect to q and the limit is taken as $q \to 0$. After some algebra:

$$\left.\frac{\partial \bar{z}}{\partial q}\right|_{q\to 0} = \left(a m^{\frac{1}{2}} + \frac{M}{m^{\frac{1}{2}}}\bar{P}_4\frac{2^{\frac{1}{3}}}{\Gamma(\frac{2}{3})}\right) q^{\frac{1}{3}} + \frac{b m^{\frac{1}{2}} 2^{\frac{1}{3}} q^{\frac{1}{3}}}{\Gamma(\frac{2}{3})} + \frac{3M\bar{P}_5 q^{\frac{5}{3}}}{2\,\Gamma(\frac{1}{3})\Gamma(\frac{2}{3})} + O\left[q^{\frac{7}{3}}\right]. \qquad \text{(B.16)}$$

Hence after substituting the expressions for M, m, b and a,

$$\left.\frac{\partial \bar{z}}{\partial \bar{\Phi}}\right|_{\bar{\Phi}\to 0} = \left(-\frac{2\overline{\tau_w}}{\mu\rho}\right) + \overline{u_1^2}\,\beta\, 2\bar{\Phi}^{\frac{1}{2}} + 2\bar{P}_4\bar{\Phi}^{\frac{1}{2}} + \bar{P}_5\bar{\Phi} + O\left[\bar{\Phi}^{3/2}\right], \qquad \text{(B.17)}$$

and after inverting this equation,

$$\left.\frac{\partial \bar{z}}{\partial \bar{\Phi}}\right|_{\bar{\Phi}\to 0} = -\frac{2\tau_w}{\mu\rho} + 2P_4\bar{\Phi}^{\frac{1}{2}} + P_5\bar{\Phi} + 2\bar{\Phi}^{\frac{1}{2}}\left\{\frac{du_1^2}{dt} + \delta\left(u_1^2(0)\right)\right\} + O\left[\bar{\Phi}^{\frac{3}{2}}\right] \qquad \text{(B.18)}$$

If this expression for $\frac{\partial z}{\partial \Phi}$ is compared with the original series

then $P_4 = -\left(\frac{2\tau_w}{\mu\rho}\right)\left(\frac{\rho V_w}{2\mu\rho\tau_w}\right)^{\frac{1}{2}}$, $P_5 = \frac{V_w}{\mu\tau_w}\left(\frac{du_1^2}{dx} - \frac{2\tau_w V_w}{\mu} + \delta(u_1^2(0))\right)$

and $P_6 = \frac{P_5 \rho V_w}{(2\mu\rho\tau_w)^{\frac{1}{2}}}$.

If equation (B.15) is inverted, an integral equation for the skin friction is obtained. However the singularity at $m = 0$ still exists for similarity flow and this is because the series for $\frac{\partial z}{\partial \Phi}$ does not satisfy the boundary condition $\frac{\partial z}{\partial \Phi} \to 0$ as $\Phi \to \infty$. If the series were modified to include this boundary condition, as shown in section (B.3), then the solution would not diverge at certain values of m. A way to include the boundary conditions is indicated by looking at the solution for $\frac{\partial z}{\partial \Phi}$ when $V_w = 0$.

B.2 A solution for $\frac{\partial z}{\partial \Phi}$ when $V_w = 0$

When $V_w = 0$ equation (B.16) reduces to

$$\frac{\partial \bar{z}}{\partial q} = \frac{b m^{\frac{1}{2}} q^{\frac{2}{3}} 2 K_{\frac{1}{3}}(q)}{\Gamma(\frac{1}{3})\Gamma(\frac{2}{3})}, \qquad (B.19)$$

where $K_{\frac{1}{3}}()$ is a modified Bessel function of the second kind. Substituting for b, m and q, equation (B.19) is

$$\frac{\partial \bar{z}}{\partial q} = \left(\frac{2}{3}\right)^{\frac{1}{3}} \frac{2}{\Gamma(\frac{1}{3})} \Phi_1^{\frac{1}{2}} \left(-\frac{2\bar{\tau}_w}{\mu\rho}\right) p^{-\frac{1}{3}} K_{\frac{1}{3}}(q), \qquad (B.20)$$

or $$\frac{\partial \bar{z}}{\partial \Phi_1} = p^{\frac{1}{2}} \Phi_1^{\frac{1}{4}} \left(\frac{2}{3}\right)^{\frac{1}{3}} \frac{2}{\Gamma(\frac{1}{3})} \left(-\frac{2\bar{\tau}_w}{\mu\rho}\right) K_{\frac{1}{3}}(q). \qquad (B.21)$$

The inversion of $\alpha^{-\frac{1}{2}\nu} p^{\frac{1}{2}\nu} K_\nu\left(2\alpha^{\frac{1}{2}} p^{\frac{1}{2}}\right)$ is $\frac{1}{2} t^{-\nu-1} e^{-\frac{\alpha}{t}}$ (Erdélyi 1954 a).

Therefore, using the Convolution theorem, the inversion of equation

COLLEGE OF AERONAUTICS LIBRARY

(B.21) is

$$\frac{\partial z}{\partial \Phi} = -\left(\frac{2}{3}\right)^{\frac{2}{3}} \frac{2}{\Gamma(\frac{1}{3})} \frac{\Phi_1^{\frac{1}{2}}}{\mu\rho} \int_0^t \tau_w (t-t_1) t_1^{-\frac{4}{3}} e^{-\frac{\left(\frac{2}{3}\right)^2 \Phi_1^{3/2}}{t_1}} dt_1 . \qquad (B.22)$$

For similarity flow this reduces to

$$\left(\frac{\partial z}{\partial \Phi}\right)_{\substack{\text{similarity} \\ v_w = 0}} = \Phi_1^{\frac{1}{2}} N \int_0^t (t-t_1)^{\frac{6m-2}{3m+3}} t_1^{-\frac{4}{3}} e^{-\left(\frac{2}{3}\right)^2 \Phi_1^{3/2}/t_1} dt_1 , \qquad (B.23)$$

where $N = \dfrac{-\left(\frac{2}{3}\right)^{\frac{2}{3}} 2K^2}{\Gamma(\frac{1}{3})\mu\rho} r^{\frac{6m-2}{3m+3}}$, $r = (2\mu\rho)^{\frac{1}{2}} \dfrac{4K}{3(m+1)}$ and

$$K^2 = f_w'' \rho^{\frac{1}{2}} \mu^{\frac{1}{2}} c^{\frac{3}{2}} = \tau_w x^{-\left(\frac{3m-1}{2}\right)}$$

The integral in equation (B.23) is a Riemann-Liouville integral (Erdélyi 1954 b) and may be written as the sum of two hypergeometric series:

$$\left(\frac{\partial z}{\partial \Phi}\right)_{\substack{\text{similarity} \\ v_w = 0}} = N\left(\frac{3}{2}\right)^{\frac{2}{3}} \alpha^{-\frac{1}{3}} t^{\frac{7m-1}{3m+3}} e^{-\frac{\alpha}{t}} \left\{ \Gamma(\tfrac{1}{3}) \left(\frac{\alpha}{t}\right)^{\frac{1}{3}} {}_1F_1\left(8m; \tfrac{2}{3}; \frac{\alpha}{t}\right) \right.$$

$$\left. - 3\Gamma(\tfrac{2}{3})\Gamma\left(\frac{9m+1}{3m+3}\right)\left(\frac{\alpha}{t}\right)^{\frac{2}{3}} {}_1F_1\left(\frac{9m+1}{3m+3}; \tfrac{4}{3}; \frac{\alpha}{t}\right) \right\}. \qquad (B.24)$$

In certain cases this equation reduces to simple forms, as for example when $m = 0$,

$$\left(\frac{\partial z}{\partial \Phi}\right)_{v_w = m = 0} = \Gamma(\tfrac{1}{3}) . N . \left(\frac{3}{2}\right)^{\frac{2}{3}} t^{-\frac{2}{3}} e^{-\frac{\alpha}{t}} . \qquad (B.25)$$

The exponential term, $e^{-\frac{\alpha}{t}}$, ensures that $\dfrac{\partial z}{\partial \Phi} \to 0$ as $\Phi_1 \to \infty$ and a term of this type will now be included in the series for $\dfrac{\partial z}{\partial \Phi}$.

B.3 A similarity solution for the skin friction

The approximate series used for $\dfrac{\partial z}{\partial \Phi}$ in section (B.1) is

$$\frac{\partial z}{\partial \Phi} = -\frac{2\tau_w}{\mu\rho} + 2\left(P_4 + \frac{du_1^2}{dt}\right)\Phi_1^{\frac{1}{2}} + P_5 \Phi_1 + O[\Phi_1^{\frac{3}{2}}]. \qquad (B.26)$$

In order to satisfy the boundary condition at infinity the series is written

$$\frac{\partial Z}{\partial \Phi} = \exp\left(-\frac{\left(\frac{2}{3}\right)^2 \Phi^{\frac{3}{2}}}{t}\right) \cdot \left\{-\frac{2\tau_w}{\mu\rho} + 2\left(P_4 + \frac{d\mu_1^2}{dt}\right)\Phi^{\frac{1}{2}} + P_5 \Phi\right\} + O\left[\Phi^{\frac{3}{2}}\right]. \quad \text{(B.27)}$$

For similarity flow the momentum equation (B.1) is

$$\frac{\partial^2 Z}{\partial \Phi^2} - \Phi^{-\frac{1}{2}} \frac{\partial Z}{\partial t} = \frac{\partial Z}{\partial \Phi} \cdot \Phi^{-\frac{1}{2}} \frac{\rho}{(2\mu\rho)^{\frac{1}{2}}} \left(\frac{r}{t}\right)^{-\frac{1}{3}} \frac{G}{K} \cdot \quad \text{(B.28)}$$

After substituting equation (B.27) into (B.28),

$$\frac{\partial^2 Z}{\partial \Phi^2} - \Phi^{-\frac{1}{2}} \frac{\partial Z}{\partial t} = I = e^{-\frac{\alpha}{t}} \left\{ A \Phi^{-\frac{1}{2}} t^{\frac{5m-3}{3m+3}} + B t^{\frac{4m-4}{3m+3}} + C \Phi^{\frac{1}{2}} t^{\frac{3m-5}{3m+3}} \right\} \quad \text{(B.29)}$$

where $A = \dfrac{-2^{\frac{1}{2}} KG}{(\mu\rho)^{\frac{1}{2}} \mu r^{\frac{5m-3}{3m+3}}}$, $B = \dfrac{2G}{K\mu}\left(\dfrac{mc^2}{K} - \dfrac{KG}{\mu}\right) \dfrac{1}{r^{\frac{4m-4}{3m+3}}}$

and $C = 2^{1/2} (\mu\rho)^{\frac{1}{2}} \dfrac{G^2}{\mu^2 K} \left(\dfrac{mc^2}{K} - \dfrac{KG}{\mu}\right) \dfrac{1}{r^{\frac{3m-5}{3m+3}}}$

The Laplace transform of $t^{\nu-1} e^{-\frac{\alpha}{t}}$ is $2\left(\frac{\alpha}{p}\right)^{\nu/2} K_\nu\left(\alpha^{\frac{1}{2}} 2p^{\frac{1}{2}}\right)$ (Erdélyi 1954 a), and therefore the transform of I is

$$\bar{I} = A\Phi^{-\frac{1}{2}} 2\left(\frac{\alpha}{p}\right)^{\frac{4m}{3m+3}} K_{\frac{3m}{3m+3}}(q) + B2\left(\frac{\alpha}{p}\right)^{\frac{7m-1}{6m+6}} K_{\frac{7m-1}{3m+3}}(q) + C\Phi^{\frac{1}{2}} 2\left(\frac{\alpha}{p}\right)^{\frac{6m-2}{6m+6}} K_{\frac{6m-2}{3m+3}}(q). \quad \text{(B.30)}$$

The method is now the same as that in section (B.1). The method of Variation of Parameters is used: an equation for $\bar{Z}$ is obtained: the boundary condition at infinity is satisfied and hence the following equation for $\overline{u_1^2}$ is derived:-

$$\Gamma\left(\tfrac{1}{3}\right)\left(\tfrac{2}{3}\right)^{\frac{2}{3}} p^{\frac{1}{3}} \overline{u_1^2} + \left(\tfrac{2}{3}\right)^{\frac{1}{3}} \Gamma\left(\tfrac{2}{3}\right) p^{-\frac{1}{3}} \left(-\frac{2\overline{\tau_w}}{\mu\rho}\right) + \frac{4}{3} \int_0^\infty \bar{I} \cdot \Phi^{\frac{1}{2}} K_{\frac{2}{3}}(q) \, d\Phi = 0 \quad \text{(B.31)}$$

It remains to evaluate the integral, which is, from equation (B.29),

$$\frac{4}{3}\int_0^\infty \bar{I}\,\bar{\Phi}_1^{\frac{1}{2}} K_{\frac{1}{3}}(q)\,d\bar{\Phi}_1 = \rho^{-\left(\frac{10m+2}{3m+3}\right)} \frac{4}{3}\left\{ \frac{A 2^{\frac{3}{3m+3}}}{} \left(\frac{3}{4}\right)^{\frac{1}{3}} \int_0^\infty q^{\frac{8m}{3m+3}+\frac{1}{3}} K_{\frac{8m}{3m+3}}(q)\, K_{\frac{2}{3}}(q)\,dq \right.$$

$$+ B.2.2^{\frac{1-7m}{3m+3}} \left(\frac{3}{4}\right) \int_0^\infty q^{\frac{7m-1}{3m+3}+1} K_{\frac{7m-1}{3m+3}}(q).K_{\frac{2}{3}}(q)\,dq$$

$$\left. + C.2.2^{\frac{2-6m}{3m+3}} \left(\frac{3}{4}\right)^{\frac{5}{3}} \int_0^\infty q^{\frac{6m-2}{3m+3}+\frac{5}{3}} K_{\frac{6m-2}{3m+3}}(q).K_{\frac{2}{3}}(q)\,dq. \right\}$$

(B.32)

But the integral, $\int_0^\infty q^\rho K_\mu(q).K_\nu(q)\,dq$, is equal to $\frac{2^{\rho-2}}{\Gamma(1+\rho)}\Gamma\left(\frac{1+\rho\mp\nu\mp\mu}{2}\right)$ (Erdélyi 1954 c), and so

$$\int_0^\infty q^{\frac{8m}{3m+3}+\frac{1}{3}} K_{\frac{8m}{3m+3}}(q).K(q)\,dq = \frac{2^{\frac{3m-5}{3m+3}}\Gamma\left(\frac{11m+3}{3m+3}\right)\Gamma\left(\frac{1}{3}\right)\Gamma\left(\frac{9m+1}{3m+3}\right)}{\Gamma\left(\frac{12m+4}{3m+3}\right)},$$

and the other two integrals in equation (B.32) are

$$\frac{2^{\frac{4m-4}{3m+3}}\Gamma\left(\frac{11m+3}{3m+3}\right)\Gamma\left(\frac{2}{3}\right)\Gamma\left(\frac{4}{3}\right)\Gamma\left(\frac{9m+1}{3m+3}\right)}{\Gamma\left(\frac{13m+5}{3m+3}\right)} \text{ and } \frac{2^{\frac{5m-3}{3m+3}}\Gamma\left(\frac{11m+3}{3m+3}\right)\Gamma\left(\frac{5}{3}\right)\Gamma\left(\frac{9m+1}{3m+3}\right)}{\Gamma\left(\frac{14m+6}{3m+3}\right)}$$

respectively.

The equation for $\overline{u_1^2}$ is therefore

$$\overline{u_1^2} = \left(\frac{2}{3}\right)^{\frac{1}{3}} \frac{\Gamma\left(\frac{2}{3}\right)}{\Gamma\left(\frac{1}{3}\right)} \rho^{-\frac{2}{3}} \left(\frac{2\tau_w}{\mu\rho}\right) - \rho^{-\left(\frac{11m+3}{3m+3}\right)} \Gamma\left(\frac{11m+3}{3m+3}\right)\Gamma\left(\frac{9m+1}{3m+3}\right)\{F\}, \quad \text{(B.33)}$$

where

$$F = \frac{A}{\Gamma\left(\frac{12m+4}{3m+3}\right)} + \frac{B}{3}\left(\frac{3}{2}\right)^{\frac{2}{3}} \frac{\Gamma\left(\frac{2}{3}\right)}{\Gamma\left(\frac{13m+5}{3m+3}\right)} + \frac{C\left(\frac{3}{2}\right)^{\frac{1}{3}}\Gamma\left(\frac{2}{3}\right)}{\Gamma\left(\frac{1}{3}\right)\Gamma\left(\frac{14m+6}{3m+3}\right)}. \quad \text{(B.34)}$$

When equation (B.33) is inverted

$$1 = \frac{2^{\frac{7}{3}}\,\Gamma\left(\frac{2}{3}\right)\Gamma\left(\frac{9m+1}{3m+3}\right)}{3^{\frac{1}{3}}(m+1)^{\frac{2}{3}}\,\Gamma\left(\frac{1}{3}\right)\Gamma\left(\frac{11m+3}{3m+3}\right)} f_w''^{\frac{4}{3}} - \frac{r^{\frac{8m}{3m+3}}\,\Gamma\left(\frac{9m+1}{3m+3}\right)}{c^2}\{F\} \qquad \text{(B.35)}$$

or, in terms of the dimensionless parameters f_w'' and f_w ,

$$1 = \frac{2^{\frac{7}{3}}\,\Gamma\left(\frac{2}{3}\right)\Gamma\left(\frac{9m+1}{3m+3}\right) f_w''^{\frac{4}{3}}}{3^{\frac{1}{3}}(m+1)^{\frac{2}{3}}\,\Gamma\left(\frac{1}{3}\right)\Gamma\left(\frac{11m+3}{3m+3}\right)} -$$

$$\Gamma\left(\frac{9m+1}{3m+3}\right)\left\{\frac{\frac{4}{3} f_w'' f_w}{\Gamma\left(\frac{12m+4}{3m+3}\right)} - \frac{2^{\frac{8}{3}} f_w}{3^{5/3} f_w''^{\frac{1}{3}}}\left(m + \frac{f_w'' f_w (m+1)}{2}\right)\frac{\Gamma\left(\frac{2}{3}\right)}{\Gamma\left(\frac{13m+5}{3m+3}\right)(m+1)^{1/3}} + \right.$$

$$\left. \frac{\Gamma\left(\frac{2}{3}\right)\,2^{\frac{7}{3}} f_w^{\,2}\,(m+1)^{\frac{1}{3}}}{\Gamma\left(\frac{1}{3}\right)\,\Gamma\left(\frac{14m+6}{3m+3}\right) f_w''^{\frac{2}{3}}\,3^{4/3}}\left(m + \frac{f_w'' f_w (m+1)}{2}\right)\right\} \qquad \text{(B.36)}$$

This equation first occurs in section 9.

APPENDIX C

A Dimensional Derivation of the Law of the Outer Region

The method follows that of Millikan (1938) but now includes a dimensionless parameter, Q, which is independent of y. Q may be a pressure gradient parameter, a transpitation velocity parameter, a relaxation parameter ..... etc.

In the region near the wall, the mean velocity distribution is assumed independent of δ but dependent on the viscosity, ν. In the outer region the mean valocity, measured relative to the free stream velocity, is assumed to depend on the boundary layer thickness, δ, but not on the viscosity. The dimensional equations for the inner and outer regions are written in the form:

Inner region: $$f_1\left(\frac{u}{u_\tau}, Q\right) = g\left(\frac{y u_\tau}{\nu}\right) \qquad (C.1)$$

Outer region: $$F_1\left(\frac{u_1 - u}{u_\tau}, \frac{u_1}{u_\tau}, Q\right) = G\left(y/\delta\right) \qquad (C.2)$$

or $$F_2\left(\frac{u}{u_\tau}, \frac{u_1}{u_\tau}, Q\right) = G\left(y/\delta\right) \qquad (C.3)$$

The equations are more general than those used by Millikan who assumed a priori that f_1 and F_2 were of a certain form.

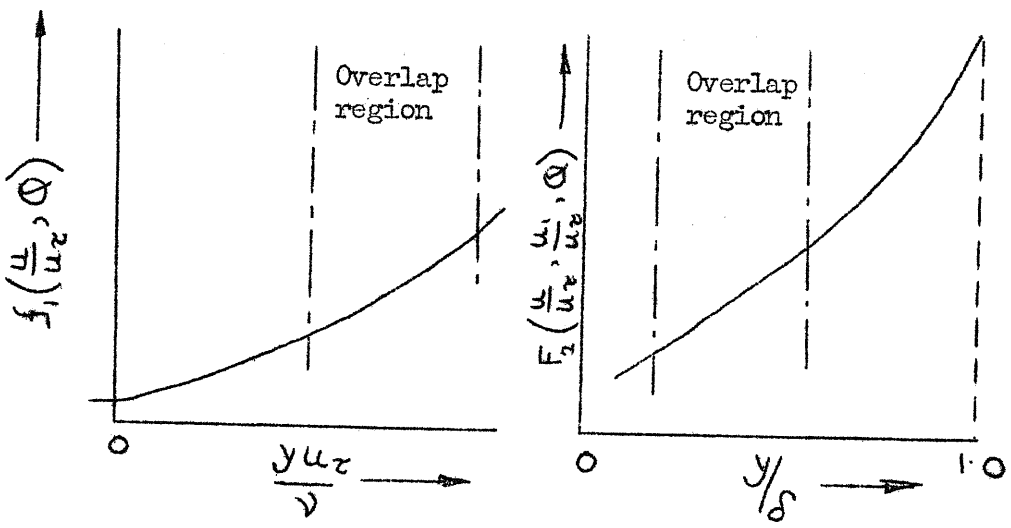

Equations (C.1) and (C.3) are differentiated with respect to y ,

$$\frac{\partial f_1\left(\frac{u}{u_\tau}, 0\right)}{\partial y} = \frac{\partial u}{\partial y} \cdot \frac{\partial f_1\left(\frac{u}{u_\tau}, 0\right)}{\partial u} = \frac{u_\tau}{\nu} g'\left(\frac{y u_\tau}{\nu}\right) \tag{C.4}$$

and $$\frac{\partial F_2\left(\frac{u}{u_\tau}, \frac{u_1}{u_\tau}, 0\right)}{\partial y} = \frac{\partial u}{\partial y} \frac{\partial F_2\left(\frac{u}{u_\tau}, \frac{u_1}{u_\tau}, 0\right)}{\partial u} = \frac{G'(y/\delta)}{\delta} \tag{C.5}$$

where g' is $\frac{\partial g}{\partial\left(\frac{y u_\tau}{\nu}\right)}$ and G' is $\frac{\partial G}{\partial(y/\delta)}$.

If an overlap region is to exist in which equations (C.1) and (C.3) are valid, the velocity gradient, $\frac{\partial u}{\partial y}$, given by the two equations must be the same in this region. If f_1 and F_2 are simply related, i.e. the form for u in both the functions is the same, then the gradients of the curves with respect to y , in the above figures, will be the same in the overlap region.

Thus $$\frac{\partial f_1}{\partial y} = \frac{\partial F_2}{\partial y} \tag{C.6}$$

and integrating with respect to y ,

$$f_1\left(\frac{u}{u_\tau}, 0\right) + f_2\left(\frac{u_1}{u_\tau}, 0\right) = F_2\left(\frac{u}{u_\tau}, \frac{u_1}{u_\tau}, 0\right). \tag{C.7}$$

From equations (C.4), (C.5) and (C.6),

$$y \frac{\partial f_1}{\partial y} = y \frac{\partial F_2}{\partial y} = \frac{y u_\tau}{\nu} \cdot g'\left(\frac{y u_\tau}{\nu}\right) = \frac{y}{\delta} G'(y/\delta) \tag{C.8}$$

but $\frac{y u_\tau}{\nu}$ and $\frac{y}{\delta}$ are formally independent, therefore

$$\frac{y u_\tau}{\nu} g'\left(\frac{y u_\tau}{\nu}\right) = \frac{y}{\delta} G'(y/\delta) = \frac{1}{K} \tag{C.9}$$

where K is a constant. Thus

$$g\left(\frac{y u_\tau}{\nu}\right) = \frac{1}{K} \operatorname{LOG}_e \frac{y u_\tau}{\nu} + C_1 \tag{C.10}$$

and $$G(y/\delta) = \frac{1}{K} \log_e \frac{y}{\delta} + C_2 \qquad (C.11)$$

The equations for the overlap region are therefore

$$f_1\left(\frac{u}{u_\tau}, Q\right) = \frac{1}{K} \log_e \frac{y u_\tau}{\nu} + C_1 \qquad (C.12)$$

or $$K\left(f_1\left(\frac{u}{u_\tau}, Q\right) - C_1\right) - \log_e \frac{\delta u_\tau}{\nu} = \log_e \frac{y}{\delta} \qquad (C.13)$$

and $$F_2\left(\frac{u}{u_\tau}, \frac{u_1}{u_\tau}, Q\right) = \frac{1}{K} \log_e \frac{y}{\delta} + C_2 \qquad (C.14)$$

or $$K\left(F_2\left(\frac{u}{u_\tau}, \frac{u_1}{u_\tau}, Q\right) - C_2\right) = K\left(f_1\left(\frac{u}{u_\tau}, Q\right) - f_2\left(\frac{u_1}{u_\tau}, Q\right) - C_2\right) = \log_e y/\delta. \qquad (C.15)$$

In view of equation (C.3), the outer region equation is

$$K\left(f_1\left(\frac{u}{u_\tau}, Q\right) - f_2\left(\frac{u_1}{u_\tau}, Q\right) - C_2\right) = K\left(G\left(\frac{y}{\delta}\right) - C_2\right) = S(y/\delta), \qquad (C.16)$$

or $$K\left(f_1\left(\frac{u_1}{u_\tau}, Q\right) - f_1\left(\frac{u}{u_\tau}, Q\right)\right) = S(1) - S(y/\delta) = F(y/\delta), \qquad (C.17)$$

where $S(y/\delta) = \log_e y/\delta$ in the overlap region.

Equations (C.16) and (C.17) will be called the equations for the outer region.

TABLE 1. Comparison of Skin Friction Results

$\frac{V_w}{u_1}$	From momentum traverses C_{fE}	Using Black and Sarnecki's theory C_f	From the 'law of the wall' equation C_f^*
0	0.0037 ± 10%		0.0040
	0.0036 "		0.0038
	0.0035 "		0.0037
0.0013	0.0028 ± 0.0003		0.0026
	0.0026 "	0.0023 ± 15%	0.0025
0.002	0.0021 "		0.0023
	0.002	0.0016 "	0.0020
0.0029	0.0019		0.0016
	0.0014	0.0015 "	0.0015
0.004	0.0013		0.0011
	0.0010	0.0009	0.0009
0.0057	---		0.00046
	---	0.0006	0.00032

TABLE 2. Mickley and Davis' Results

$\frac{y_w}{u_1}$	Station	c_f as evaluated by Mickley and Davis	Including the Pressure Gradient Term		c_f* from the 'law of the wall' equation
			c_{fA}	c_{fB} †	
0.003	E	0.00136			0.0019
	G	0.00097		0.00175	0.0017
	H	0.00087		0.00165	0.0014
	I	0.00068	0.0008	0.0016	0.0013
	J	0.00066	0.00094	0.0014	0.0011
	K	0.00054	0.00087	0.0013	0.00105
	L	0.00058	0.00098	0.0014	0.0009
	M	0.0005	0.0005	0.0013	0.0009
	N	0.0005	0.0005		0.00085
0	J	0.00349	Only a very small correction required.		0.00318
	K	0.00329			0.00311
	L	0.00332			0.00292
	M	0.00307			0.00295

† Fig. 33 shows the distribution of u_1 along the working section. Curve A was used to evaluate c_{fA} and curve B to evaluate c_{fB}.

Constants for the Preston Tube

TABLE 3.

t	I_1	k	log k
0	1.5706	0.0424	$\bar{2}$.6274
0.5	1.5603	0.0426	$\bar{2}$.6298
1.0	1.5161	0.0437	$\bar{2}$.6405

TABLE 4.

t	I_1	I_2	I_3
0	1.5706	1.5706	1.5706
0.68	1.54	1.53	1.53
1.0	1.5161	1.51	1.50

TABLE 5. Constants used by Different Authors

	Schultz-Grunow (1947)	Clauser (1954)	Present Values	Coles (1954)
K	0.39	0.41	0.418	0.42
B	5.93	5.6	5.8	5.10
$\Phi(1)$			8.2	7.90
C_1	3.34	3.60	3.56	4.05
C_2		22.0	26.4	29.0
C_3			189.5	
C_4			1792	

TABLE 6. The universal function $S(y/\delta)$

$S(y/\delta)$	y/δ	$S(y/\delta)$	y/δ
- 4.04	0.0174	- 1.62	0.19
- 3.68	0.0251	- 1.35	0.23
- 3.22	0.0398	- 0.7	0.35
- 2.87	0.0575	- 0.32	0.43
- 2.58	0.0794	+ 0.175	0.55
- 2.30	0.105	0.57	0.67
- 2.03	0.138	0.875	0.80
- 2.0	0.140	1.05	1.0

TABLE 7. Values for K and B

	K	B	KB
Schultz-Grunow (1947)	0.39	4.1	1.6
Klebanoff and Diehl (1951)	0.43	4.8	2.0
Clauser	0.41	4.9	2.0
Coles	0.40	5.1	2.0
Dutton	0.42	5.8	2.4
Ludwieg and Tillmann (1949)	0.44	6.0	2.7

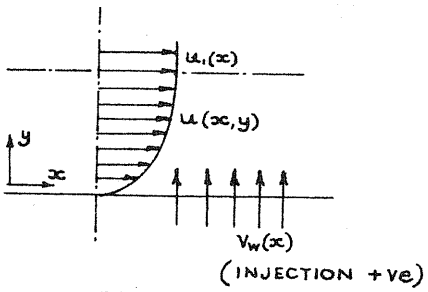

FIG. 1

THE x & y COORDINATES

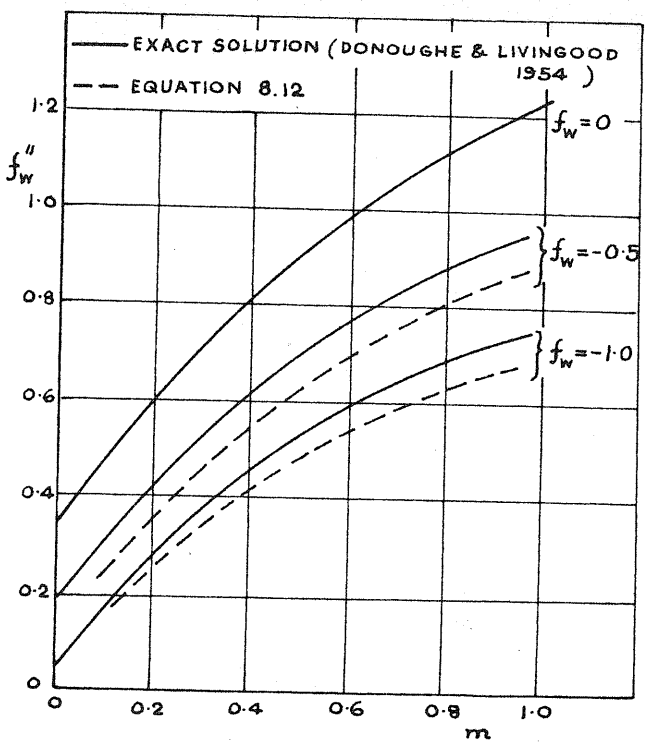

FIG. 2 VARIATION OF SKIN FRICTION PARAMETER, f_w'', WITH EULER NUMBER, m

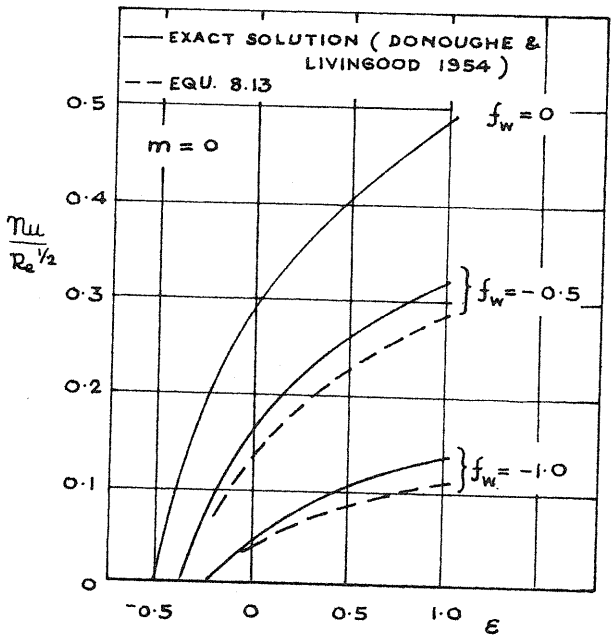

FIG. 3 HEAT TRANSFER TO A POROUS WALL WITH VARIABLE WALL TEMPERATURE

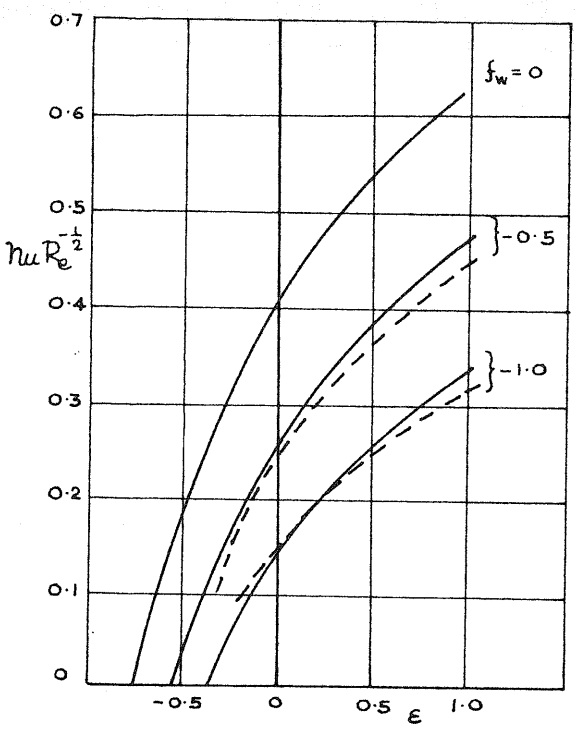

FIG. 4 $m = 0.5$

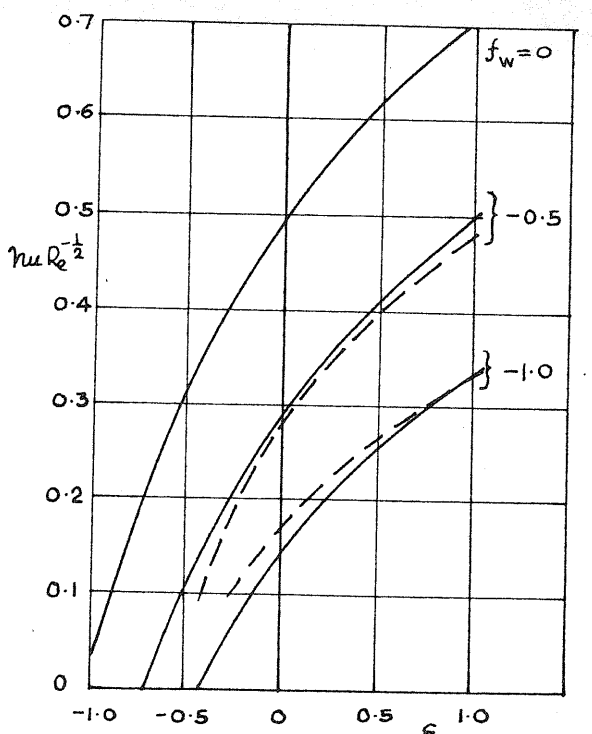

FIG. 5 $m = 1.0$

——— EXACT SOLUTION (DONOUGHE & LIVINGOOD 1954)
– – – EQUATION 8.13

HEAT TRANSFER TO A POROUS WALL WITH VARIABLE TEMPERATURE

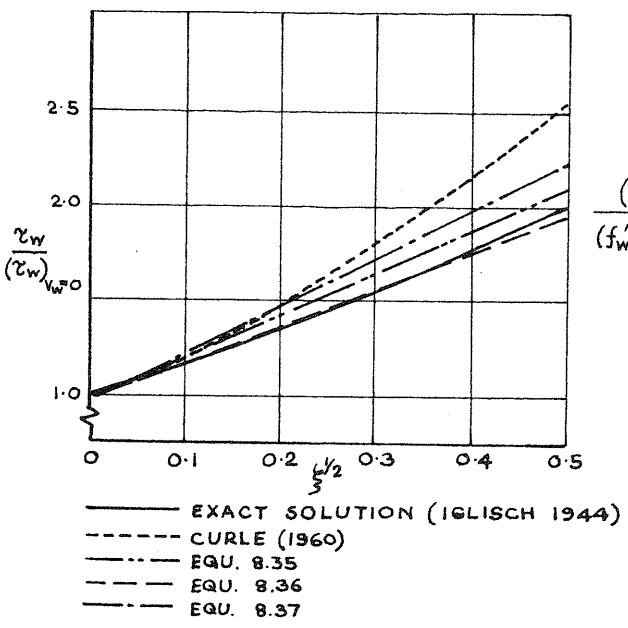

FIG. 6 SKIN FRICTION FOR A FLAT PLATE WITH UNIFORM SUCTION

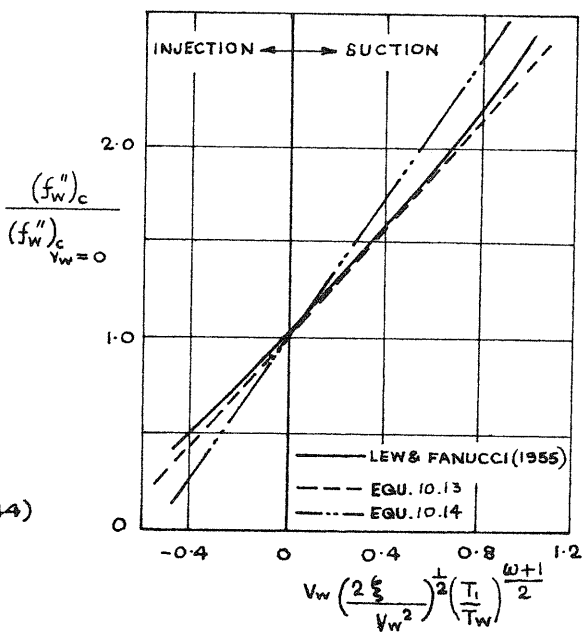

FIG. 7 SKIN FRICTION — COMPRESSIBLE SOLUTION

$\xi = \frac{V_w^2 x}{u_1 \nu}$

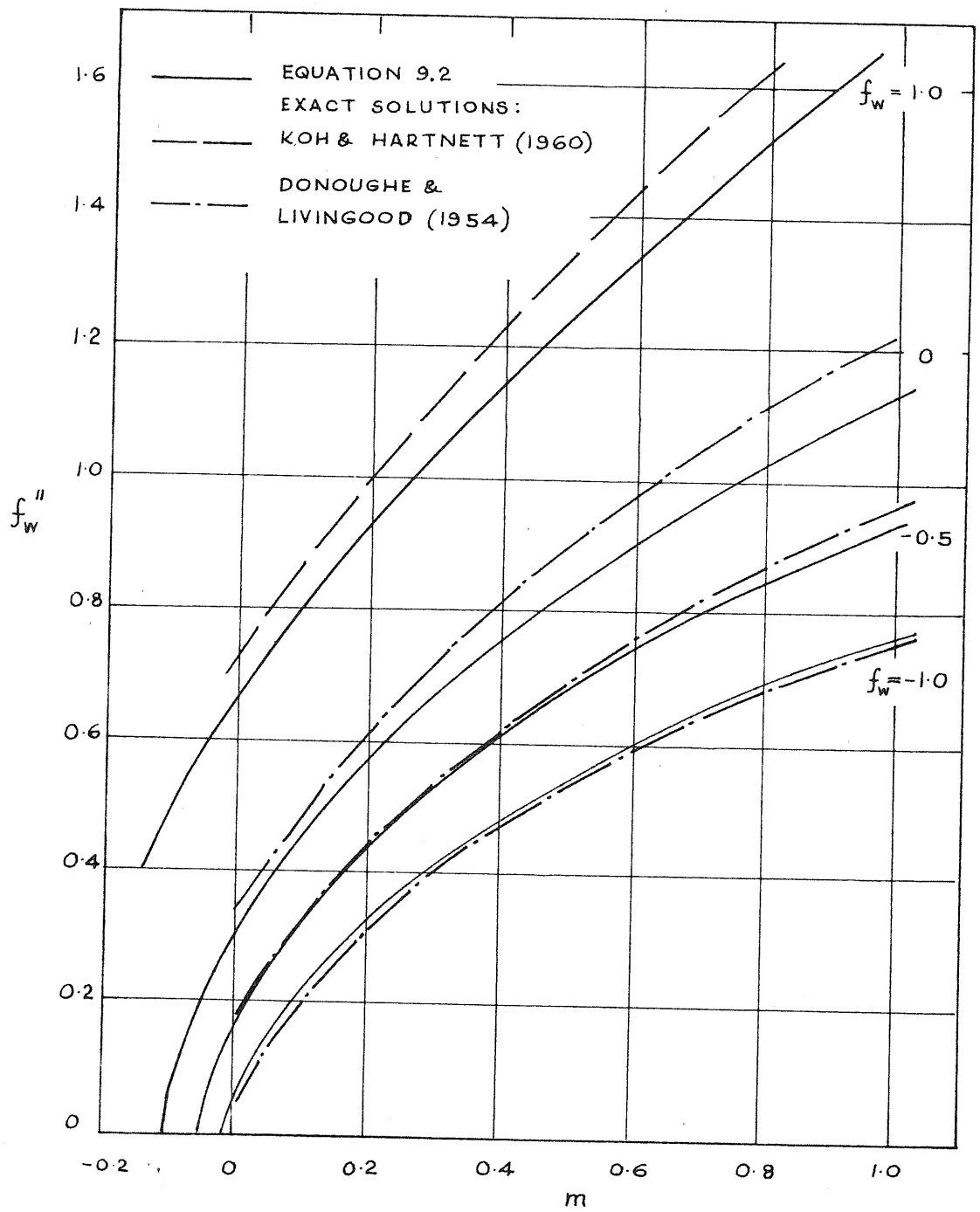

FIG. 8 VARIATION OF SKIN FRICTION PARAMETER, f_w'', WITH EULER NUMBER, m.

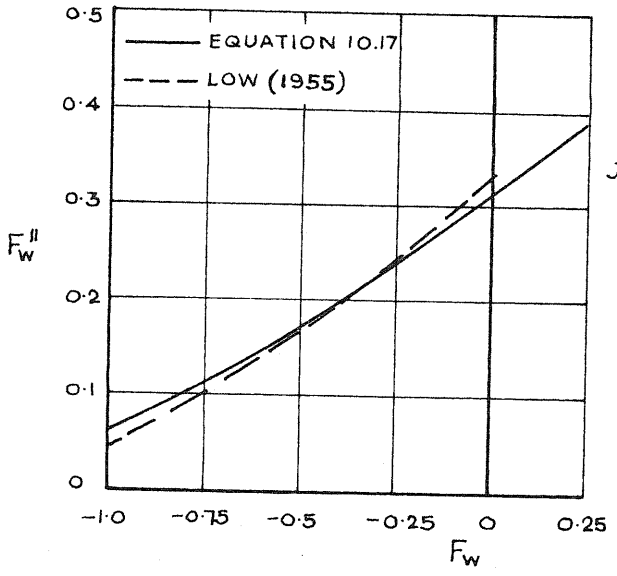

FIG. 9

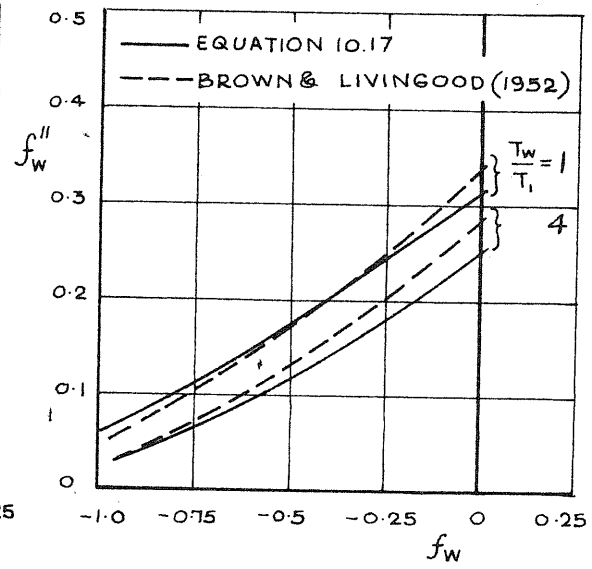

FIG. 10

VARIATION OF SKIN FRICTION WITH INJECTION ($\omega = 0.7$)

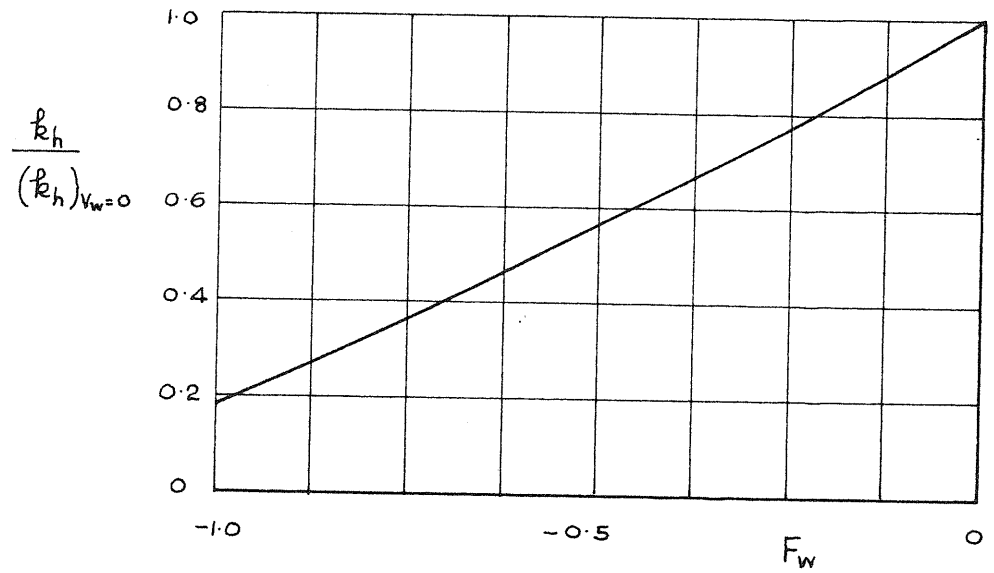

FIG. 11 VARIATION OF THE STANTON HEAT TRANSFER COEFFICIENT, ρk_h, WITH INJECTION

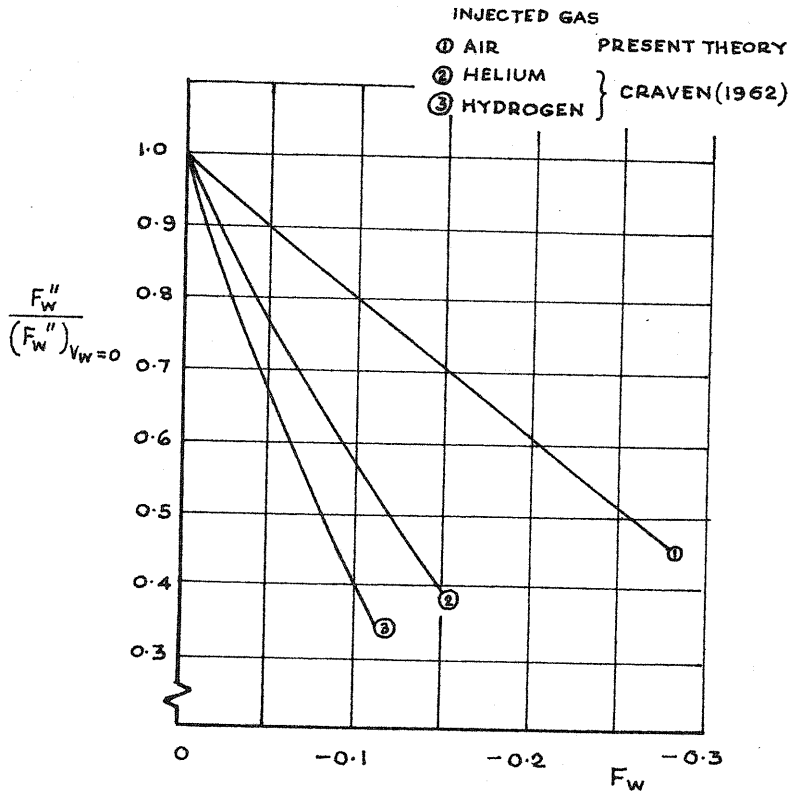

FIG. 12 EFFECT OF FOREIGN GAS INJECTION ON SKIN FRICTION (UNIFORM INJECTION VELOCITY $M_1 = 4$, $T_w = T_1$)

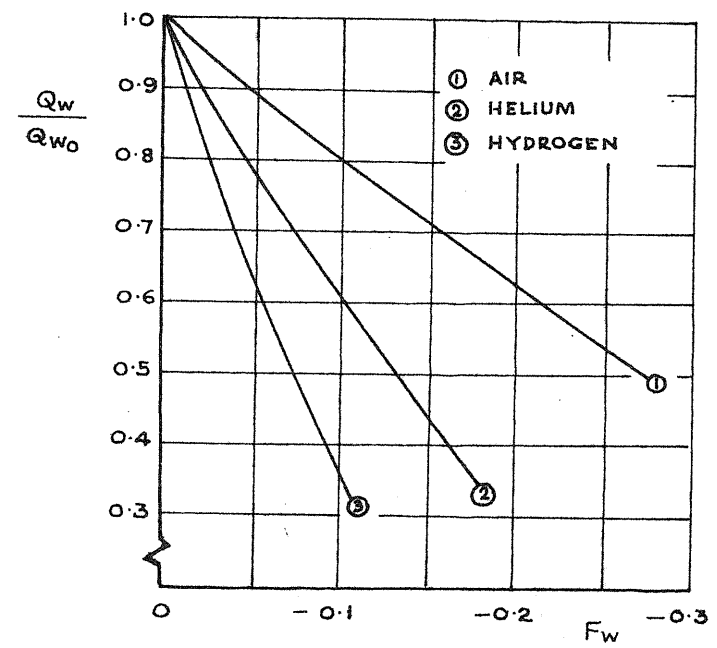

FIG. 13 EFFECT OF FOREIGN GAS INJECTION ON HEAT TRANSFER RATE (UNIFORM INJECTION VELOCITY $M_1 = 4$, $T_w = T_1$)

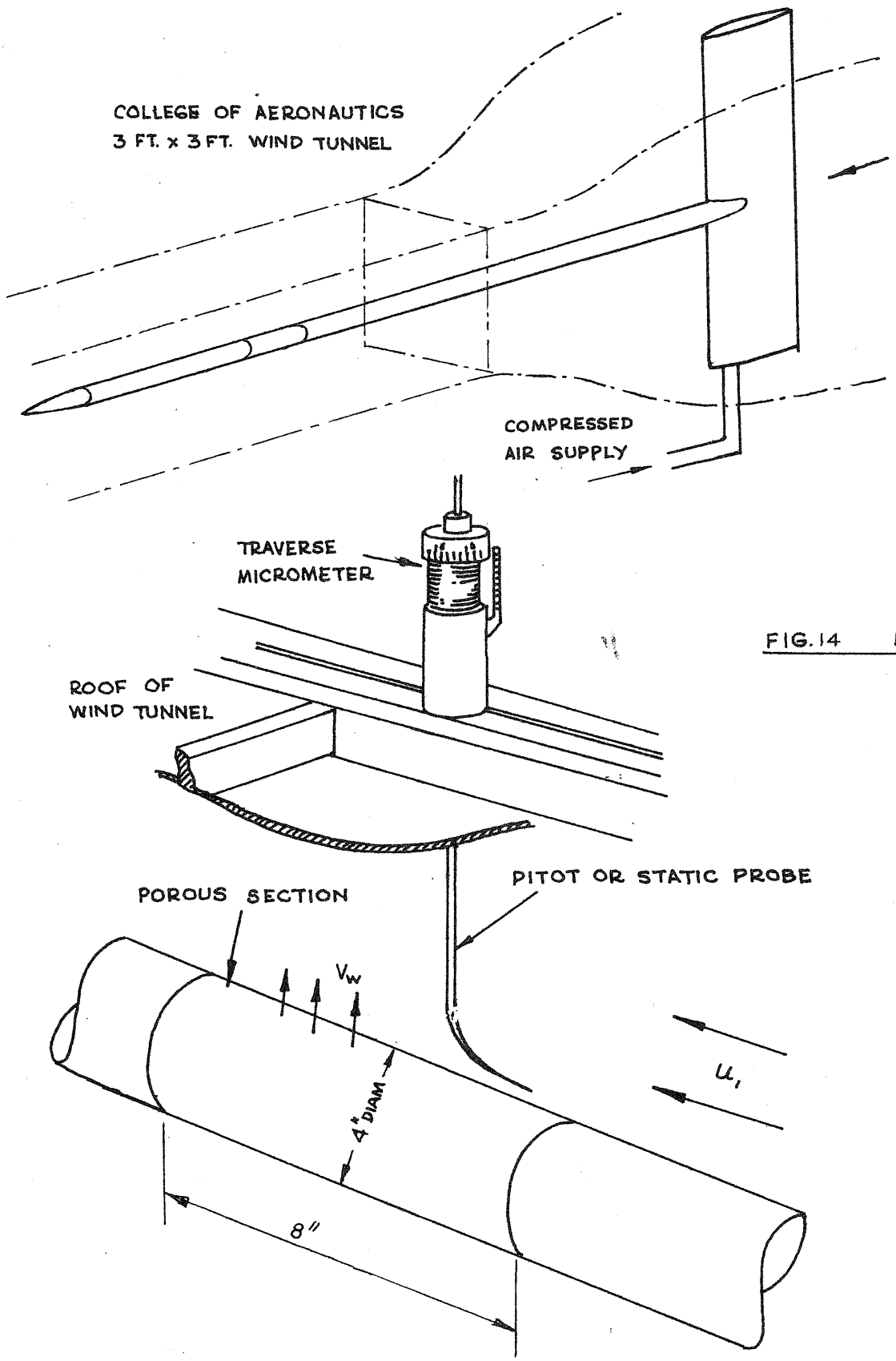

FIG. 14 MODEL 1

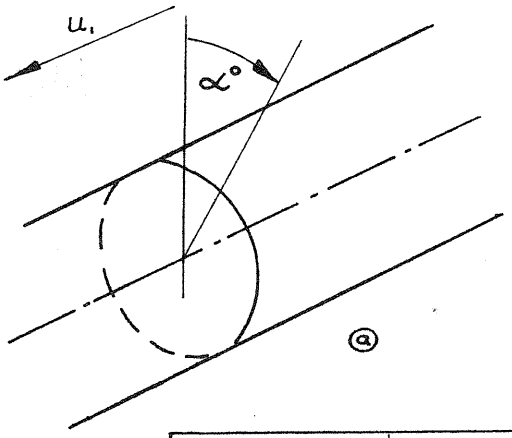

ⓐ

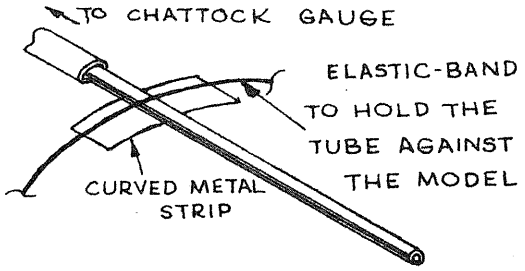

ⓑ THE PRESTON TUBE

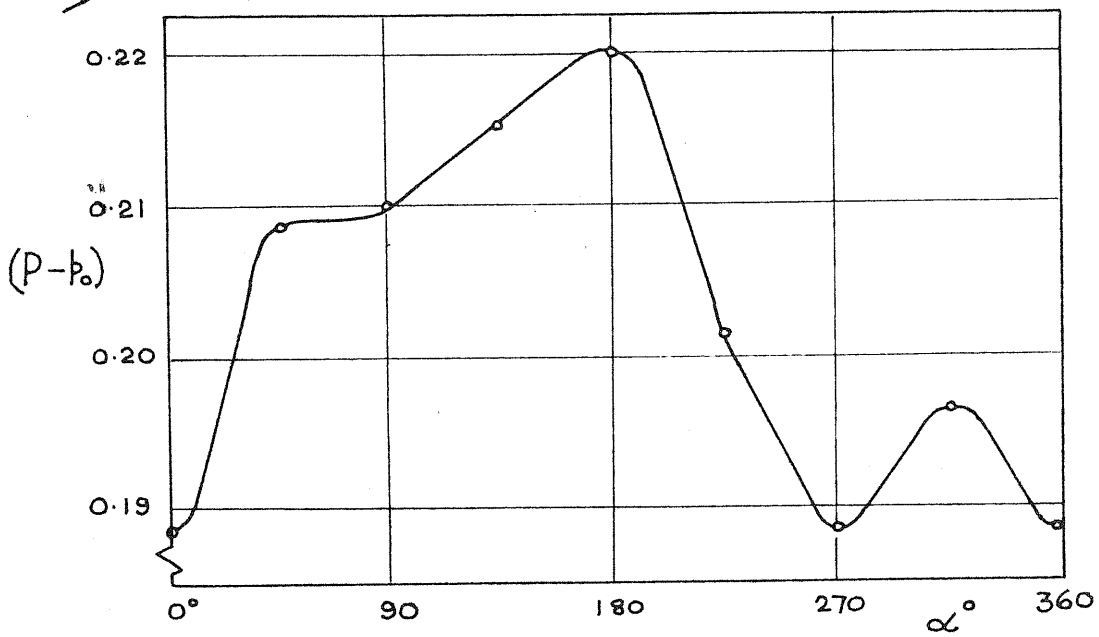

ⓒ MODEL 1

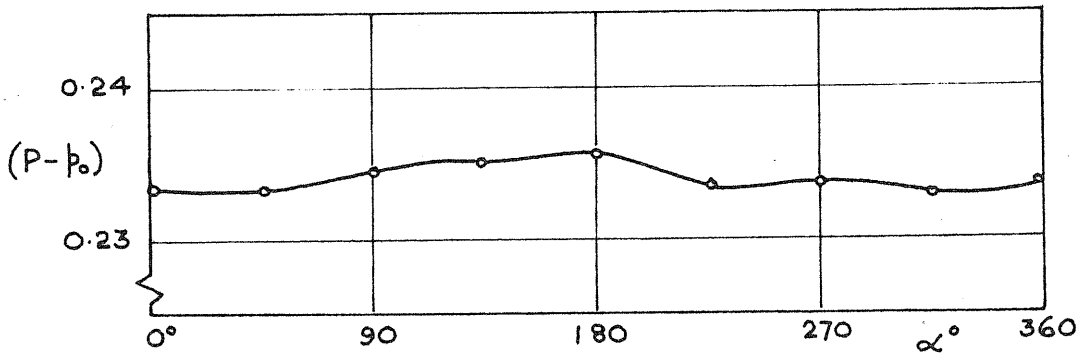

ⓓ MODEL 2

FIG. 15 PRESTON TUBE READINGS ROUND THE MODELS

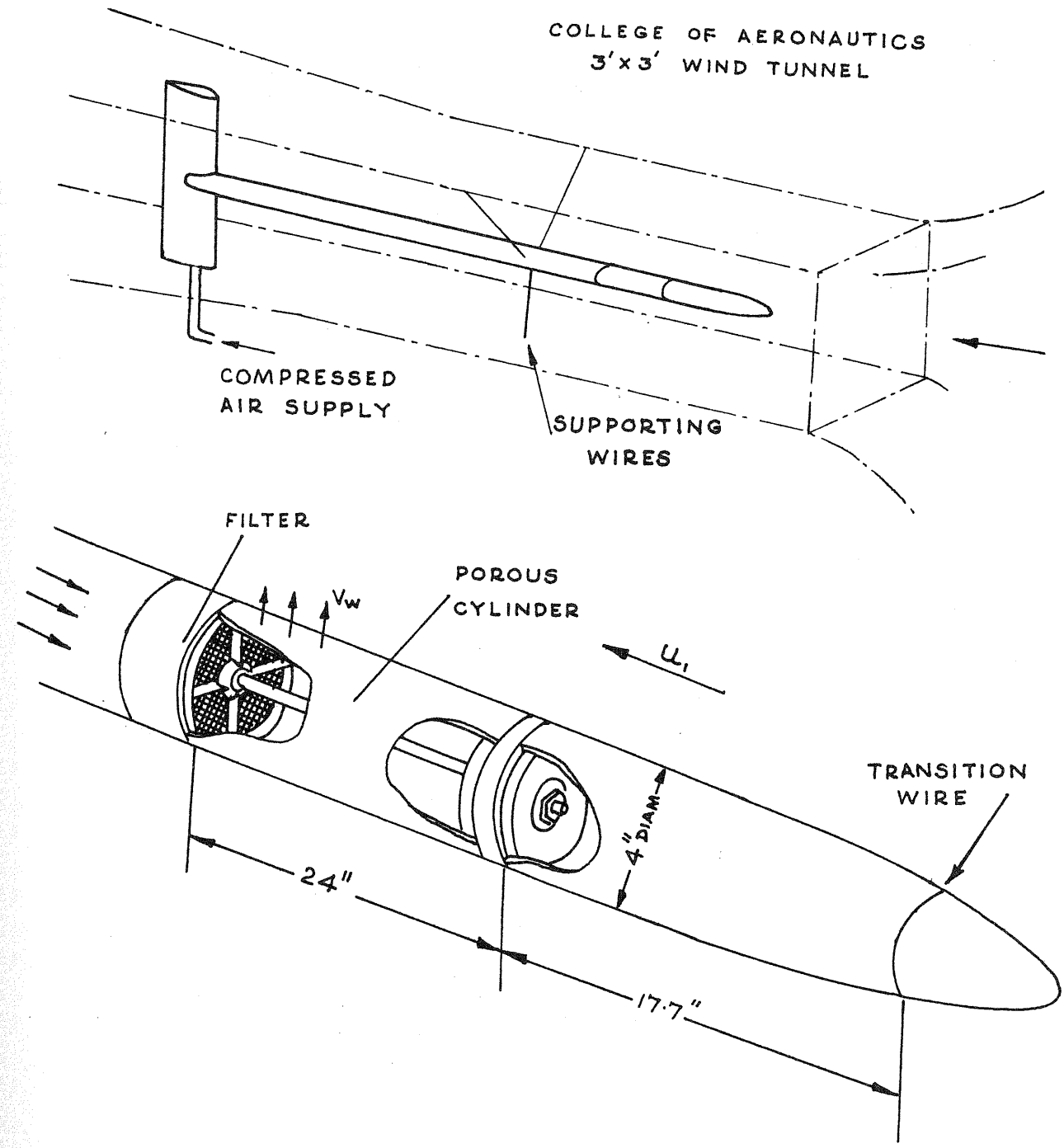

FIG. 16 MODEL 2

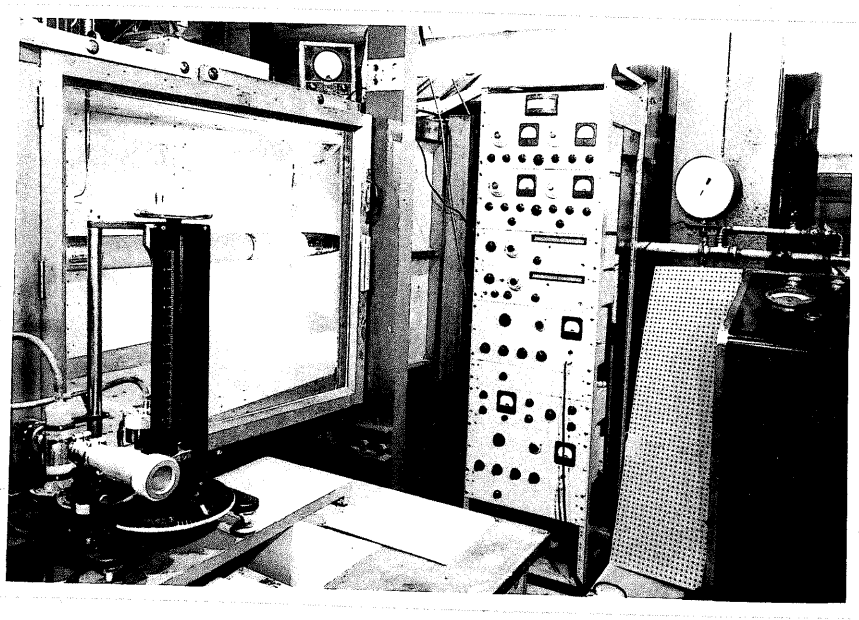

FIG. 17 MODEL 2 - THE WIND TUNNEL WORKING SECTION

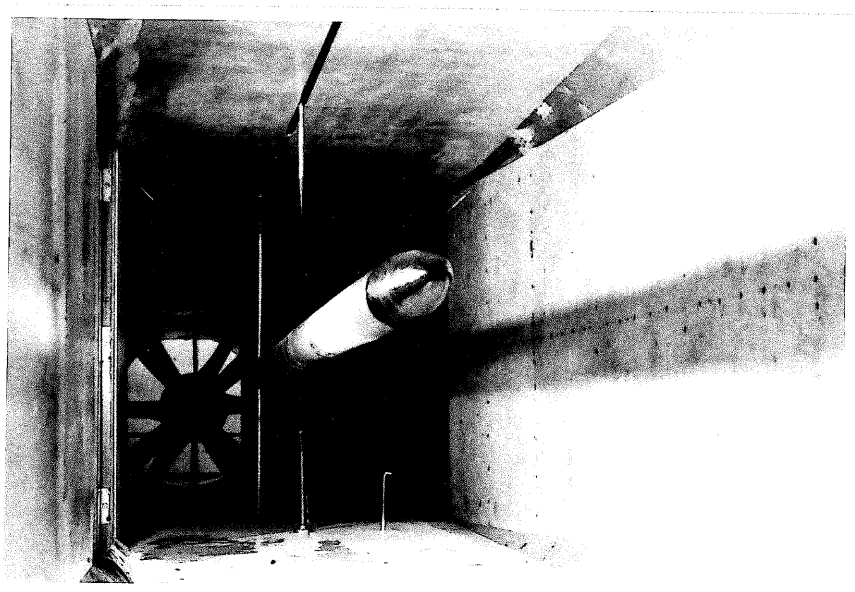

FIG. 18 MODEL 2 - PHOTOGRAPH TAKEN FROM THE WIND TUNNEL CONTRACTION

C.I.T. ENGINEERING AERONAUTICS LIBRARY

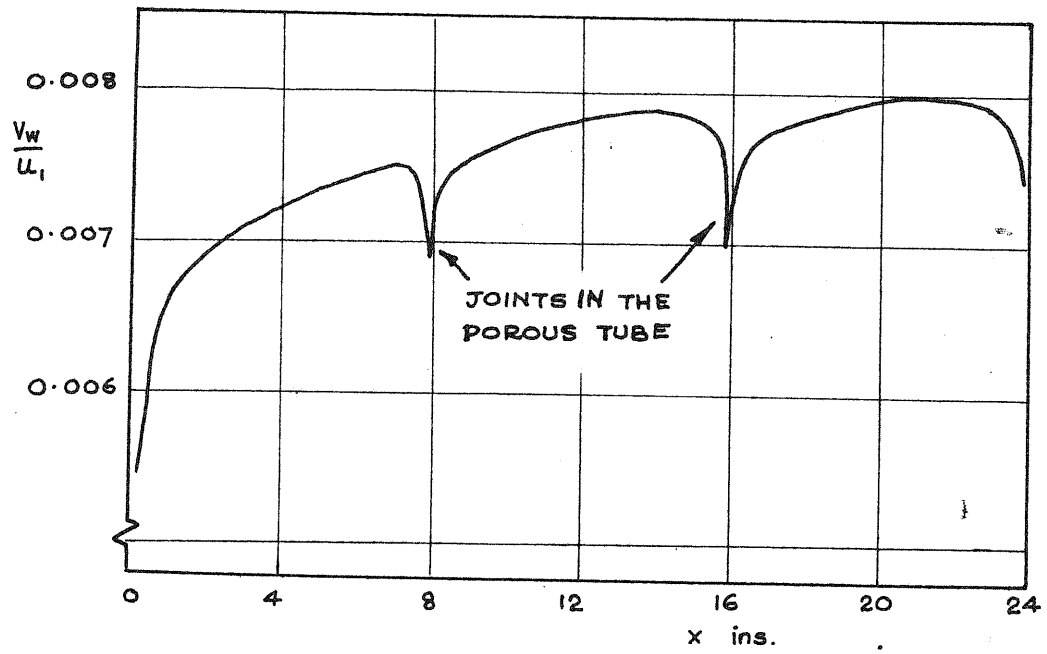

FIG. 19 THE APPROXIMATE INJECTION VELOCITY DISTRIBUTION

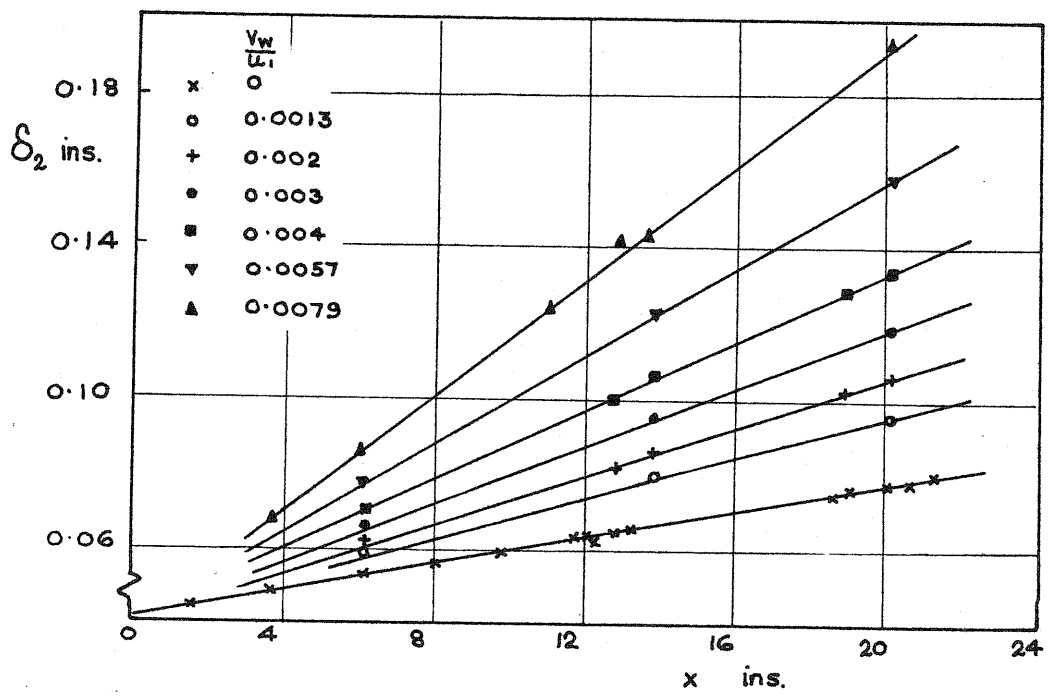

FIG. 20 THE MOMENTUM THICKNESS ALONG THE CYLINDER

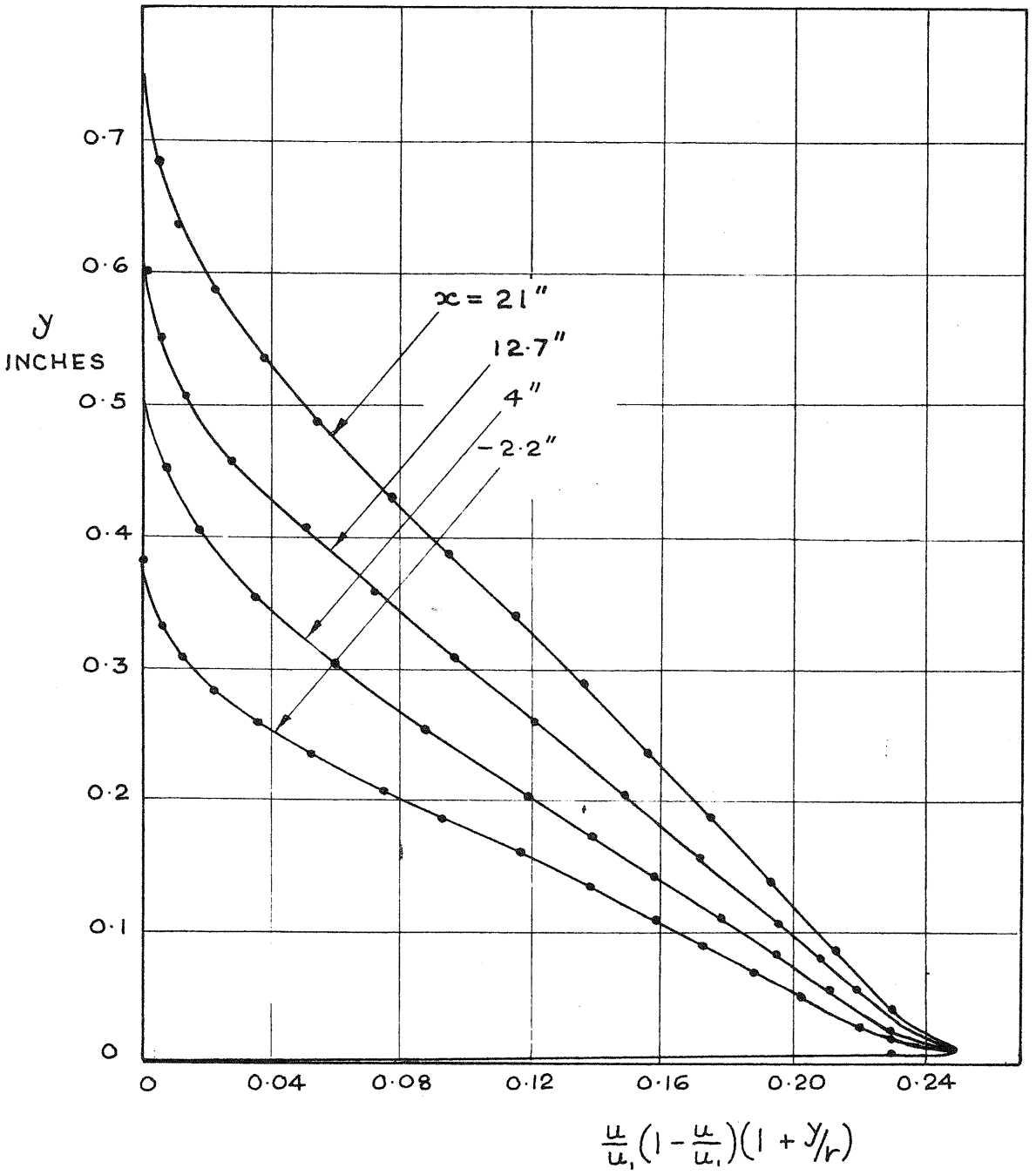

FIG. 21 MOMENTUM CURVES WHEN $V_w = 0$

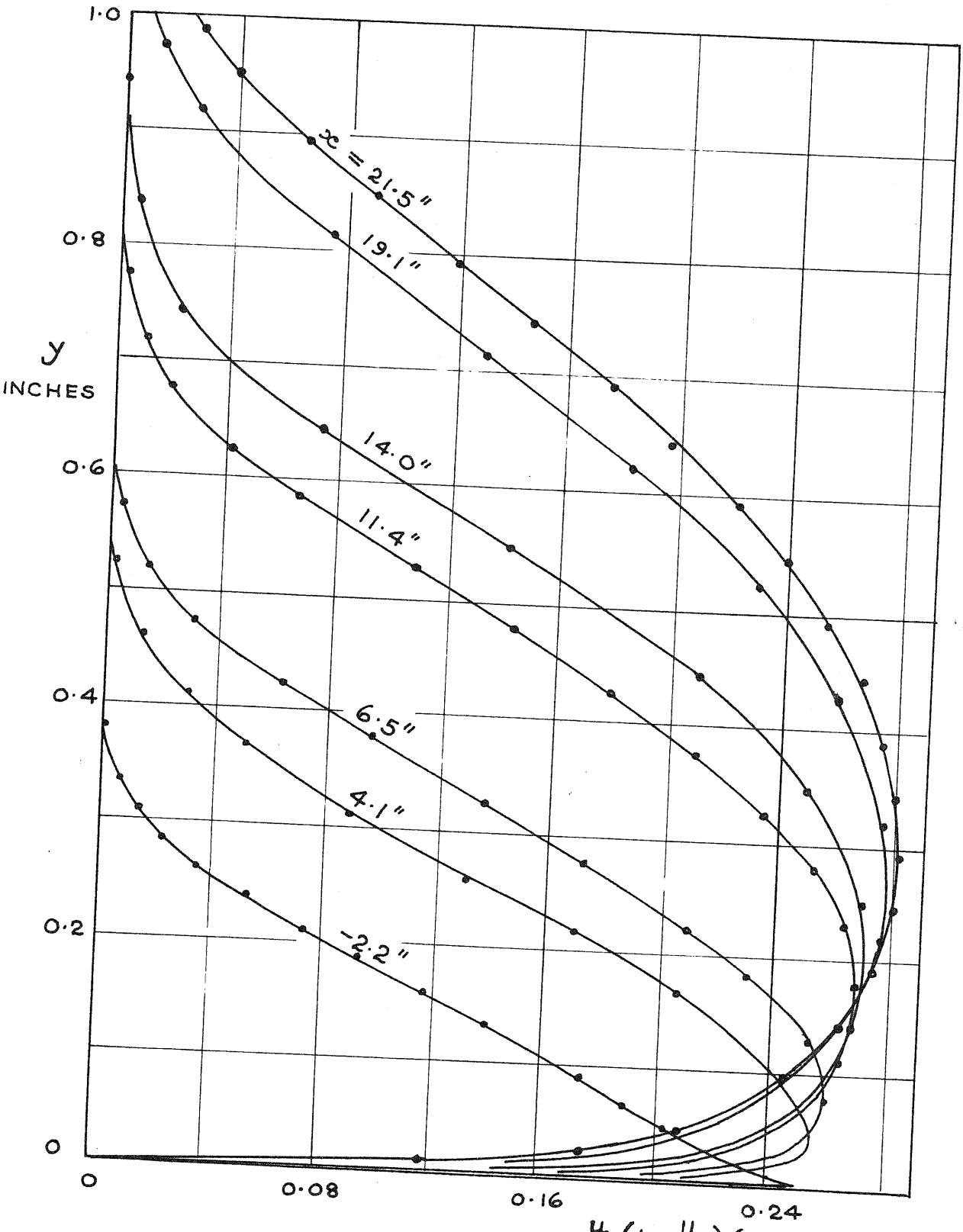

FIG. 22 MOMENTUM CURVES

$\frac{v_w}{u_1} = 0.0079$

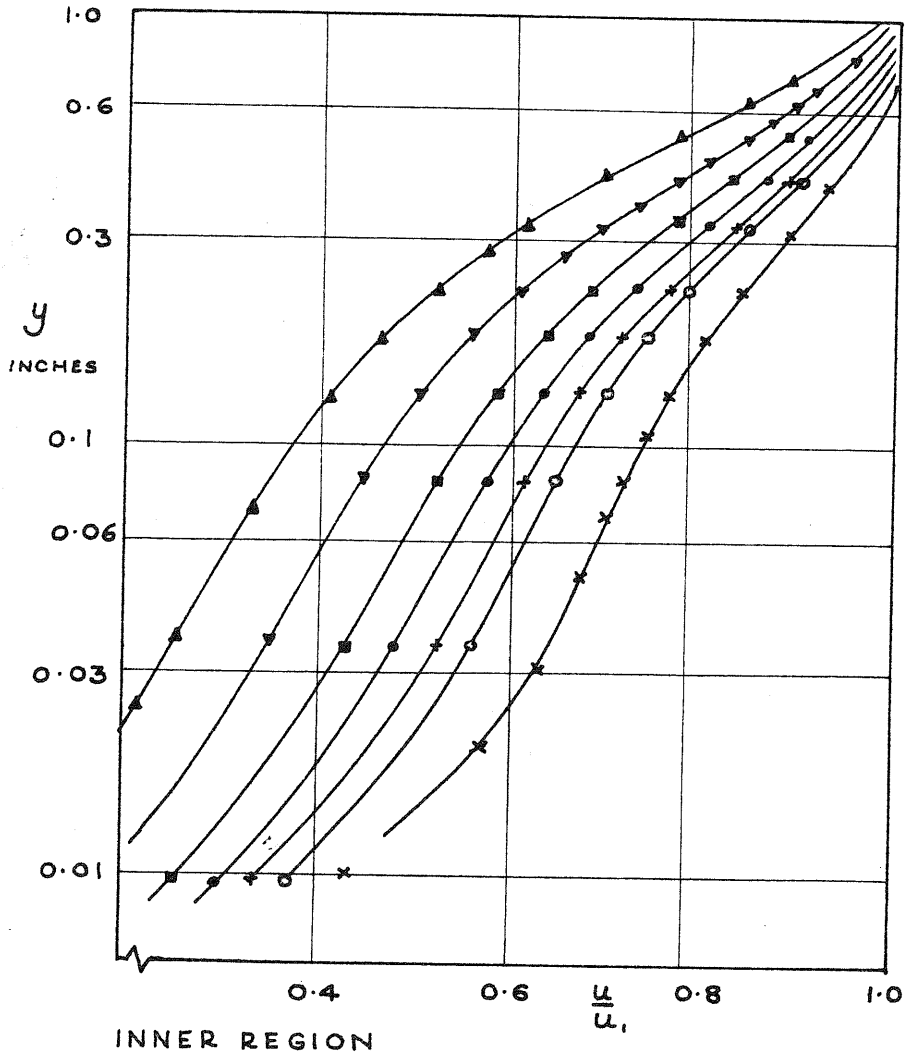

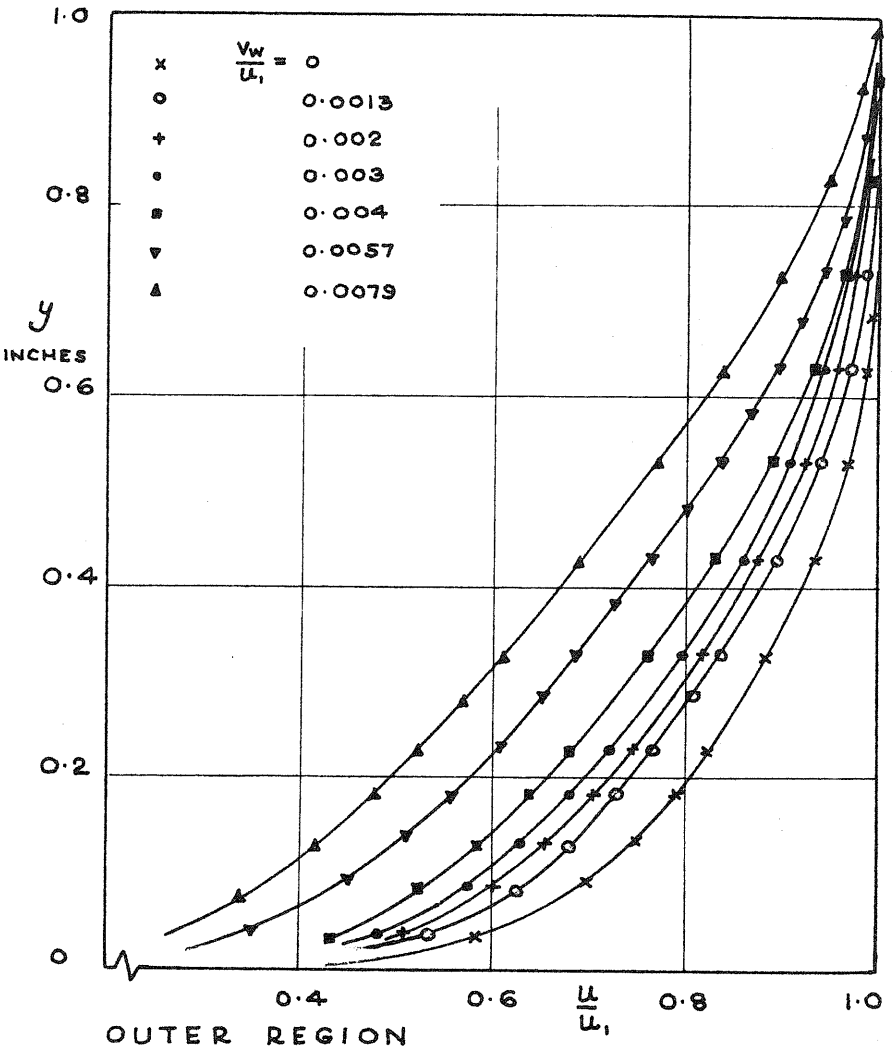

FIG. 23 VELOCITY PROFILES AT X = 20 INCHES

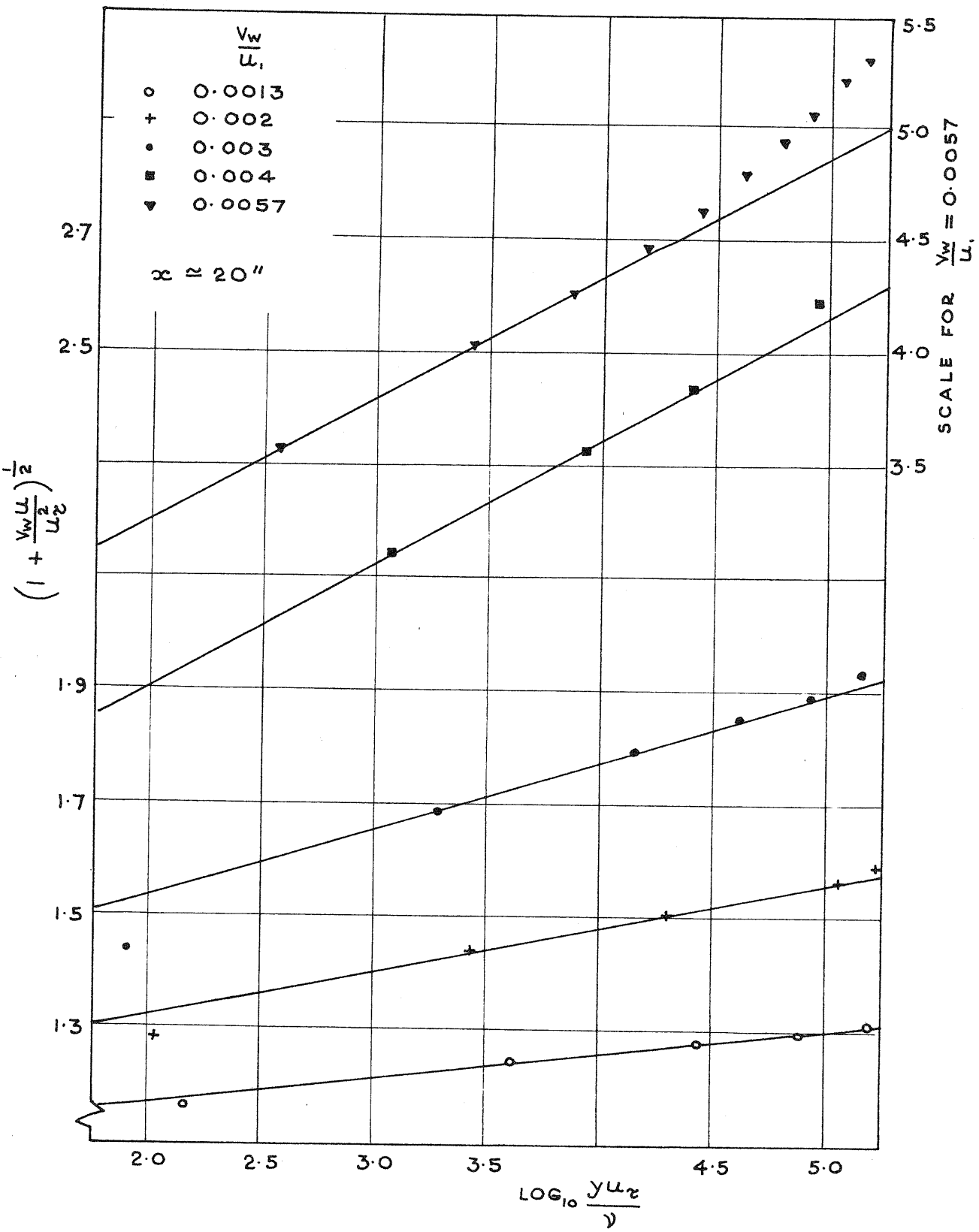

FIG. 24 VELOCITY PROFILES COMPARED WITH MICKLEY & DAVIS' THEORY

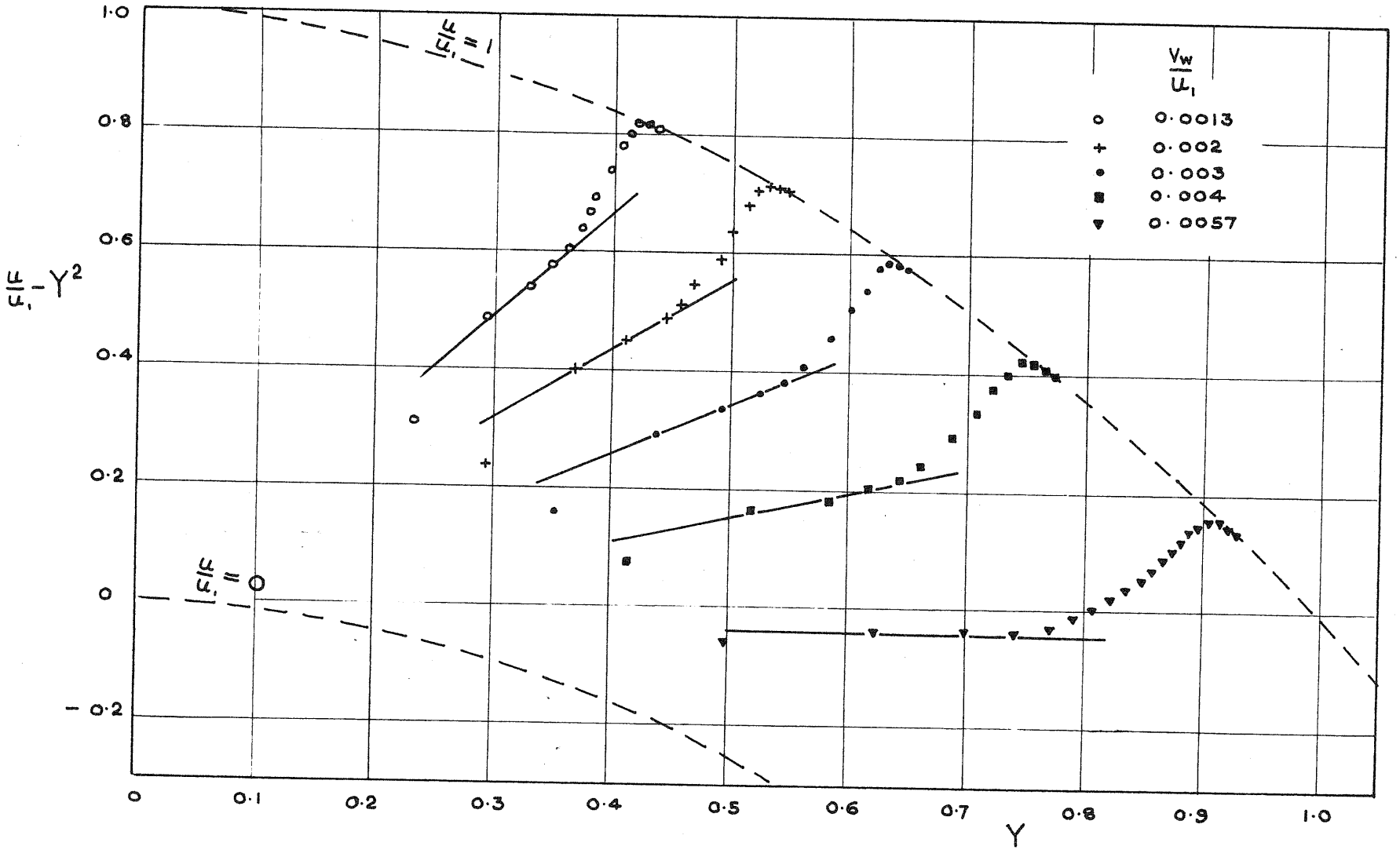

FIG. 25 VELOCITY PROFILES COMPARED WITH BLACK & SARNECKI'S THEORY

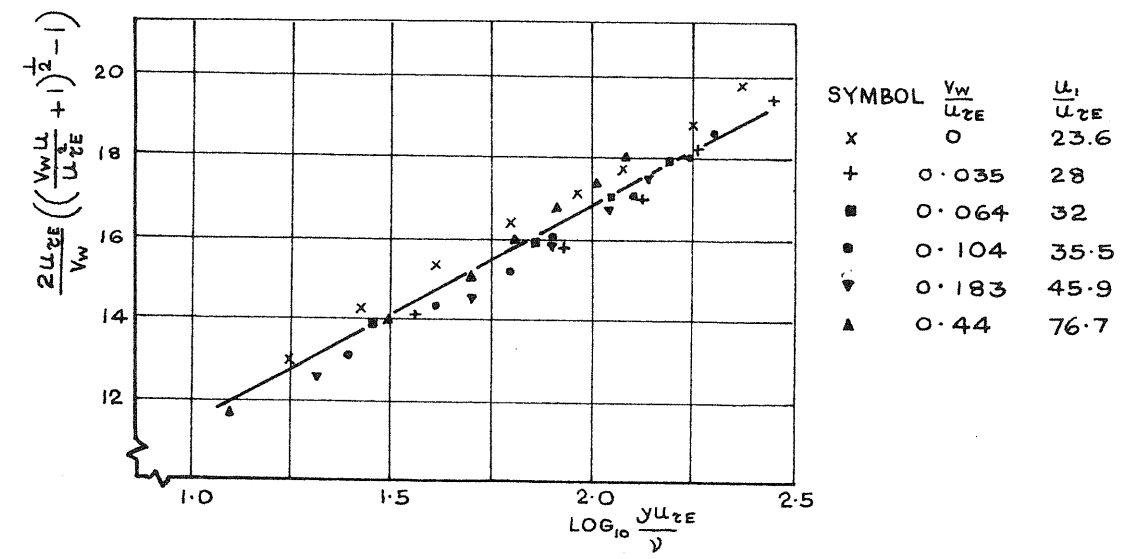

FIG. 26 EXPERIMENTAL RESULTS COMPARED WITH EQUATION 19.3

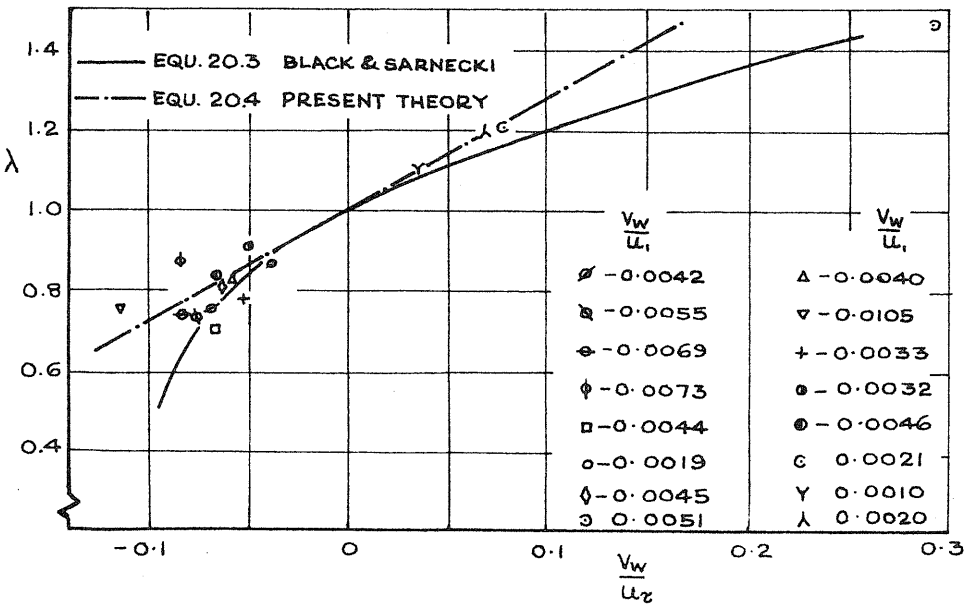

FIG. 27 VARIATION OF THE PROFILE PARAMETER λ WITH TRANSPIRATION

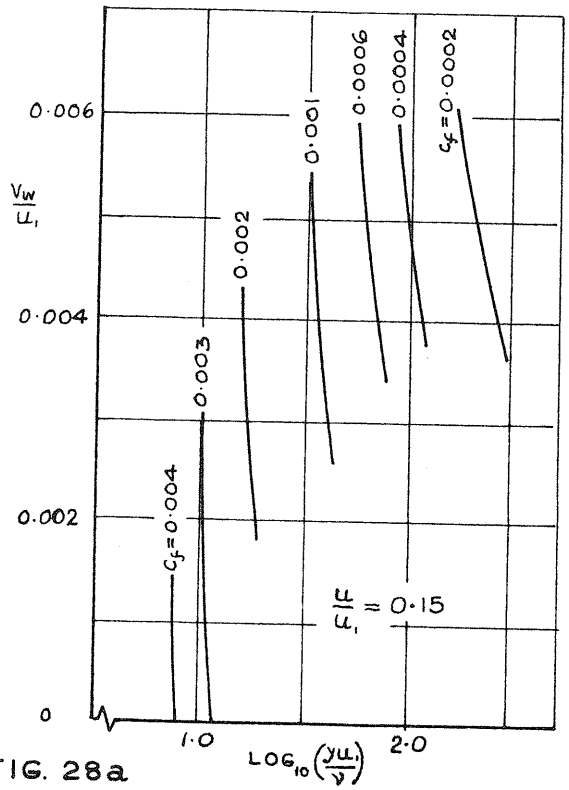

FIG. 28a

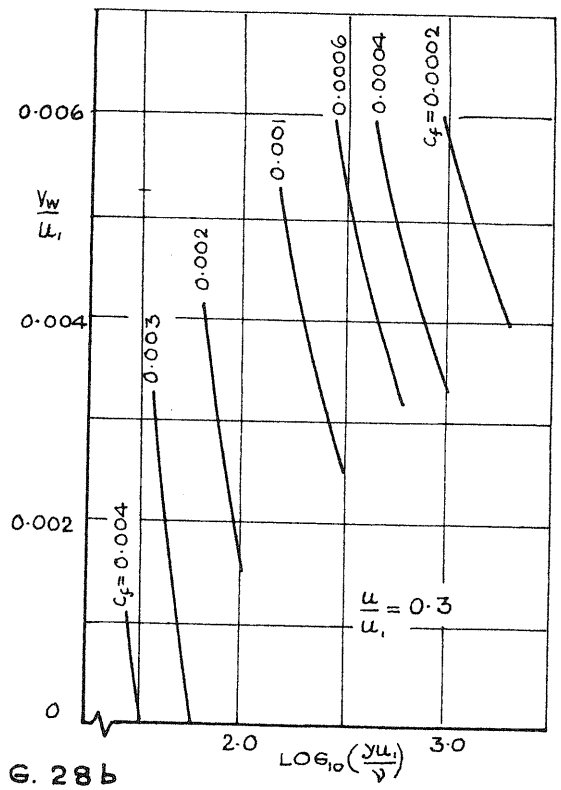

FIG. 28b

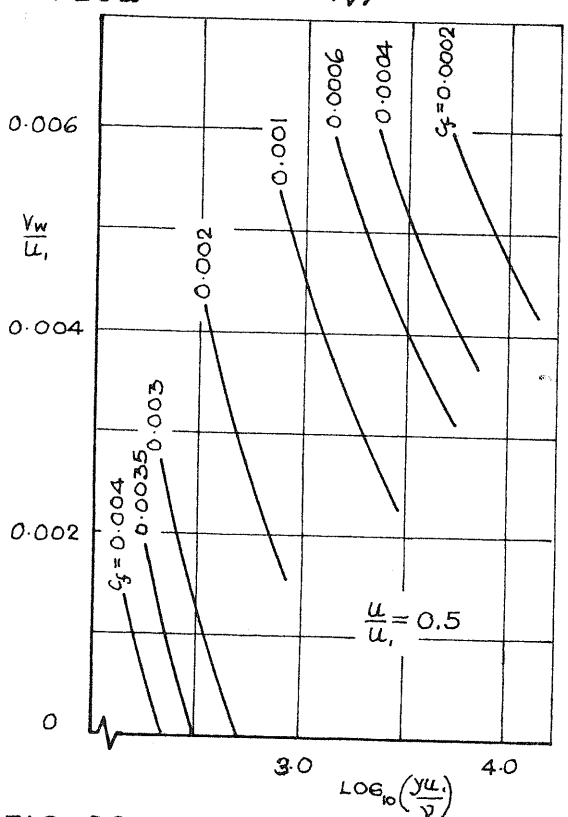

FIG. 28c

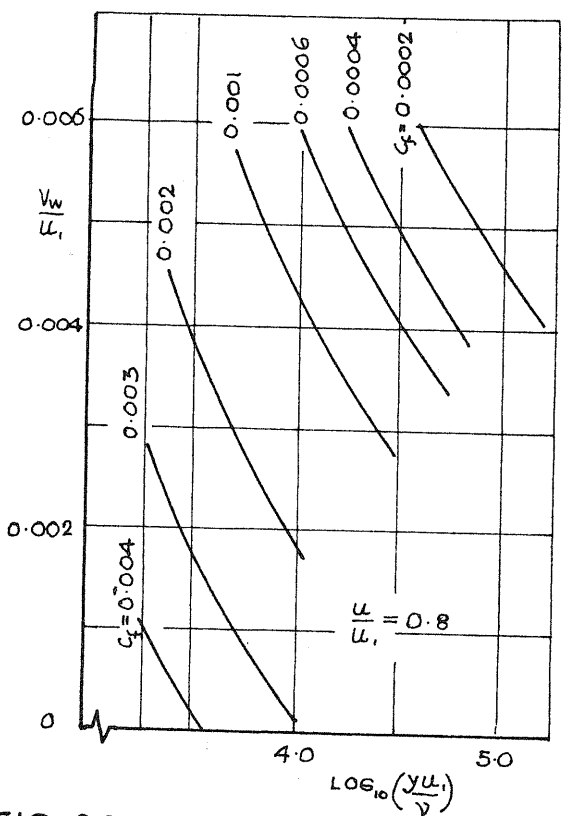

FIG. 28d

CURVES OF EQUATION 21.1

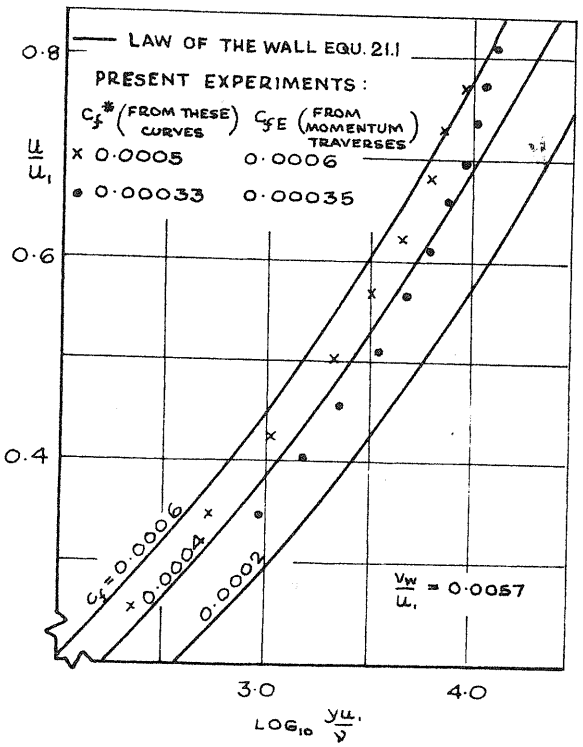

FIG. 29 SKIN FRICTION FROM VELOCITY TRAVERSE

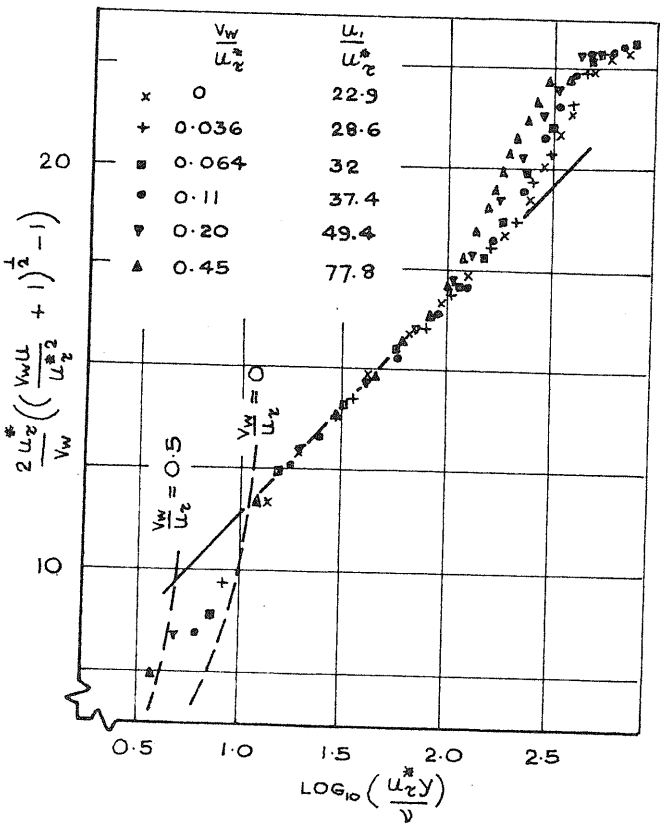

FIG. 30 EXPERIMENTAL RESULTS USING THE LAW OF THE WALL EQU. 21.1

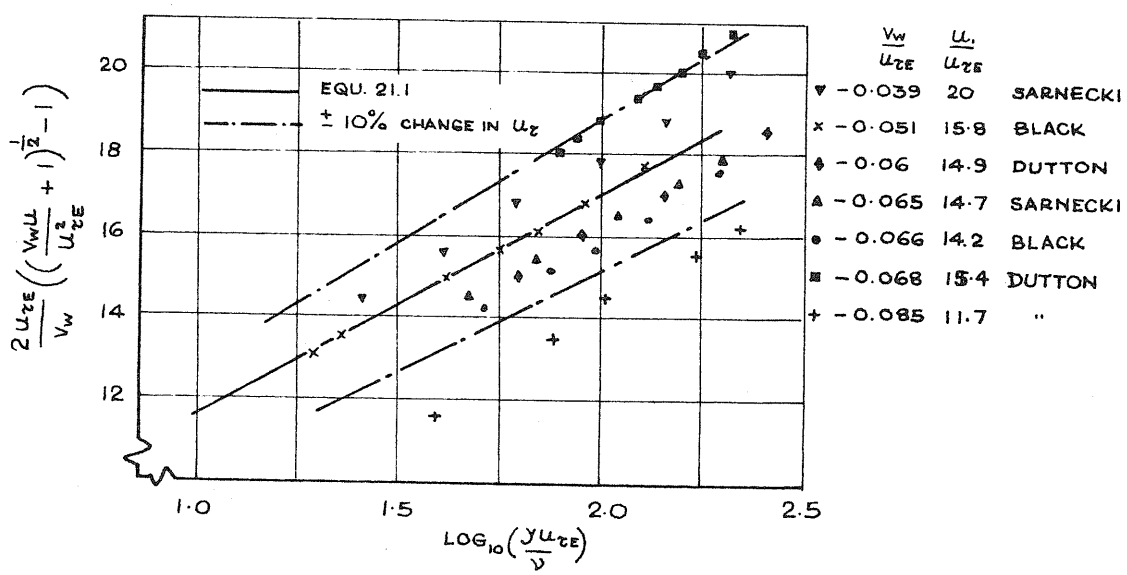

FIG. 31 PREVIOUS EXPERIMENTAL RESULTS

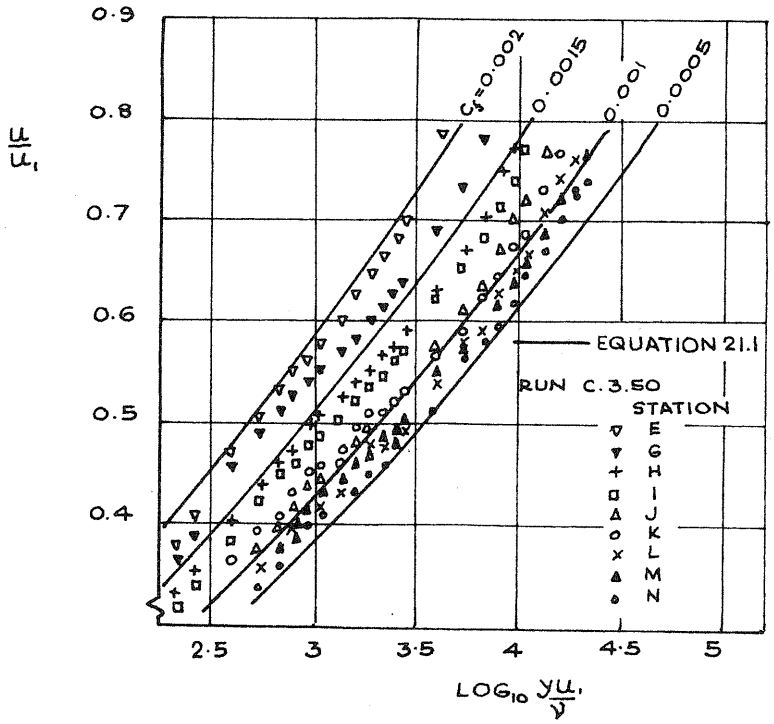

FIG. 32 VELOCITY PROFILES - MICKLEY & DAVIS (1957)

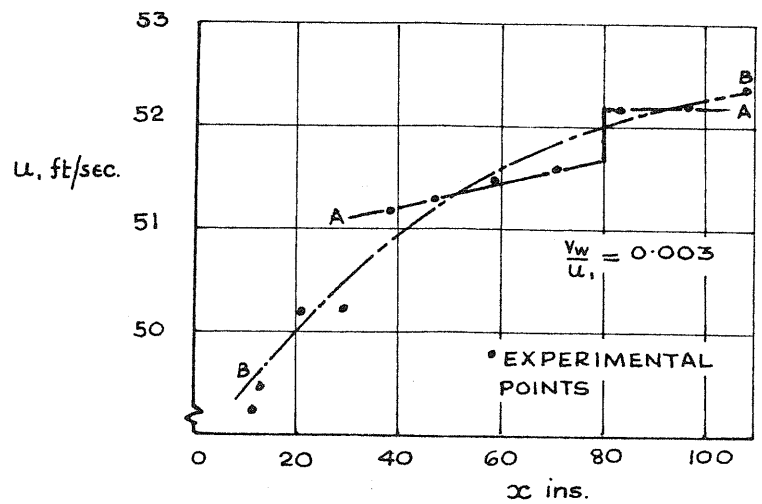

FIG. 33 FREE STREAM VELOCITY VARIATION (RUN C.3.50 - MICKLEY & DAVIS 1957)

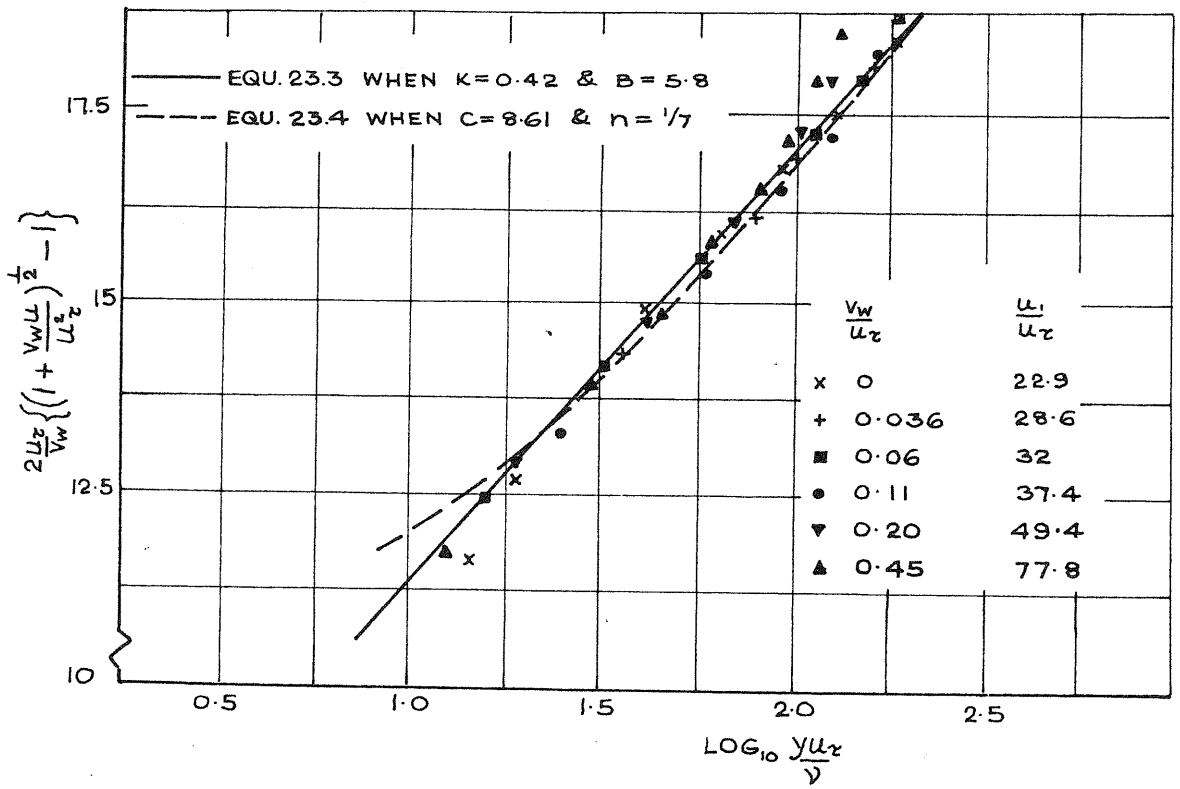

FIG. 34 THE OVERLAP REGION

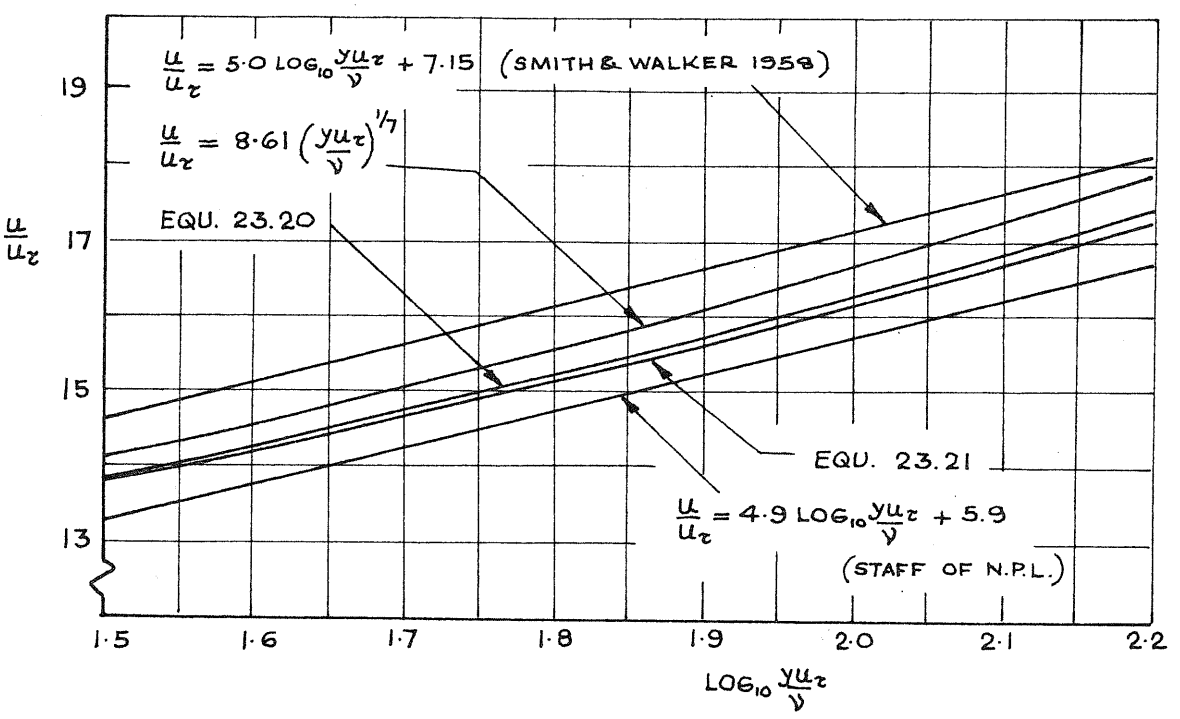

FIG. 35 FORMULAE FOR THE OVERLAP REGION

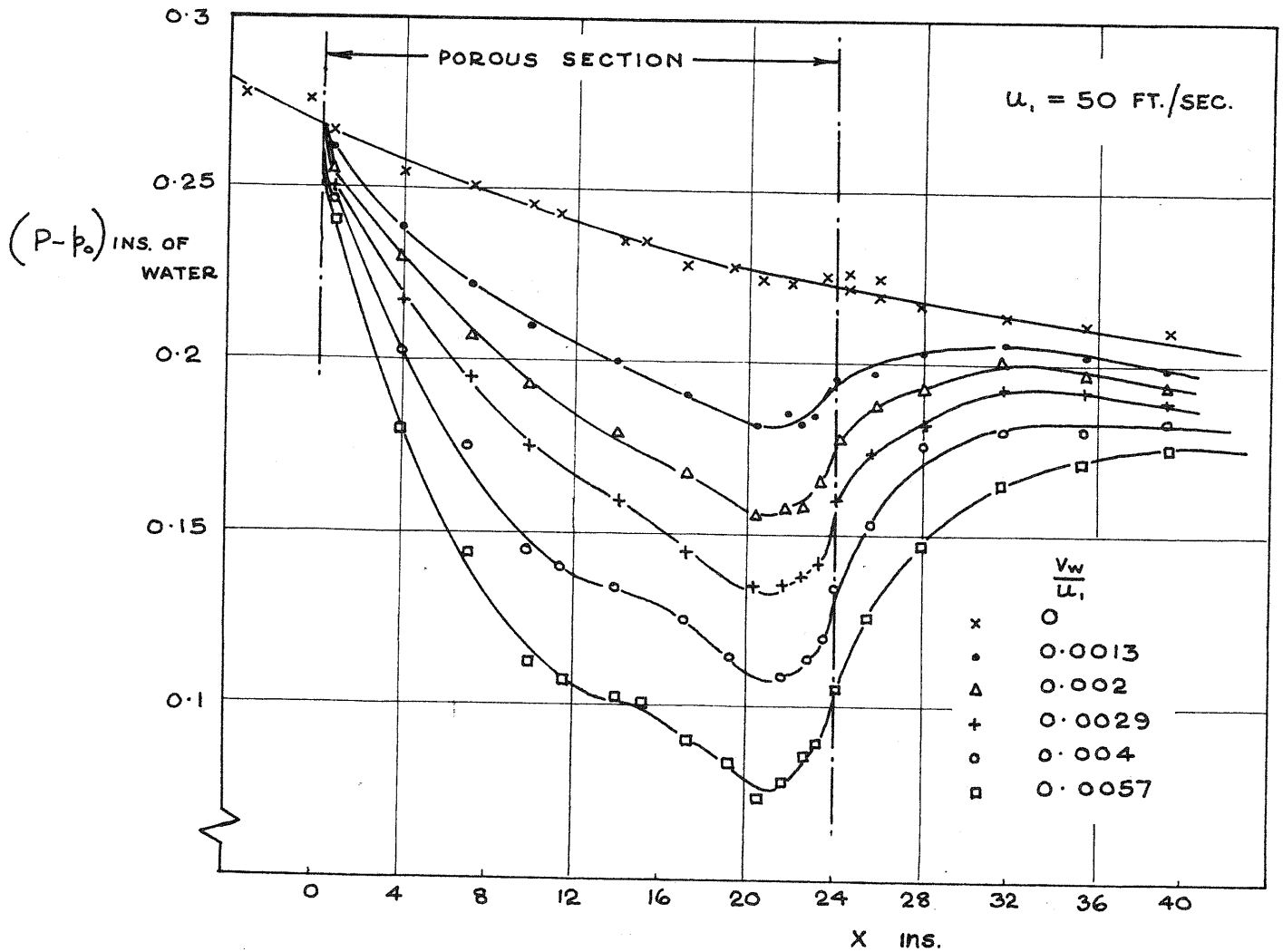

FIG.36 THE PRESSURE RECORDED WITH THE PRESTON TUBE

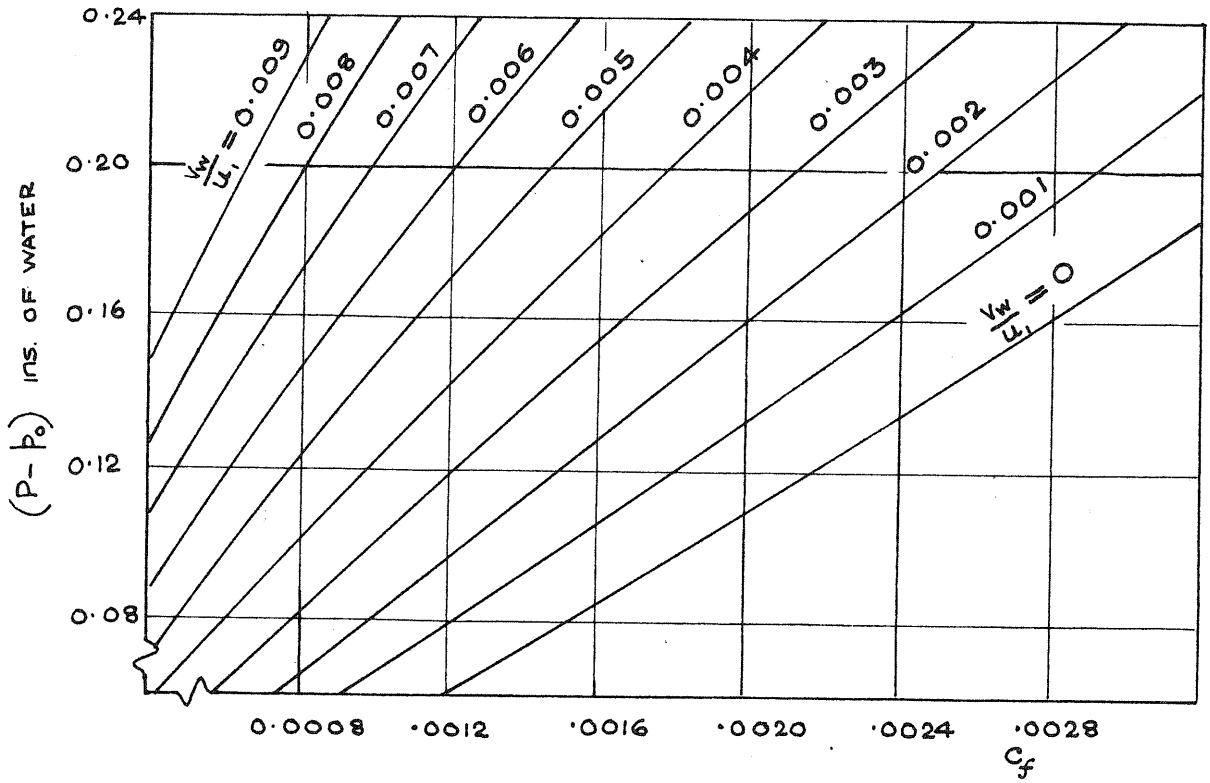

FIG.37 EQUATION 23.23 WHEN $u_1 = 50$ FT./SEC.

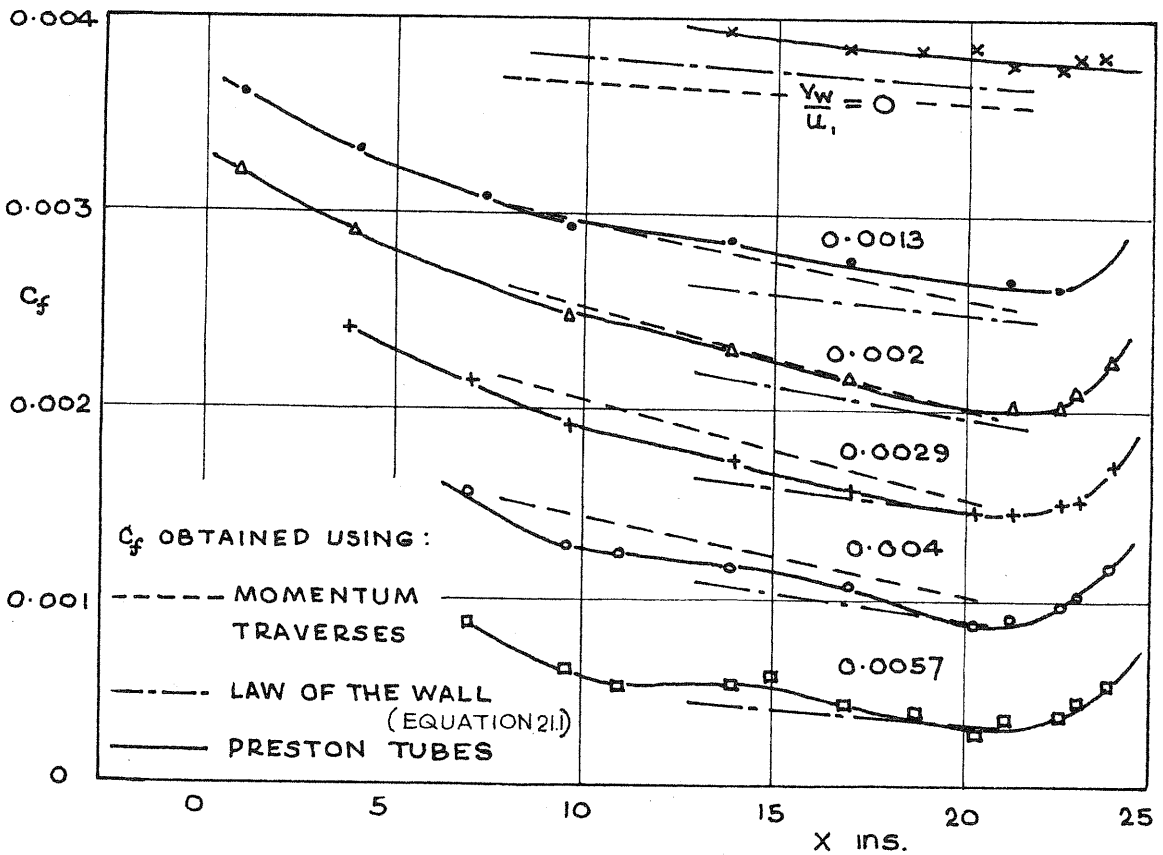

FIG.38 VARIATION OF SKIN FRICTION ALONG THE MODEL.

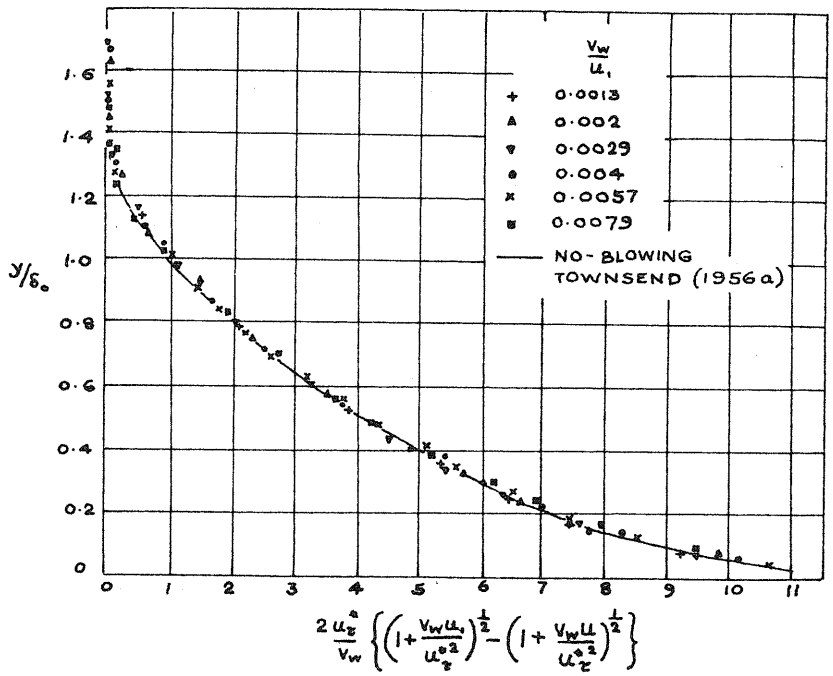

FIG. 39 VELOCITY DEFECT CURVE

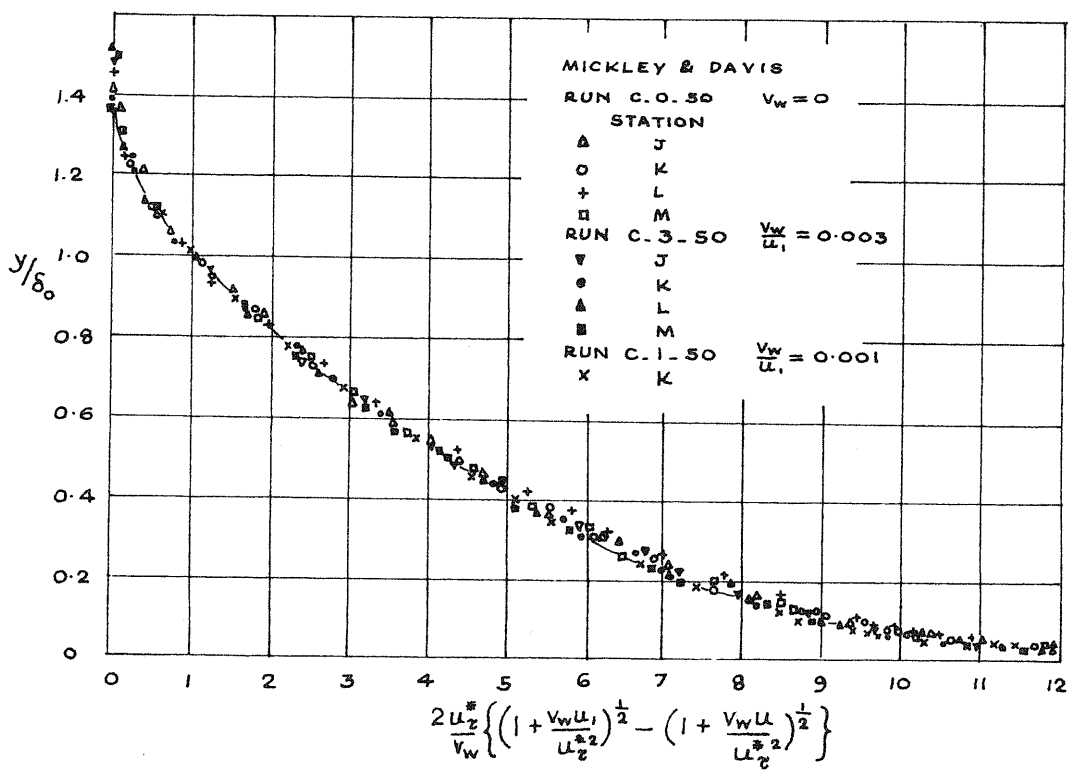

FIG. 40 VELOCITY DEFECT CURVE OR OUTER REGION CURVE

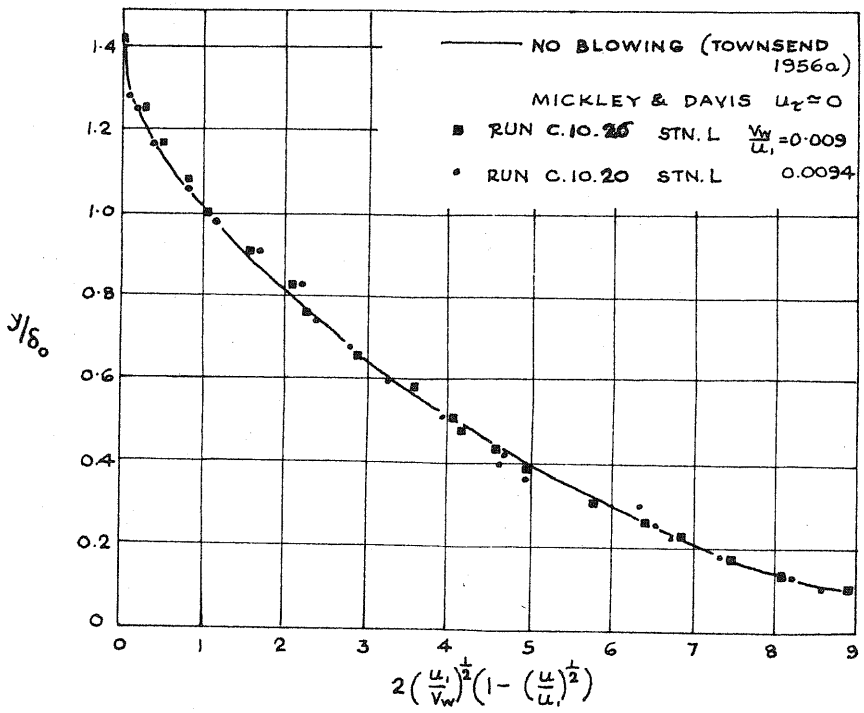

FIG. 41 THE OUTER REGION CURVE

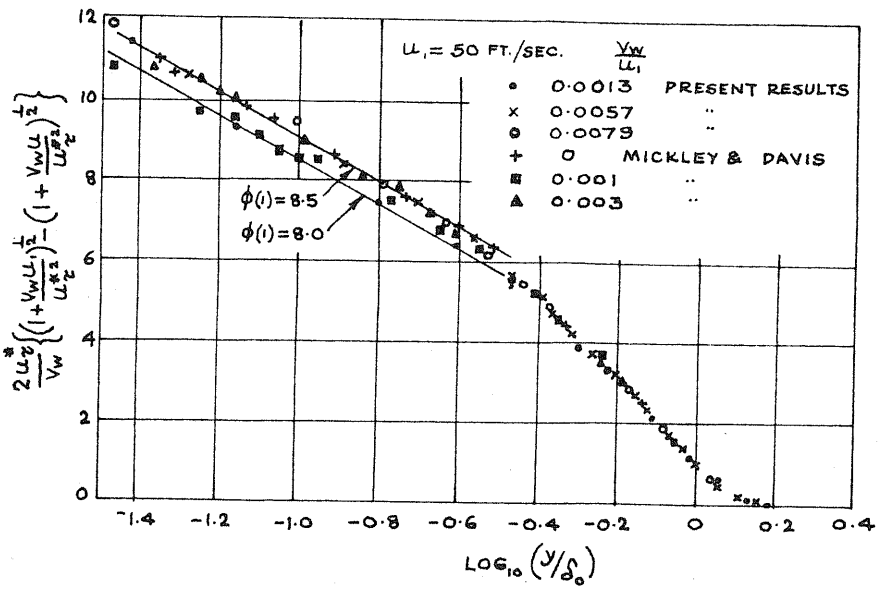

FIG. 42 THE OUTER REGION CURVE – LOGARITHMIC PLOT

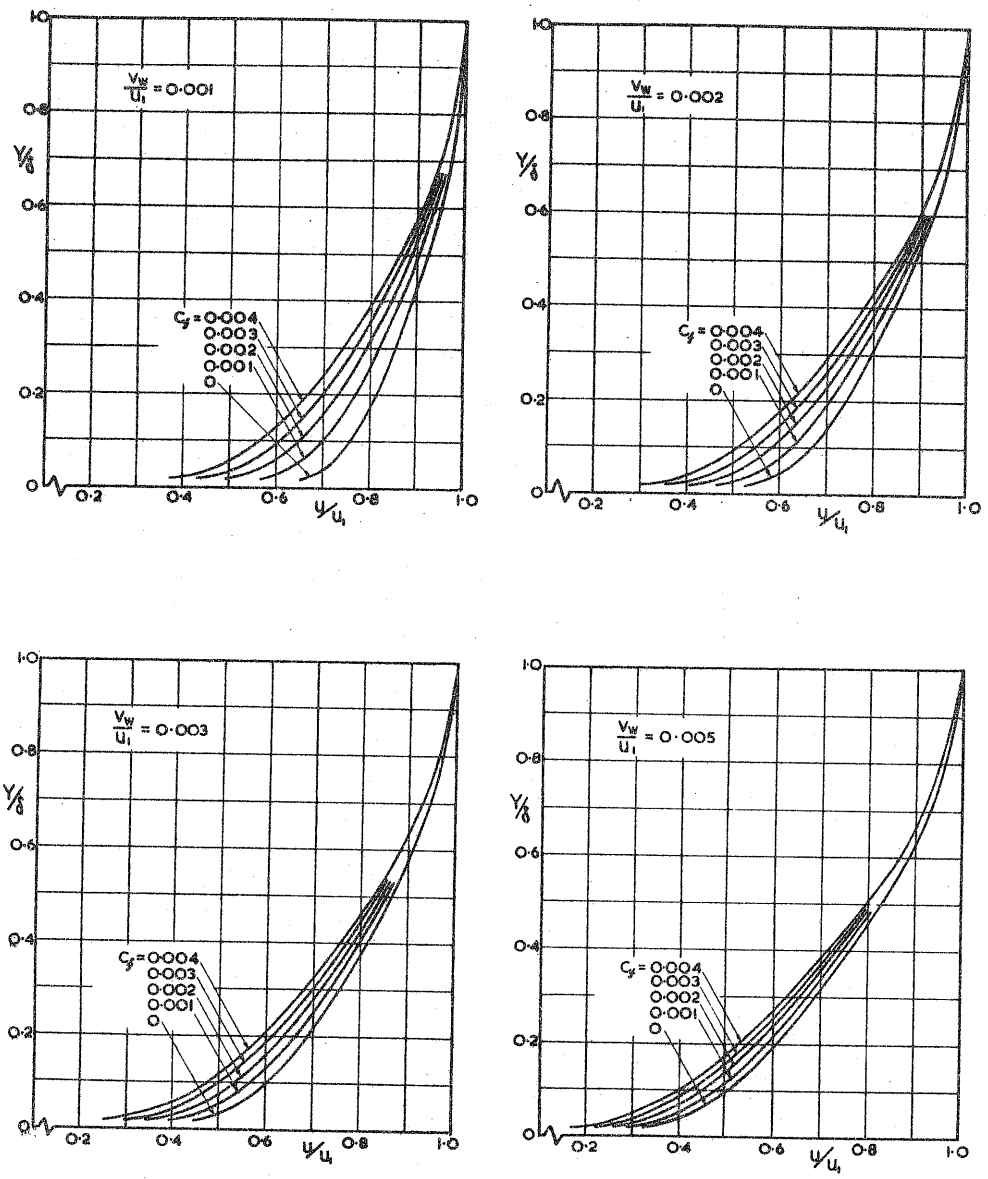

FIG.43 VELOCITY PROFILES WITH INJECTION.

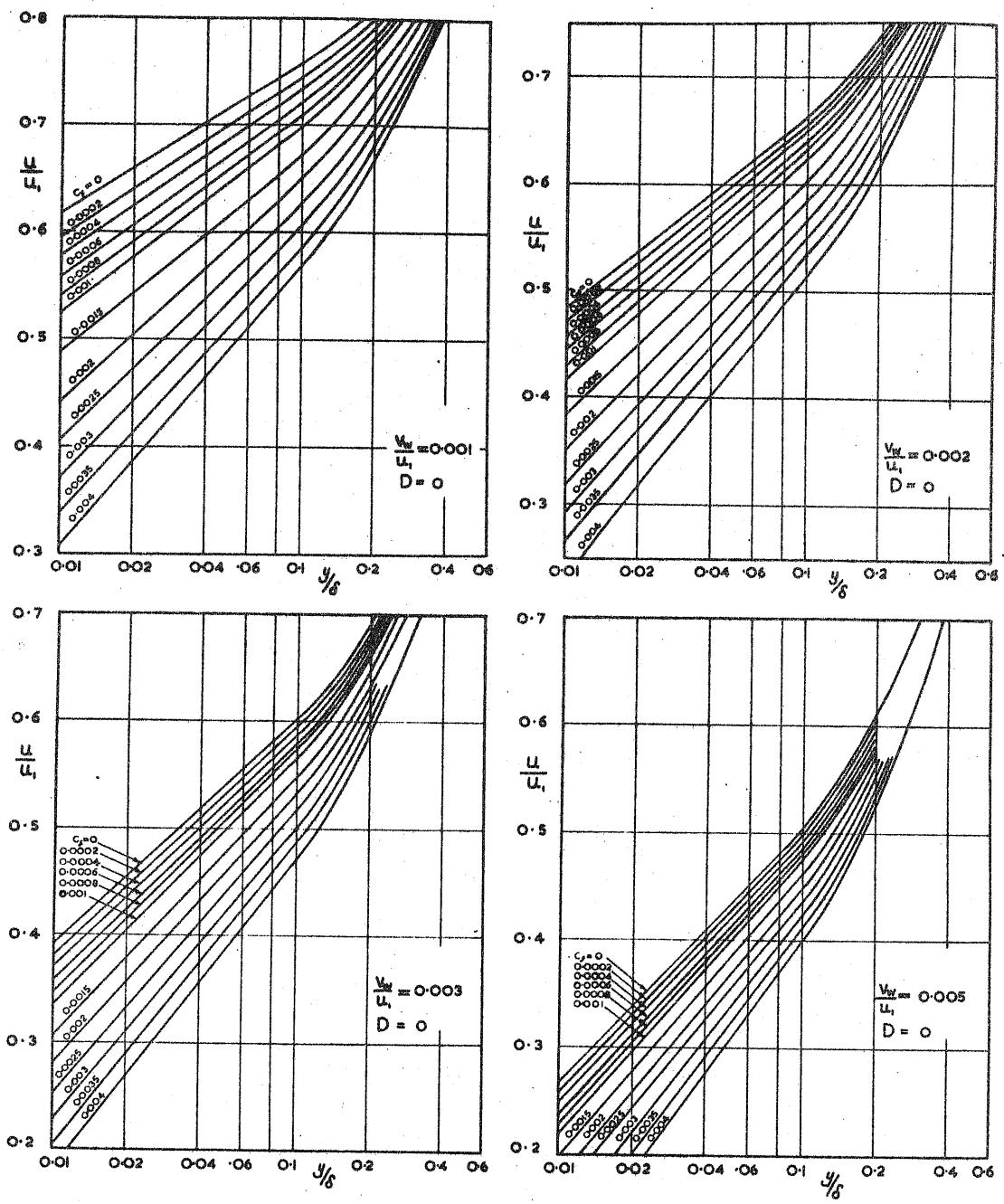

FIG. 44 THE INNER REGION WITH INJECTION

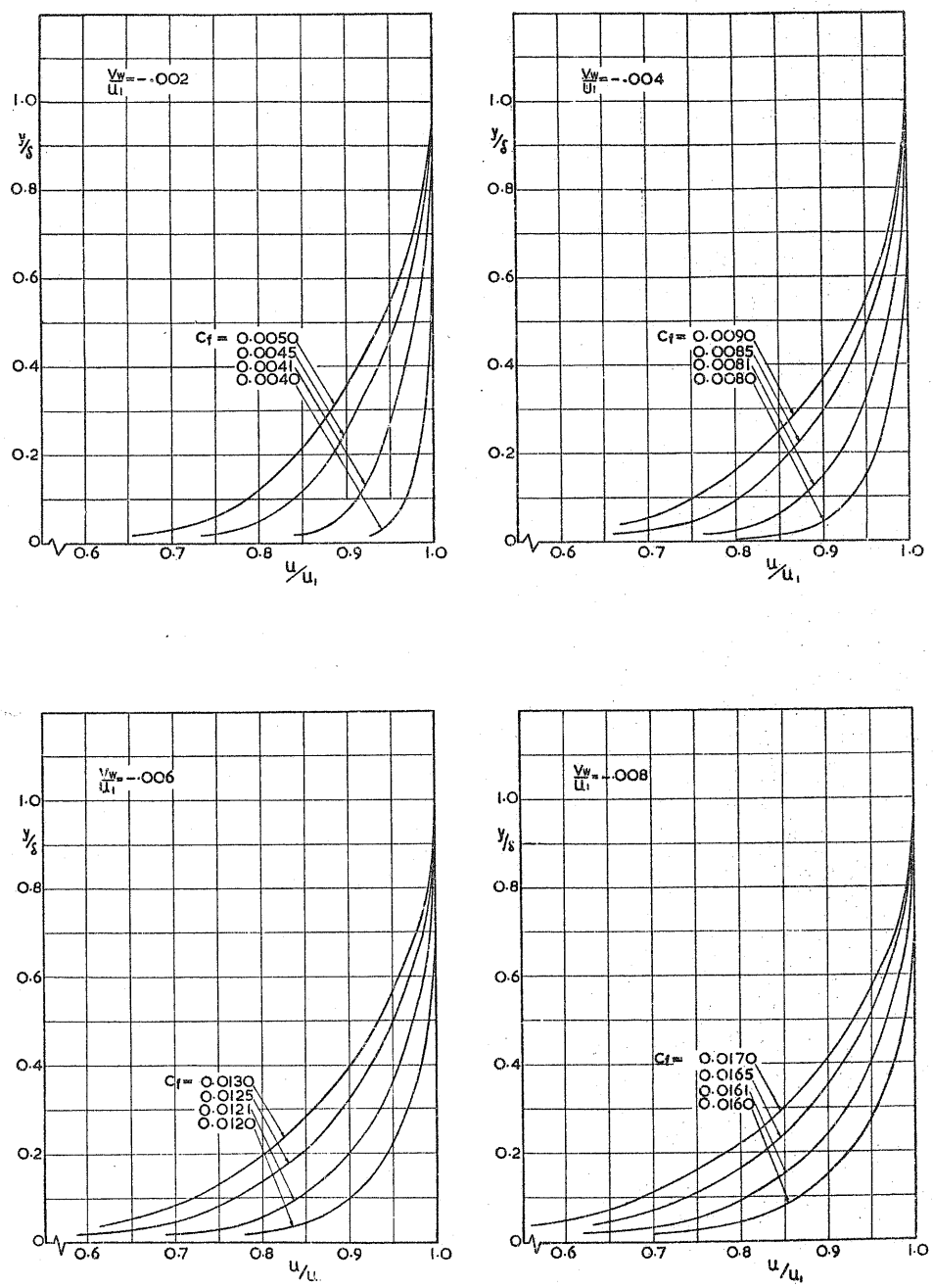

FIG.45 VELOCITY PROFILES WITH SUCTION

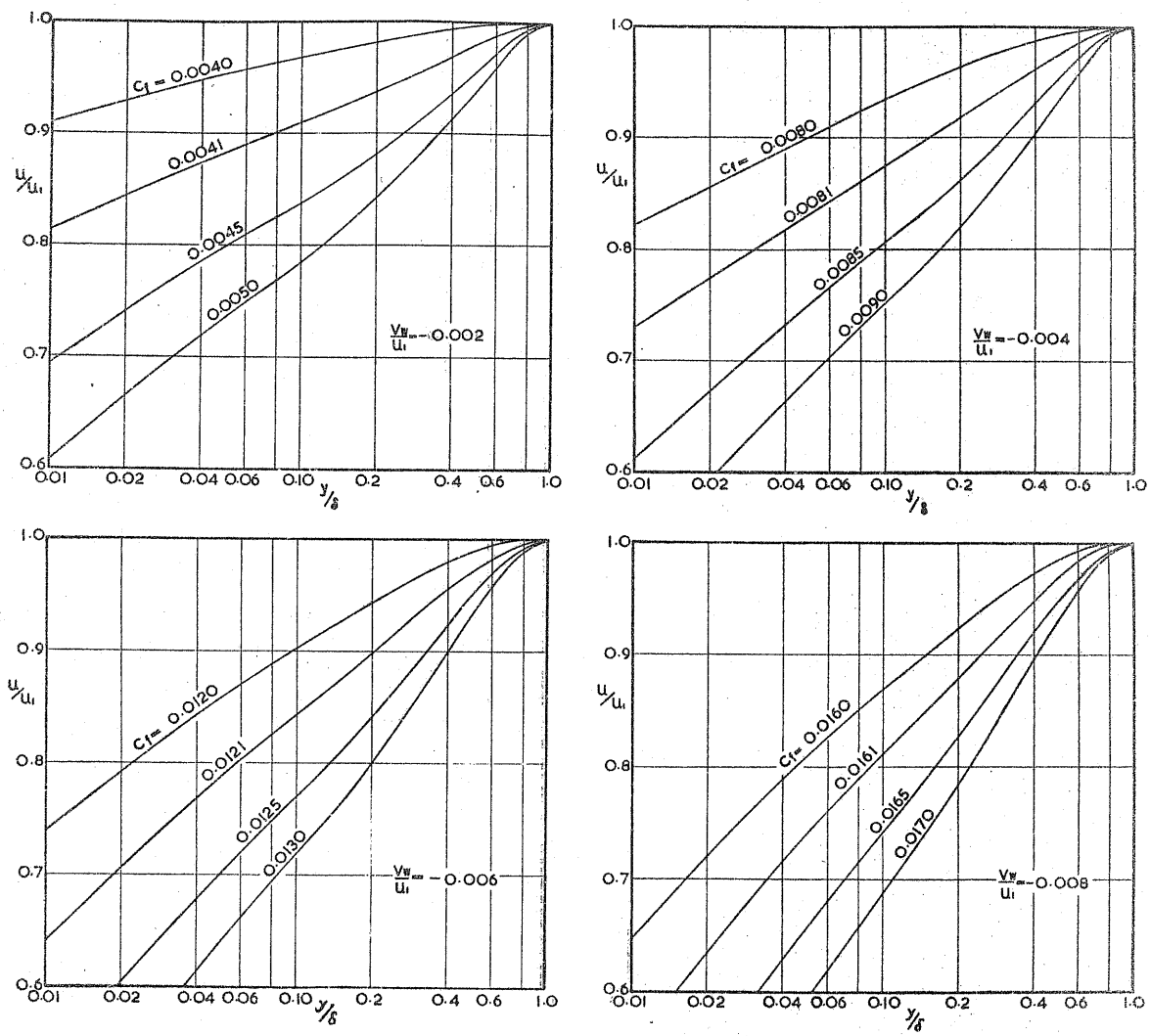

FIG.46 THE INNER REGION WITH SUCTION

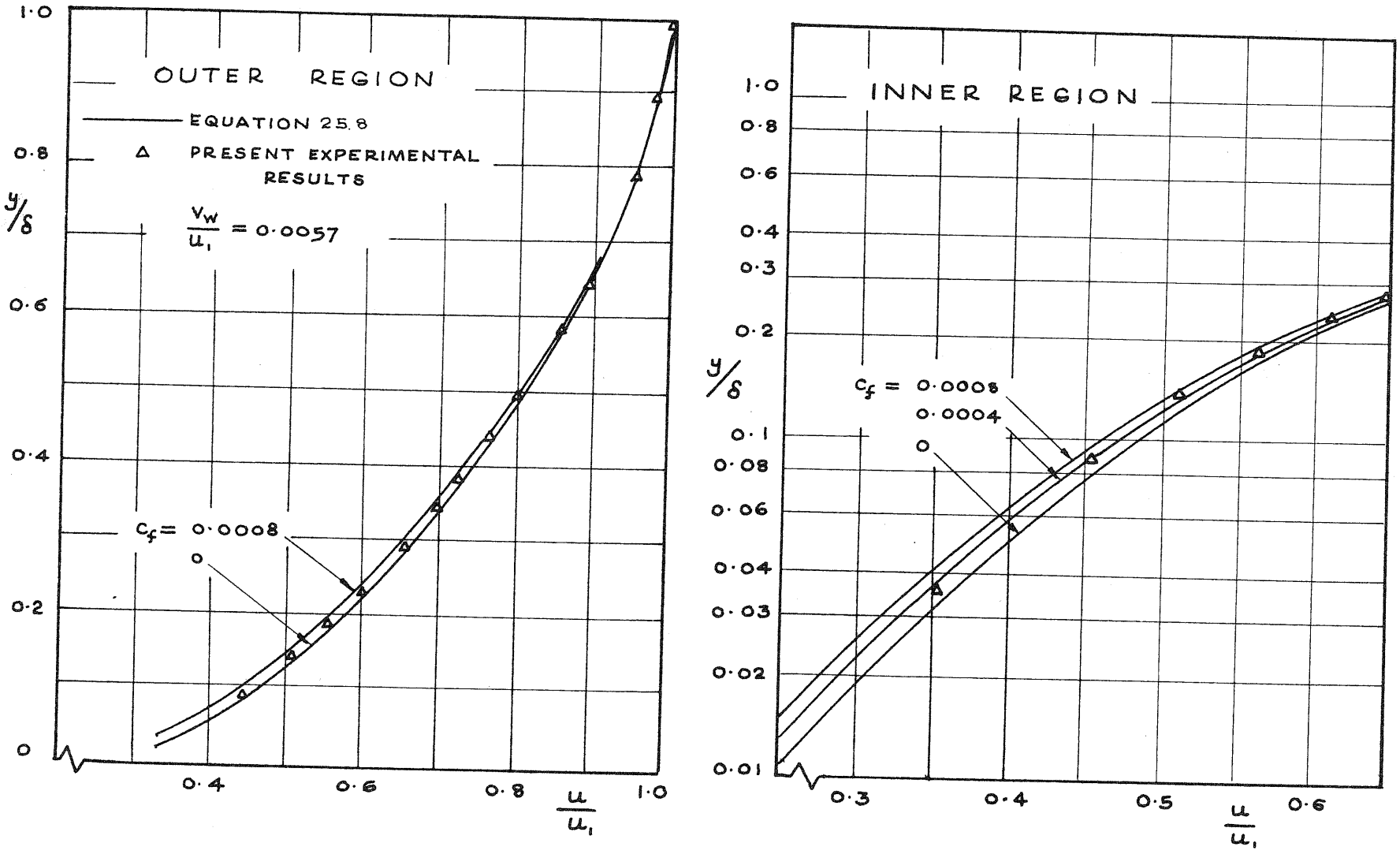

FIG. 47 VELOCITY PROFILES WITH INJECTION

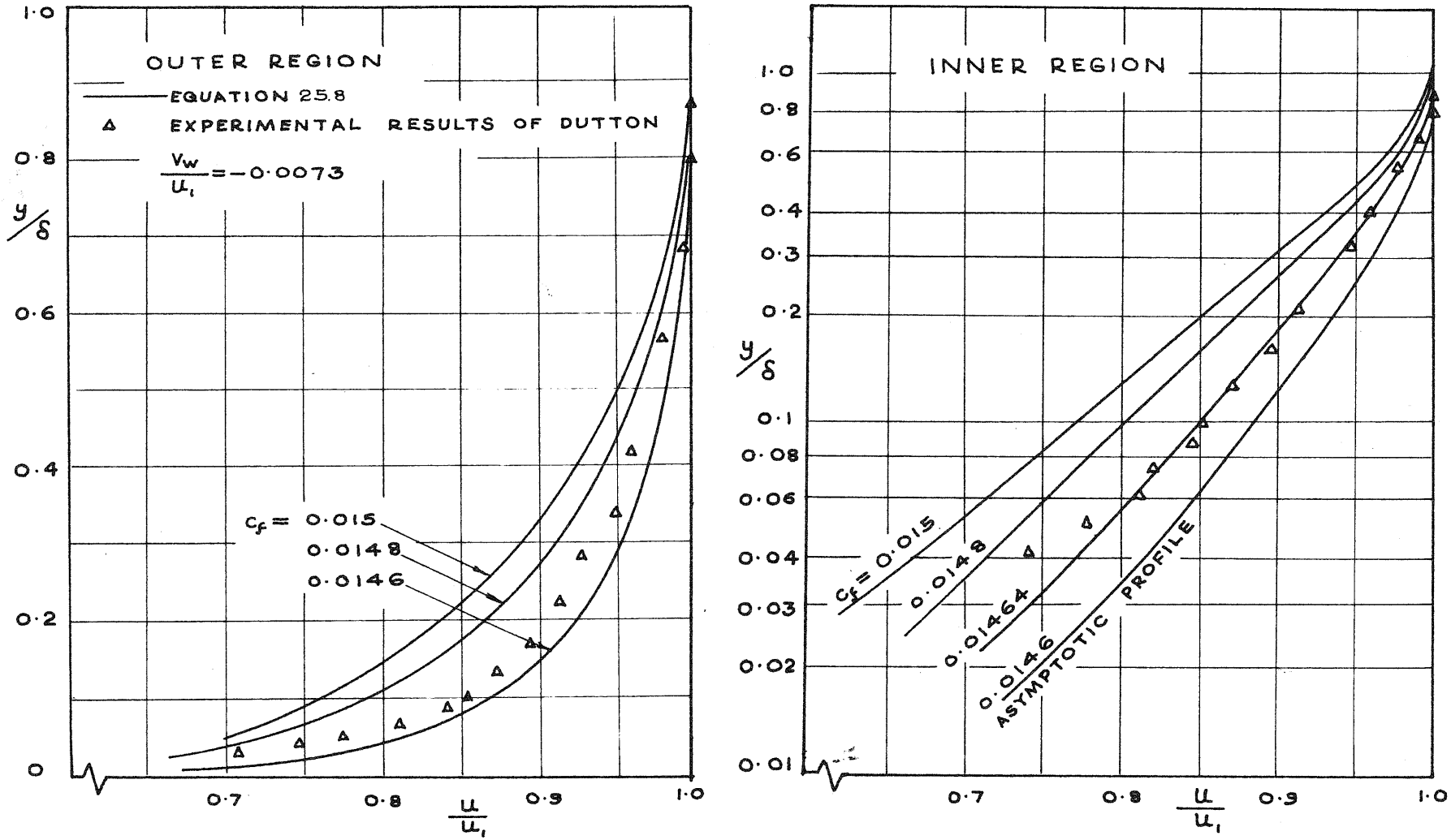

FIG. 48 VELOCITY PROFILES WITH SUCTION

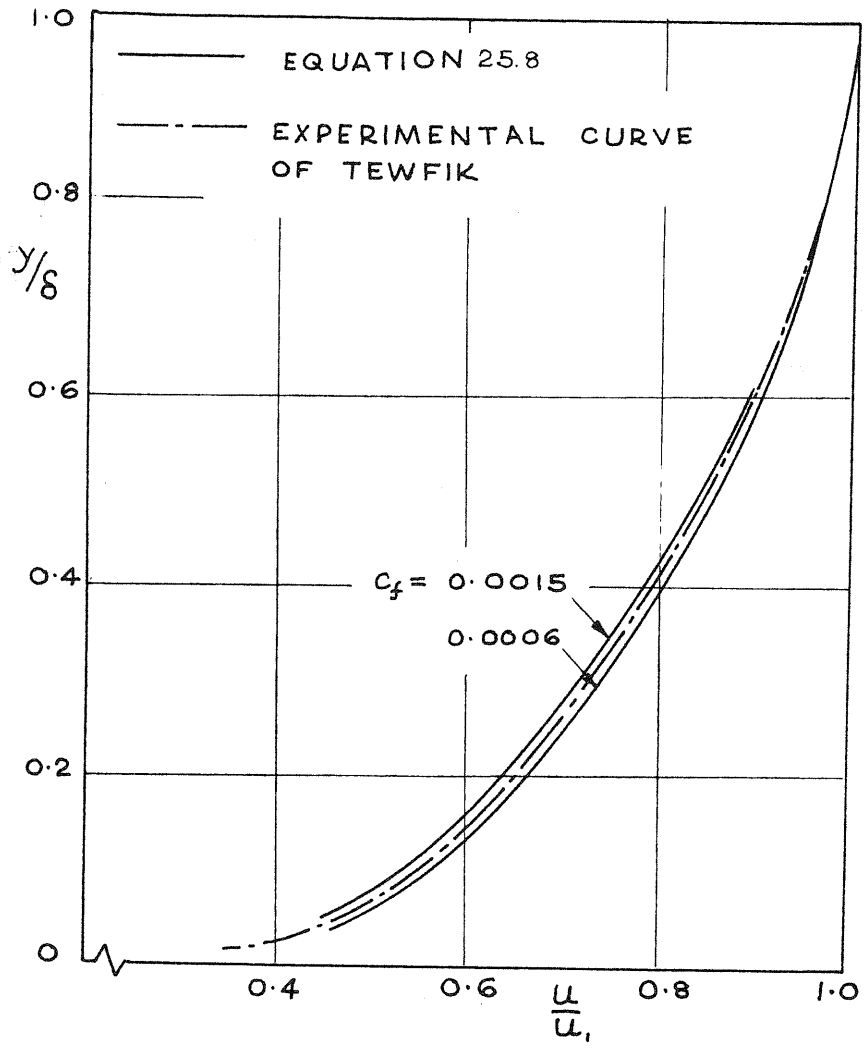

OUTER REGION

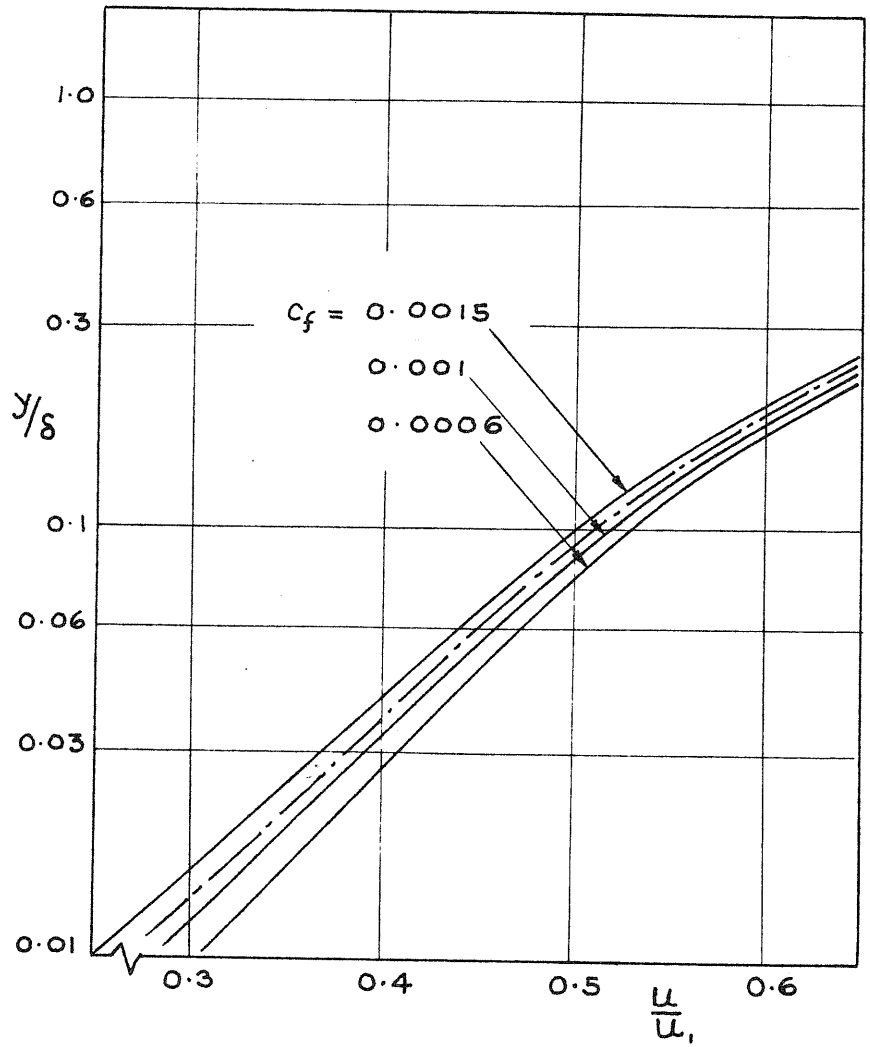

INNER REGION

FIG. 49 VELOCITY PROFILE OF TEWFIK

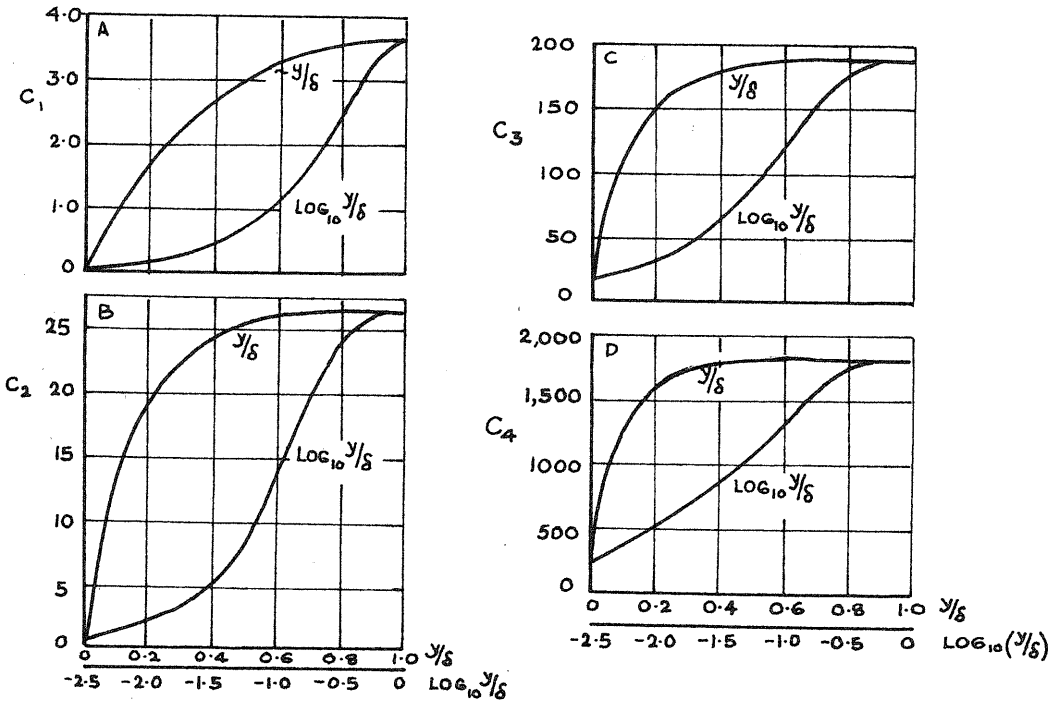

FIG. 50 THE VARIATION OF THE PROFILE PARAMETERS C_1, C_2, C_3 & C_4 (EQU. 26.5)

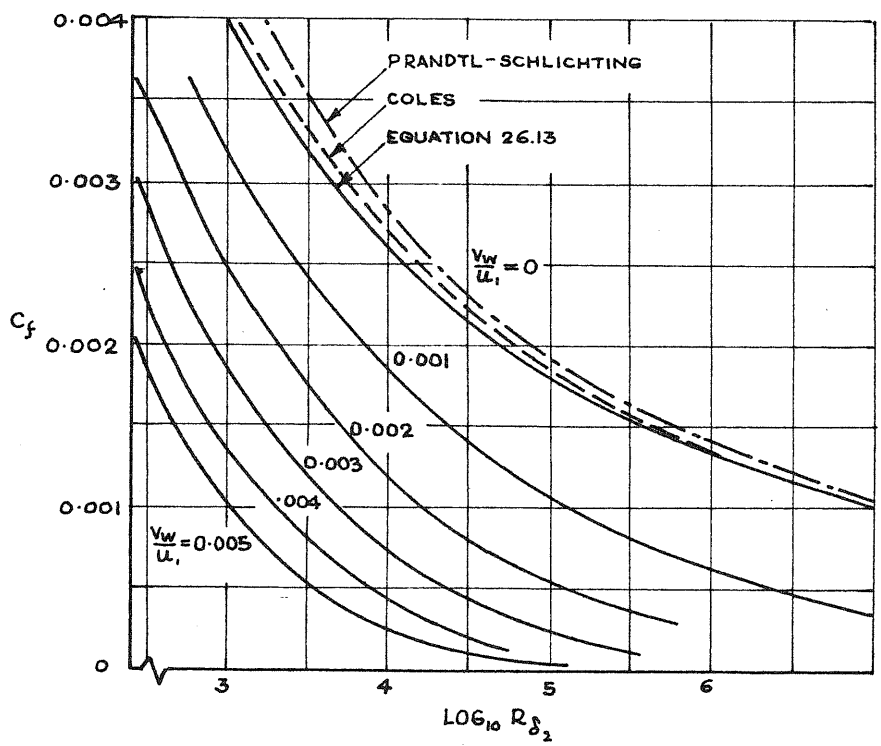

FIG. 51 THE VARIATION OF SKIN FRICTION WITH REYNOLDS NUMBER, R_{δ_2}. (EQU. 26.13)

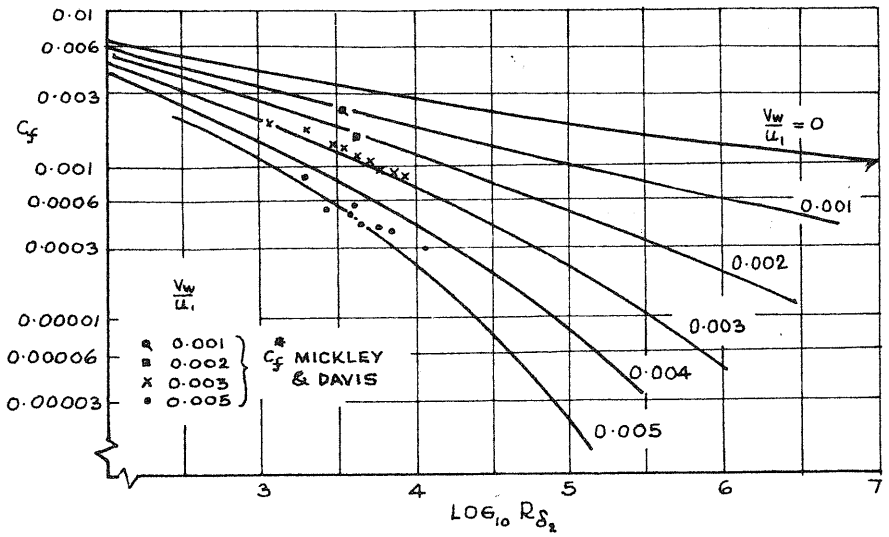

FIG. 52 VARIATION OF SKIN FRICTION WITH REYNOLDS NUMBER, R_{δ_2} (EQUATION 26.13)

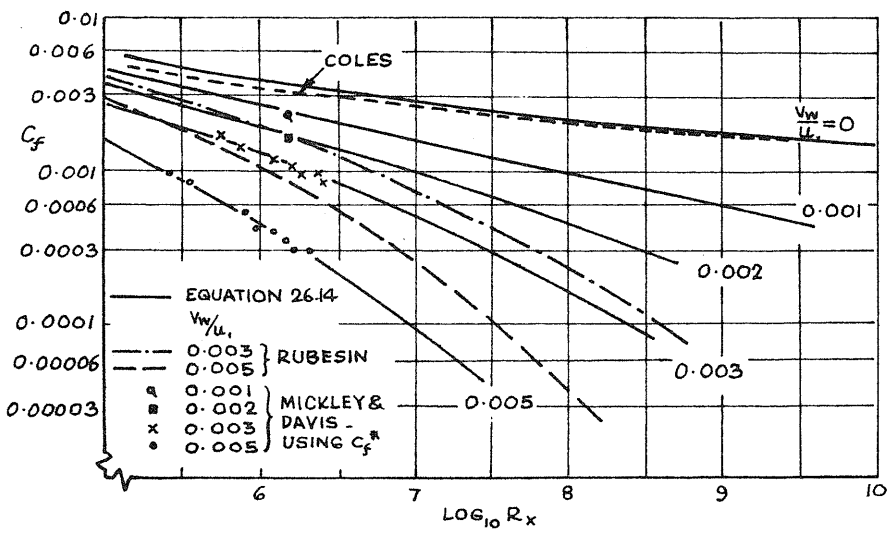

FIG. 53 VARIATION OF SKIN FRICTION WITH REYNOLDS NUMBER, R_x.

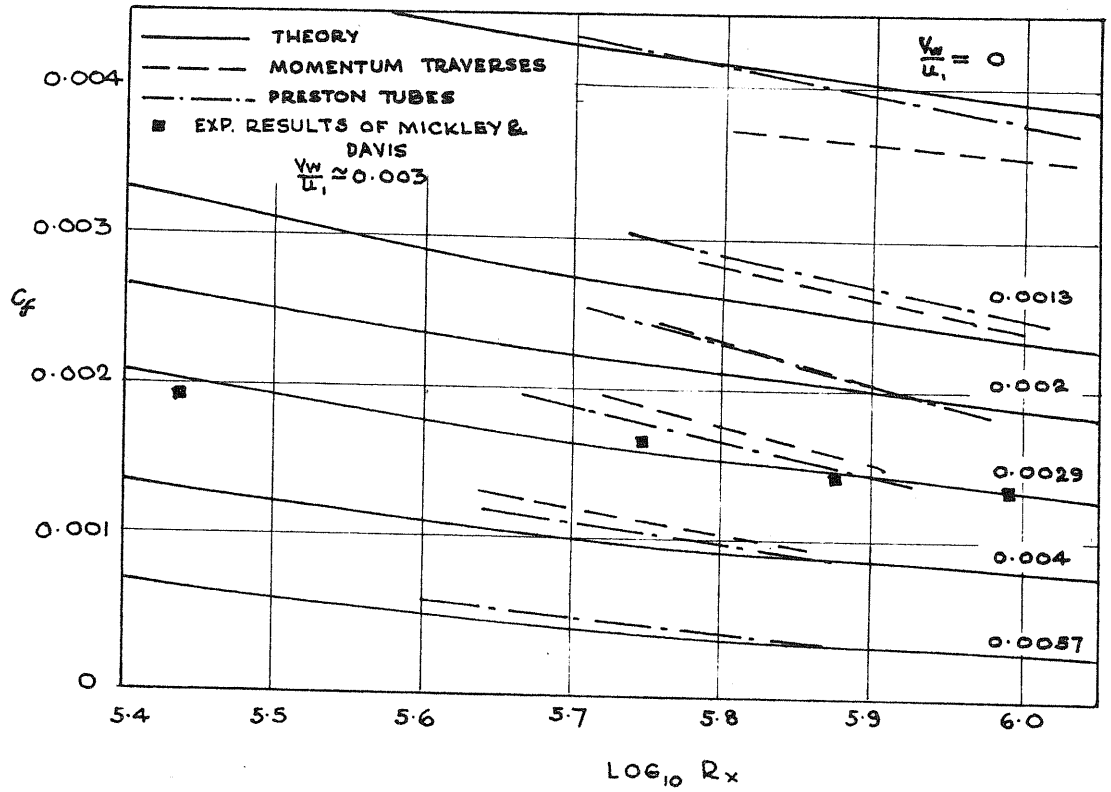

FIG. 54 VARIATION OF SKIN FRICTION WITH REYNOLDS NUMBER, R_x

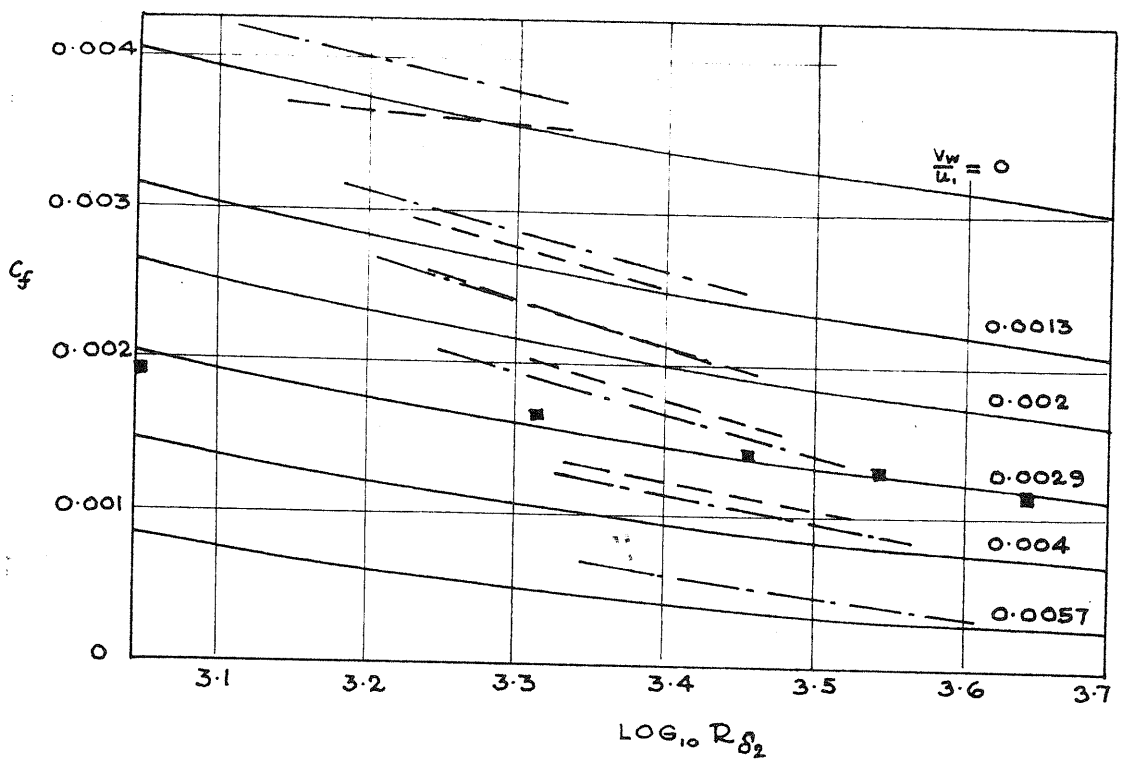

FIG. 55 VARIATION OF SKIN FRICTION WITH REYNOLDS NUMBER, R_{δ_2}

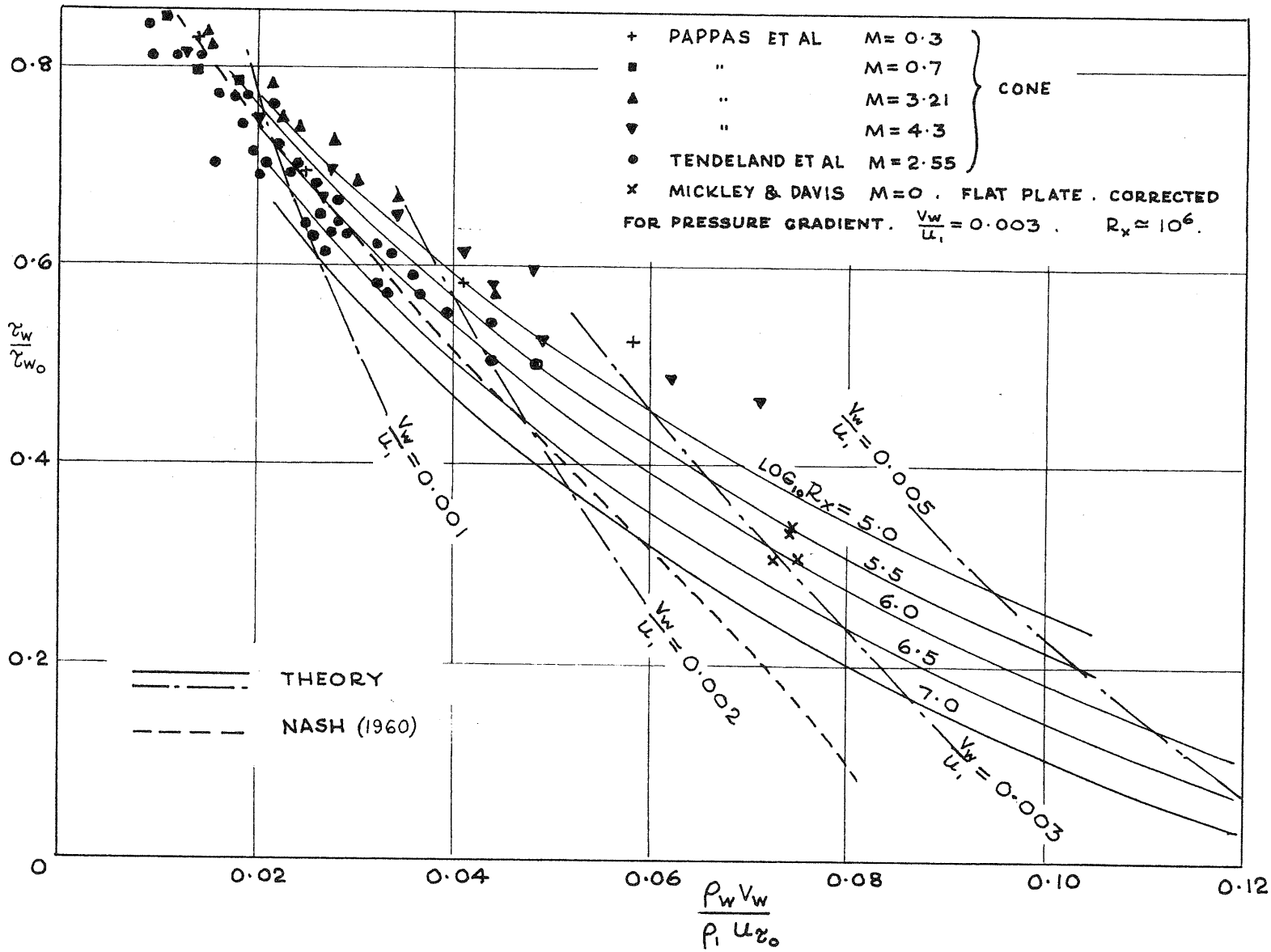

FIG. 56 CORRELATION OF SKIN FRICTION

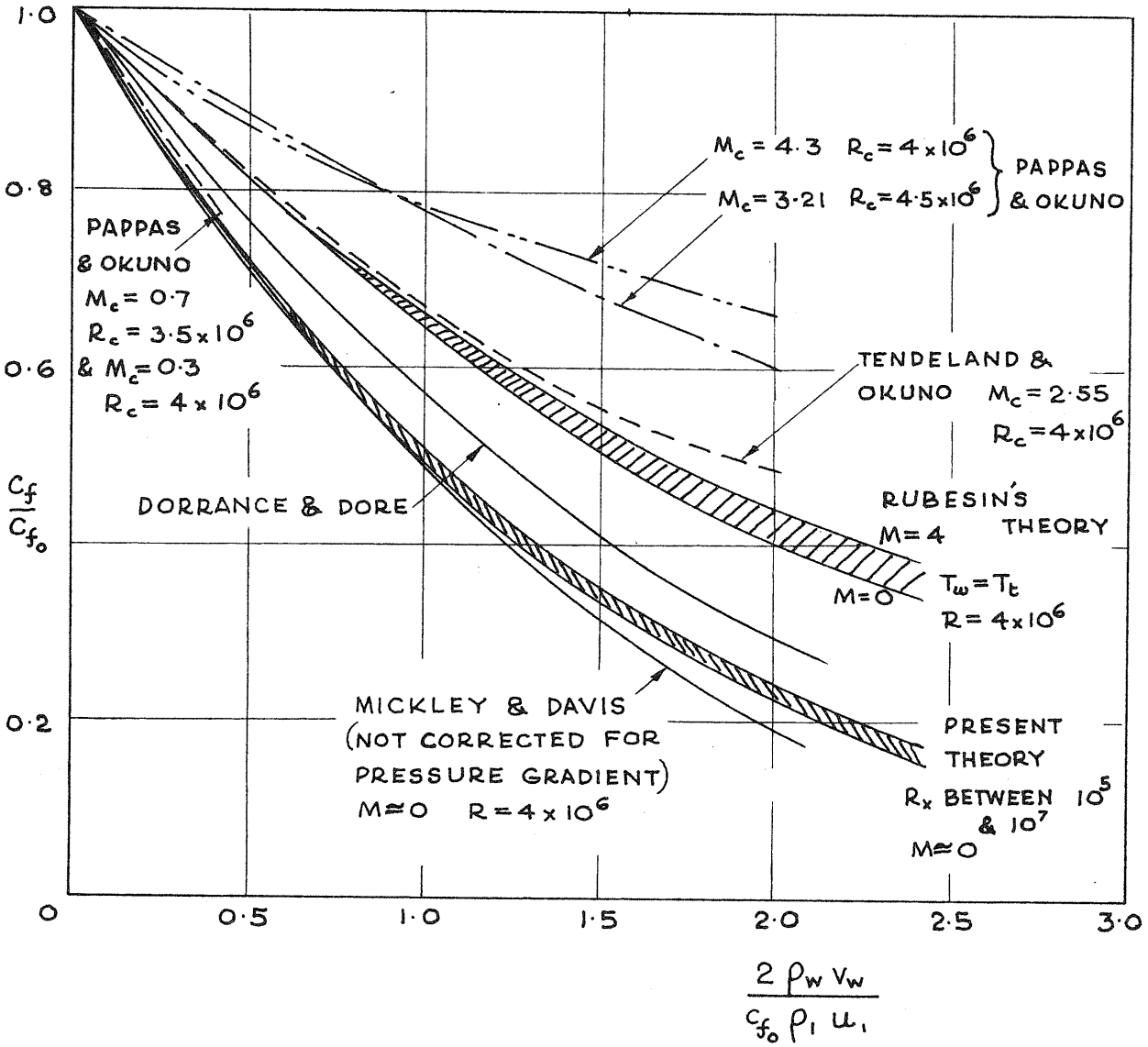

FIG. 57 COMPARISON OF THEORETICAL AND EXPERIMENTAL EFFECTS OF AIR INJECTION

OF AERONAUTICS LIBRARY

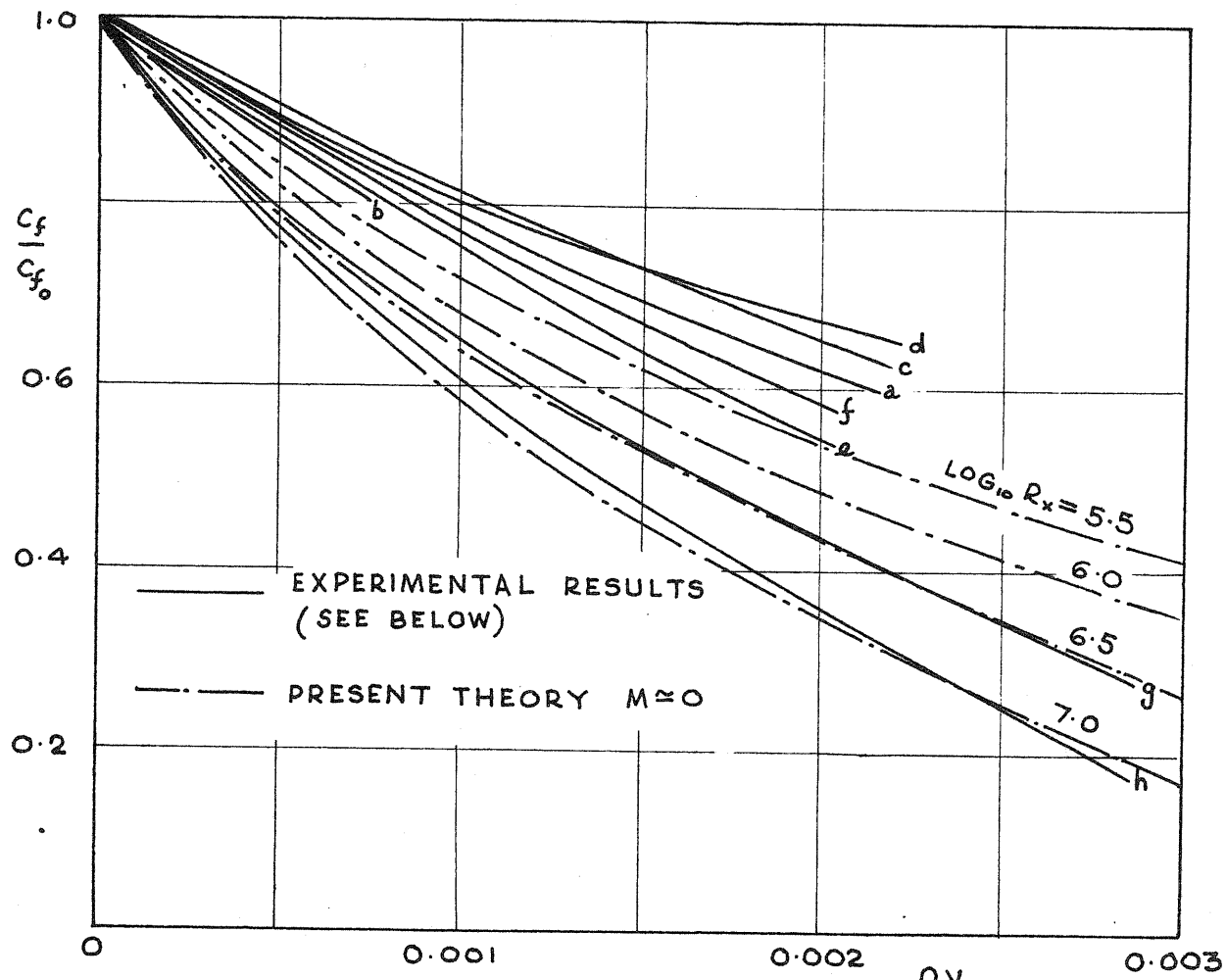

		M_c	$R_c \times 10^{-6}$	
a	PAPPAS & OKUNO	0·3	0·87	CONES (OVERALL SKIN FRICTION)
b	"	0·3	4·03	
c	"	3·21	5·86 , 4·42 , 2·95	
d	"	4·35	4·68 , 3·25	
e	TENDELAND & OKUNO	2·55	6·25	
f	"	2·55	8·56	
g	MICKLEY & DAVIS	M≃0	$R_x = 0.5 \times 10^6$	FLAT PLATE (LOCAL SKIN FRICTION)
h	"	M≃0	$R_x = 3 \times 10^6$	

(g&h NOT CORRECTED FOR PRESSURE GRADIENT)

FIG.58 CORRELATION OF SKIN FRICTION MEASUREMENTS WITH INJECTION

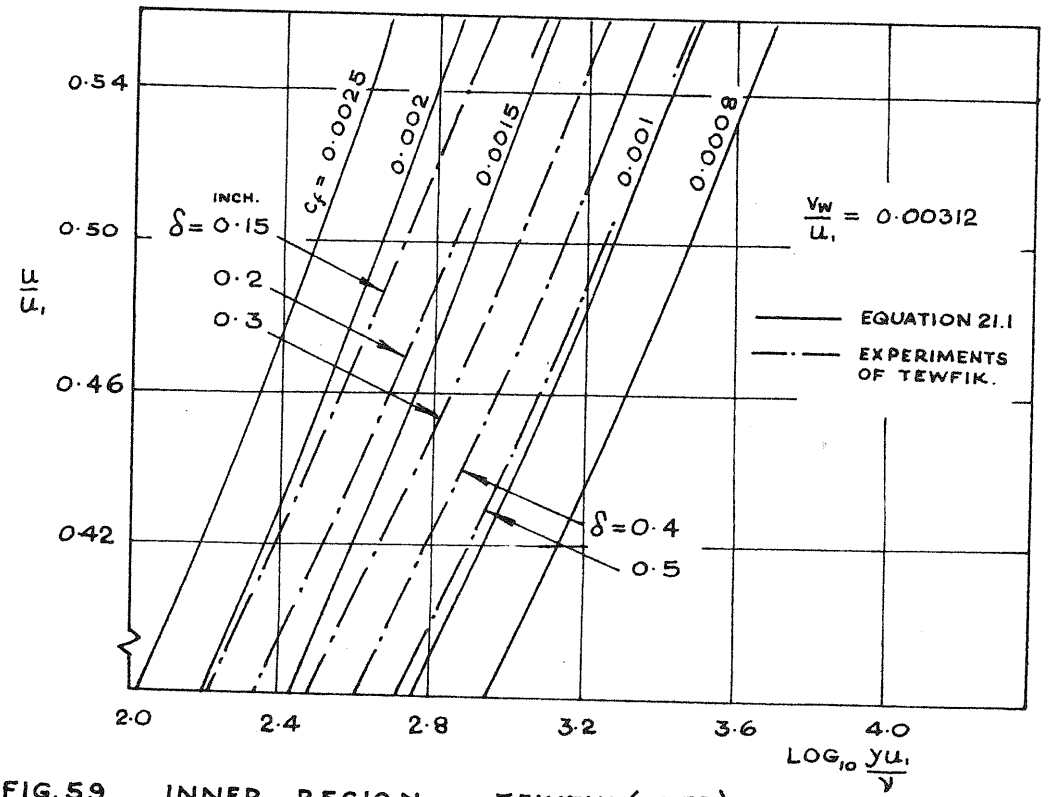

FIG. 59 INNER REGION - TEWFIK (1963)

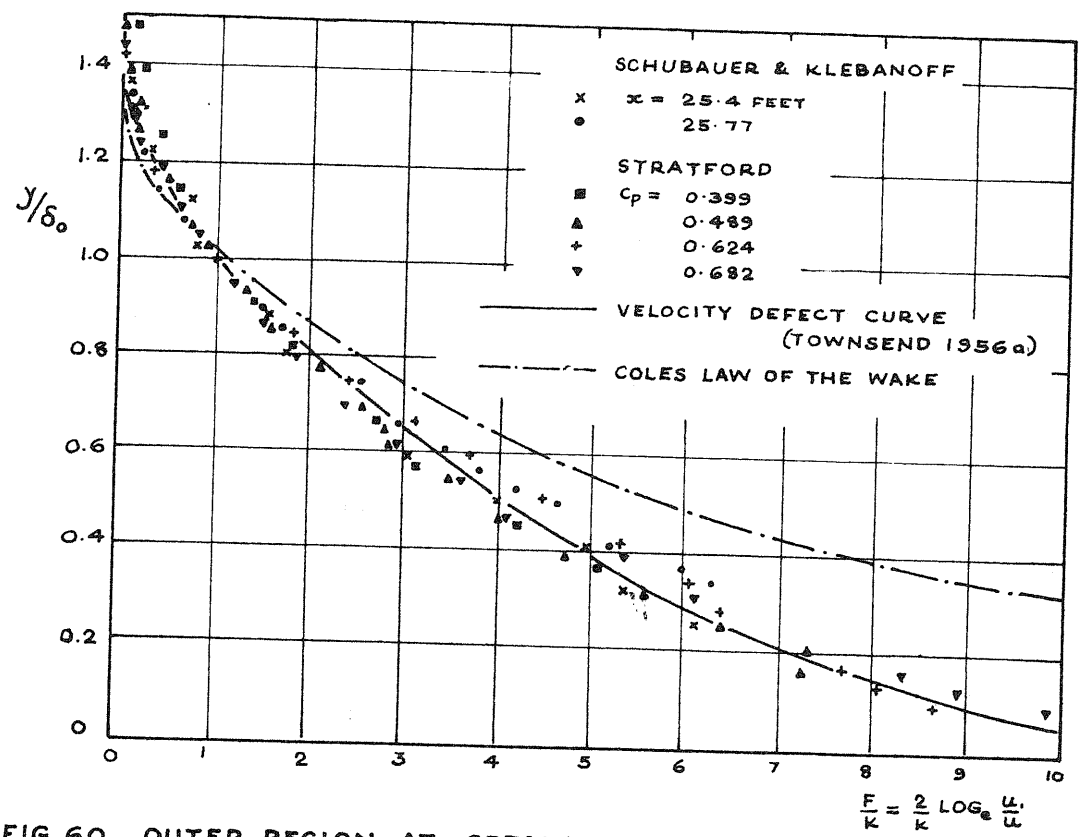

FIG. 60 OUTER REGION AT SEPARATION

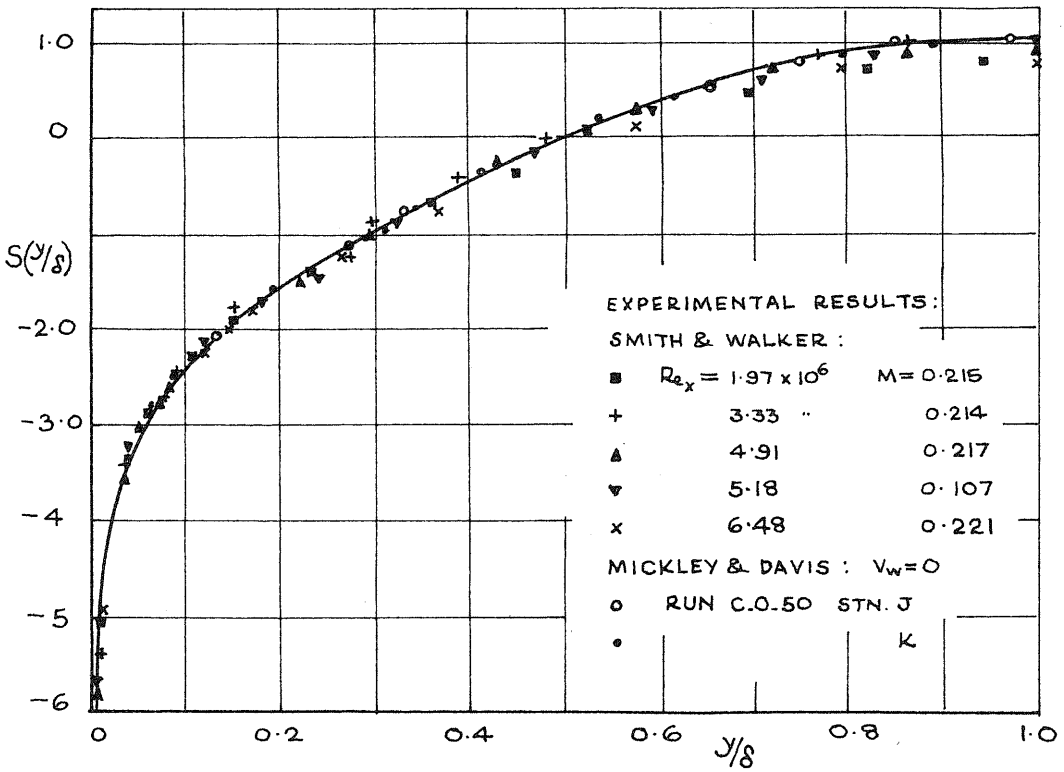

FIG. 61 THE FUNCTION $S(y/\delta)$

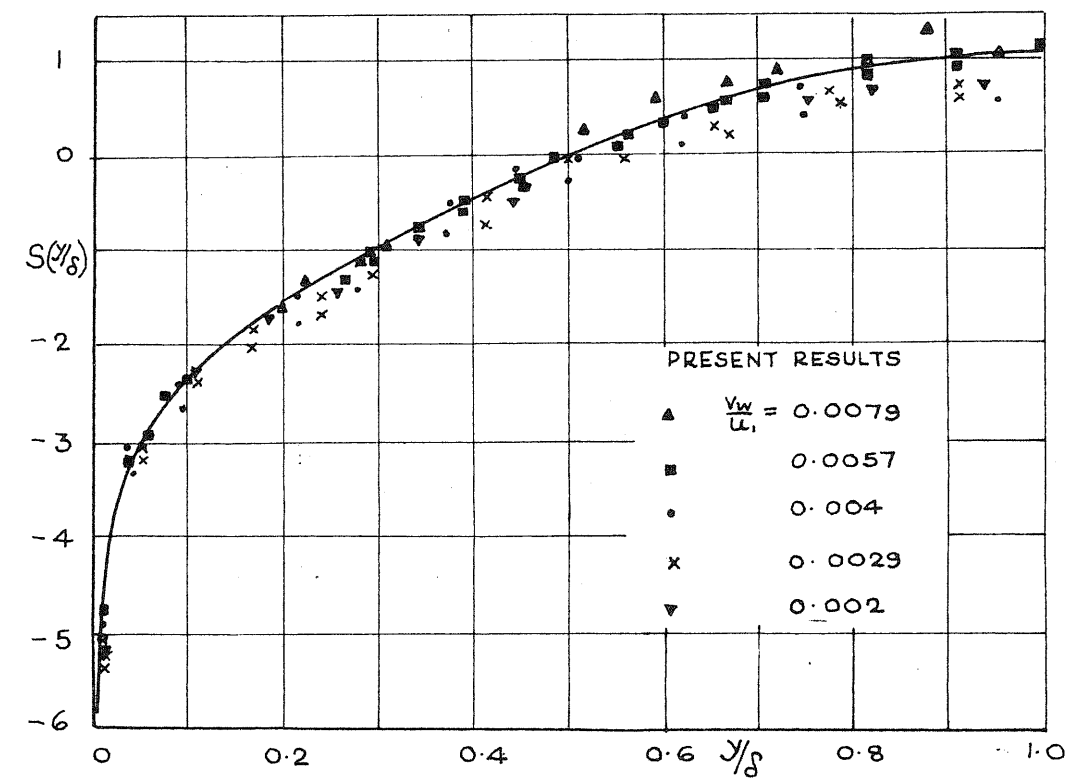

FIG. 62 THE FUNCTION $S(y/\delta)$

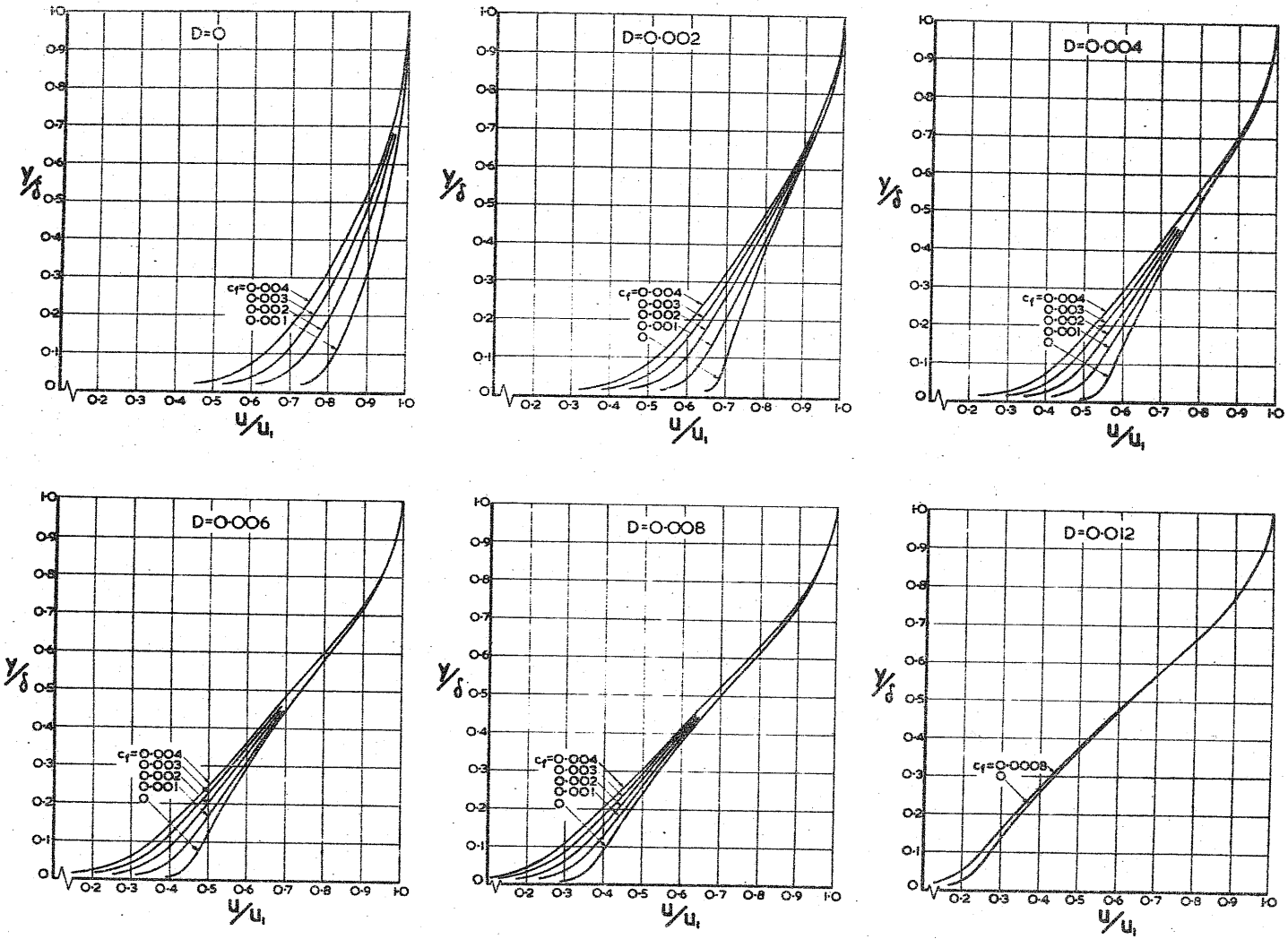

FIG.63 VELOCITY PROFILES IN A PRESSURE GRADIENT.

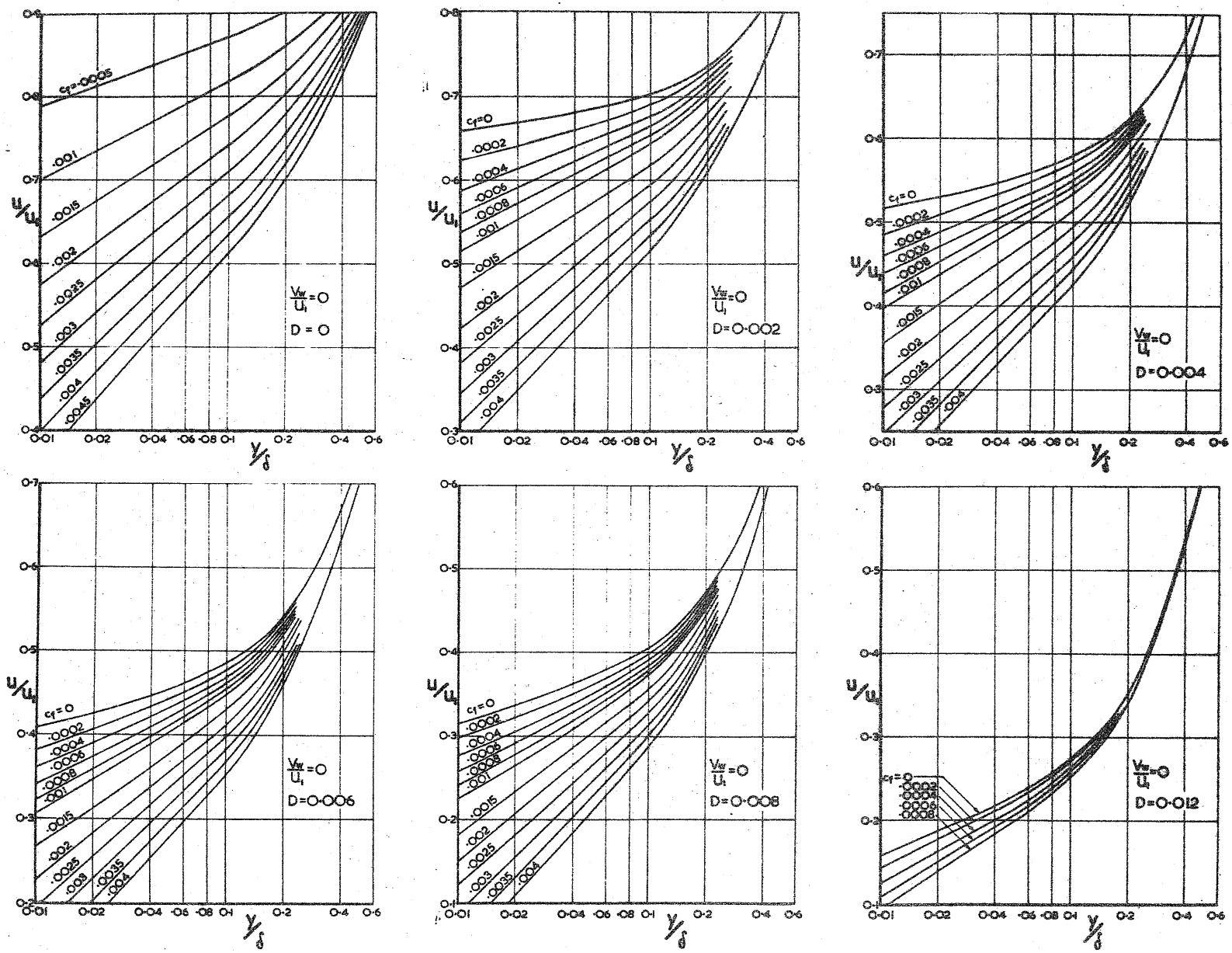

FIG.64 THE INNER REGION IN A PRESSURE GRADIENT.

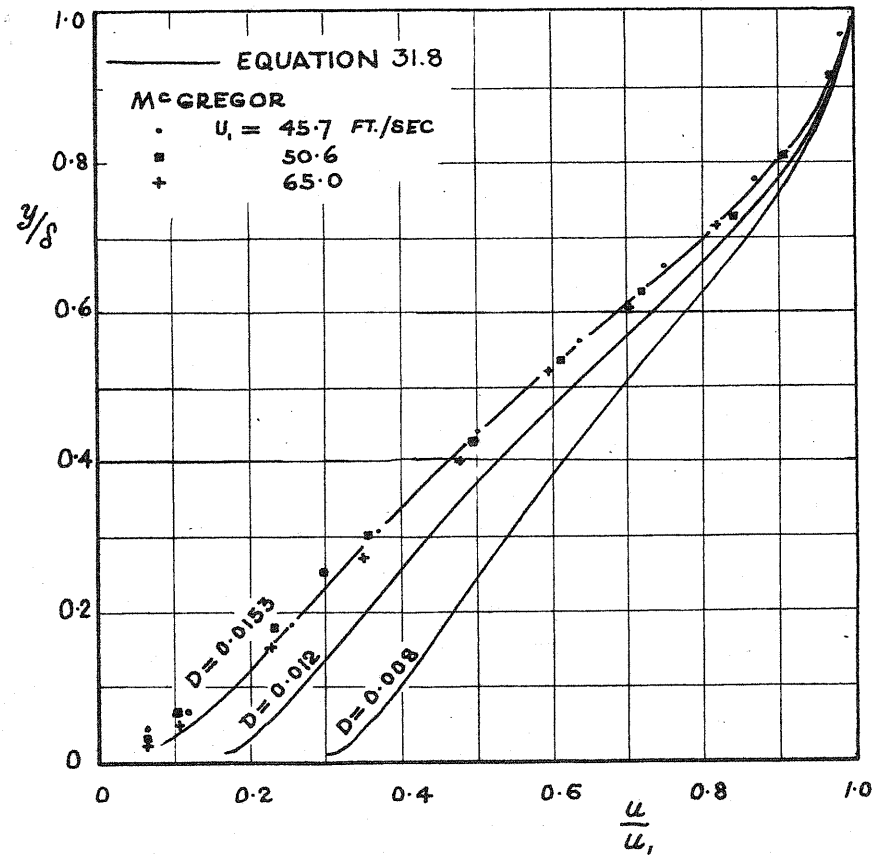

FIG. 65 REATTACHMENT PROFILES

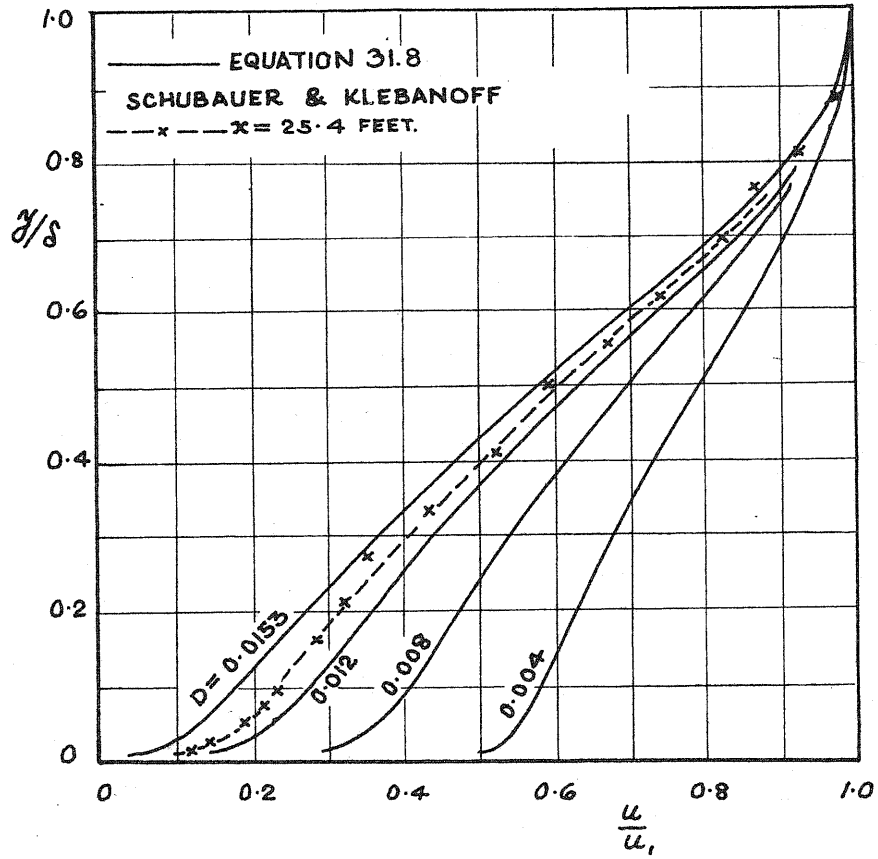

FIG. 66 SEPARATION PROFILES

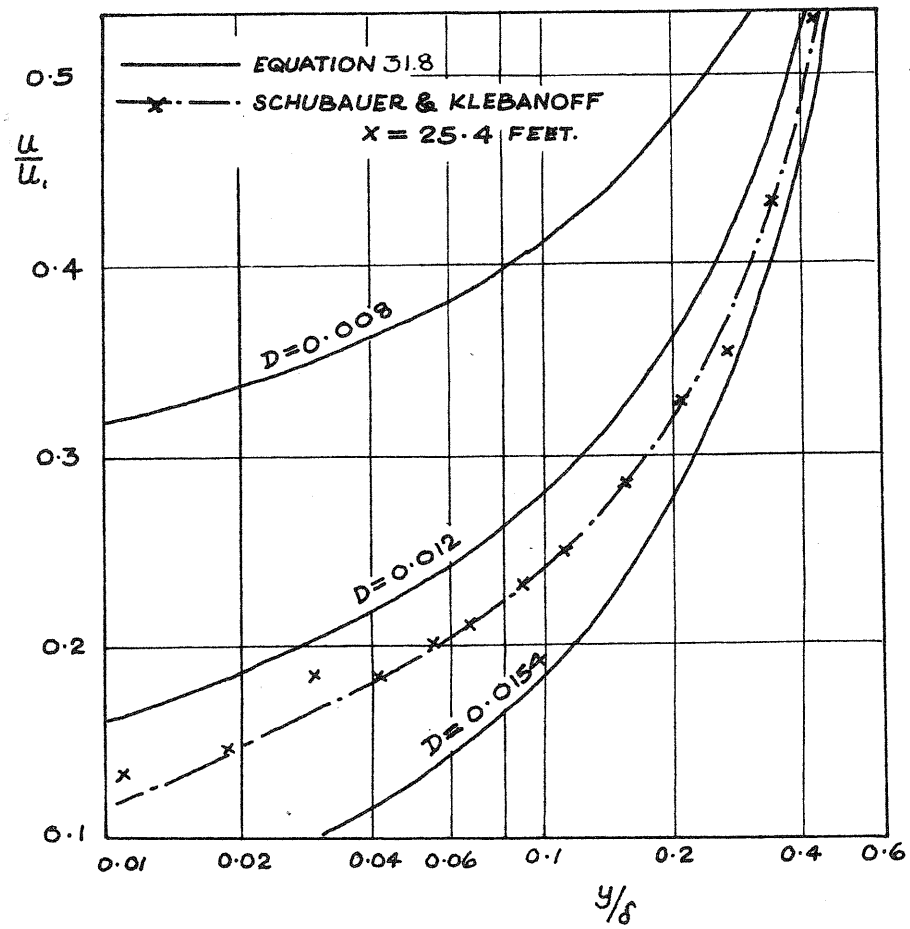

FIG.67 SEPARATION PROFILE IN THE INNER REGION

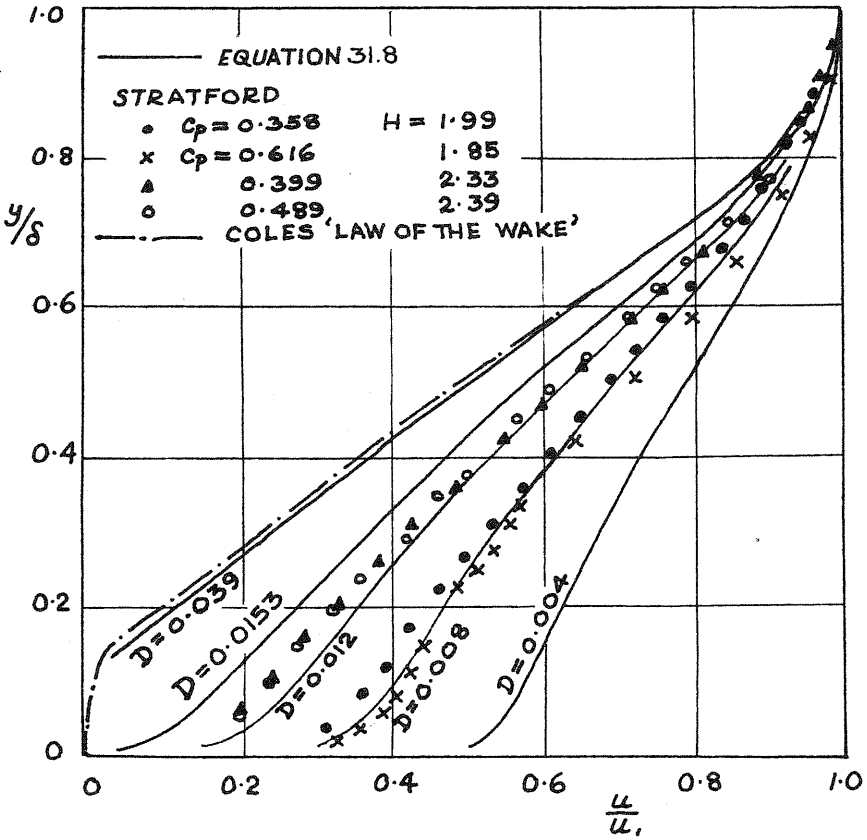

FIG. 68 SEPARATION PROFILES

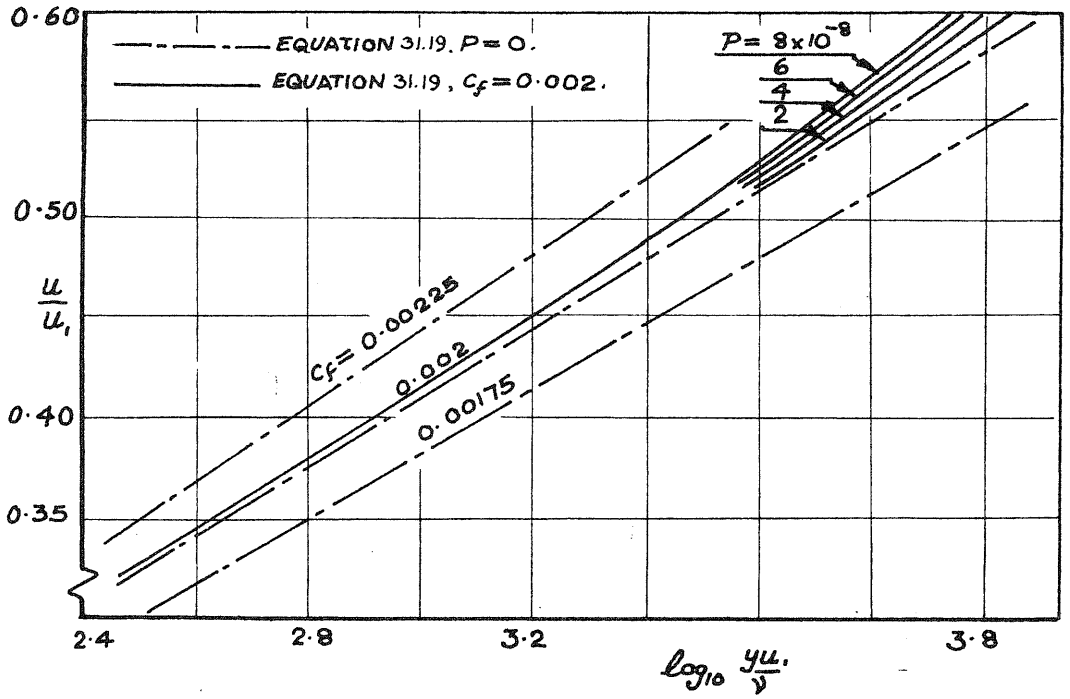

FIG. 69 THE INNER REGION EQUATION 31.19 $C_f = 0·002$

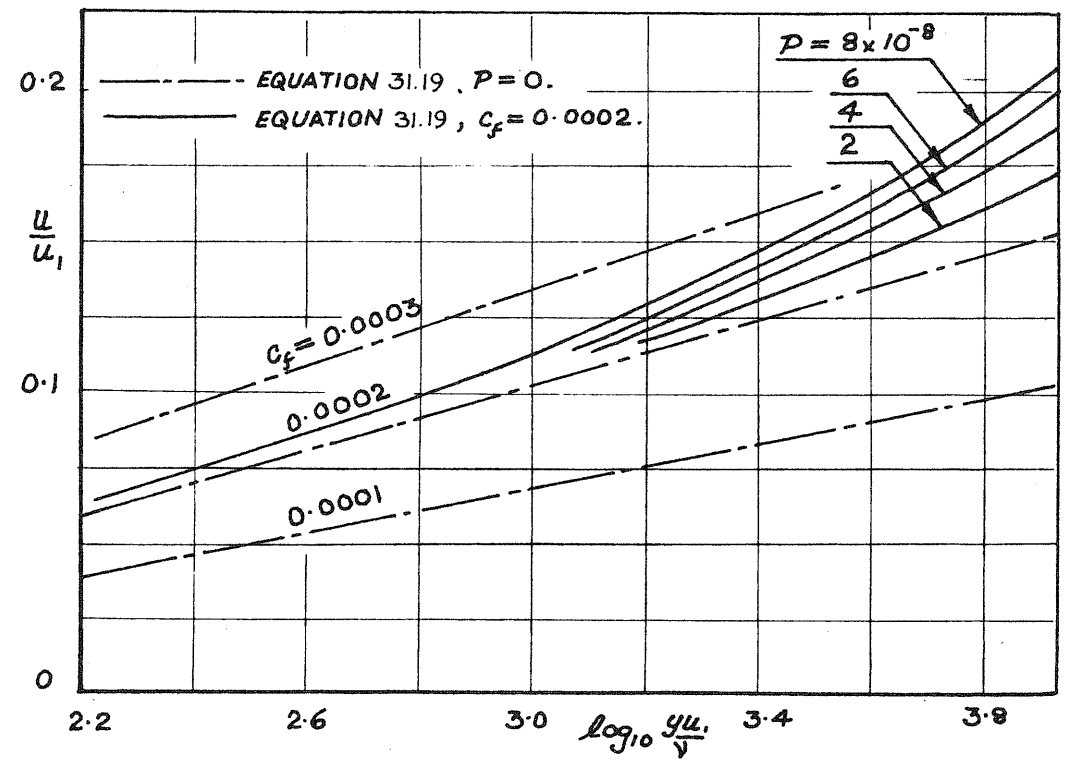

FIG. 70 THE INNER REGION EQUATION 31.19 $C_f = 0·0002$

$$P = -\frac{\nu}{u_1^2} \cdot \frac{du_1}{dx}.$$

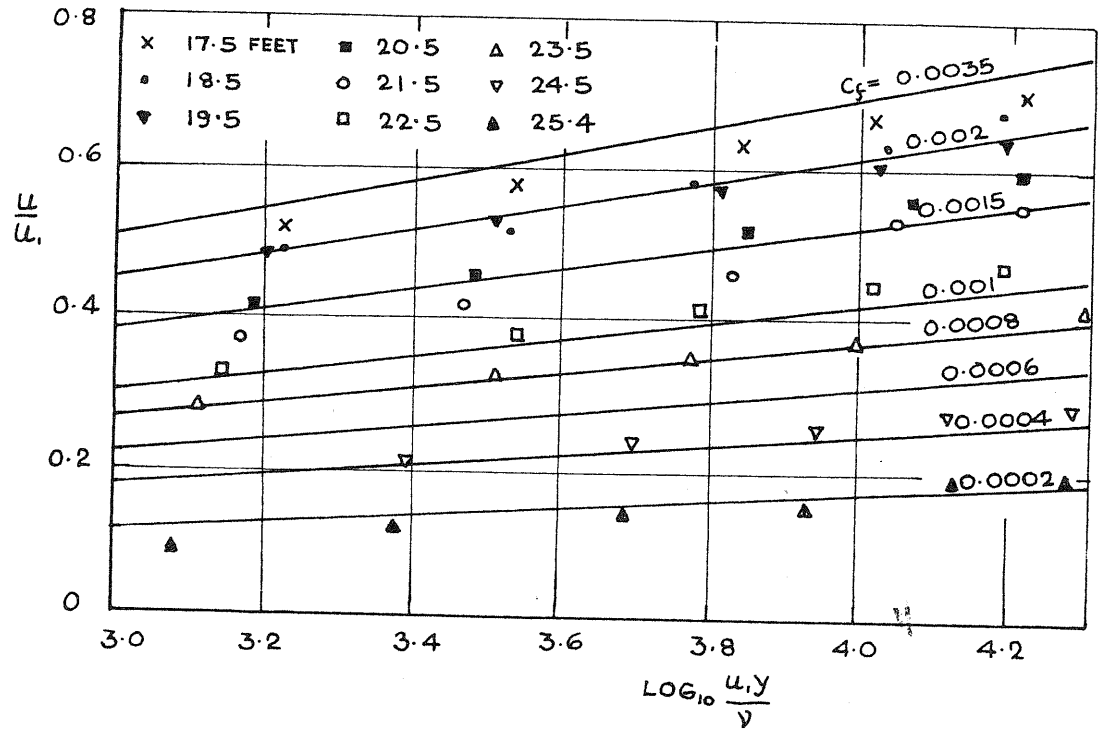

FIG. 71 THE LAW OF THE WALL AND SCHUBAUER & KLEBANOFF'S EXPERIMENTAL RESULTS

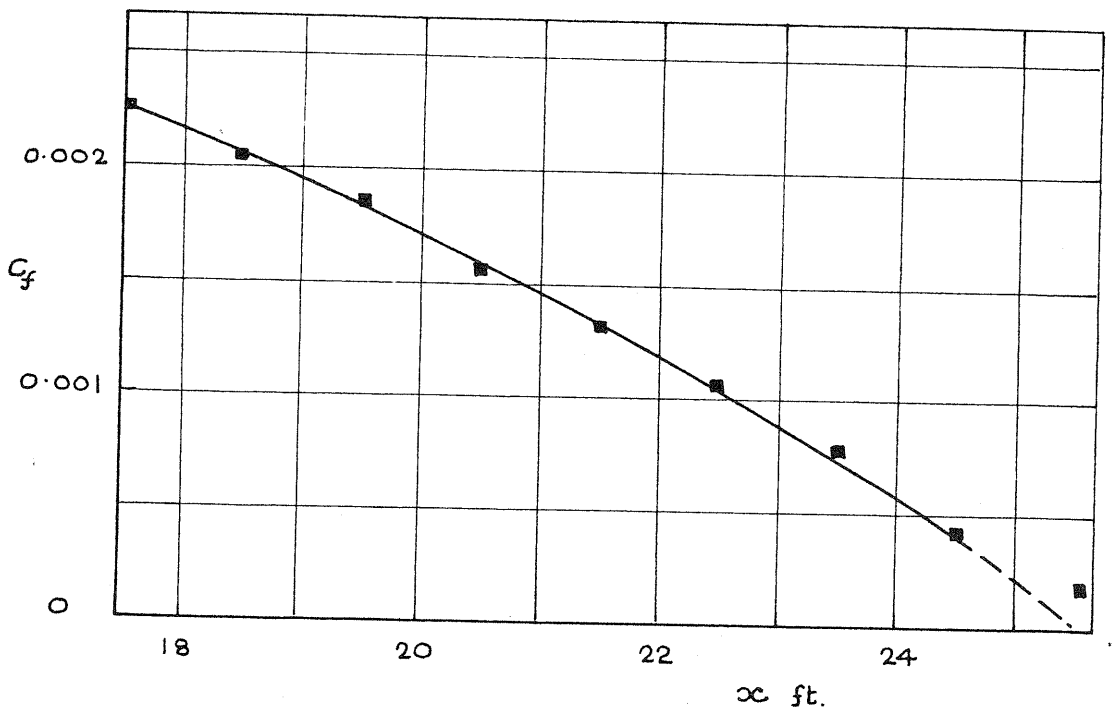

FIG. 72 THE APPROXIMATE SKIN FRICTION DISTRIBUTION IN SCHUBAUER & KLEBANOFF'S EXPERIMENTS

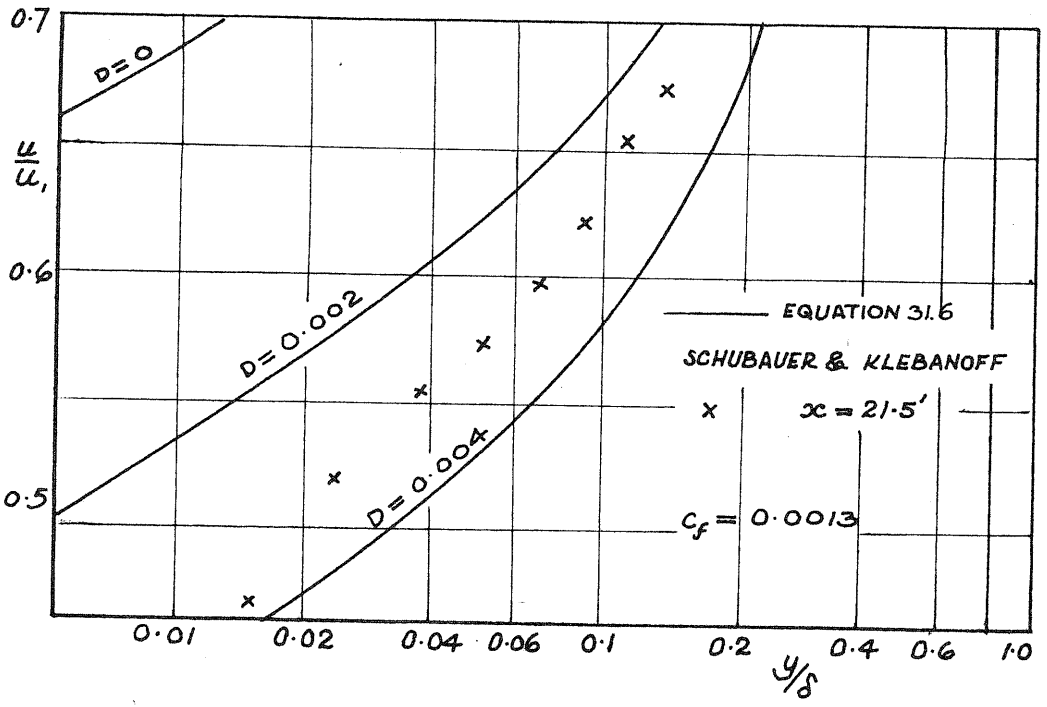

FIG. 73 ESTIMATING THE APPARENT PRESSURE GRADIENT

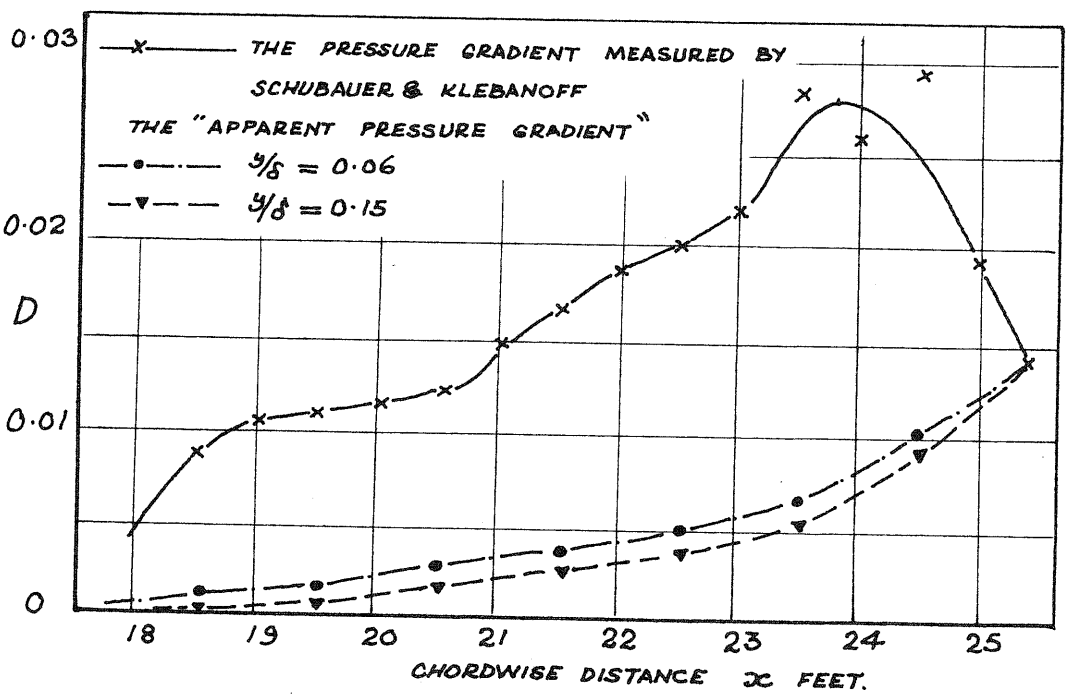

FIG. 74 DISTRIBUTION OF PRESSURE GRADIENT

$$D = -\frac{\delta}{u_1}\frac{du_1}{dx}$$

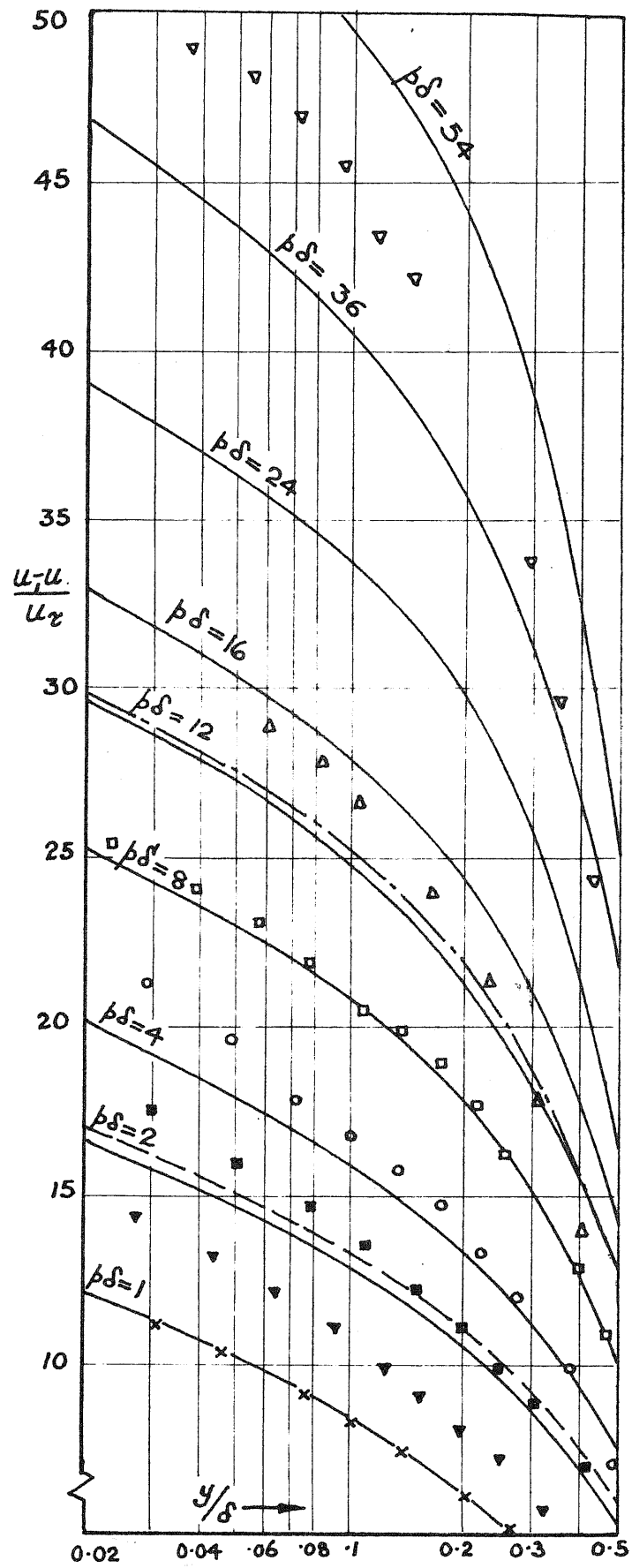

FIG. 75 THE INNER REGION $\frac{u_1-u}{u_\tau}$ AGAINST y/δ.

——— EQUATION 31.21

SCHUBAUER & KLEBANOFF

x	x = 17·5′
▽	19·5′
■	20·5′
o	21·5′
□	22·5′
△	23·5′
▽	24·5′

CLAUSER:

PRESSURE DISTRIBUTION

– – – – 1.

—·—·— 2.

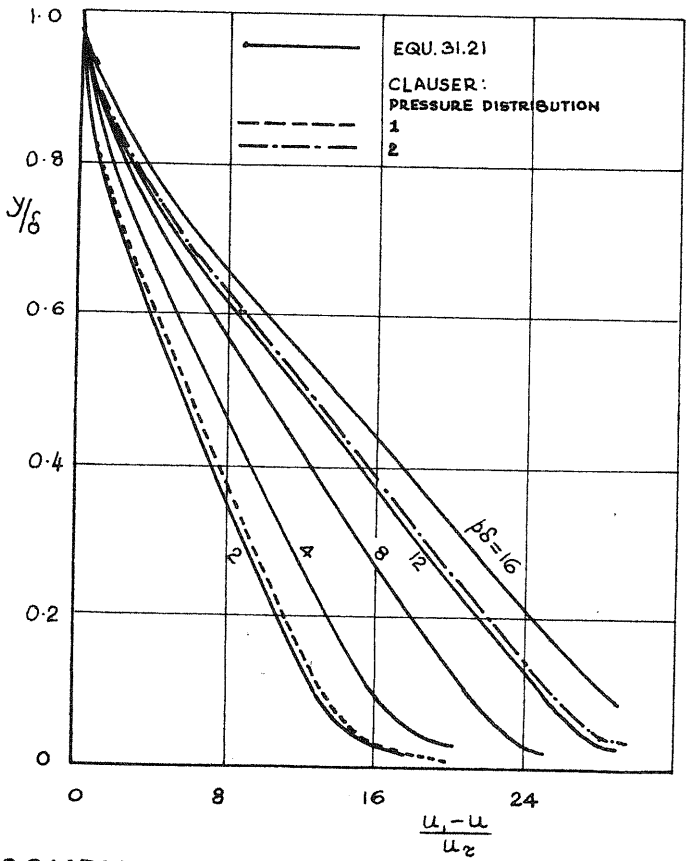

FIG. 76 COMPARISON BETWEEN EQU. 31.21 AND THE EXPERIMENTAL RESULTS OF CLAUSER

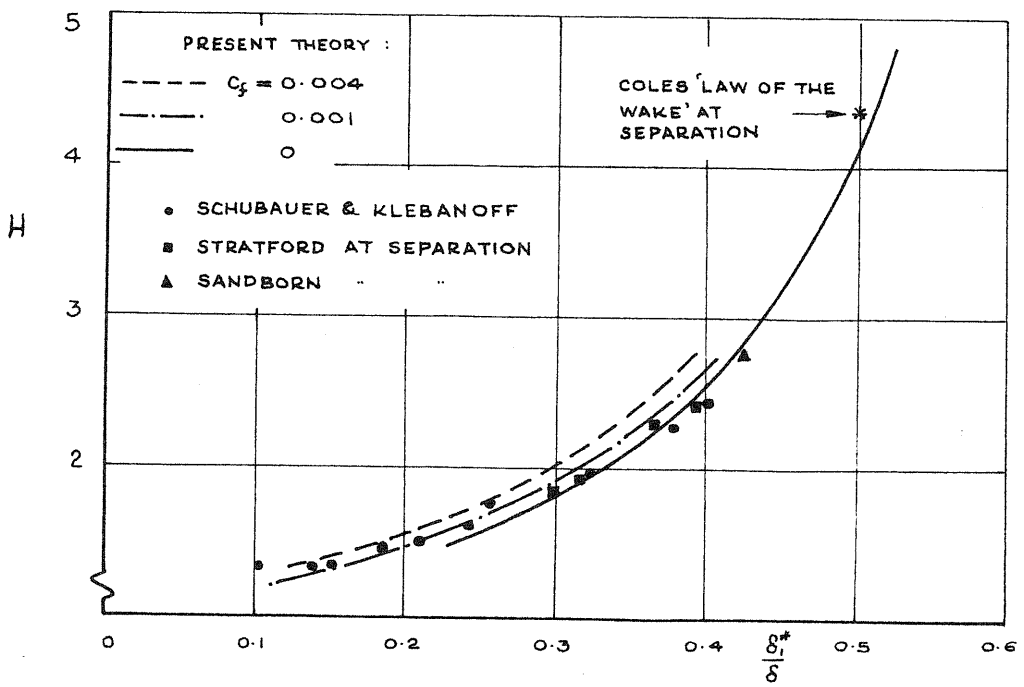

FIG. 77 VARIATION OF δ_1/δ WITH H

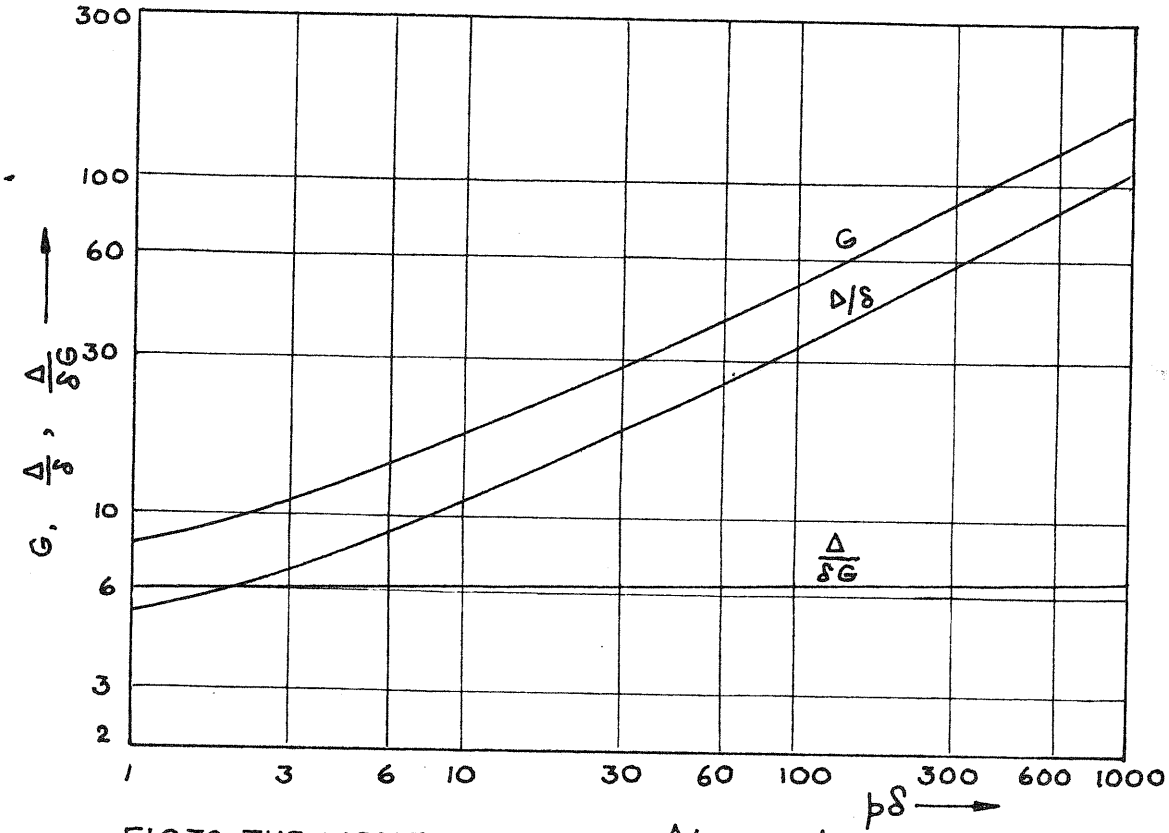

FIG.78 THE VARIATIONS IN G, Δ/δ AND $\Delta/\delta G$ WITH $p\delta$.

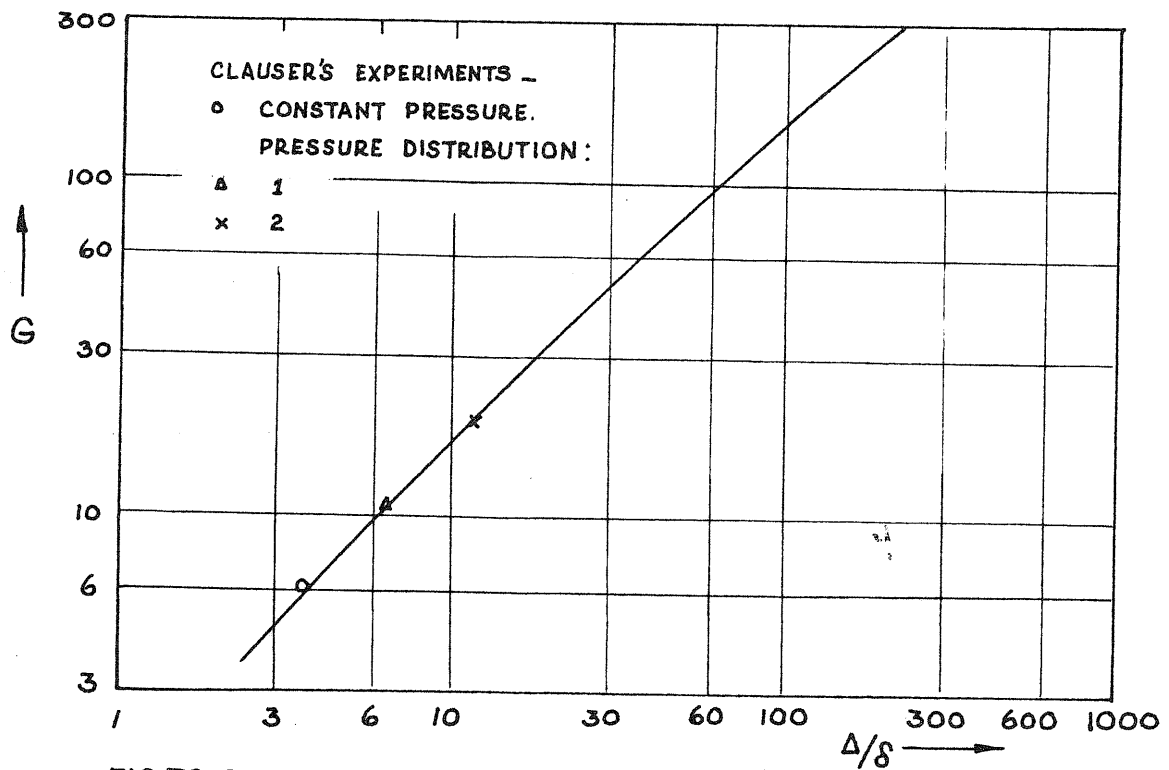

FIG.79 RELATIONSHIP BETWEEN G AND Δ/δ

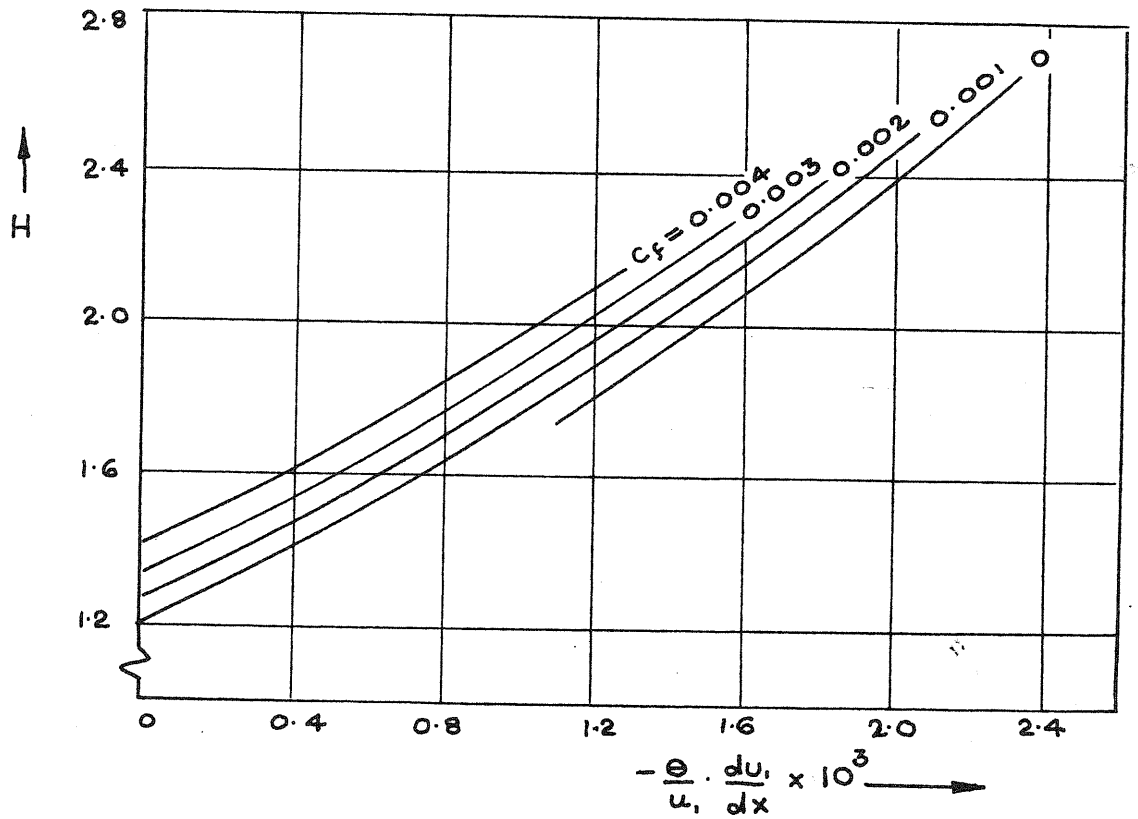

FIG. 80 VARIATION OF A PRESSURE GRADIENT TERM WITH H.

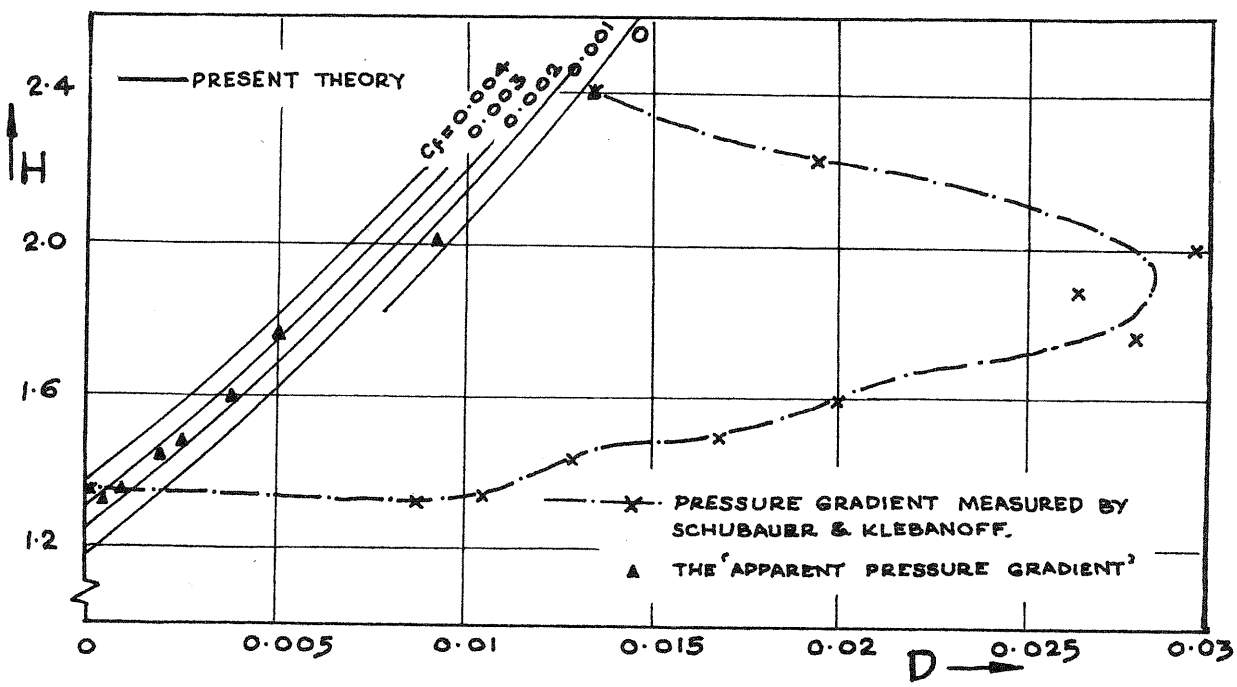

FIG. 81 VARIATION OF THE PRESSURE GRADIENT PARAMETER WITH H.

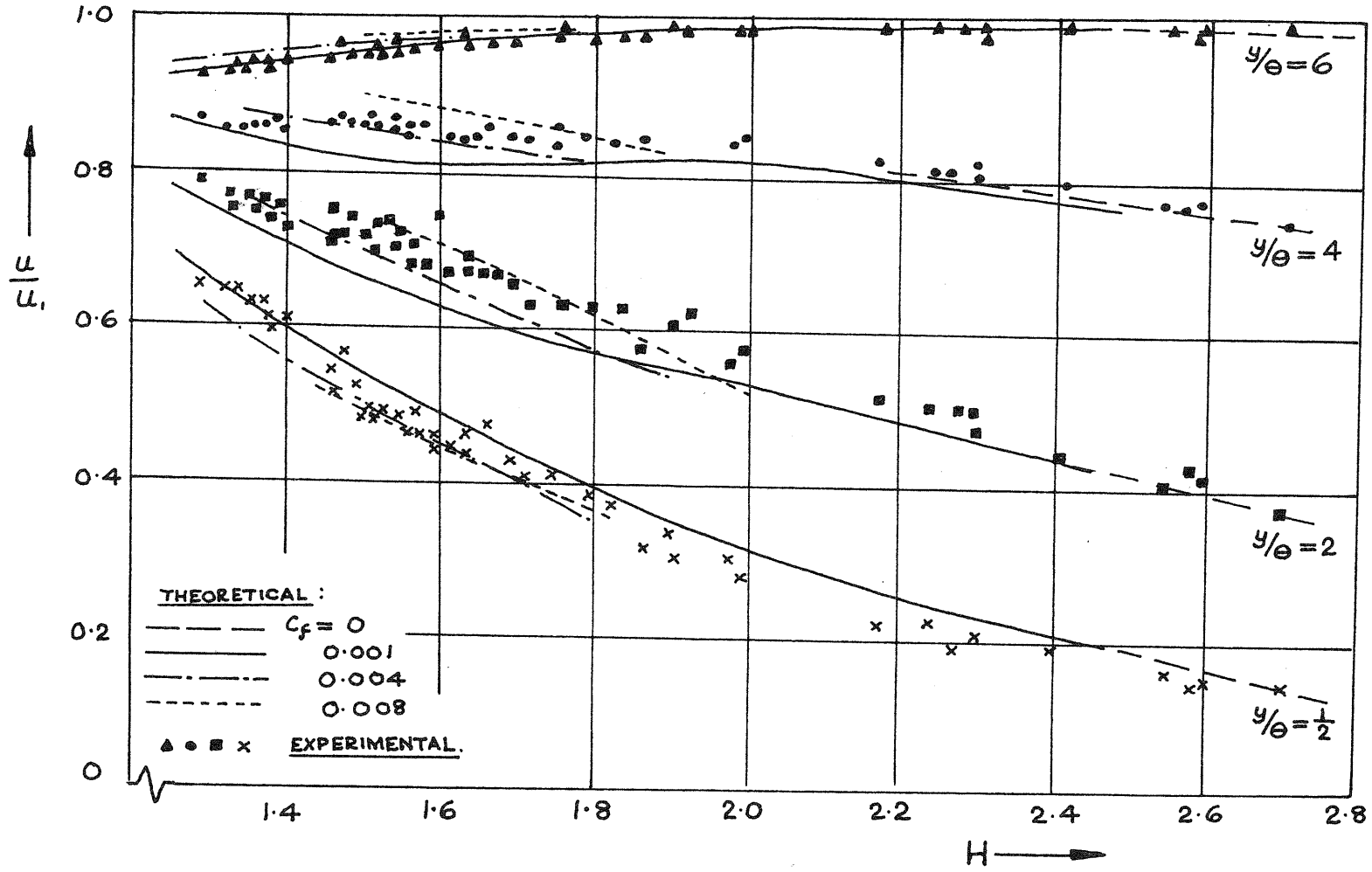

FIG. 82 EXPERIMENTAL RESULTS OF VON DOENHOFF & TETERVIN

$\frac{u}{u_1} \sim H$

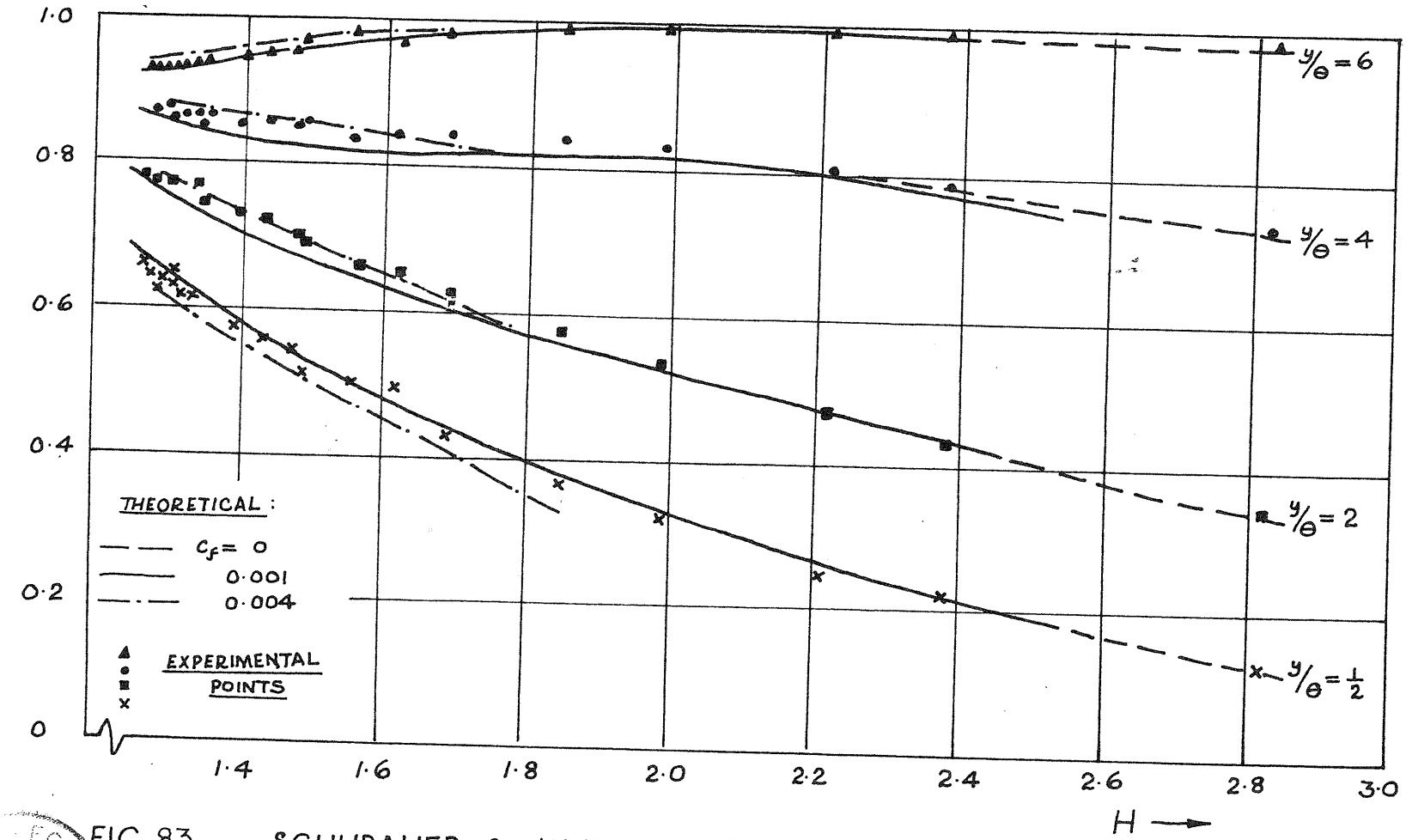

FIG. 83 SCHUBAUER & KLEBANOFF'S EXPERIMENTAL RESULTS. $u/u_1 \sim H$.

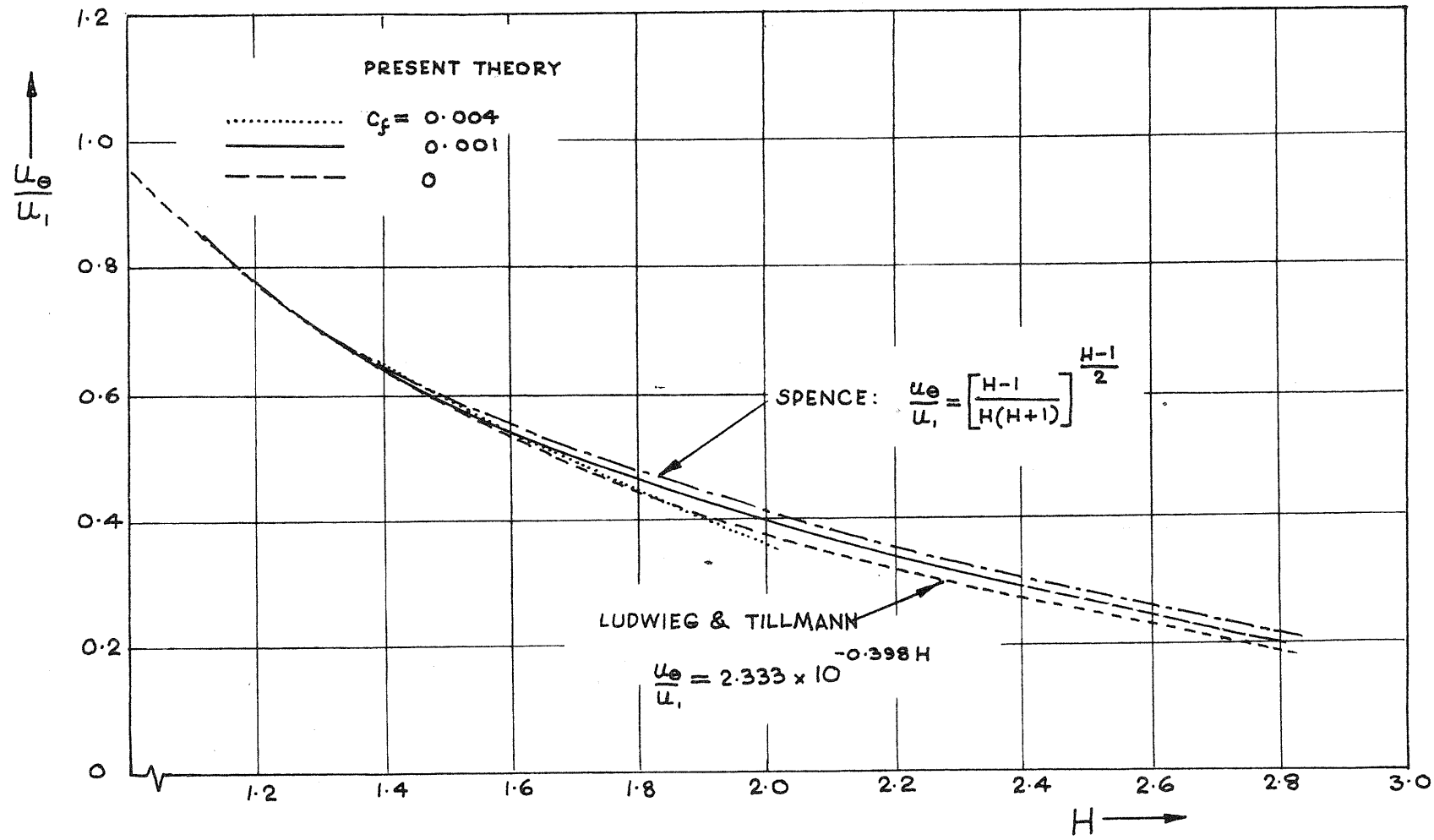

FIG. 84 THE PARAMETER u_e/u_1 AS FUNCTION OF H.

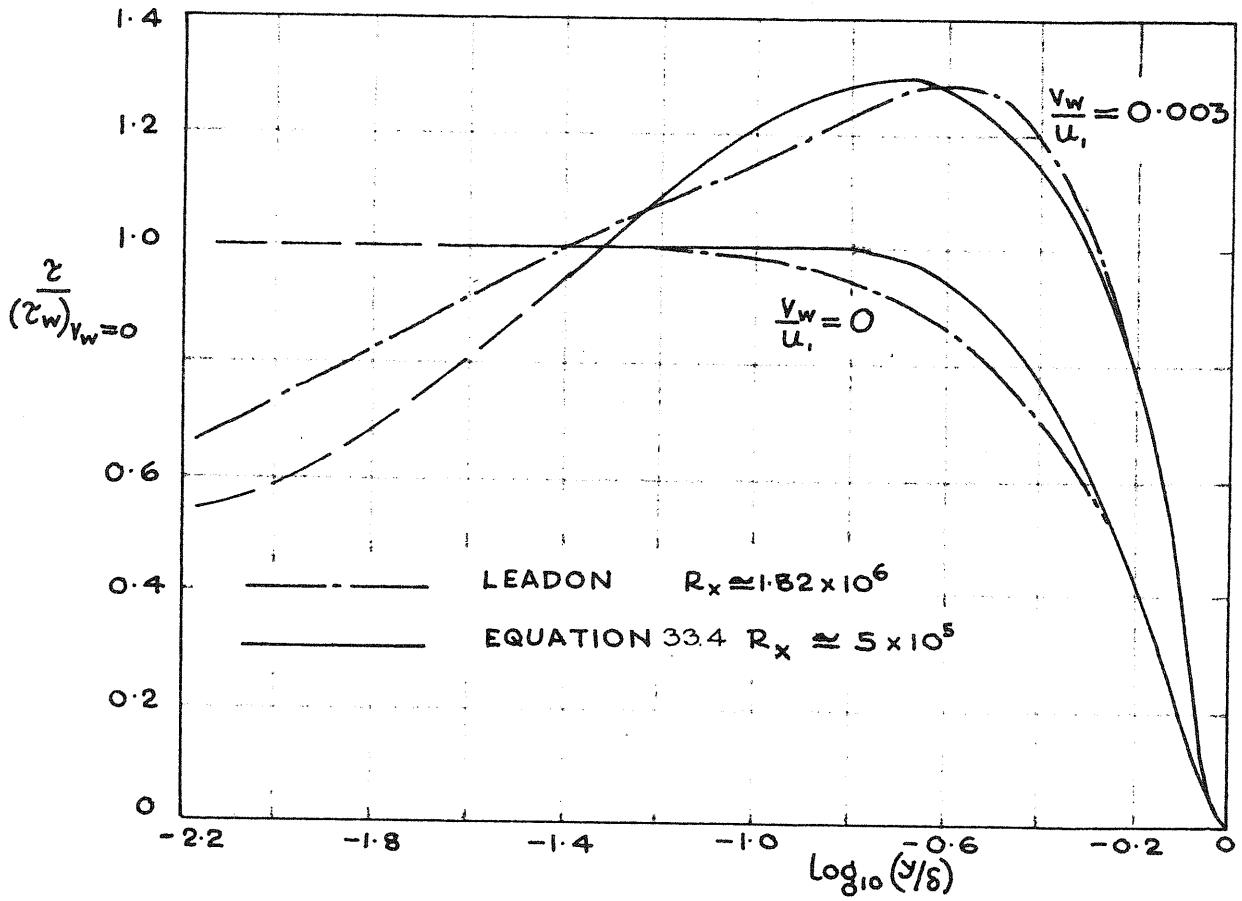

FIG. 85 SHEAR DISTRIBUTION CALCULATED BY LEADON FROM MICKLEY AND DAVIS' RESULTS

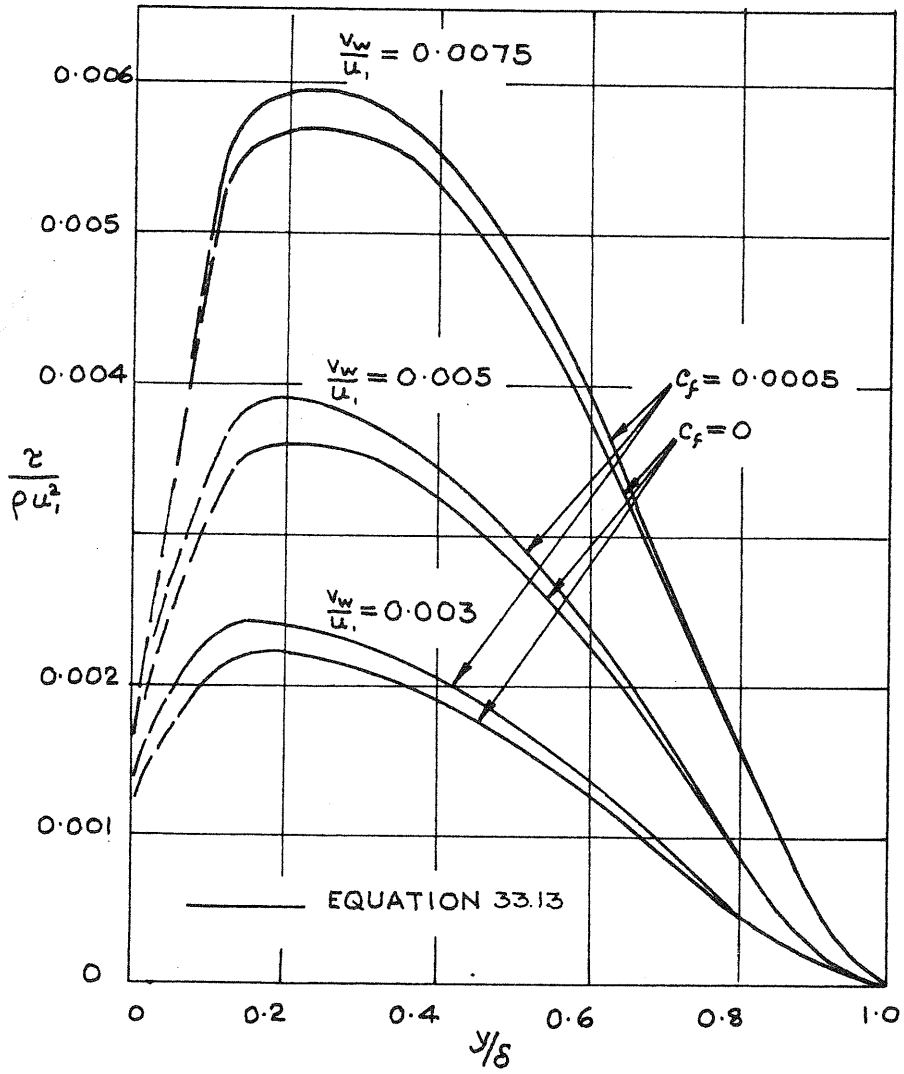

FIG. 86 INJECTION

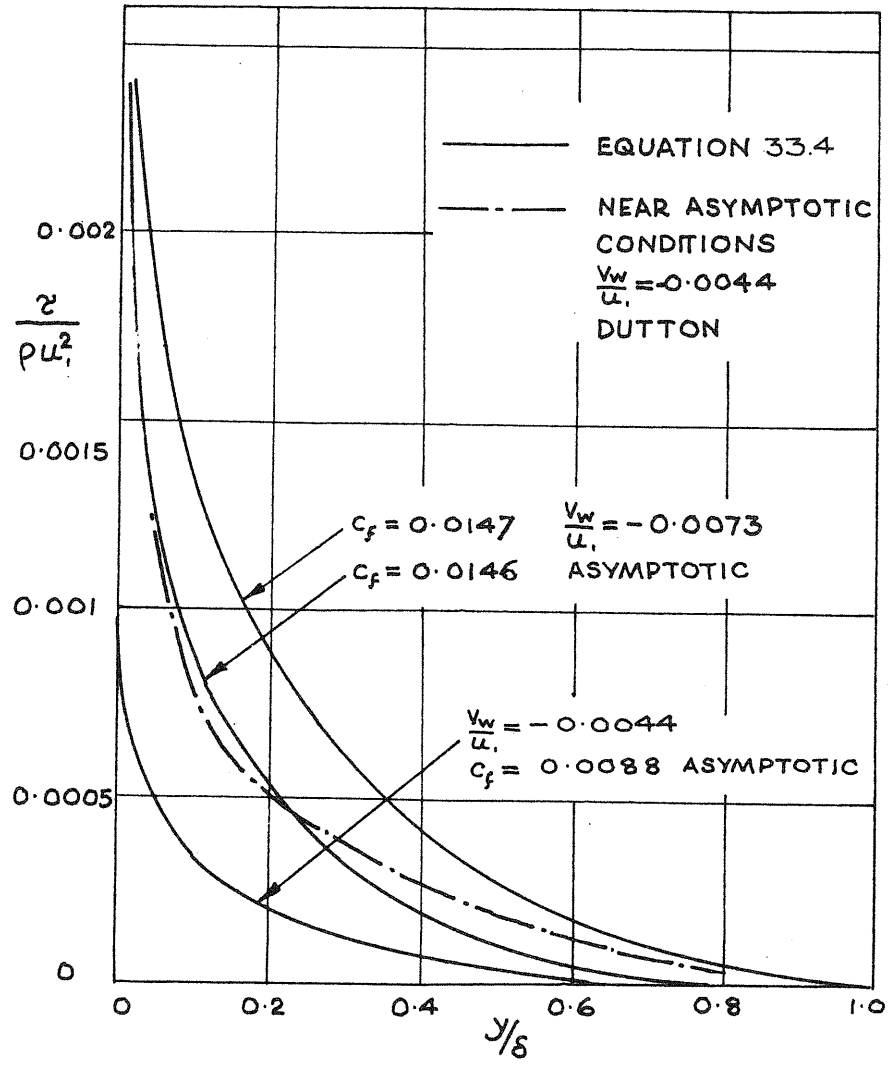

FIG. 87 SUCTION

SHEAR STRESS DISTRIBUTIONS

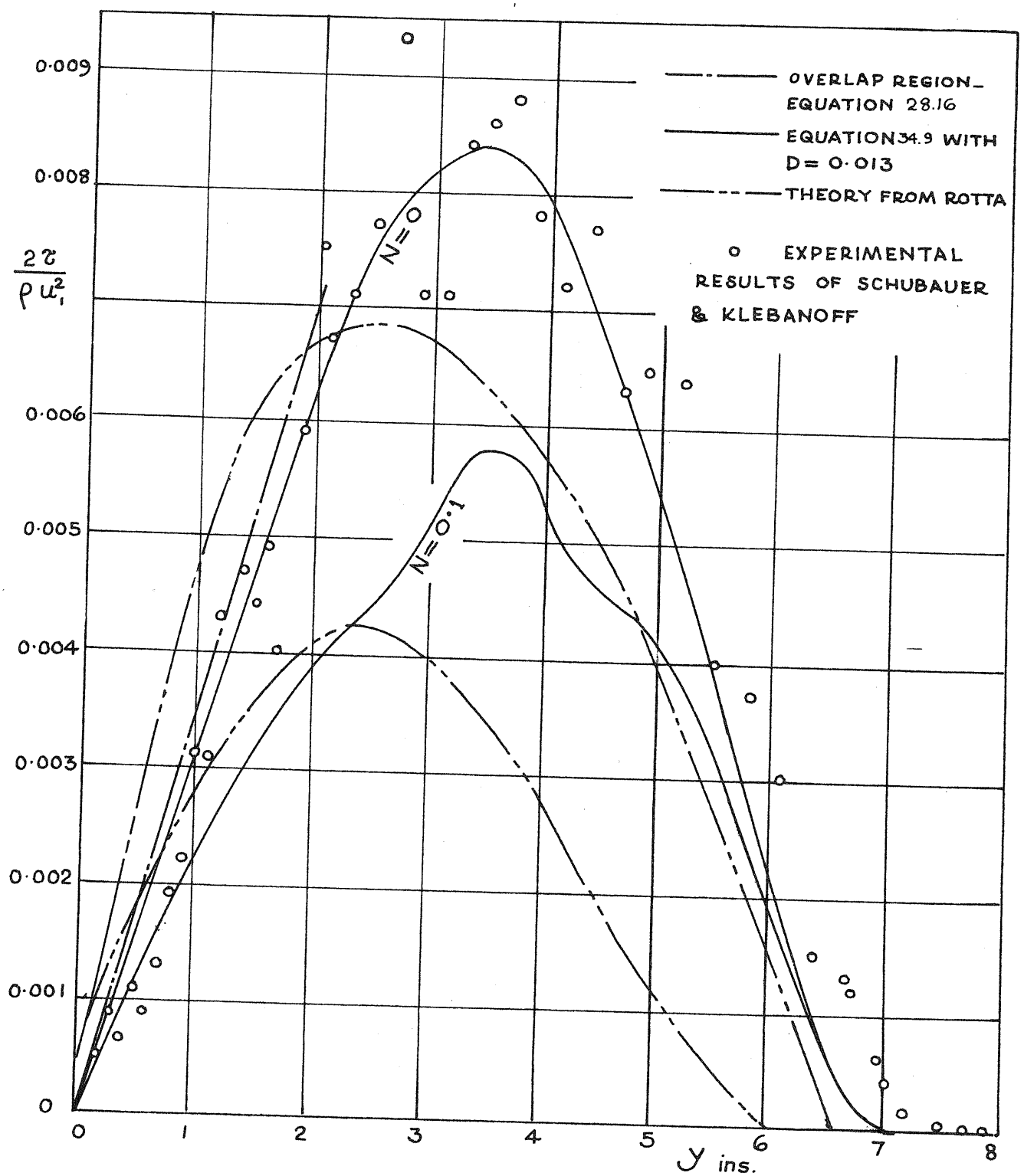

FIG. 88 SHEAR STRESS DISTRIBUTION AT SEPARATION

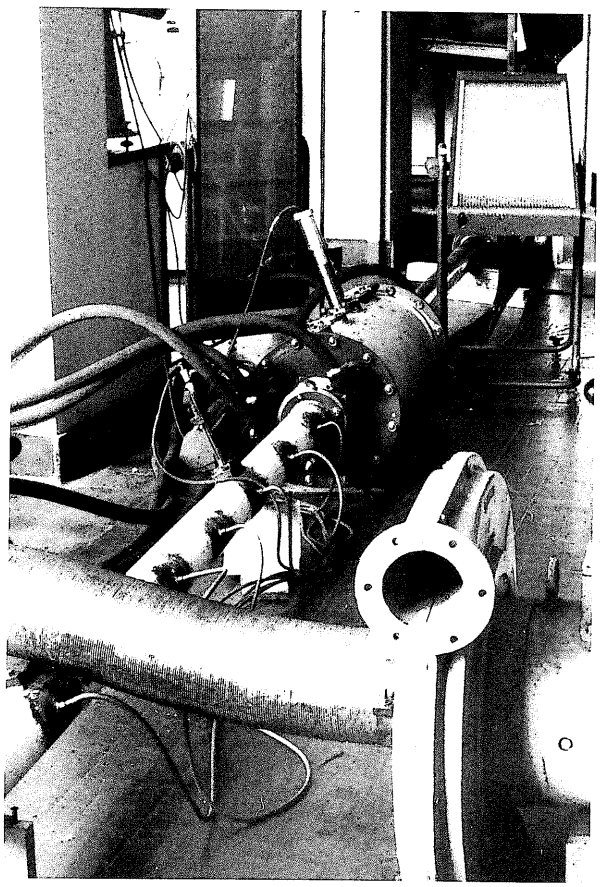

FIG. 89. PIPE FLOW APPARATUS.

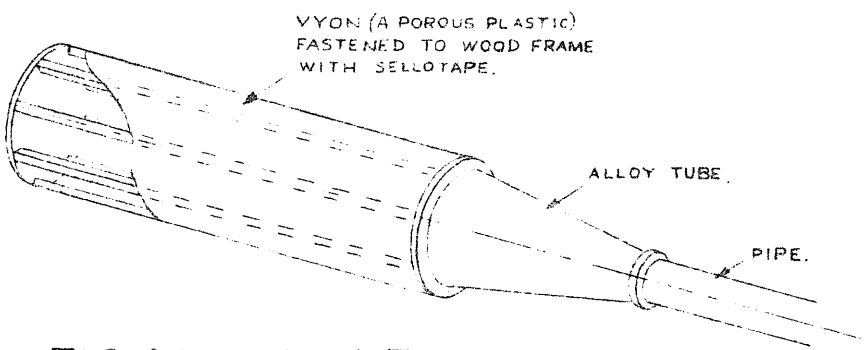

FIG. 90. INTAKE.

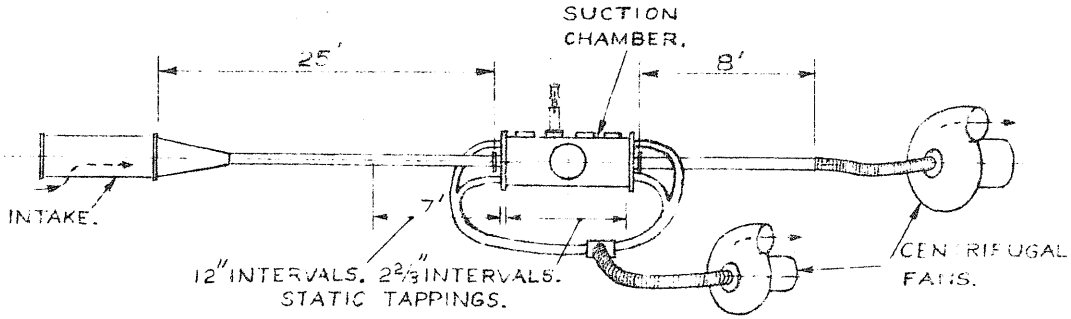

FIG. 91. LAYOUT OF APPARATUS.

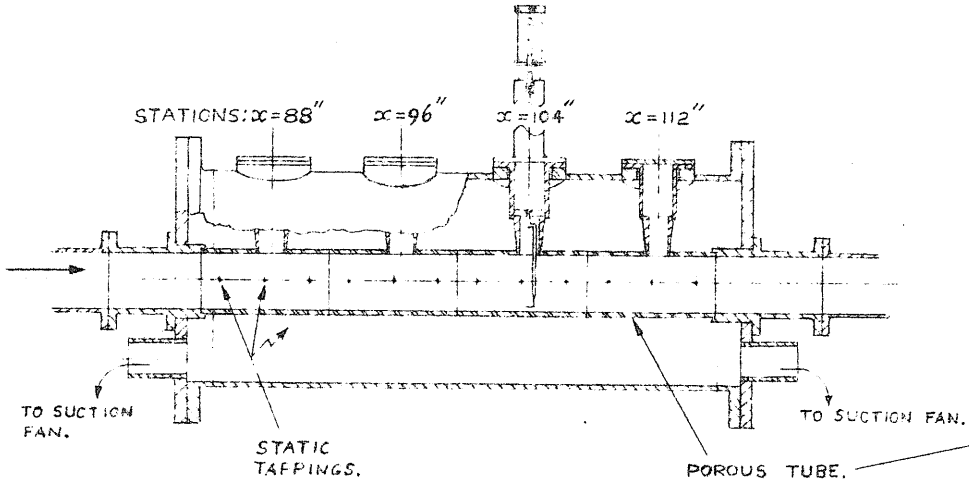

SUCTION CHAMBER

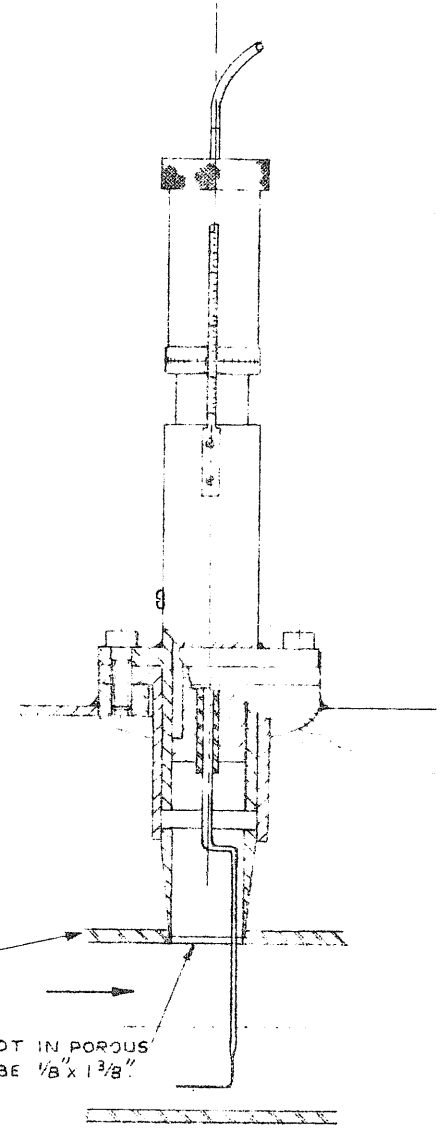

TRAVERSING GEAR.

FIG. 92. APPARATUS

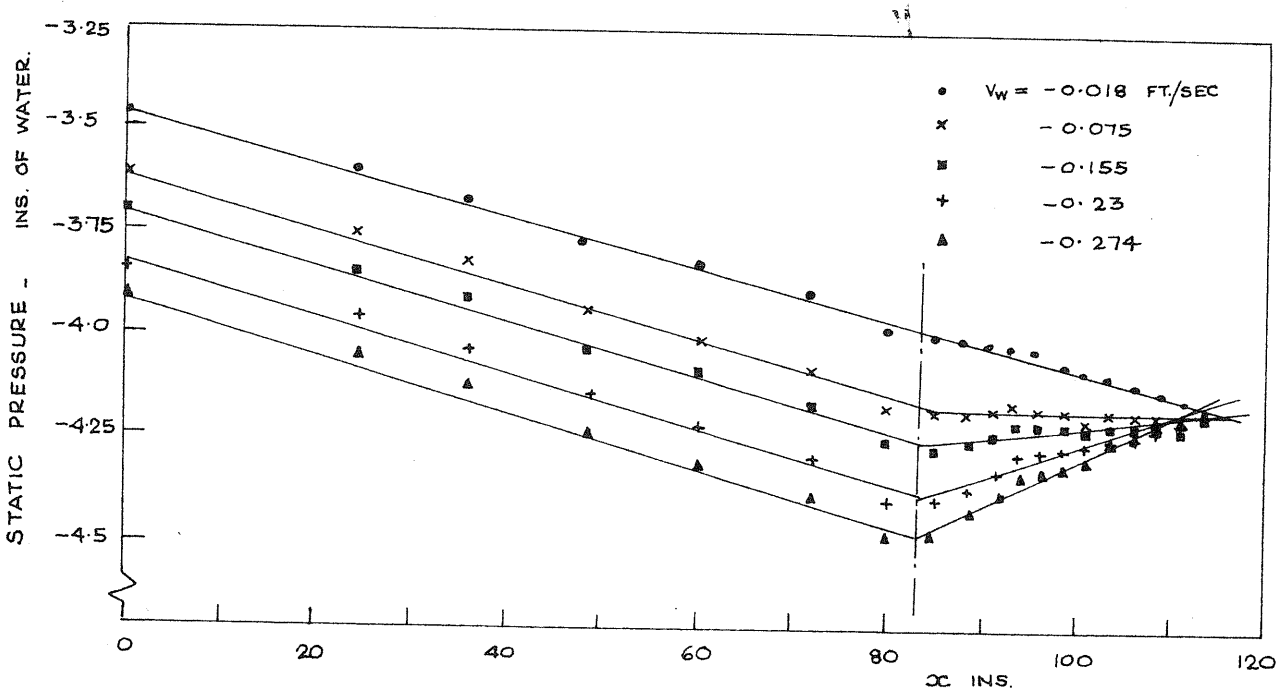

FIG. 93 A

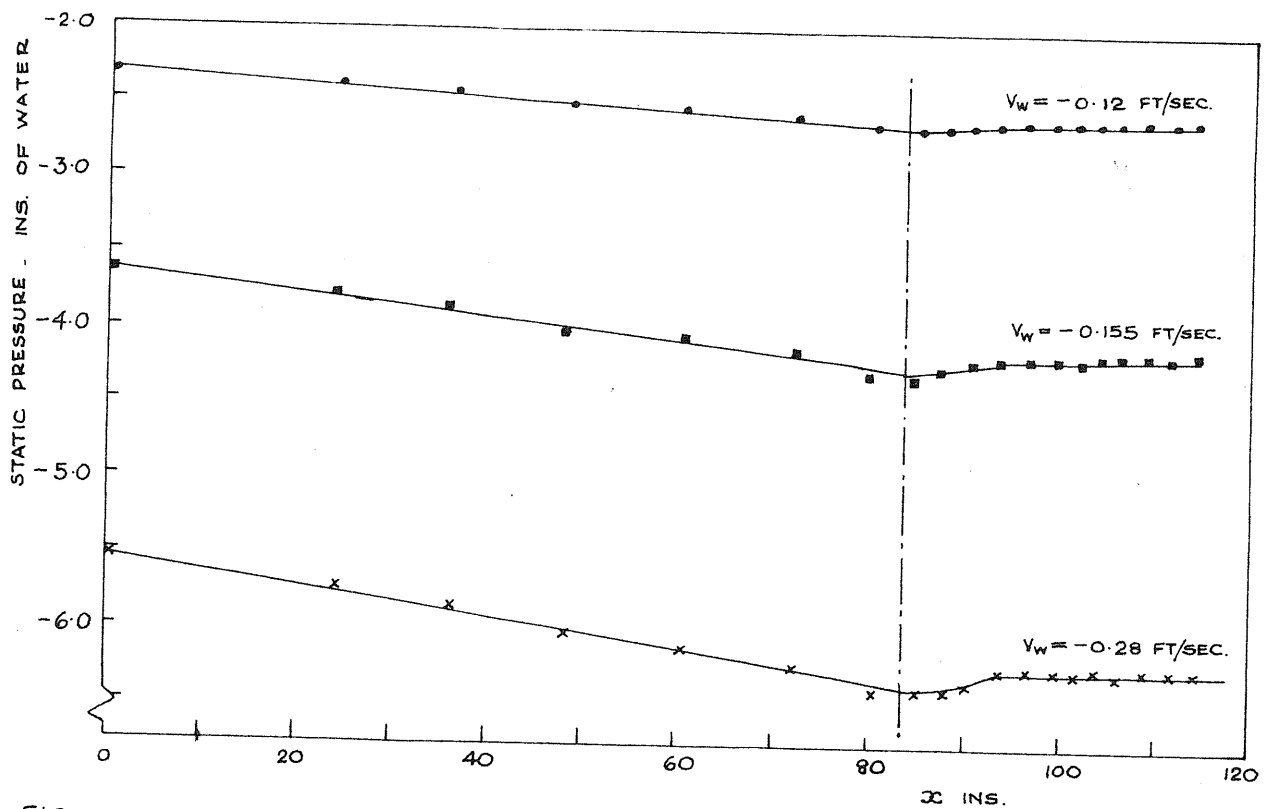

FIG. 93 B

STATIC PRESSURE DISTRIBUTION ALONG THE PIPE

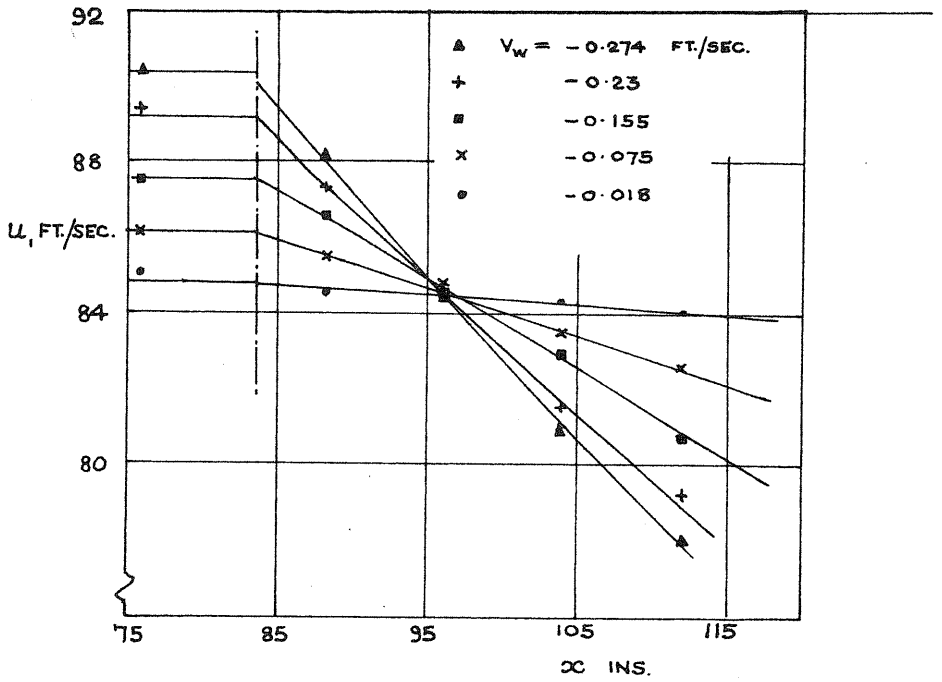

FIG. 94A

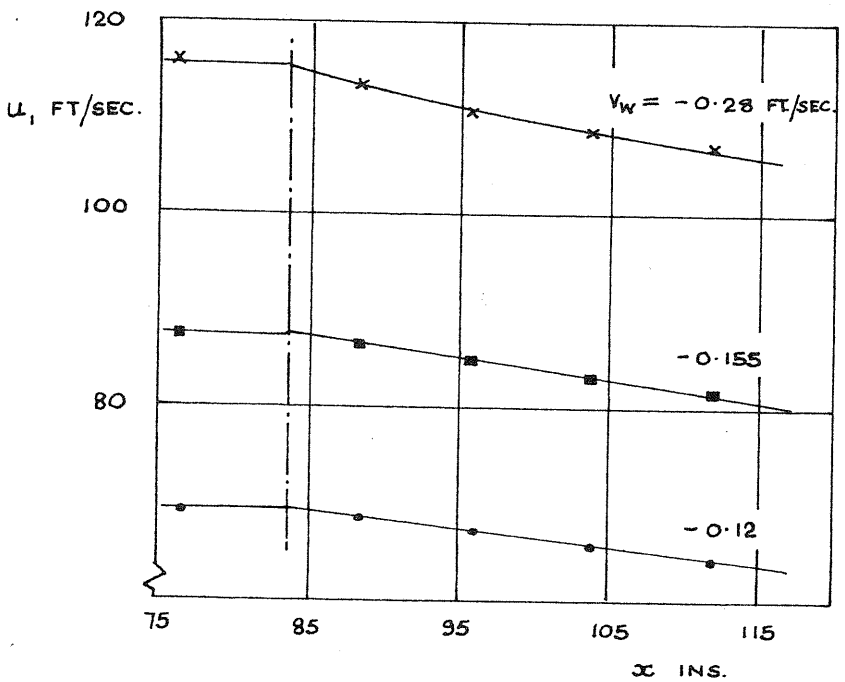

FIG. 94 B

VELOCITY DISTRIBUTION ALONG CENTRE-LINE OF PIPE

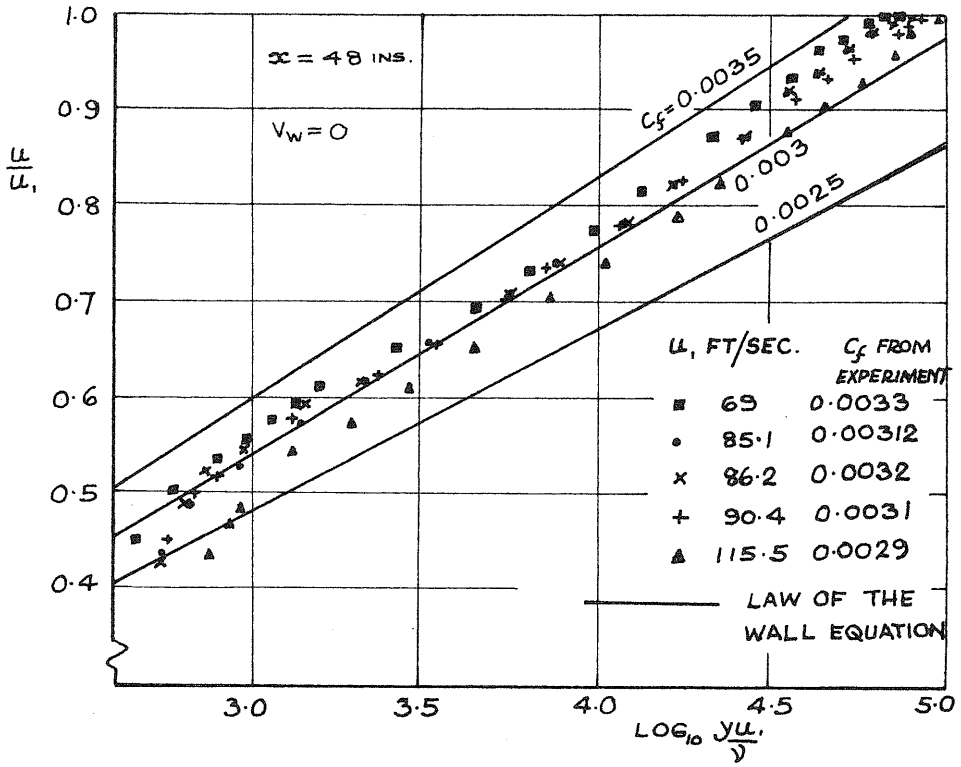

FIG.95 VELOCITY PROFILES IN PIPE FLOW – $V_w = 0$

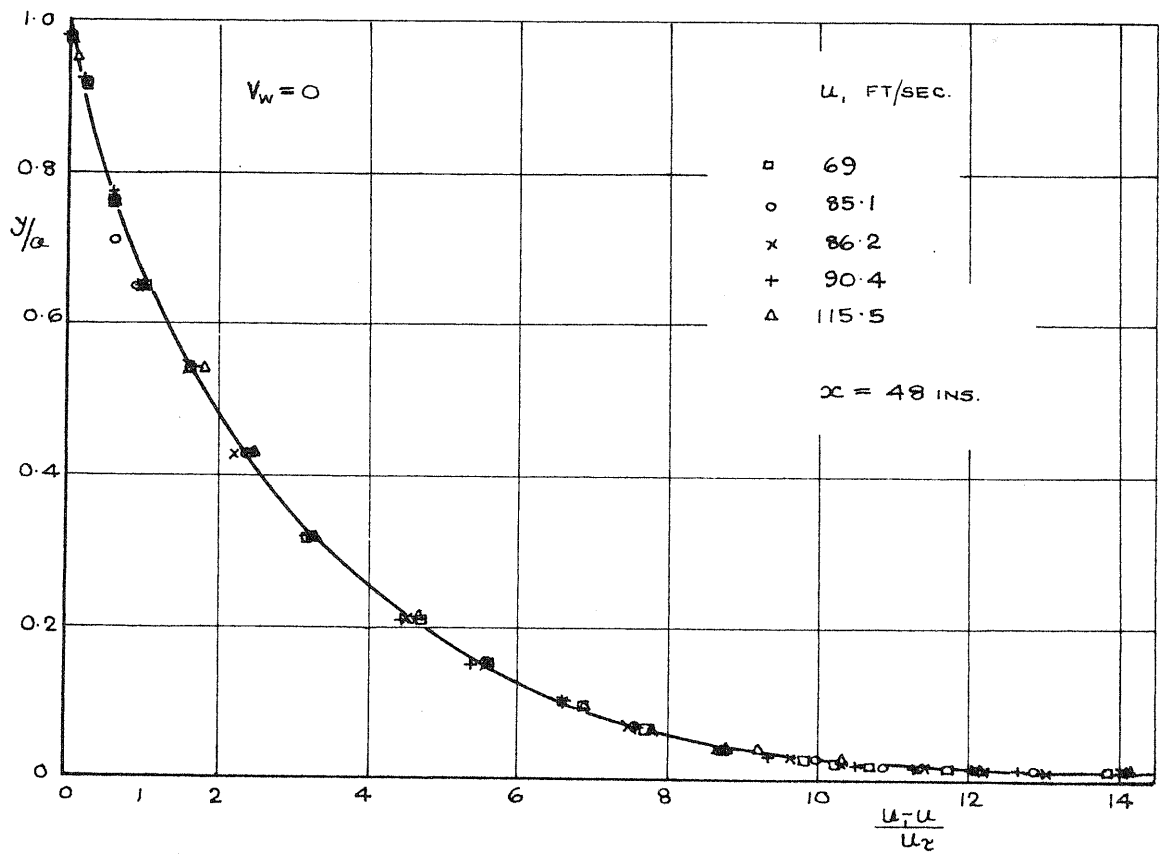

FIG. 96 THE OUTER REGION CURVE – PIPE FLOW

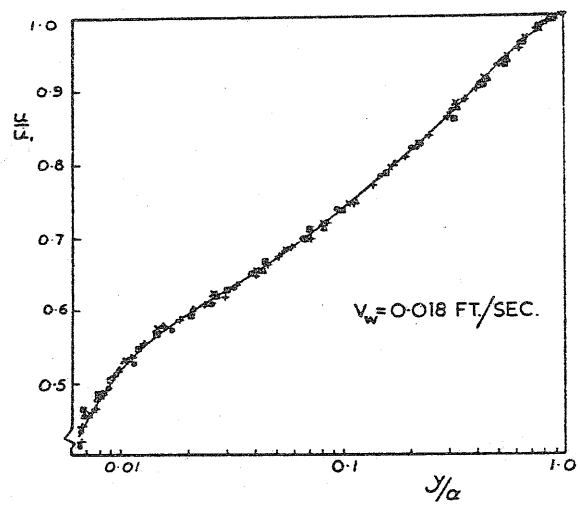

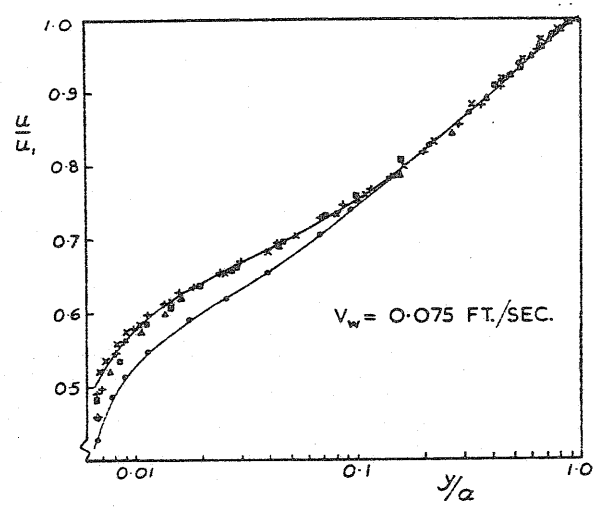

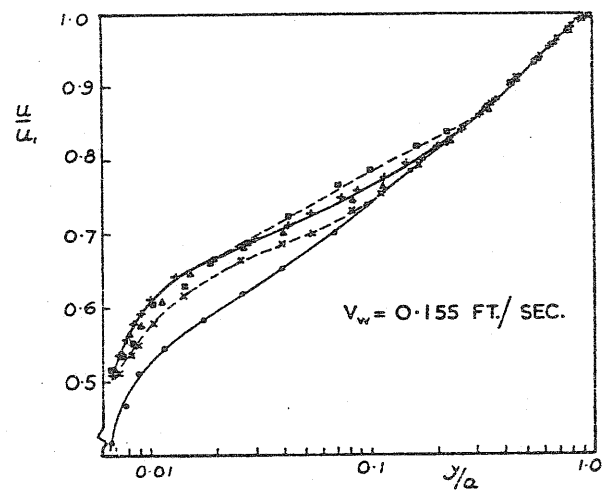

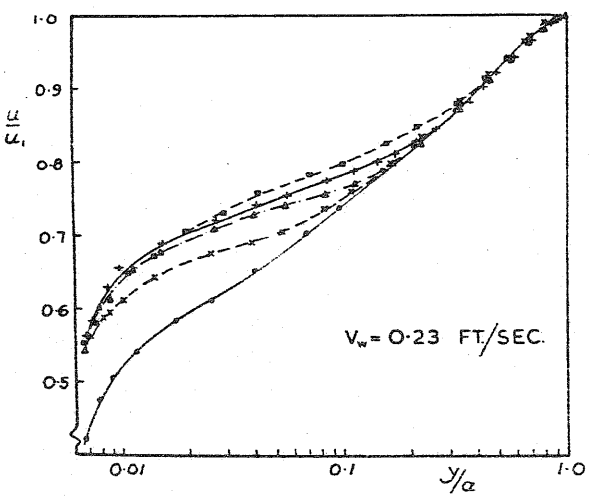

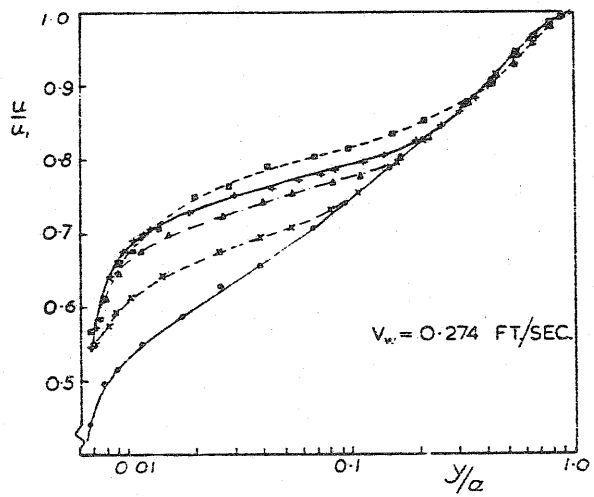

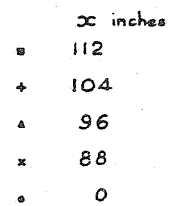

FIG. 97 VELOCITY PROFILES WITH SUCTION — PIPE FLOW $u_1 \simeq 80$ FT./SEC.

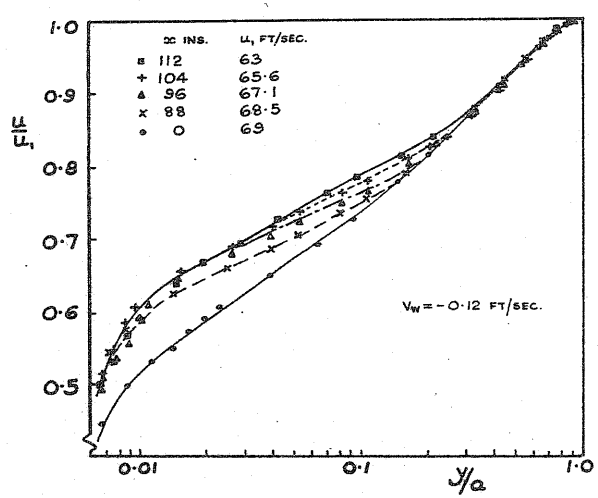

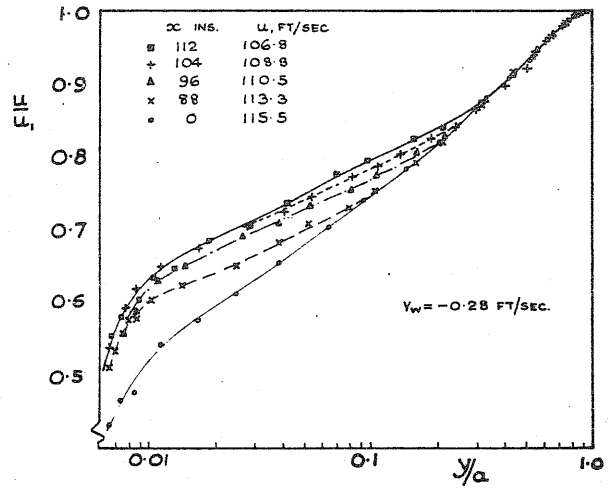

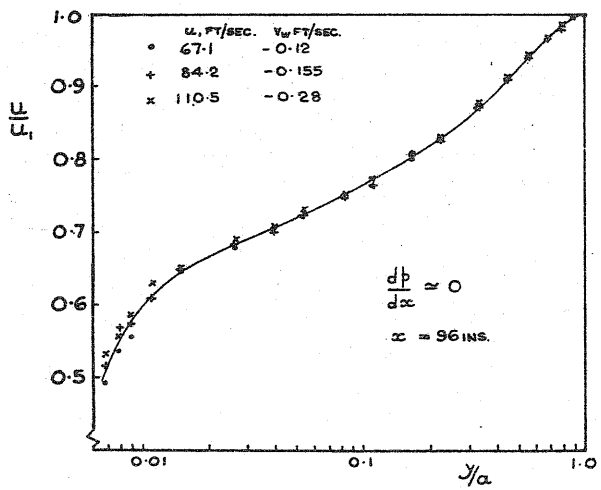

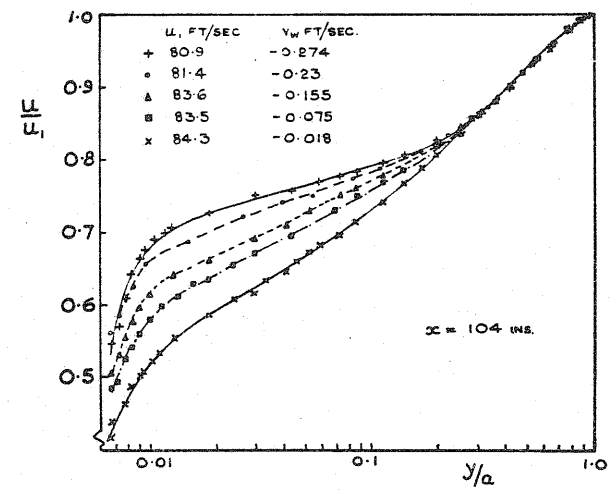

FIG. 98 VELOCITY PROFILES WITH SUCTION — PIPE FLOW

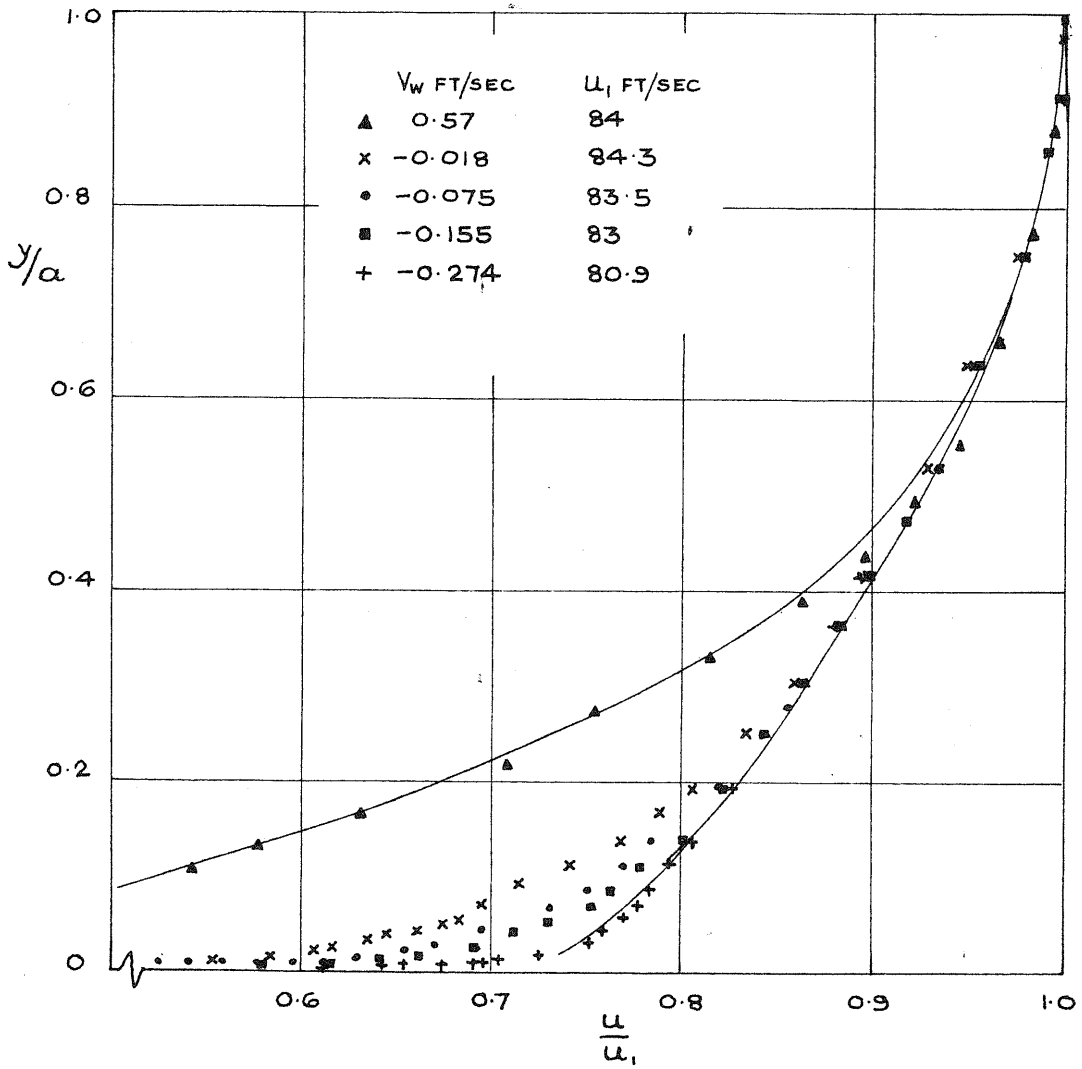

FIG. 99 VELOCITY PROFILES IN PIPE FLOW

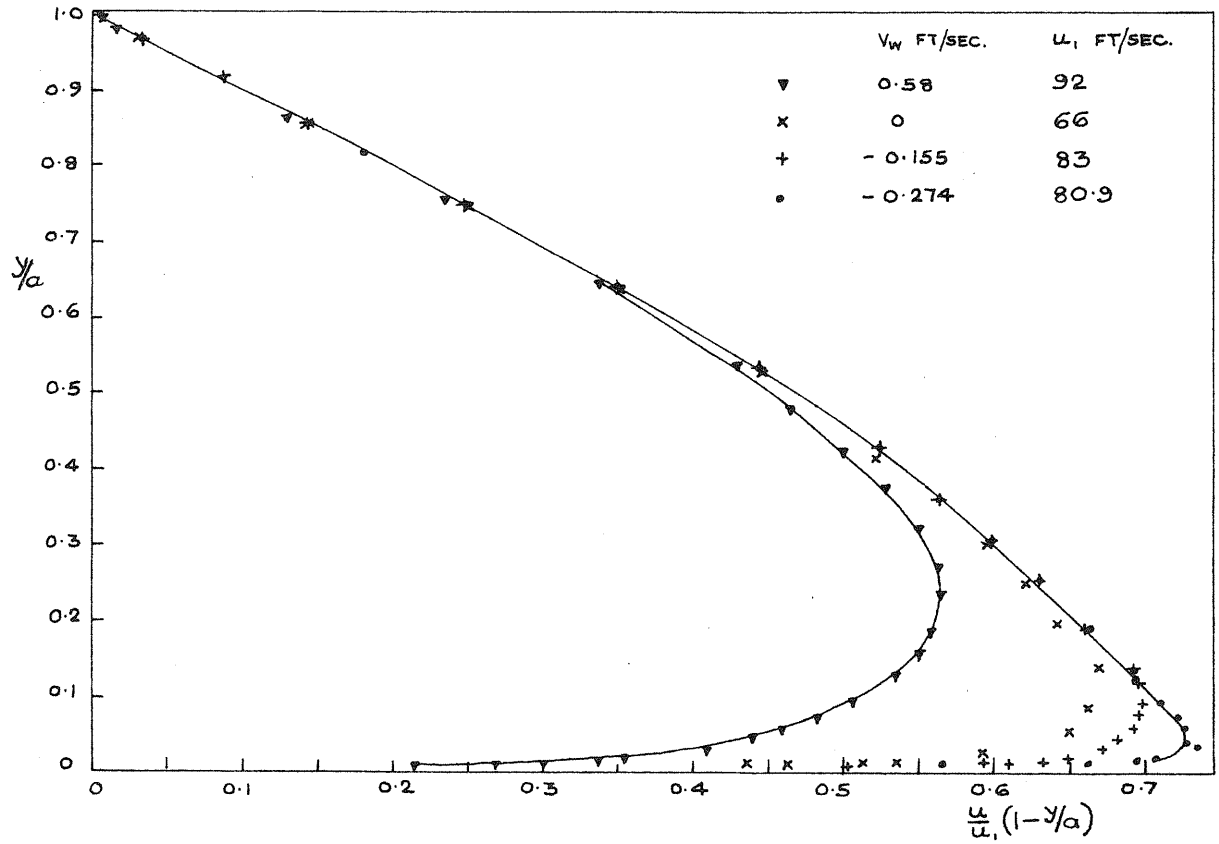

FIG. 100 CURVES USED TO EVALUATE V_w

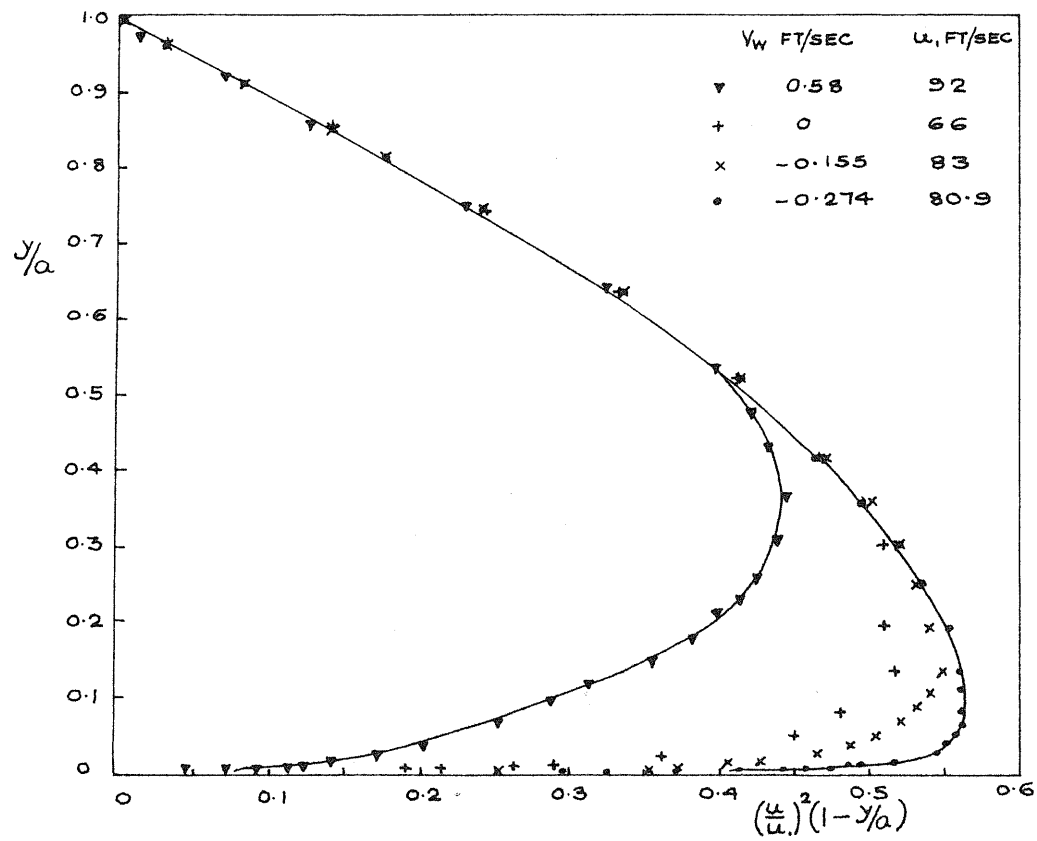

FIG. 101 CURVES USED TO EVALUATE THE SKIN FRICTION

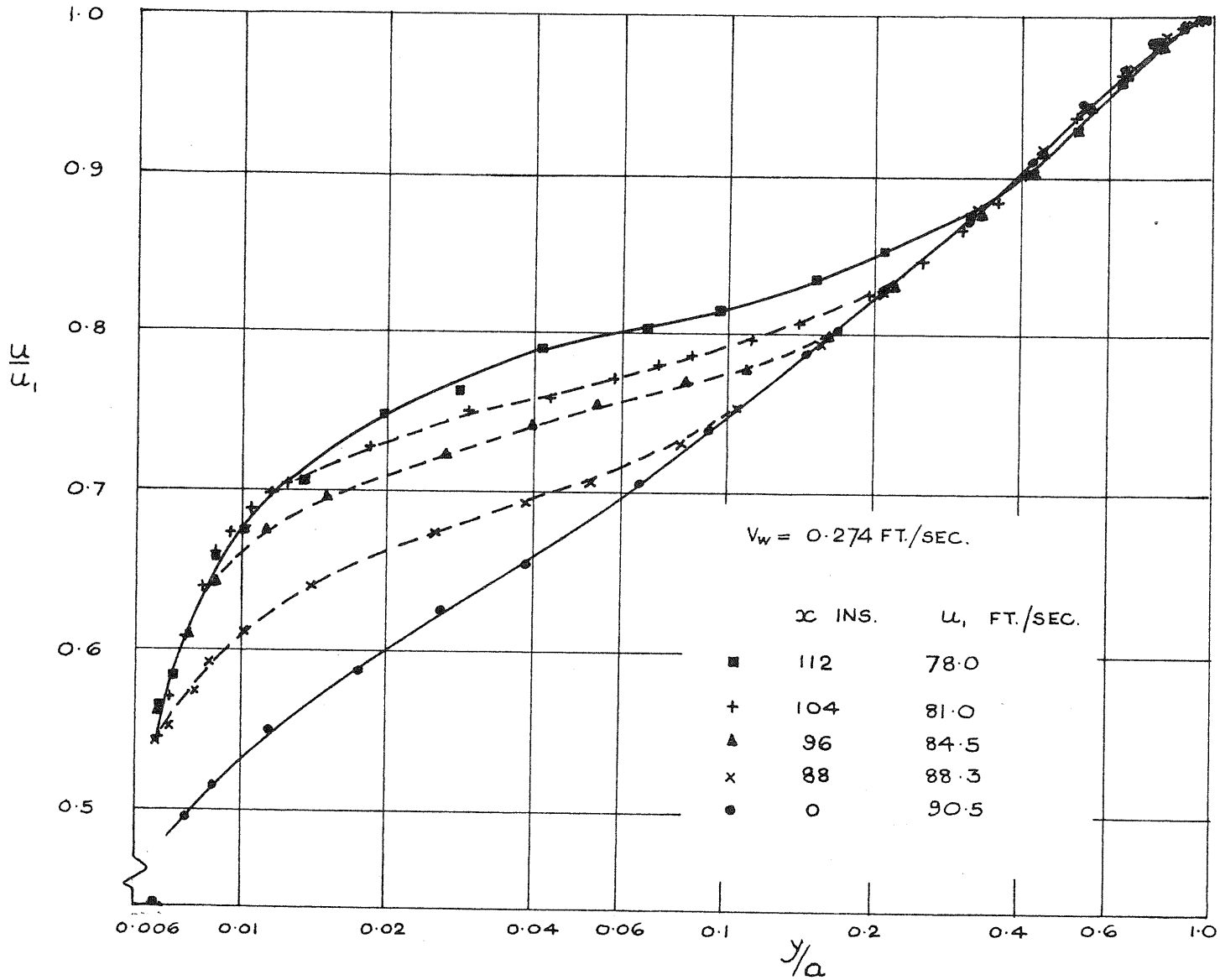

FIG. 102 VELOCITY PROFILES WITH SUCTION - PIPE FLOW

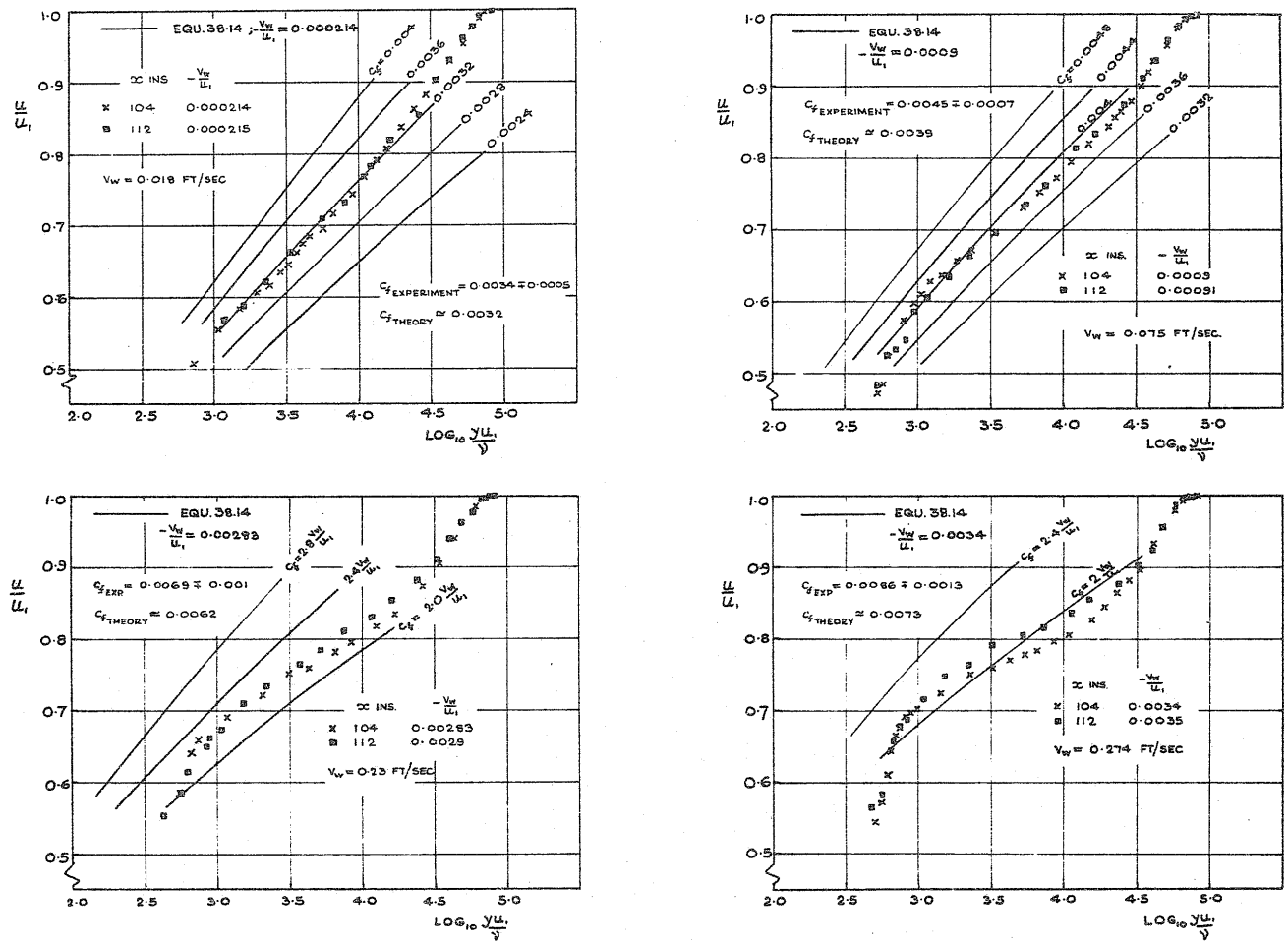

FIG. 103 INNER REGION VELOCITY PROFILES – PIPE FLOW

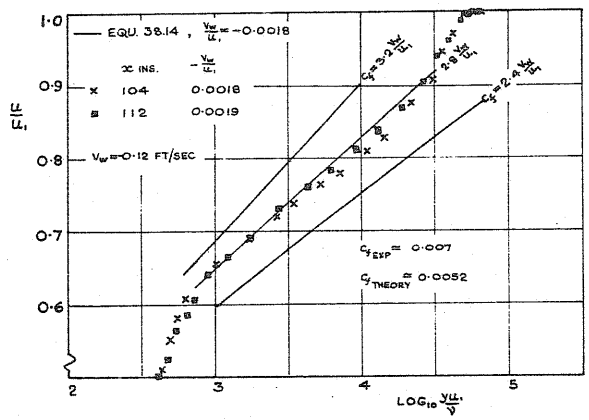

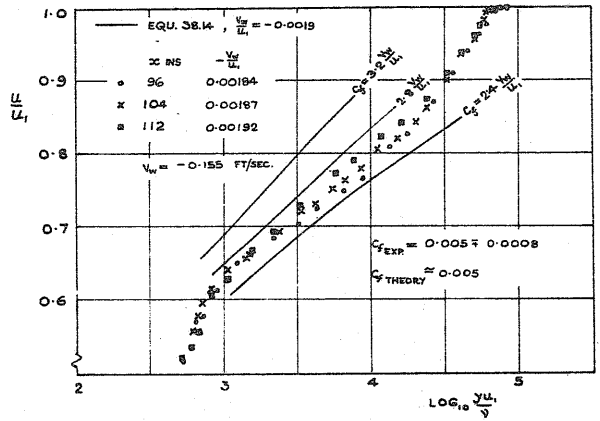

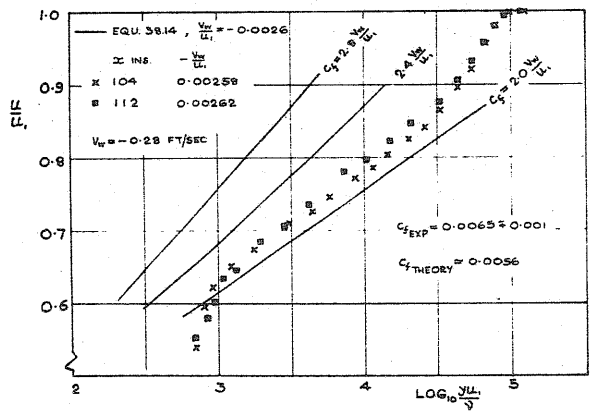

FIG. 104 INNER REGION VELOCITY PROFILES – PIPE FLOW

CRANFIELD INSTITUTE OF TECHNOLOGY

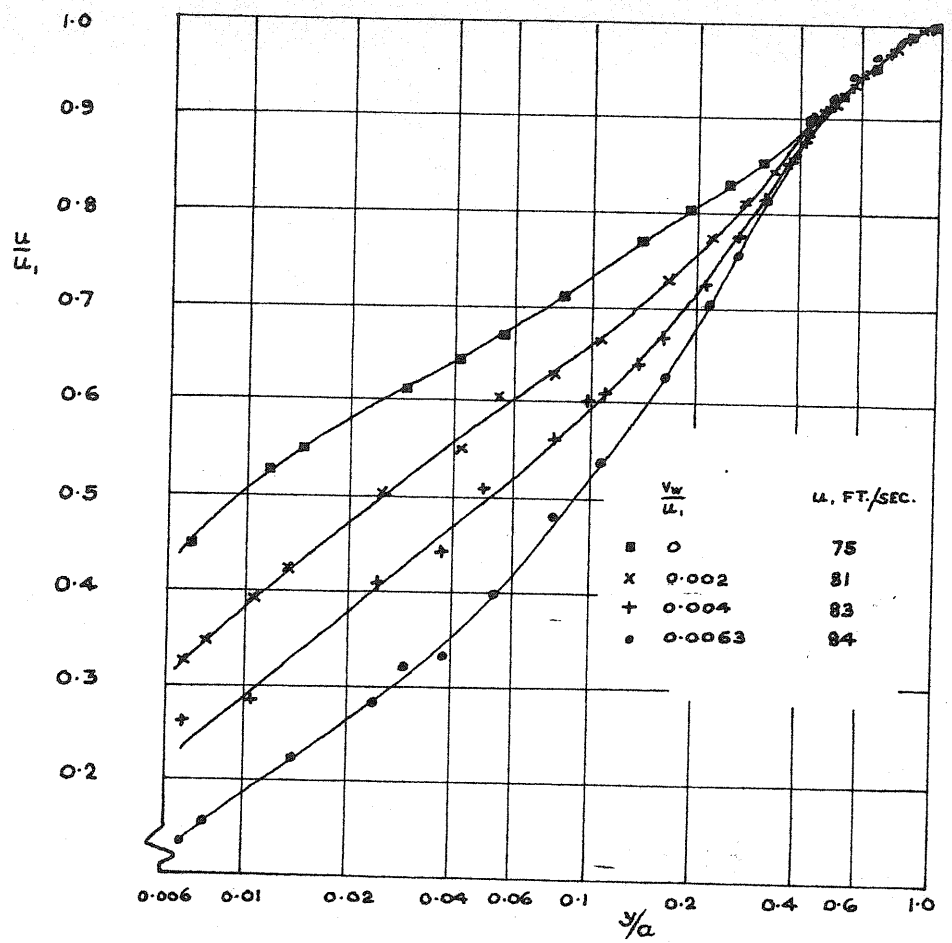

FIG. 105 VELOCITY PROFILES WITH INJECTION – PIPE FLOW

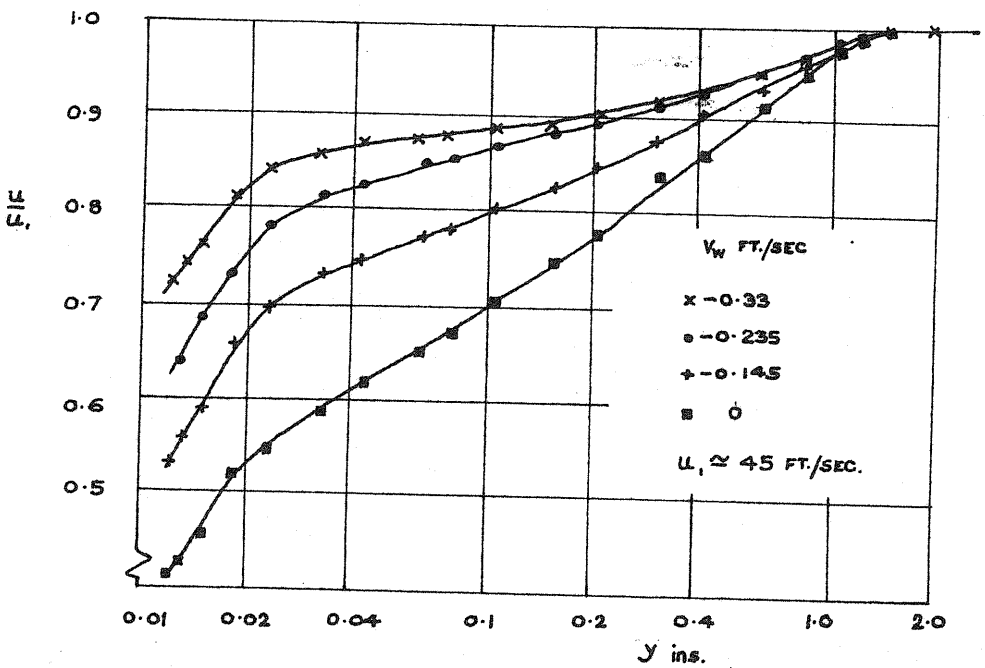

FIG. 106 VELOCITY PROFILES WITH SUCTION – ENTRY LENGTH CONDITIONS

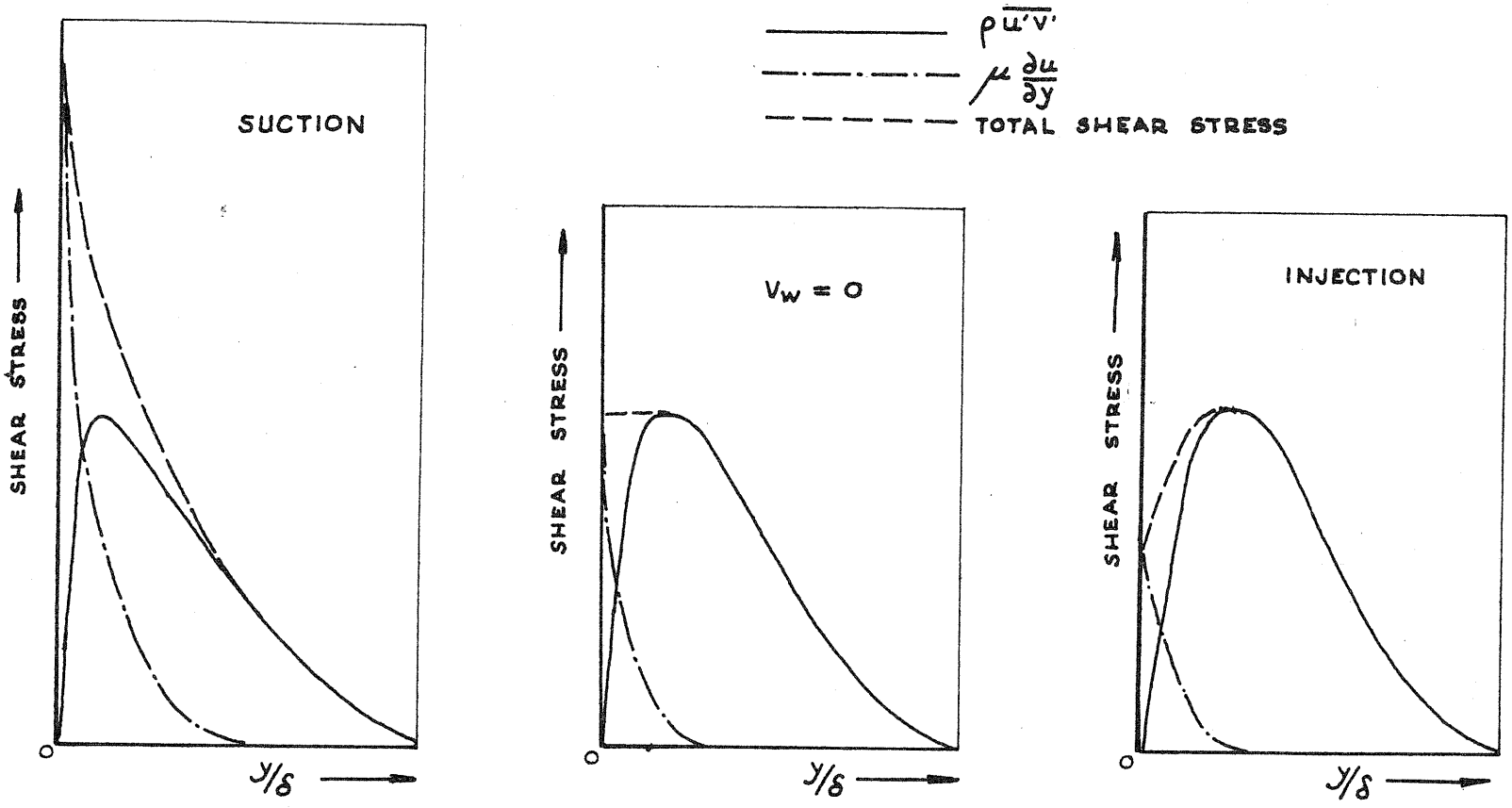

FIG. 107 A COMPARISON BETWEEN THE SHEAR STRESSES WITH SUCTION AND INJECTION (NOT TO SCALE)